

# **Formation of MHC Class II – Peptide Multimers**

**Walaa Wilson Matta Saweirs**

**BSc(Hons.Med.Sci.), MBChB (Hons.), MRCP (UK)**



## Acknowledgements

I would like to thank:

The Medical Research Council for their financial support in awarding me a research fellowship;

My two supervisors, Professor Neil Turner and Dr Richard Phelps, for their guidance and support throughout the research work, without which this project would not have been possible;

Our amazing laboratory technicians, Pat Swan and Davina Wojtacha, for all their technical help and support, and without whom this project would have been far more of a struggle;

Drs Andrew Devitt and Julia Marley for their help with the FACS techniques and analysis;

Dr Simone Brown for providing the beads used in FACS analysis, as well as incisive discussions regarding the findings of the FACS analysis;

Drs Juan Zou, Nick Sargent, and Matthew King for technical help and discussions;

Dr Chris Bellamy for providing the histopathology figure of Goodpasture's Disease;

And of course my wife, Tracey, without whose support and distraction I would have been unable to finish this task with a sound mind.



## **Dedication**

I would like to dedicate this work to Tracey, Sophie and Suzanna. They have seen this project from its inception and to its rather prolonged written completion.

# Contents

<b>ACKNOWLEDGEMENTS.....</b>	<b>I</b>
<b>DEDICATION.....</b>	<b>II</b>
<b>CONTENTS.....</b>	<b>III</b>
<b>DECLARATION.....</b>	<b>VI</b>
<b>ABSTRACT.....</b>	<b>VII</b>
<b>INDEX OF TABLES AND FIGURES .....</b>	<b>IX</b>
<b>NOMENCLATURE AND ABBREVIATIONS.....</b>	<b>XII</b>
1    NOMENCLATURE .....	XII
2    ABBREVIATIONS .....	XIII
<b>CHAPTER 1: INTRODUCTION.....</b>	<b>1</b>
1    INTRODUCTION .....	1
2    AUTOIMMUNITY, NEPHRITIS AND THE CELLULAR IMMUNE RESPONSE.....	1
3    GOODPASTURE’S DISEASE.....	9
4    ESTABLISHED METHODS OF T CELL ASSESSMENT .....	17
5    MAJOR HISTOCOMPATIBILITY COMPLEX MULTIMERS.....	22
6    CONCLUDING REMARKS .....	43
<b>CHAPTER 2: MATERIALS AND METHODS.....</b>	<b>49</b>
1    MATERIALS .....	49
2    NUCLEIC ACID METHODS.....	52
3    HYBRIDOMA CELL CULTURE.....	58
4    INSECT CELL CULTURE AND PROTEIN PRODUCTION METHODS.....	61
5    BACTERIAL PROTEIN PRODUCTION METHODS.....	65
6    CELL LYSATE PREPARATION .....	70
7    PROTEIN IDENTIFICATION METHODS.....	71
<b>CHAPTER 3: RESULTS (I) .....</b>	<b>79</b>
1    INTRODUCTION .....	79
2    CONSTRUCTION OF RECOMBINANT I-E <sup>D</sup> T <sup>D</sup> PCBIRA.....	80
3    EXPRESSION OF RECOMBINANT I-E <sup>D</sup> T <sup>D</sup> BIRA - PRELIMINARY WORK .....	86

4	CHARACTERISATION OF EXPRESSION OF RECOMBINANT I-E <sup>D</sup> TBIRA .....	88
5	DISCUSSION.....	97
<b>CHAPTER 4: RESULTS (II).....</b>		<b>100</b>
1	INTRODUCTION.....	100
2	DESIGN OF ACID-BASE LEUCINE ZIPPER-ASSOCIATED HLA-DR15 AND HLA-DR7 MOLECULES .....	101
3	CONSTRUCTION OF LEUCINE ZIPPER ASSOCIATED HLA-DR $\alpha$ CHAIN.....	105
4	CONSTRUCTION OF LEUCINE ZIPPER LINKED HLA-DR $\beta$ CHAINS .....	110
5	EXPRESSION OF LEUCINE ZIPPER-ASSOCIATED HETERODIMERIC HLA-DR15 CONSTRUCT ..	115
6	EXPRESSION OF LEUCINE ZIPPER-ASSOCIATED HETERODIMERIC HLA-DR7 CONSTRUCT ....	130
7	DISCUSSION.....	133
<b>CHAPTER 5: RESULTS (III) .....</b>		<b>137</b>
1	INTRODUCTION.....	137
2	CONSTRUCTION OF SINGLE-CHAIN MHC CLASS II MOLECULES .....	139
3	EXPRESSION OF SINGLE-CHAIN TETRAMER BUILDING BLOCKS IN <i>E. COLI</i> .....	150
4	PURIFICATION OF SCTBB PROTEINS .....	166
5	DISCUSSION.....	175
<b>CHAPTER 6: RESULTS (IV).....</b>		<b>178</b>
1	INTRODUCTION.....	178
2	LEUCINE ZIPPER-ASSOCIATED HETERODIMERIC HLA-DR TETRAMER BUILDING BLOCKS ...	178
3	SINGLE-CHAIN TETRAMER BUILDING BLOCKS .....	191
4	DISCUSSION.....	206
<b>CHAPTER 7: CONCLUSIONS.....</b>		<b>210</b>
1	INTRODUCTION.....	210
2	FORMATION OF TETRAMER BUILDING BLOCKS .....	211
3	FUNCTIONAL ASSESSMENT OF TETRAMER BUILDING BLOCKS .....	219
4	SENSITIVITY AND SPECIFICITY OF MHC CLASS II MULTIMERS.....	222
5	APPLICATION OF MHC CLASS II MULTIMERS .....	225
6	FUTURE WORK .....	230
<b>CHAPTER 8: REFERENCES.....</b>		<b>236</b>
<b>APPENDIX 1 .....</b>		<b>267</b>
1	I-E <sup>D</sup> TBIRA HETERODIMER CONSTRUCTS .....	267
2	HLA-DR ZIPPER CONSTRUCTS .....	268
3	PEPTIDE BINDING CASSETTE CONSTRUCT.....	268

**APPENDIX 2.....269**

**APPENDIX 3.....270**

1 TRANSFORMATION AND AMPLIFICATION OF DNA IN COMPETENT CELLS .....270

2 AGAROSE MINI GELS.....270

3 SDS-PAGE GELS .....270

4 ANTIBODY PURIFICATION .....270

5 BACTERIAL INCLUSION BODY PREPARATION .....271

6 NICKEL CHELATION CHROMATOGRAPHY .....271

7 MISCELLANEOUS SOLUTIONS .....273

## **Declaration**

This work contains no material which has been accepted for the award of any other degree or diploma in any university or tertiary institution and, to the best of my knowledge and belief, contains no material previously published or written by another person, except where due reference has been made in the text.

Walaa Wilson Matta Saweirs

1<sup>st</sup> June, 2005

## Abstract

A quantitative and qualitative analysis of the various sub-types of antigen-specific CD4<sup>+</sup> T cells in autoimmunity is important because they have a central role in an immune response. Although it has been possible to study the humoral response in detail in many autoimmune diseases, the analysis of antigen-specific T cells lags far behind. A major impediment has been the innate low affinity of the T cell receptor for its bipartite ligand – MHC plus peptide. The arrival of MHC class I tetramers shed new light on the CD8<sup>+</sup> T cell response, and provided one solution to these challenges. Although monomeric HLA binding is of too low an affinity to be useful in T cell labelling, fluorochrome labelled tetrameric HLA-peptide complexes bind stably to antigen-specific CD8<sup>+</sup> T cells due to the higher avidity gained by multimerisation. These MHC-peptide TCR interactions are, therefore, able to detect specific cellular immune responses in a similar way to the way antigen-antibody interactions have been used to examine the humoral immune response. There is currently no evidence that this technique overestimates the number of antigen-specific T cells. The need to explore the role of CD4<sup>+</sup> T cells in autoimmunity and infection has lead several groups to try to develop MHC class II tetramers. All have met with varying technical difficulties, primarily because successful MHC class II multimer formation requires the conformationally correct interaction of three components –  $\alpha$  and  $\beta$  chain, and peptide – rather than the two in MHC class I. However, the successes that have been reported suggested that MHC class II tetramer analysis could be undertaken and applied to examine autoimmune T cell populations.

I chose Goodpasture's disease as a pilot autoimmune disease to explore the potential of MHC class II tetramers. Although Goodpasture's disease is an uncommon autoimmune disorder that causes rapidly progressive glomerulonephritis and lung haemorrhage, it provides an amenable model for tetramer analysis of autoreactive T cells for a number of reasons:

- The 'Goodpasture' antigen is known

- Both predisposing and protective HLA class II molecules have been identified
- Three nested sets of naturally processed peptides from the antigen that are presented bound to HLA-DR15 have been identified biochemically.

Here I describe the formation of functional recombinant MHC class II proteins that are capable of being multimerised to form fluorochrome labelled multimeric complexes. Two different approaches have been used. One approach utilised the *Drosophila* S2 expression system and adapted the C-terminals of the MHC class II alpha and beta chains through the addition of an acid-base leucine zipper motif in order to maintain the stability of their heterodimeric association in solution. Protein tags were also added to the C-terminals together with the BirA site-specific biotinylation sequence. Both HLA-DR15 and HLA-DR7 were adapted in this way. The other, more novel approach, utilised a bacterial expression system and aimed to improve the heterodimeric chain pairing of the MHC class II peptide-binding domain through the construction of a two-domain single chain MHC class II peptide, linking the  $\beta$ 1 domain directly to the  $\alpha$ 1 domain, similar to the rat RT1b construct of Burrows *et al* (Burrows et al., 1999). HLA-DR15, HLA-DR7 and I-E<sup>d</sup> were adapted in this way. The conformationally correct nature of both of these approaches and their peptide-specific binding are demonstrated.

## Index of Tables and Figures

TABLE 1 – CELL LINES .....	51
TABLE 2 – ANTIBODIES USED.....	73
FIGURE 1.1 – PATHOLOGY OF GOODPASTURE’S DISEASE .....	10
FIGURE 1.2 – $\alpha$ 3- $\alpha$ 4- $\alpha$ 5 TYPE (IV) COLLAGEN PROTOMER NETWORK.....	11
FIGURE 1.3 – THE $\alpha$ 3- $\alpha$ 4- $\alpha$ 5 (IV) NC1 HEXAMER .....	13
FIGURE 1.4 – MHC I PEPTIDE BINDING GROOVE .....	23
FIGURE 1.5 – MHC II PEPTIDE BINDING GROOVE .....	23
FIGURE 1.6 – MHC CLASS I TETRAMER.....	25
FIGURE 1.7 – LEUCINE ZIPPER ASSOCIATED MHC CLASS II TETRAMER.....	38
FIGURE 1.8 – “CLASSICAL” TETRAMER DESIGN .....	39
FIGURE 1.9 – IMMUNOGLOBULIN SCAFFOLD BASED OLIGOMERS.....	40
FIGURE 1.10 – PEPTIDE BACKBONE OLIGOMERISATION.....	42
FIGURE 1.11 – SINGLE CHAIN MHC CLASS II.....	43
FIGURE 1.12 – DIAGRAM OF TBB APPROACHES .....	47
FIGURE 3.1 – I-E <sup>D</sup> CONSTRUCT COMPARISON .....	81
FIGURE 3.2 – NUCLEOTIDE AND AMINO ACID SEQUENCES OF I-E <sup>D</sup> $\beta$ TBIRA .....	83
FIGURE 3.3 – THE PEPTIDE-BINDING CASSETTE.....	85
FIGURE 3.4 – A20 CELL LYSATE SAMPLES WITH I-E <sup>D</sup> -SPECIFIC MONOCLONAL ANTIBODIES .....	87
FIGURE 3.5 – BALB/C SPLEEN LYSATE SAMPLES WITH I-E <sup>D</sup> -SPECIFIC MONOCLONAL ANTIBODIES .....	88
FIGURE 3.6 – I-E <sup>D</sup> TRANSCRIPTION ASSESSED BY RT-PCR.....	89
FIGURE 3.7 – ASSESSMENT OF I-E <sup>D</sup> TBIRA PRODUCTION BY STABLY TRANSFECTED S2 CELLS .....	92
FIGURE 3.8 – IMMUNOPRECIPITATION OF I-E <sup>D</sup> TBIRA.....	93
FIGURE 3.9 – CYTOSPIN OF S2 CELLS TRANSFECTED WITH I-E <sup>D</sup> TBIRA (+/- BAND3) STAINED USING 2G9 .....	94
FIGURE 4.1 – ALIGNMENT OF I-A AND HLA-DR PEPTIDE SEQUENCES .....	102
FIGURE 4.2 – HLA-DR ZIPPER-ASSOCIATED CONSTRUCT .....	104
FIGURE 4.3 – CONSTRUCTION OF HLA-DRA WITH ACIDIC LEUCINE ZIPPER .....	106
FIGURE 4.4 – WSA1 NUCLEOTIDE SEQUENCE.....	107
FIGURE 4.5 – ACID LEUCINE ZIPPER AND POLYHISTIDINE SEQUENCE OF WSA2.....	108
FIGURE 4.6 – HLA-DRAZ PROTEIN SEQUENCE.....	109



FIGURE 4.7 - CONSTRUCTION OF DRB WITH ZIPPER .....	111
FIGURE 4.8 – WSB1-07 AND WSB1-15 NUCLEOTIDE SEQUENCES.....	112
FIGURE 4.9 – BASIC LEUCINE ZIPPER, C-MYC TAG AND BIRA SEQUENCE FOR WSB2.....	113
FIGURE 4.10 – HLA-DRB15Z AND -DR7Z PEPTIDE SEQUENCES.....	114
FIGURE 4.11 – DR15 AND DR7 mRNA RT-PCR.....	116
FIGURE 4.12 – MONOCLONAL ANTIBODY BINDING TO HLA-DR CONSTRUCTS .....	117
FIGURE 4.13 – HLA-DR15LZ & HLA-DR7LZ SUPERNATANT ASSESSMENT .....	118
FIGURE 4.14 – ASSESSMENT OF CELL-ASSOCIATED HLA-DR15LZ TBB.....	119
FIGURE 4.15 – ASSESSMENT OF HLA-DR15LZ PRODUCTION IN SERUM-FREE MEDIUM.....	122
FIGURE 4.16 –WESTERN BLOT STAINED WITH DA6.147 FOLLOWING DA6.231 IMMUNOPRECIPITATION .....	124
FIGURE 4.17 – METAL CHELATION EXTRACTION OF $\alpha$ CHAIN PULLS DOWN $\beta$ CHAIN .....	126
FIGURE 4.18 – CONCENTRATION OF LARGE-SCALE PRODUCTION OF HLA-DR15LZ TBB.....	128
FIGURE 4.19 – PROTEIN LOSSES USING A POROS <sup>®</sup> MC COLUMN.....	128
FIGURE 4.20 – FINAL PURIFICATION OF HLA-DR15LZ TBB.....	129
FIGURE 4.21 – ASSESSMENT OF CELL-ASSOCIATED HLA-DR7LZ TBB.....	131
FIGURE 4.22 – WESTERN BLOT SHOWING WEAK HLA-DR7LZ EXPRESSION.....	132
FIGURE 5.1 – ALIGNMENT OF HLA-DR, IE <sup>D</sup> AND RTB.....	140
FIGURE 5.2 – OUTLINE OF I-E <sup>D</sup> SINGLE-CHAIN CONSTRUCT FORMATION .....	142
FIGURE 5.3 – FORMATION OF IE <sup>D</sup> SC FUSION PROTEIN.....	144
FIGURE 5.4 – IE <sup>D</sup> SC DNA SEQUENCE.....	145
FIGURE 5.5 – OUTLINE OF HUMAN SINGLE-CHAIN FORMATION .....	147
FIGURE 5.6 – SEQUENCE OF HLA-DR $\alpha$ 1 DNA .....	148
FIGURE 5.7 – SEQUENCE FOR HLA-DR7SC AND DR15SC.....	149
FIGURE 5.8 – ASSESSMENT OF IE <sup>D</sup> SC TBB PROTEIN PRODUCTION.....	152
FIGURE 5.9 – PI OF I-E <sup>D</sup> SC TBB .....	153
FIGURE 5.10 – ANION EXCHANGE OF IE <sup>D</sup> SC TBB.....	154
FIGURE 5.11 – ASSESSMENT OF ANION EXCHANGE SEPARATION OF IE <sup>D</sup> SC TBB .....	155
FIGURE 5.12 – OUTLINE OF PET25B-BIRA SC TBB FORMATION .....	158
FIGURE 5.13 – SEQUENCE PET25B(BIRA) USING T7 PROMOTER PRIMER.....	159
FIGURE 5.14 – NUCLEOTIDE SEQUENCES OF PET25B-IE <sup>D</sup> SC TBB, -DR15SC TBB & -DR7SC TBB .....	160
FIGURE 5.15 – PROTEIN SEQUENCES OF SC TBB CONSTRUCTS .....	162
FIGURE 5.16 – IE <sup>D</sup> SC TBB PEPTIDE PRODUCTION.....	163
FIGURE 5.17 – DR7SC TBB PEPTIDE PRODUCTION.....	164
FIGURE 5.18 – DR15SC TBB PEPTIDE PRODUCTION.....	164
FIGURE 5.19 – HIS-TAG <sup>®</sup> PURIFICATION OF DR7SC TBB.....	167

FIGURE 5.20 – ASSESSMENT OF IMIDAZOLE CONCENTRATION FOR HIS-TAG PURIFICATION.....	168
FIGURE 5.21 – SDS-PAGE GEL MOBILITIES OF THE SCTBBS .....	170
FIGURE 5.22 – DR15SC TBB REFOLDING WITHOUT REDOX SHUFFLE (ANTI-HSV TAG).....	172
FIGURE 5.23 – REFOLDING SCTBB(DR15) USING REDOX SHUFFLE .....	173
FIGURE 6.1 - IMMUNOPRECIPITATION WITH L243 TO INVESTIGATE THE OCCURRENCE OF $\alpha\beta$ HETERODIMERS .....	180
FIGURE 6.2 - L243 IMMUNOPRECIPITATION ANALYSIS OF HLA-DR15LZTBB.....	181
FIGURE 6.3 – FLUORESC EIN-TAGGED PEPTIDE (FL-E-23-R) COMPARED TO PEPTIDE P3B .....	183
FIGURE 6.4 – GATING ON DYNAL <sup>®</sup> BEADS .....	186
FIGURE 6.5 – HLA-DR15LZ TBB BINDS TO FL-E-23-R.....	187
FIGURE 6.6 – HLA-DR15LZ TBB PEPTIDE BINDING COMPETITION .....	189
FIGURE 6.7 – LACK OF DMSO EFFECT ON HLA-DR15LZ TBB PEPTIDE BINDING .....	190
FIGURE 6.8 – ASSESSMENT OF HLA-DR15LZ TBB BINDING TO BEADS .....	191
FIGURE 6.9 – L243 IMMUNOPRECIPITATION OF HLA-DR15SC TBB AND HLA-DR7SC TBB .....	192
FIGURE 6.10 – ASSESSMENT OF BIOTINYLATION OF SCTBB .....	194
FIGURE 6.11 – FACS ANALYSIS OF HLA-DR15SC REFOLDED WITH FL-E-23-R IN THE PRESENCE/ABSENCE OF CITRATE BUFFER.....	196
FIGURE 6.12 – OPTIMISING PEPTIDE-BINDING CONDITIONS OF HLA-DR15SC WITH FL-E-23-R .....	198
FIGURE 6.13 – HLA-DR15SC PEPTIDE-BINDING INHIBITION (I) .....	200
FIGURE 6.14 - HLA-DR15SC PEPTIDE-BINDING INHIBITION (II) .....	201
FIGURE 6.15 – EFFECT OF DMSO UPON FLUORESCENCE INTENSITY .....	203
FIGURE 6.16 – OPTIMISATION OF BEAD, HLA-DR15SC TBB AND FL-E-23-R CONCENTRATIONS .....	204

# Nomenclature and Abbreviations

## 1 Nomenclature

HLA-DRAz – HLA-DRA1\*0101 acid leucine zipper-associated construct

HLA-DRB15z – HLA-DRB1\*1501 base leucine zipper-associated construct

HLA-DRB7z – HLA-DRB1\*0701 base leucine zipper-associated construct

HLA-DR15LZ – HLA-DR15 leucine zipper heterodimeric construct

HLA-DR7LZ – HLA-DR7 leucine zipper heterodimeric construct

HLA-DR15sc – HLA-DR15 $\beta_1\alpha_1$ BirA single-chain fusion protein/DNA construct

HLA-DR7sc – HLA-DR7 $\beta_1\alpha_1$ BirA single-chain fusion protein/DNA construct

I-E<sup>d</sup> – Native murine I-E<sup>d</sup>

I-E<sup>d</sup>t – Truncated extracellular I-E<sup>d</sup> as per Wallny *et al* (Wallny et al., 1995)

I-E<sup>d</sup> $\alpha$ t – Extracellular I-E<sup>d</sup> alpha chain

I-E<sup>d</sup> $\beta$ tBirA – Extracellular I-E<sup>d</sup> beta chain with carboxy terminus BirA biotinylation sequence

I-E<sup>d</sup> $\beta$ tPCBirA – As above with linked amino terminus peptide-binding cassette

I-E<sup>d</sup> $\beta$ tPCBirA-Band3 – As above with a Band3 peptide covalently linked via the peptide-binding cassette

I-E<sup>d</sup>tBirA – Truncated extracellular I-E<sup>d</sup> protein with BirA at the C-terminus of the  $\beta$  chain

I-E<sup>d</sup>tBand3 – As above, with covalently linked Band 3 peptide

I-E<sup>d</sup>sc – I-E<sup>d</sup> $\beta_1\alpha_1$ BirA single-chain fusion protein/DNA construct

IzTBB – Leucine zipper-associated heterodimeric tetramer building block

pUC19BirA – pUC19 vector containing the BirA cDNA sequence

pUC19 $\alpha$ 1BirA – Above containing HLA-DR $\alpha_1$  cDNA sequence 5' of BirA cDNA

scTBB – Single-chain fusion protein tetramer building block

TBB – Tetramer building block

## 2 Abbreviations

ANCA – Anti-neutrophil cytoplasmic antibody

AP – Alkaline phosphatase conjugate

$\alpha 3(\text{IV}) \text{NC1}$  –  $\alpha 3$  Type IV collagen NC1 domain

APC – Antigen presenting cell

BCIP – 5-bromo-4-chloro-3-indolyl phosphate

bp – Base pairs

BirA – Site-specific biotinylation sequence

BSA – Bovine serum albumin

BSP – Bir A enzyme substrate peptide

CEA – Carcinoembryonic antigen

CFSE – 5-(and -6)-Carboxyfluorescein diacetate succinimidyl ester

CNS – Central nervous system

CTL – Cytotoxic T lymphocyte

DAPI - 4',6-Diamidino-2-phenylindole

DMSO - Dimethyl sulphoxide

DNA – deoxyribonucleic acid

DTT - Dithiothreitol

dNTP – Dideoxy nucleic acid triphosphate

EAG – Experimental allergic glomerulonephritis

EBV – Epstein-Barr virus

EDTA – Ethylenediaminetetraacetic acid

ELISA – Enzyme-linked immunosorbent assay

FACS – Fluorescent-activated cell sorting

FCA – Freund's complete adjuvant

FITC - Fluorescein Isothiocyanate

GBM – Glomerular basement membrane

GnHCl - Guanidine hydrochloride

HA – Haemagglutinin

HEPES – 4-(2-Hydroxyethyl)piperazine-1-ethanesulphonic acid

HIV – Human immunodeficiency virus

HLA – Human leukocyte antigen

HSV-2 – Herpes simplex virus type 2

HTLV-I – Human T cell lymphotropic virus type I

IDA – Iminodiacetic acid	OD – Optical density
IDDM – Insulin dependent diabetes mellitus	PBMC – Peripheral blood mononuclear cell
IgG – Immunoglobulin gamma	PBS – Phosphate buffered saline
IL-2 – Interleukin 2	PCR – Polymerase chain reaction
IPTG – Isopropyl- $\beta$ -D-galactopyranoside	pMHC – Peptide MHC complex
kD – Kilo Daltons	PMSF – Phenylmethanesulfonyl fluoride
LB – Luria-Bertani bacterial media	pMT – Metallothionein promoter
LCMV - Lymphocytic choriomeningitis virus	RBC – Erythrocyte
MBP – Myelin basic protein	RNA – Ribonucleic acid
MCC – Moth cytochrome c	rpm – Revolutions per minute
MgCl <sub>2</sub> – Magnesium chloride	RT-PCR – Reverse transcription polymerase chain reaction
MHC – Major Histocompatibility Complex	Sf9 – <i>Spodoptera frugiperda</i> pupal ovarian cell line
mRNA – Messenger RNA	SLE – Systemic lupus erythematosus
MW – Molecular weight	SOB – Hanahan's broth bacterial media
MWCO – Molecular weight cut-off	TCR – T cell receptor
NaCl – Sodium chloride	T <sub>H</sub> 1 – Class I T helper lymphocytes
NaOH – Sodium hydroxide	T <sub>H</sub> 2 – Class II T helper lymphocytes
NBT - Nitrotetrazolium blue chloride	T <sub>R</sub> 1 – Class I regulatory CD4 <sup>+</sup> T lymphocytes
NC1 – First non-collagenous domain of collagen chain	UV – Ultraviolet
(NH <sub>4</sub> ) <sub>2</sub> SO <sub>4</sub> – Ammonium sulphate	w/v – weight per volume
NiCl – Nickel chloride	
NP40 - Nonidet® P40	

# **Chapter 1**

## **Introduction**

# Chapter 1

## Introduction

### 1 Introduction

Before discussing MHC multimers in some detail, I feel that it would be appropriate to provide some background to autoimmune glomerulonephritis and the role of T cells within this. I will also provide an overview of the established methods of T cell assessment before describing the aims behind this thesis.

### 2 Autoimmunity, Nephritis and the Cellular Immune Response

#### 2.1 Autoimmunity - General concepts

Autoimmune diseases can be broadly distinguished by two main patterns – those primarily restricted to a single organ and those that are systemic. Classical examples of the former include multiple sclerosis (MS) affecting neuronal axons of the central nervous system, type I insulin-dependent diabetes mellitus (IDDM) affecting the pancreatic islets, and Goodpasture's disease affecting the glomerular and alveolar basement membranes. Systemic lupus erythematosus (SLE) and rheumatoid arthritis provide examples of the latter.

It is thought that these autoimmune diseases are initiated in a similar manner to protective adaptive immune responses by the activation of antigen-specific T cells. Such activation can result in direct and indirect tissue injury. Cytotoxic CD8<sup>+</sup> T cells and macrophages inappropriately activated by CD4<sup>+</sup> T cells can result in marked tissue damage. This damage may be furthered by autoantibodies produced by self-reactive B cells through inappropriate CD4<sup>+</sup> T cell help. These processes also lead to activation of the other components of the humoral response such as complement

factors. Although the final response pathways are similar, many questions remain (Theofilopoulos, 1995):

- The principles governing the nature and extent of the autoimmune process
- The nature of the inciting antigen
- The nature of the environmental factors precipitating the process
- The nature of the genes that predispose and accelerate the autoimmune process
- The discriminating characteristics of auto-pathogenic T cells and antibodies
- The nature of the mechanisms that control relapses and remissions

In the majority, if not all, cases, these questions remain largely unanswered. Recent data points to a genetic bias towards autoimmunity in the form of an “autoimmune profile” that was evident even in first-degree relatives of those with both organ-specific and systemic autoimmune disease (Maas et al., 2002). Such a profile may form a basis for more specific genetic and environmental factors that affect the nature and extent of autoimmune disease. One such specific factor is the inciting antigen, which remains obscure for many human autoimmune diseases, particularly the systemic diseases. For although the autoantibodies and their corresponding antigens may be apparent, ambiguities remain as to their relevance in terms of disease initiation, particularly when there is a large diversity of autoantibodies in a particular disease process. Moreover, the role and specificity of auto-reactive T cells remains elusive (Abbas et al., 1996, Roncarolo and Levings, 2000). A better knowledge of the inciting antigen and its relationship to auto-reactive T cells would, therefore, act as a springboard to a greater understanding of the autoimmune disease process by permitting a more thorough dissection of the other factors involved and their mechanistic relationship. One human autoimmune disease where a greater understanding of the inciting antigen has been gained is Goodpasture’s Disease (*vide infra*).



## 2.2 Human Glomerulonephritis – The role of the cellular immune response

Human glomerulonephritis may be divided into those diseases that primarily affect the glomeruli and those where the glomerular damage is secondary to a more systemic disease process. In both instances some diseases will have a better-defined inciting antigen than others, which are currently idiopathic. The initial work that established the immune aetiology of glomerulonephritis concentrated on the role of the humoral arm of the immune system (Reviewed in (Robson, 2000)). The central hypothesis at that time was that the presence of immune complexes within the glomeruli initiated a common pathway of activation of the complement system resulting in neutrophil recruitment and platelet activation with consequent glomerular injury. However, this hypothesis has proven inadequate at explaining the diversity of glomerulonephritis and the tendency of glomerular lesions to sclerose (Rovin and Schreiner, 1991).

Initial studies in human glomerulonephritis showed the presence of monocytes within the glomeruli particularly in the context of cellular crescents (Magil and Wadsworth, 1982), although the suggestion at that time was more of a clearance role for these cells (Magil and Wadsworth, 1981). Further work involving more than 340 renal biopsy samples stained using the non-specific esterase reaction to detect monocytes revealed the presence of these cells in proliferative glomerulonephritis. Indeed, it was found that monocyte infiltration correlated with proteinuria, cellular crescents and neutrophil infiltration, strongly suggesting a direct role for these cells in glomerular injury (Ferrario et al., 1985). Using a panel of monoclonal antibodies Hooke *et al* (Hooke et al., 1987) found that in proliferative glomerulonephritis monocyte and granulocyte numbers significantly increased within the glomerular tuft, without any significant changes to intra-glomerular T cell numbers. However, they did find significant increases in interstitial T cell numbers in cases of proliferative glomerulonephritis, and an inverse correlation between total interstitial leukocyte count and renal function.

The absence of a significant increase in intra-glomerular T cell numbers was not born out by other studies using different panels of monoclonal antibodies. Nolasco *et al* (Nolasco et al., 1987) found significant increases in overall intra-glomerular leukocyte numbers in proliferative glomerulonephritis, with a significant increase in CD4<sup>+</sup> T cells in crescentic biopsies, almost exclusively seen within glomerular tufts. This finding was particularly notable in anti-glomerular basement membrane disease. Moreover, a significant correlation between total intra-glomerular T cell and monocyte numbers was found. This finding was noted in another study (Bolton et al., 1987), which also found an association between interstitial leukocyte infiltration and renal function. Furthermore, the authors went on to suggest an inverse correlation between CD4<sup>+</sup> T cells and responsiveness to pulse methylprednisolone therapy, with anti-GBM disease biopsies revealing the most marked increase in CD4<sup>+</sup> T cells within glomeruli. Neale *et al* also published similar findings with respect to intra-glomerular T cell infiltration and fibrin deposition in proliferative glomerulonephritis (Neale et al., 1988). Markovic-Lipkovski *et al* (Markovic-Lipkovski et al., 1990) found indications of activation of infiltrating leukocytes within and around affected glomeruli in cases of proliferative glomerulonephritis. Once again, there was a predominance of CD4<sup>+</sup> T cells particularly in cases of rapidly progressive glomerulonephritis. These findings would suggest more strongly a significant role for the cellular arm of the immune system, particularly the orchestrating CD4<sup>+</sup> T cells, in proliferative glomerulonephritis. The importance of the cellular arm of the immune system is particularly well highlighted by a more recent study of pauci-immune (ANCA-positive) rapidly progressive glomerulonephritis. In this disease the humoral components are usually absent, but a significant influx of T cells with the majority expressing a memory phenotype (CD45RO) is seen, together with macrophages and a local up-regulation of tissue factor indicating cellular activation (Cunningham et al., 1999). The discrepancies seen between studies may be explained by a multitude of reasons including timing of biopsies in relation to disease initiation (Markovic-Lipkovski et al., 1990) as well as antibody sensitivity and specificity.

Expanding on this foundation of the role of the cellular arm of the immune response in glomerulonephritis, one must also begin to consider the relative predominance of specific components of the cellular response. A growing number of T cell subtypes have been identified in both murine models and human disease (Mosmann and Sada, 1996). The role of these within the context of glomerulonephritis has been postulated to explain the different patterns of glomerulonephritis, although a greater understanding of the role of these T cell subtypes is still needed to provide a basis for therapeutic intervention (Reviewed in (Holdsworth et al., 1999)).

### **2.3 Experimental Crescentic Glomerulonephritis – The role of the cellular immune response**

The role of cell-mediated immunity in glomerulonephritis has been more clearly demonstrated in experimental models (Alderwegen et al., 1997, Rovin and Schreiner, 1991). The importance of such immunity is particularly well demonstrated by the models of crescentic glomerulonephritis, which were one of the first to establish an immunological role in such conditions.

Crescentic glomerulonephritis was first induced in sheep by repeated administration of heterologous crude GBM preparations in Freund's complete adjuvant (Stebay, 1962). Stebay noted the presence of anti-GBM antibodies to the heterologous immunising GBM in sheep dying of nephritis, but further postulated a possible role for sensitised cells. Direct evidence of the role of such "sensitised cells" came a decade later when Bhan *et al* (Bhan et al., 1978) used an implanted antigen model of crescentic glomerulonephritis. The group transferred rabbit gamma globulin-sensitised lymph node cells into Lewis rats that had been administered rabbit anti-rat GBM immunoglobulin. This group found that only those rats given lymph node cells from donors sensitised to rabbit gamma globulin showed segmental cellular crescents with necrosis in their glomeruli, whereas those rats given serum

from the same sensitised donors only showed linear immunoglobulin staining within their glomeruli.

To this point the evidence for a role for cell-mediated immunity has been obtained within the context of functional humoral immunity. A chicken model of experimental allergic glomerulonephritis (EAG) developed by Bolton *et al* (Bolton *et al.*, 1984) provided more specific evidence for cellular immunity. In this model chickens were immunised with bovine glomeruli in FCA and were noted to develop proliferative crescentic glomerulonephritis with linear deposition of IgG. In the group of chemically bursectomized chickens, IgG deposition was seldom noted yet there was no significant difference in glomerular proliferation and crescent formation between the groups. There was, therefore, no correlation between IgG deposition and proliferative changes within the glomeruli. This group went on to transfer EAG by using sensitised mononuclear cells eluted from nephritic kidneys, with these cells being characterised as lymphocytes (Bolton *et al.*, 1988). Transfer of eluted immunoglobulin from nephritic kidneys resulted in linear IgG deposition on glomeruli but without proliferative changes.

Based on Steblay's classic model of crescentic glomerulonephritis, Pusey *et al* developed a rat model of EAG using a single injection of homologous GBM preparation in FCA as the inciting agent in Brown Norway rats (Pusey *et al.*, 1991). They noted that although the injection of the homologous GBM preparation alone resulted in the production of anti-GBM antibodies, it was only with the addition of FCA that glomerular IgG deposition and nephritis occurred. This finding would indicate a role for T cells in the pathogenesis of glomerulonephritis and would also be in keeping with the other animal models discussed below. This group have used this model of EAG to investigate the pivotal role of T cells in disease pathogenesis (Reynolds *et al.*, 1991, Reynolds *et al.*, 1993). They have also documented disease prevention through the use of T cell blocking antibodies (Reynolds *et al.*, 2002, Reynolds and Pusey, 1994, Reynolds *et al.*, 2000). This work is reviewed by Nikolic-Paterson (Nikolic-Paterson, 2001). Using this model, other groups have attempted to map the T cell epitopes (Luo *et al.*, 1996). Further confirmation for the role of CD4<sup>+</sup> T cells in mediating crescentic glomerulonephritis has been recently

obtained by Wu *et al* using the same model (Wu *et al.*, 2002). This group demonstrated that transfer of sensitised  $\alpha 3$  Type IV NC1-specific T cell lines resulted in classic crescentic changes within glomeruli although without the antibody deposition.

Using a murine model of EAG, Kalluri *et al* (Kalluri *et al.*, 1997) immunised different mouse strains with bovine  $\alpha 3$  Type IV collagen NC1 domains. Although all strains developed antibodies to the bovine antigen, only certain mouse strains developed glomerulonephritis. This variability was seen to be linked to the murine I-A<sup>s</sup> region suggesting a role for the T cell repertoire in disease development.

Using an implanted antigen model of crescentic glomerulonephritis similar to that previously used (Bhan *et al.*, 1978), the group led by Holdsworth and Tipping have performed a series of experiments that not only reveal T cell participation in this model of crescentic glomerulonephritis, but also shed some light on the role of CD4<sup>+</sup> T cell subsets. Their basic model is a result of rats being pre-immunised with sheep globulin in FCA subcutaneously before being administered sheep anti-rat GBM antibody. Using this model the group was able to demonstrate the accumulation of intra-glomerular T cells preceding macrophage accumulation, with the administration of cyclosporin abrogating both the accumulation of T cells and macrophages, as well as proteinuria (Tipping *et al.*, 1985). As a further refinement, the group performed a T cell depletion experiment using anti-CD5 and anti-CD4 monoclonal antibodies 24 hours after administering the sheep anti-rat GBM antibody. This resulted in a significant reduction in CD4<sup>+</sup> T cells within glomeruli, with a significant attenuation of macrophage accumulation and crescent formation without altering the formation of anti-sheep globulin (Huang *et al.*, 1994). The fact that T cell depletion did not completely abolish glomerular injury in this model could suggest that other mechanisms also contribute, although the time delay to depletion would not fully support this suggestion. Further cell depletion studies using anti-CD4 or anti-CD8 monoclonal antibody or macrophage depletion by microencapsulated clodronate indicated that both CD4<sup>+</sup> and CD8<sup>+</sup> T cells were necessary for glomerular macrophage recruitment and glomerular injury in the

Sprague-Dawley rats studied. Moreover, there was no evidence that the CD8<sup>+</sup> T cells acted in a directly cytotoxic manner (Huang et al., 1997b). In order to perform these experiments cell deletion knockout mice were used homozygous for CD4 and/or CD8 deficiency. In this setting the mice were not sensitised prior to the induction of glomerulonephritis using sheep anti-mouse GBM immunoglobulin. Crescentic glomerulonephritis with severe renal injury developed after 14 to 21 days in wild type mice, but was more or less completely abrogated in CD4<sup>-/-</sup> and combined CD4/CD8 <sup>-/-</sup> mice. In these mice there was a significant reduction in macrophage numbers and glomerular injury, once again highlighting the pivotal role of CD4<sup>+</sup> T cells in this model of crescentic glomerulonephritis (Tipping et al., 1998). Taking the planted antigen model one stage further, the group used the same principle in immunoglobulin heavy chain ( $\mu$ ) deficient mouse strain. These  $\mu$  chain deficient mice do not develop mature B cells nor do they produce immunoglobulin. Despite the complete lack of immunoglobulin there was no significant effect on the development of proliferative crescentic glomerulonephritis (Li et al., 1997). These final two experiments were replicated by Rosenkranz *et al* (Rosenkranz et al., 2000) who also showed the importance of  $\gamma\delta$  T cells in this model of crescentic glomerulonephritis.

The importance of the cellular immune system in glomerulonephritis has also been shown in murine lupus nephritis. Previous work had shown the importance of B cells (Chan and J. Shlomchik, 1998), but the role of antibodies in this model was unclear. Using an antibody-deficient strain of the lupus-prone MRL/*lpr* mouse Chan *et al* (Chan et al., 1999) were able to demonstrate interstitial nephritis, vasculitis and glomerular injury indicating an antibody-independent mechanism for renal and vascular disease in this model. This model not only shows the importance of the cellular immune system, but also indicates alternative roles for B cells as antigen presenting cells (APC's) or cytokine producers activating T cells.



## 2.4 Summary

The pivotal role of the cellular arm of the immune system within autoimmune glomerulonephritis has been demonstrated through both human pathological assessment using monoclonal antibodies, and experimental animal models. In the latter case specific cellular depletion experiments clearly point to a central role for T cells in glomerulonephritis and crescent formation. However, T cells are a heterogeneous group of cells with different antigen specificities, cytokine release profiles, and effector functions. Although the role of this group of cells is clearly key to autoimmune glomerulonephritis, and autoimmune disease in general, a greater understanding of the T cell phenotypes involved is necessary. Therefore, a better way of assessing the T cell phenotypes in autoimmune disease is needed. This has been the impetus behind the development of MHC multimers (*vide infra*).

## 3 Goodpasture's Disease

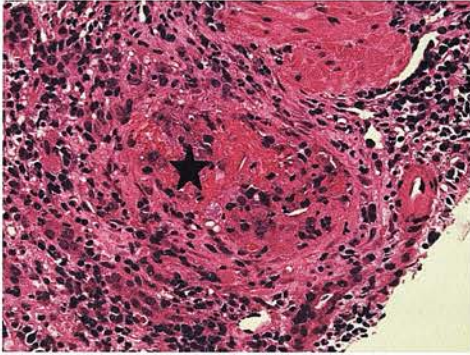
### 3.1 Aetiology and Pathogenesis

Goodpasture's disease is a clinical condition characterised by rapidly progressive glomerulonephritis (Figure 1.1a), pulmonary haemorrhage in 50 – 75% of cases, and the presence of autoantibodies to a specific component of the glomerular and alveolar basement membrane that is seen as linear IgG staining within glomeruli (Figure 1.1b). The disease affects people of both sexes and all ages, although there are two incidence peaks in the third and sixth decades of life (Hudson et al., 2003, Savage et al., 1986, Turner and Rees, 1996). The pathogenic nature of the autoantibodies was established by Lerner (Lerner et al., 1967), and has since been well documented by several clinical observations (Phelps, 2000). Although the primary target for the autoimmune response has been well defined, and is localised to the non-collagenous (NC1) domain of the  $\alpha 3$  chain of type IV collagen (Butkowski et al., 1987, Saus et al., 1988, Wieslander et al., 1984, Wieslander et al., 1987), the inciting factors have not been clearly defined. As with the majority of autoimmune

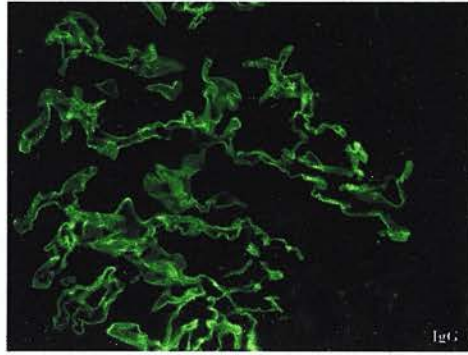
conditions, both genetic and environmental factors appear to be involved in disease aetiology.

**Figure 1.1 – Pathology of Goodpasture's Disease**

**a) Haematoxylin & eosin stain**



**b) Anti-IgG immunofluorescence**



A renal biopsy of a patient with Goodpasture's disease showing a haemorrhagic cellular crescent occupying the glomerular space (\* in a) as well as the linear deposition of IgG along the glomerular basement membrane stained by direct immunofluorescence (b). (Courtesy of Dr C. Bellamy)

There is strong evidence for HLA-linked disease susceptibility to Goodpasture's disease, with certain HLA Class II alleles being more frequently found in patients than controls (Fisher et al., 1997, Phelps and Rees, 1999, Rees et al., 1984). Although one possibility for this linkage is that of linkage disequilibrium of other associated genes, the nature of the association with respect to the exact HLA-DR loci involved strongly suggests that the association is due to the HLA-DRB1 alleles themselves and their peptide-binding characteristics (Phelps et al., 2000, Phelps and Rees, 1999). These strong MHC associations, when taken together with the experimental work outlined above, would suggest that the autoimmune process in this disease is likely to be T cell dependent. This notion is strengthened by the class-switched nature of the autoantibody response that also indicates the need for CD4<sup>+</sup> T cell help (Segelmark et al., 1990). Furthermore, recent work has found an increased frequency of  $\alpha 3(\text{IV})$  NC1 reactive CD4<sup>+</sup> T cells during the acute disease process (Salama et al., 1999, Salama et al., 2001). However, environmental factors also appear to be important in precipitating the disease process, with reports of Goodpasture's disease being precipitated by lithotripsy and exposure to hydrocarbon fumes (Turner and Rees, 1996).

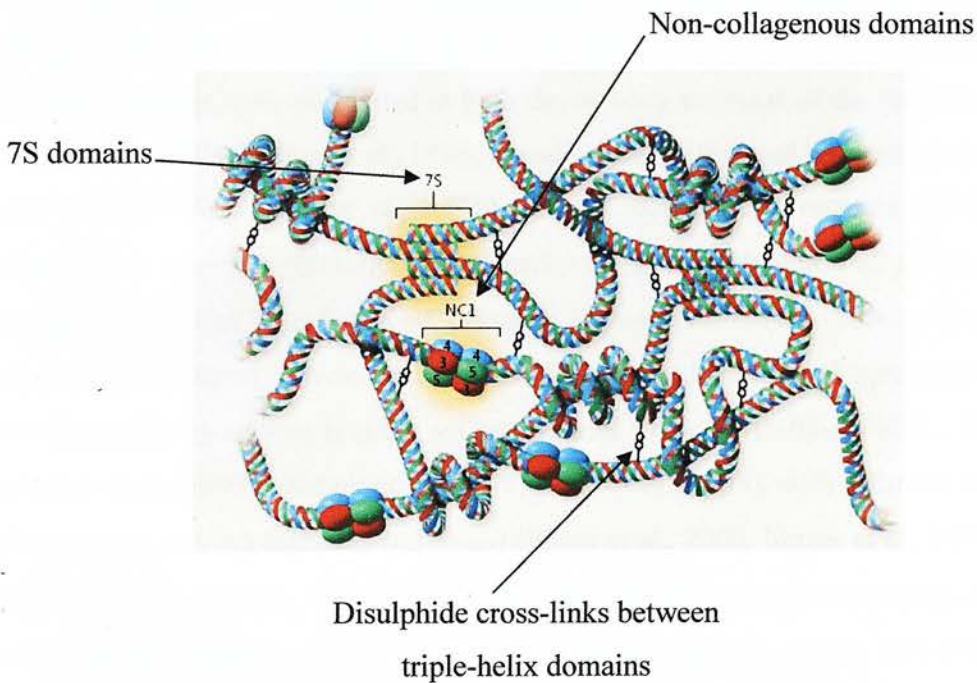


## 3.2 The Goodpasture Auto-antigen

### 3.2.1 The antibody epitope

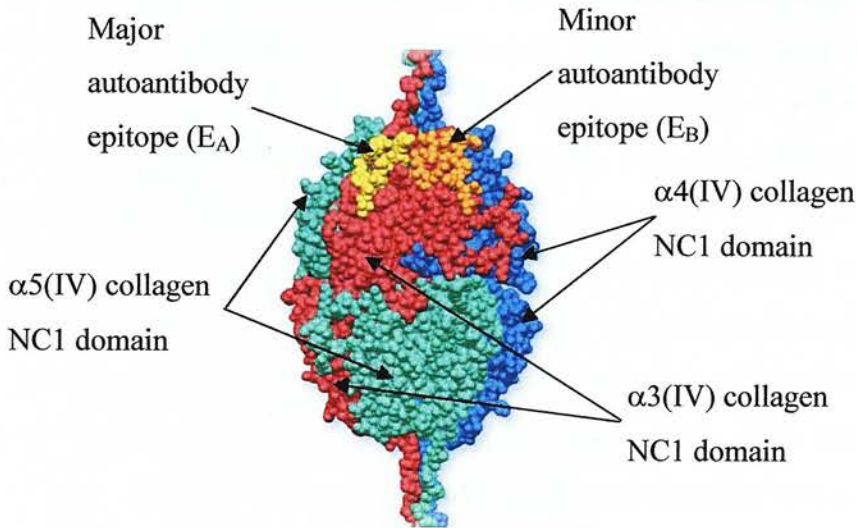
The Goodpasture antigen was initially localised to the non-collagenous domain of Type (IV) collagen (Figure 1.2) (Wieslander et al., 1984, Wieslander et al., 1987, Wieslander et al., 1985), before being finally isolated in 1988 by Hudson and co-workers who localised the antigen to the NC1 domain of the newly discovered  $\alpha 3(\text{IV})$  collagen chain (Butkowski et al., 1987, Saus et al., 1988). The human Goodpasture antigen was later cloned and confirmed to be the NC1 domain of  $\alpha 3(\text{IV})$  collagen (Turner et al., 1992).

Figure 1.2 –  $\alpha 3\text{-}\alpha 4\text{-}\alpha 5$  Type (IV) collagen protomer network



In the glomerular basement membrane each type (IV) collagen protomer is composed of  $\alpha 3$ ,  $\alpha 4$  and  $\alpha 5$  (IV) collagen chains in a trimeric association. Protomers create basement-membrane networks by uniting at their NC1 domains to form a hexameric interface, and also uniting four 7S domains at the N-terminal. The  $\alpha 3\text{-}\alpha 4\text{-}\alpha 5$  (IV) network differs from other type (IV) collagen networks due to its greater number of disulfide cross-links between the triple helical domains, which increases its resistance to proteolysis. Adapted from (Hudson et al., 2003).

The pathogenic nature of the autoantibody response in Goodpasture's Disease was demonstrated via passive transfer experiments conducted by Lerner *et al* (Lerner *et al.*, 1967). The presence and nature of these circulating antibodies was later confirmed by Wilson *et al* (Wilson and Dixon, 1973). The autoantibody response has been demonstrated to be specific to the NC1 domain of  $\alpha 3(\text{IV})$  collagen in separate laboratories (Dehan *et al.*, 1996, Derry *et al.*, 1991, Neilson *et al.*, 1993, Saus *et al.*, 1988, Turner *et al.*, 1994). Further, the antibodies appeared to have restricted specificity (Hellmark *et al.*, 1994, Meyers *et al.*, 1998). Subsequent work has endeavoured to dissect out the antibody binding epitopes, and in so doing has alluded to both the conformational and cryptic nature of these epitopes (Hellmark *et al.*, 1997, Kalluri *et al.*, 1991, Leinonen *et al.*, 1999). Initial studies were performed using linear peptide sequences and provided conflicting data on the epitopes, although there was concordance on the limited heterogeneity of the antibody response. Epitopes were postulated at both the carboxy terminal of the NC1 domain (Kalluri *et al.*, 1991, Kalluri *et al.*, 1996, Penadés *et al.*, 1995) and the amino terminal (Levy *et al.*, 1997, Levy *et al.*, 1996). Later studies used recombinant DNA technology to engineer chimeric NC1 domains using a combination of  $\alpha 1$  type IV collagen and  $\alpha 3$  type IV collagen NC1 domain sequences in order to better define the autoantibody epitopes. These later studies have resulted in a broad agreement that the major antibody epitope is at the amino terminus ( $\alpha 3_{17-31}$ ) (Hellmark *et al.*, 1999a, Hellmark *et al.*, 1999b, Netzer *et al.*, 1999, Ryan *et al.*, 1998), with a further minor epitope at the carboxy terminus ( $\alpha 3_{127-141}$ ) (Borza *et al.*, 2000, Netzer *et al.*, 1999) of the  $\alpha 3(\text{IV})$  NC1 domain. More recent work has furthered our understanding of the conformational nature of the major autoantibody epitope using site-directed mutagenesis. This has highlighted key amino acid residues within this epitope that are important to its tertiary and quaternary structure (David *et al.*, 2001, Gunnarsson *et al.*, 2000). Although the homologous nature of both the major and minor autoantibody epitopes was alluded to in earlier work (Netzer *et al.*, 1999), the significance of this has only been recently realised with the crystallographic determination of the Goodpasture antigen by Hudson and co-workers (Borza *et al.*, 2002, Sundaramoorthy *et al.*, 2002) (Figure 1.3).

**Figure 1.3 – The  $\alpha 3$ - $\alpha 4$ - $\alpha 5$  (IV) NC1 hexamer**

The three-dimensional structure and the location of epitopes were determined by computer modeling of the crystal structure of the  $\alpha 1$ - $\alpha 1$ - $\alpha 2$ (IV) NC1 hexamer and the apparent quaternary structure of the  $\alpha 3$ - $\alpha 4$ - $\alpha 5$ (IV) NC1 hexamer. The hexamer is composed of two  $\alpha 3$  monomers (red), two  $\alpha 4$  monomers (blue), and two  $\alpha 5$  monomers (green). The locations of the major EA (yellow) and minor EB (orange) regions that encompass two dominant epitopes for Goodpasture antibodies are depicted. The epitopes reside in the  $\alpha 3$ (IV) NC1 domain, near the triple helical junction, and they are partially sequestered by interactions with the  $\alpha 5$ (IV) and  $\alpha 4$ (IV) NC1 domains, respectively. Adapted from (Hudson et al., 2003)

### 3.2.2 The CD4<sup>+</sup> T cell epitope

Unlike the B cell mediated antibody response, CD4<sup>+</sup> T cells recognize their antigenic epitopes in the form of processed peptides in association with MHC Class II molecules on the surface of antigen presenting cells. Furthermore, the affinity of the immunoglobulin-like T cell receptor is a thousand-fold weaker than the typical antibody affinity for its ligand such that the binding interaction alone cannot be used to identify the T cell epitope. Two approaches have therefore been employed in order to ascertain the presence and identity of T cell epitopes within the Goodpasture antigen.

The first approach assesses the proliferative responses of T cells when incubated with antigen presenting cells that have been pulsed with  $\alpha 3(\text{IV})$  NC1. Certainly, this approach has demonstrated that T cells from patients with Goodpasture's disease specifically proliferated when incubated with either purified or recombinant  $\alpha 3(\text{IV})$  NC1 domains (Derry et al., 1995, Marelli-Berg et al., 1996). This approach has allowed the formation of some short-term  $\text{CD4}^+$  T cell lines specific for  $\alpha 3(\text{IV})$  NC1 and restricted by HLA-DR (Marelli-Berg et al., 1996). The approach has since been refined to delineate the T cell epitopes more precisely using overlapping peptides to two major areas ( $\alpha 3_{71-90}$  and  $\alpha 3_{131-150}$ ), and two minor areas ( $\alpha 3_{1-20}$  and  $\alpha 3_{31-50}$ ) (Cairns et al., 2003, Cairns et al., 1999). Two of these epitopes are close to the major ( $\alpha 3_{31-50}$ ) and minor ( $\alpha 3_{131-150}$ ) antibody epitopes. Although this provides valuable information on T cell epitopes, it does not provide information concerning the specific cell phenotypes. Therefore, significant problems still remain with this. Foremost amongst these is the relatively low frequency of antigen-specific T cells in peripheral blood such that their *in vitro* expansion may result in the expansion of apparently irrelevant T cell populations (Merkel et al., 1996), at the expense of poorly proliferating yet autoantigen-specific T cells. This latter issue was addressed to a small extent by the more recent study of Cairns *et al* that utilised cytokine analysis of the responding T cells and blocking monoclonal antibodies against MHC antigens (Cairns et al., 2003). This study confirmed that the proliferative cell response to the  $\alpha 3(\text{NC1})$  peptides was mediated by T cells restricted predominantly by HLA-DR. However, the techniques used bulk T cell cultures that are likely to have blurred important details of the responses seen.

The second approach utilized biochemical techniques to tease out which peptides from the  $\alpha 3(\text{NC1})$  domain are processed and displayed to T cells for their immune recognition. This approach has identified three groups of peptides each centred on a common core sequence and about the length of the MHC Class II peptide-binding groove ( $\alpha 3_{21-40}$ ,  $\alpha 3_{61-80}$ ,  $\alpha 3_{161-180}$ ). Interestingly, the naturally processed and presented peptide nested sets had intermediate affinity for HLA-DR15. The inference from this finding is that antigen presentation to T cells in this situation is affected more by processing constraints rather than antigen-MHC Class II



affinity (Phelps, 2000, Phelps et al., 2000, Phelps et al., 1998, Phelps et al., 1996). These findings, however, must be taken in the context of the contrived *in vitro* system from which they were found.

Despite the drawbacks of the two separate approaches, there does appear to be some agreement between them. The data from the T cell proliferation experiments show that two of the four epitopes ( $\alpha 3_{31-50}$  and  $\alpha 3_{71-90}$ ) overlap two of the naturally processed epitopes ( $\alpha 3_{21-40}$  and  $\alpha 3_{61-80}$ ). These epitopes overlap with the antibody epitopes. More recent work indicates the exquisite sensitivity of the postulated T cell epitopes to cleavage by endosomal proteases (Phelps, personal communication). This would appear to reiterate the suggestion of processing constraints affecting peptide presentation.

### 3.3 A Model Disease

Studies on autoimmunity to date have focused on experimental work using inbred animal strains, primarily mouse and rat models of various autoimmune disease processes. Few of these models are clearly defined with respect to their inciting antigen, MHC linkage or their relationship to their human counterparts, and as such dissecting out disease mechanisms becomes difficult. In contrast to this lack of clarity, Goodpasture's disease, although an uncommon clinical entity, is emerging as an archetypal autoimmune disease in many ways.

First, the auto-antigenic target has been clearly established as the  $\alpha 3(\text{NC1})$  domain of type IV collagen as indicated above. Furthermore, recombinant expression of this antigen has been established enabling more detailed dissection of the antigenic epitopes (Hudson et al., 1993a, Hudson et al., 1993b, Turner et al., 1992). This has more recently resulted in the identification of the crystallographic structure of the antigen (Sundaramoorthy et al., 2002). The unequivocal determination of an inciting antigen with such clarity is certainly uncommon amongst autoimmune conditions (Elson and Barker, 2000). Furthermore, the

relatively small size of the antigen permits for more detailed examination of the interactions between antigenic peptides and MHC Class II molecules.

Second, and in addition to the above, information is gathering as to the processing and presentation of  $\alpha 3(\text{IV})$  NC1 (Phelps et al., 1998, Phelps et al., 1996). This information is simply not available for any other autoimmune disease or experimental model. To date this information has enabled more detailed assessment of the autoimmune response in this disease setting (Cairns et al., 2003). Furthermore, such dissection of the antigen has enabled the identification of not only the antibody-binding epitopes, but has also led to the identification of the main T cell epitopes.

Third, there are distinct HLA associations (Fisher et al., 1997, Huey et al., 1993, Phelps and Rees, 1999, Rees et al., 1984). The positive association of HLA-DRB1\*1501 with Goodpasture's disease is amongst the strongest reported for autoimmune diseases. Other HLA-DRB1 alleles also appear to influence disease outcome from susceptibility (HLA-DRB1\*04) through neutrality (HLA-DRB1\*03) to protection (HLA-DRB1\*07) (Phelps and Rees, 1999). Although such an association could be related to linkage disequilibrium of an associated gene, current work would indicate that the association is directly related to the peptide-binding characteristics of the HLA molecules themselves (Phelps et al., 2000, Phelps and Rees, 1999). The limited number of alleles involved also simplifies further analysis.

Fourth, Goodpasture's disease has a consistent presentation and course across populations. It has a definite period of onset and tends to present as a severe glomerulonephritis that progresses to end-stage renal failure within weeks to months. It is usually a "one-shot" disease rather than a relapsing-remitting disease like some autoimmune conditions. Effective treatment protocols are available and activity can be monitored through an assessment of autoantibody levels (Reviewed in (Phelps and Turner, 2000, Turner and Rees, 1996)). The relatively well-defined nature of disease initiation and termination with or without therapy would allow assessment and comparison of the immune response over the entire period of disease activity and

recovery. This may well provide further information into tolerance breakdown and recovery in autoimmune diseases.

Fifth, although quite good rat models exist, murine models of Goodpasture's disease are being actively developed both within inbred strains and in HLA-DR transgenic animals (Dr Phelps, *personal communication*). Furthermore, several stable T cell clones and hybridomas which recognise human  $\alpha 3(\text{IV})\text{NC1}$ -derived peptides have been generated in Balb/c mice (Bowie *et al*, Aberdeen, unpublished) and in HLA-DR15 transgenic mice (Marley *et al*, Edinburgh, unpublished).

The detailed knowledge of both the antigen and HLA-DR association therefore provide a unique opportunity to study the cellular arm of the immune response within an autoimmune disease in man, whilst the presence of a murine disease model allows for more detailed parallel investigation. Furthermore, such detailed knowledge also provides the exceptional prospect of utilising recent innovations in T cell assessment through the use of MHC Class II tetramer technology *vide infra*.

## 4 Established Methods of T cell Assessment

### 4.1 Identifying Antigen-specific T cells

The role of the cellular arm of the immune system in general and in association with the humoral arm in autoimmune disease states is well documented (Janeway *et al*, 2001). However, a major obstacle to the study of human autoimmunity has been the difficulty of identifying the autoantigen-specific T lymphocytes that are fundamental to the initiation and perpetuation of the autoimmune response. T cells are more difficult to characterise than plasma cells due to their more diverse functionality, and the technical difficulty of studying their membrane-bound receptors as compared to secreted antibodies. As a result of these difficulties, many techniques have been developed to identify, enumerate and characterise autoantigen-specific T lymphocytes to date, however, their sensitivity,

specificity and utility have not always been ideally suited to the task in hand (Reviewed in (Hickling, 1999)). The main techniques are briefly described below. Other techniques are available for use in murine models exploiting the possibility of TCR transgenic animals through the use of specific V region monoclonal antibodies (McHeyzer-Williams and Davis, 1995) and multiparameter flow cytometry (McHeyzer-Williams et al., 1996). However, these techniques are not extendable to human studies.

## 4.2 Lymphoproliferation Assay

This assay relies upon antigen-specific T cells proliferating in response to their specific antigen. This is usually measured from the incorporation of tritiated thymidine into their DNA. PBMC's are incubated in the presence of either the test antigen or a control stimulus for 3-7 days before tritiated thymidine is added for 6-18 hours prior to assessing the amount of incorporated radiolabel. The amount of incorporated radiolabel provides a measure of DNA synthesis for the whole cell population, and needs to be compared to a similar cell population that has only been incubated in culture medium or in the presence of a control antigen. The results are usually expressed as a ratio or stimulation index.

This assay provides a good indication of T cell division in response to a test antigen, but does not necessarily reflect the complete response of the T cell population to the stimulus. Some T cells may simply respond through cytokine release without undergoing proliferation. Therefore, it does not allow for assessment of individual cell responses, and in its simplest state is neither sensitive nor quantitative enough to allow a longitudinal comparison of the numbers of antigen-specific T cells in a series of PBMC samples (Hickling, 1999).



### 4.3 Limiting-Dilution Assay

Limiting dilution analysis estimates the 'precursor frequency' of T cells with a particular specificity. Successful application of this technique requires antigen-specific precursors within the PBMC population that both respond and survive over the culture period, and a means of analysing this response through proliferation, cytokine production or cytotoxicity.

Multiple lymphoproliferation assays are prepared using an excess of specific antigen, growth factors and irradiated antigen-presenting cells, to which dilutions of the cell population under investigation are added such that the only limiting parameter is the number of antigen-specific T cells present. At least 24 replications of each dilution are set up. The cells are cultured for 10-14 days to allow differentiation and expansion. Functional assays can then be used to assess cytokine production within the culture supernatant or cytotoxicity of the expanded T cell population within each microtitre well. Assuming that 'single-hit' kinetics apply, the number of non-responding wells follows a Poisson distribution, and from this statistical approaches can be used to calculate the precursor cell frequency.

The assay is not only critically dependent upon cell survival *in vitro* and a detectable functional end-point, it is critically dependent on a clear distinction between 'positive' and 'negative' wells. The definition of a 'positive' well may involve defining a threshold, and in so doing the estimate of precursor frequency can be greatly affected by even the slightest alteration of this subjective threshold. Although there have been developments of this technique, the overall drawbacks remain unchanged. Furthermore, the assay does not provide a measure of the effector function of the responding cells, and serves only to give an indication of T cell responsiveness (Ford and Burger, 1983). This has been recognized recently in the comparison of this technique to that of MHC tetramers, with the latter demonstrating the functionally diverse nature of the polyclonal response to a single antigen (Lim et al., 2000).

Despite these drawbacks, much has been gleaned using this technique as regards T cell frequency and effector type in the setting of autoimmune disease in general (Zhang et al., 1994), and specifically in the context of Goodpasture's Disease (Lightstone et al., 2001, Salama et al., 1999, Salama et al., 2001). Salama *et al* found increased frequencies of CD4<sup>+</sup> T cells reactive with  $\alpha$ 3(IV) NC1 during acute Goodpasture's Disease (ranging from 1:6300 to 1:65000), with the numbers decreasing during recovery (Salama et al., 2001).

#### 4.4 ELISPOT Assay

The ELISPOT assay is an adaptation of the antigen-capture ELISA technique into a more sensitive method for measuring the responses of T cell populations to their cognate antigen. The assay detects the production of cytokines by activated antigen-specific T cells that have been incubated *in vitro* with the antigen of interest. The PBMC population of interest is incubated with the antigen of interest for 18-36 hours before adding the cells to microtitre wells that have been pre-coated with an anti-cytokine antibody. If an activated T cell is secreting the cytokine of interest it will be captured by the coating antibody. Once the cells are removed from the wells a second antibody to the cytokine that is enzyme labelled can be added to reveal the presence of cytokine-producing cells by the visualised 'spots' in the wells (Hickling, 1999, Tough and Sprent, 1998).

This assay is 20-100 fold more sensitive than the LDA in measuring the frequency of specific T cells (Murali-Krishna et al., 1998, Tough and Sprent, 1998). The disadvantages of this technique include the need for manual enumeration of the spots so adding subjectiveness to the process, the requirement for at least a period of *in vitro* incubation, and the difficulty of determining whether individual cells are capable of secreting mixtures of cytokines as has been postulated (Abbas et al., 1996, Kelso, 1995).

## 4.5 Intracellular Cytokine Analysis

Flow cytometry techniques have been developed to allow the analysis of intracellular cytokines to assess the frequency and phenotype of antigen-specific T cell populations. This technique allows for the simultaneous analysis of multiple cytokines at the level of a single T cell (Waldrop et al., 1997), although the cells require permeabilisation. The cells of interest are stimulated for about 5 hours with the antigen of interest in the presence of an inhibitor of intracellular protein transport (eg brefeldin A) to promote the intracellular accumulation of cytokines. The cells are then fixed and permeabilised before being stained for the presence of the cytokines of interest using directly conjugated anti-cytokine monoclonal antibodies.

The technique allows for the analysis of large numbers of T cells in a short period of time as well as enabling better phenotypic assessment of individual T cells within the stimulated T cell population. Like the ELISPOT assay, this technique is not reliant upon cell proliferation and the minimal stimulation times improve assay sensitivity. The major disadvantages, however, are that the T cells have to be killed and permeabilised in order to detect them, and that the antigenic specificity of individual T cells cannot be assessed.

## 4.6 Cell Surface Affinity Matrix Assay

This technique was developed as a refinement of the above in order to allow for the analysis and sorting of live cells according to the molecules secreted. In essence an artificial matrix specific to the cytokine of interest is created on the cell surface using bi-specific antibodies prior to the cells being activated with the antigen of interest for a defined period of time. The secreted cytokines bind to the matrix and are subsequently labelled with specific fluorescent or magnetic reagents to allow for cytometric analysis and sorting of the live cells. In order to prevent diffusion of the selected cytokine away from the secreting cell, the growth medium is made more viscose during the stimulation period (Manz et al., 1995).

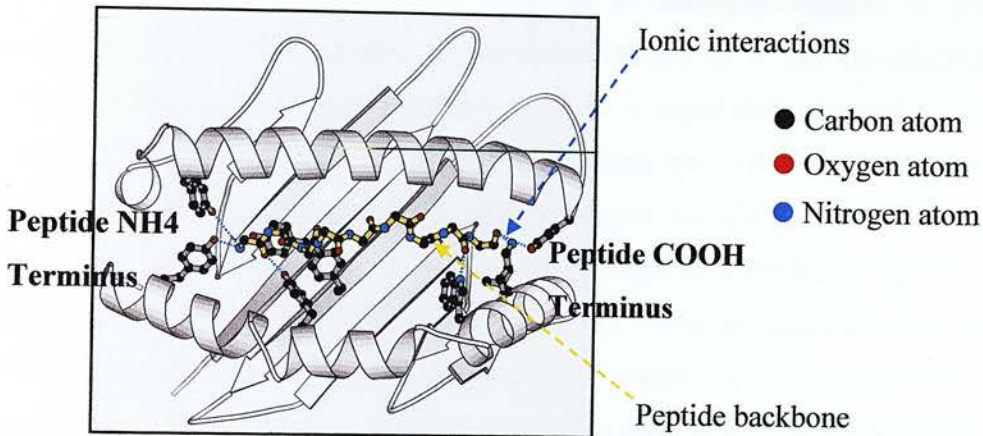
Although a sensitive technique that allows for the isolation of live T cells, one of the main drawbacks is that the affinity matrix is specific to only one cytokine. Nevertheless, it has been successfully used to isolate functionally active antigen-specific CD8<sup>+</sup> T cells (Oelke et al., 2000).

## 5 Major Histocompatibility Complex Multimers

### 5.1 The T Cell Receptor Ligand

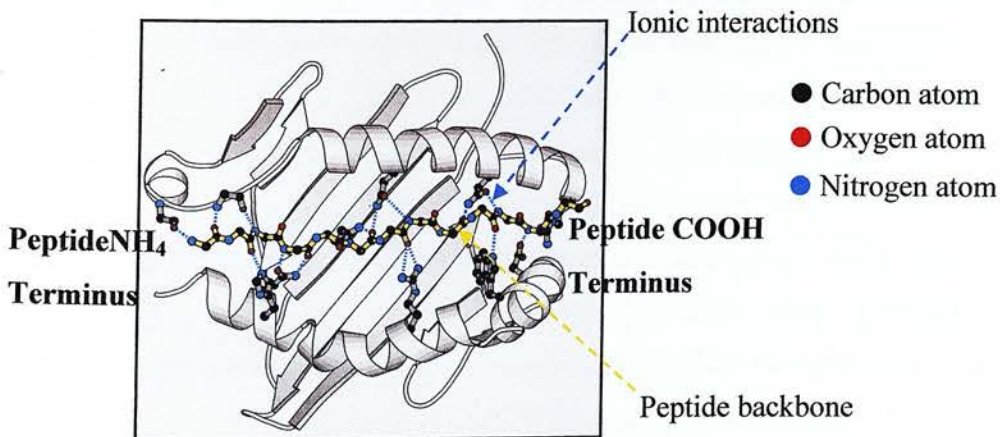
Over the last decade the crystal structures of TCRs and TCR-ligand complexes have been elucidated (Reinherz et al., 1999). In contrast to immunoglobulins, T cells only recognise their cognate antigens on cell surfaces in association with self-MHC molecules. Furthermore, the cognate antigen is a small peptide derived from the processing of the whole antigen, varying in length from 8-10 amino acids (MHC Class I – CD8<sup>+</sup> T cell interaction) (Falk et al., 1991, Hunt et al., 1992, VanBleek and Nathenson, 1990) to 13-17 amino acids (MHC Class II – CD4<sup>+</sup> T cell interaction) (Chicz et al., 1993, Chicz et al., 1992, Rudensky et al., 1992, Rudensky et al., 1991). The peptide antigen is held within a defined peptide-binding groove formed by the MHC molecule (Buus et al., 1987), with the nature of the groove differing between MHC Class I (Figure 1.4) and Class II (Figure 1.5) molecules (Gauthier et al., 1998, Smith et al., 1998, Stern et al., 1994). The assessment of TCR-ligand interactions has been difficult not only due to the membrane-bound nature of the primary molecules but also due to their very low affinity which has required technological innovations for its assessment (Reviewed in (Davis et al., 1998)).

Figure 1.4 – MHC I peptide binding groove



Peptides are bound to the MHC class I molecules by their ends. At the amino terminus a cluster of tyrosine residues common to all MHC class I molecules form hydrogen bonds with the bound peptide, while a second cluster of residues form hydrogen bonds and ionic interactions with the carboxy terminus of the bound peptide (Janeway et al., 2001).

Figure 1.5 – MHC II peptide binding groove



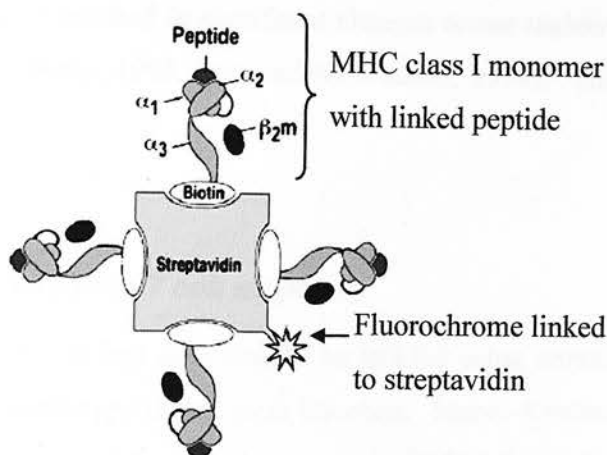
Peptides are bound to MHC class II molecules by a series of hydrogen bond interactions along the length of the binding groove that is open at both ends. At the amino terminus the hydrogen bonds are made with the MHC class II polypeptide backbone, whereas over the length of the peptide interactions are with the side chains of highly conserved amino acid residues (Janeway et al., 2001).



One of the major problems with previously established techniques for tracking antigen-specific T cells is their use of surrogate markers of antigen specificity and/or their reliance on functional assays of T cell proliferation or cytokine secretion that may therefore result in a significant underestimation of antigen-specific T cell numbers. Moreover, by their nature these techniques would be unable to provide clear phenotypic data on antigen-specific T cells. Unlike the B cell compartment where ligand binding can be used to specifically track B cells (Hayakawa et al., 1987, McHeyzer-Williams et al., 1991), the inherently low affinity of the bipartite T cell ligand has hampered this as a tracking technique (Davis et al., 1998, Matsui et al., 1991). Therefore, in order to utilise the TCR-ligand interaction as a tracking technique one must have information regarding both the TCR-MHC restriction as well as knowledge of the bound antigenic peptides related to the specific MHC restriction.

## 5.2 Development of MHC Class I Multimers

Altman *et al* have developed a technique to circumvent the fast dissociation rate of monomeric soluble peptide-MHC complexes from their T cell ligand (Altman et al., 1996). Soluble peptide-MHC complexes were formed into multimeric units enabling more than one TCR per antigen-specific T cell to be bound, slowing their inherently fast dissociation rate and increasing the avidity of the complex through this simultaneous and serial engagement process (Matsui et al., 1994). By linking these multimeric complexes to a fluorochrome they could be used as an immunological stain (Figure 1.6). This approach involved the production of soluble HLA-A2 alpha chains (Garboczi et al., 1992) that had been modified at the COOH-terminus by the addition a 15-amino acid substrate peptide for BirA-dependent biotinylation (BSP) (Schatz, 1993). The alpha chains were produced in *E.coli* as inclusion bodies and refolded in the presence of  $\beta_2$ -microglobulin and the specific antigenic peptide prior to purification and biotinylation. The COOH-terminus biotinylation served to both correctly orientate the refolded monomers and tetramerise them by binding to phycoerthyrin-labeled avidin in a 4:1 molar ratio.

**Figure 1.6 – MHC Class I tetramer**

A schematic adapted from (Hugues et al., 2002) illustrating four MHC Class I units each with a linked peptide covalently bound to fluorochrome-labelled streptavidin. This illustrates the archetype MHC Class I tetramer.

Using this strategy and refolding with two different HLA-A2-restricted HIV epitopes – Gag (77-85) and reverse transcriptase Pol (309-317) – the investigators were not only able to specifically stain HLA-A2-restricted HIV-specific CTL lines and clones, but were also able to demonstrate the antigen-specific functionality of the stained cells by using cytotoxicity assays. The reagents were also able to identify antigen-specific CD8<sup>+</sup> T cells from an HLA-A0201<sup>+</sup> HIV-seropositive donor's peripheral blood mononuclear cells using flow cytometry. The specificity of the isolated cells was confirmed using peptide-dependent cytotoxicity. The frequency of antigen-specific T cells identified using these reagents was seen to be in keeping with estimates from TCR cDNA libraries and 10- to 50-fold greater than frequencies previously obtained using LDA. The utility of this methodology was further demonstrated by using it to phenotype the antigen-specific CD8<sup>+</sup> T cells isolated (Altman et al., 1996).

This technique has revolutionised the study of complex antigen-specific CD8<sup>+</sup> T cell populations. The approach, including monomer formation in *E.coli*, has

now become a standard technique for tracking and analysing antigen-specific CD8<sup>+</sup> T cells and has resulted in significant changes to our understanding of CD8<sup>+</sup> T cell dynamics (Doherty, 1998, Ogg and McMichael, 1998). These are outlined briefly below:

### 5.2.1 *The anti-viral T cell response*

One of the first questions to be tackled using tetramers was that of T cell number and phenotype during viral infection. Murali-Krishna *et al* (Murali-Krishna *et al.*, 1998) assessed the T cell response in C57BL/6 and BALB/c mice during the course of a primary infection by the lymphocytic choriomeningitis virus (LCMV). This group found the size of the specific viral response to be higher than previously demonstrated using LDA. 23% of CD8<sup>+</sup> T cells in C57BL/6 mice and 56% of CD8<sup>+</sup> T cells in BALB/c mice were found to be specific to the single LCMV epitope tested using MHC class I tetramers, and were also noted to be functional using an IFN $\gamma$  ELISPOT assay. Therefore, the suggestion from this is that the T cell proliferation seen with viral infections is primarily antigen-specific, rather than bystander activation. Moreover, in following the course of the immune response, it was found that only approximately 5% of the activated CD8<sup>+</sup> T cells entered into the memory pool, with the size of this pool being dependent on the initial response burst size. This finding of antigen-specific expansion rather than bystander activation was also found in humans in the context of Epstein-Barr virus (EBV) infection (Callan *et al.*, 1998).

Extending their initial development of MHC class I tetramers, Ogg *et al* (Ogg *et al.*, 1998) used HLA-A\*0201 tetramers loaded with either HIV Gag (77-85) or HIV Pol (476-484) to assess the correlation between HIV-specific CTL activity and plasma RNA viral load. Using two-colour FACS staining they were able to detect tetramer-positive cells at levels as low as 0.02% of CD8<sup>+</sup> T cells, finding a significant positive correlation between tetramer staining and fresh cytotoxicity using <sup>51</sup>Cr-release cytotoxic assay. They were also able to show an inverse association between HLA-A\*0201-restricted HIV-specific effector CTLs and plasma viral RNA



load. Gray *et al* {Gray, 1999 #65} independently confirmed the frequency of HIV-specific CD8<sup>+</sup> T cells, although their findings showed that the tetramer-positive cells were primarily of memory rather than effector phenotype. Moreover, they showed that anti-retroviral therapy reduces both viral RNA load and activated HIV-specific CTLs, suggesting that without consistent stimulation antigen-specific CTLs disappear.

The pattern of immune response has also been followed during bacterial infection. Using the model of *Listeria monocytogenes* infection of BALB/c mice Busch *et al* (Busch *et al.*, 1998) were able to demonstrate synchronous changes in *L.monocytogenes*-specific CTL populations differing in epitope specificity.

### 5.2.2 Evolution of the T cell response

Further studies using *L.monocytogenes* epitope loaded MHC class I tetramers revealed that activated effector CTL proliferation could occur in the absence of the specific antigen, but that memory CTL generation required antigen presentation. Moreover, the memory response is established before the completion of the primary T cell response (Busch *et al.*, 2000). The maturation of the CTL memory response was also assessed using a novel approach based on MHC class I tetramer association and dissociation rates in the context of an *L.monocytogenes* epitope. This technique showed an increase in overall T cell affinity for antigen as the memory T cells expanded to form recall effector T cells (Busch and Pamer, 1999). The idea of clonal maturation of the immune response is supported independently by a study using multiparameter flow cytometry (McHeyzer-Williams *et al.*, 1996).

Similar work on CD8<sup>+</sup> T cell populations was also carried out using the LCMV model that revealed the stochastic nature of the memory T cell pool (Blattman *et al.*, 2000). This latter group did not, however, find the same affinity maturation in the T cell response as noted above.

### 5.2.3 Characterization of auto-antigen specific T cells

MHC class I tetramers have also been used to characterize the TCR affinity to a potential auto-antigenic peptide over the course of development of overt diabetes in NOD mice (Amrani et al., 2000). This group found an outgrowth of T cells expressing higher avidity TCRs as the disease progressed, with the TCR reactivity becoming more focused in terms of epitope recognition.

Taking this one stage further, self-specific T cells have been traced using MHC class I tetramer technology in the context of a transgenic mouse with an oligoclonal self-specific T cell population (Visser et al., 2000). In this model, C57BL/10 mice express influenza nucleoprotein (NP) fragment 328-498 under the control of the H-2K promoter resulting in negative selection of T cells expressing a transgenic TCR specific for NP<sub>366-374</sub>. Despite this selection, T cells with TCRs having a low avidity for NP<sub>366-374</sub> were found using murine MHC class I (D<sup>b</sup>) tetramers loaded with NP<sub>366-374</sub>. This indicates that, at least in this model, low avidity T cells can escape negative selection mechanisms, and that tetramer technology can be used to identify these self-reactive T cells.

### 5.2.4 Sensitivity and specificity of peptide-MHC class I tetramers

Although the specificity of this technique was assessed in each of the studies above, Burrows *et al* (Burrows et al., 2000b) further investigated the fine specificity of the approach. The group used a panel of EBV responsive CTL clones and a panel of HLA-B8 tetramers loaded with either the relevant EBV epitope or single amino acid variants of this. The study clearly demonstrated the ability of the tetramers to stain specific clones with an intensity that correlated with the peptide activity in cytotoxicity assays irrespective of the tetramer staining temperature. Moreover, tetramer staining of fresh PBMCs was just as specific as T cell clones. One interesting point found in this study was that a peptide-MHC complex that binds an antigen-specific T cell might be a null ligand for the T cell, and as such fail to induce a productive signal (agonist or antagonist). The findings were replicated in a different system, although in this instance null ligands did not bind to antigen-

specific T cells (Buslepp *et al.*, 2001). Broadly speaking these studies suggest that peptide-MHC tetramer staining correlates with the functional avidity of CTL clones. A study by Derby *et al* (Derby *et al.*, 2001) would add a cautionary note to this broad statement, as they found that two intermediate-avidity clones showed an inverse relationship with tetramer staining that was not entirely accounted for by compensating for TCR levels. Once again, the staining temperature did not affect the final outcome. A study by Echchakir *et al* also found a lack of correlation (Echchakir *et al.*, 2002). Therefore, the correlation with functional avidity may not be as direct as initially suggested, rather the association may be related to tetramer binding stability (Dutoit *et al.*, 2002).

MHC class I tetramers have also been used to select CD8<sup>+</sup> T cells for cloning. Dunbar *et al* (Dunbar *et al.*, 1998) used HLA-A2 tetramers loaded with influenza matrix protein peptide 58-66 to identify and phenotype reactive CD8<sup>+</sup> T cells from PBMCs of HLA-A2<sup>+</sup> individuals. They were able to identify antigen-specific T cells at levels as low as 1 in 58,000 PBMCs, and were also able to phenotype and clone these cells. Lim *et al* (Lim *et al.*, 2000) used HLA-A2 loaded with HTLV-I Tax11-19 peptide to isolate Tax 11-19-reactive T cells from PBMCs of an HLA-A\*0201-expressing patient with HTLV-I-associated myelopathy. Of the 25 tetramer binding CTL clones tested 17 different clonal populations were identified by determination of TCR V $\beta$ -chain usage. The cytotoxic effector function of the 9 clones tested was found to be nearly identical, in broad agreement with the suggestion that tetramer staining correlates with CTL functional avidity. Despite their similarities in cytotoxicity assays, these clones were qualitatively different in terms of proliferation and cytokine production, highlighting the benefits of this technology at better delineating T cell phenotype.

The findings above highlight one of the advantages of this T cell assay technique in being independent of T cell survival, expansion or effector function. One caveat to this advantage, however, was raised by a study of plasma membrane lipid-rafts and TCR arrangement on CD8<sup>+</sup> T cells (DrakeIII and Braciale, 2001). This study found that disruption of plasma membrane lipid organisation resulted in a loss of tetramer binding without altering TCR levels, and further indicated that there

is a transition to tetramer binding upon activation of antigen-specific CTLs. This finding would, therefore, suggest that the technique might not be able to identify naïve-resting CTLs. Further work independently confirmed this notion, showing differences between the binding of dimeric peptide-MHC complexes to naïve and activated CD8<sup>+</sup> T cells at low concentrations of dimeric peptide-MHC complex (Fahmy et al., 2001). This latter group also highlighted the role of lipid rafts in TCR rearrangement, and showed that the addition of cholesterol to naïve CD8<sup>+</sup> T cells enhanced their avidity for the dimeric peptide-MHC complexes at low concentrations of complex.

The studies performed with MHC class I tetramers have all used a double-labelling approach with anti-CD8 antibodies. The possibility of such antibodies blocking tetramer interaction has been raised indicating that CD8 may play a critical role in the initial interaction between peptide-MHC class I tetramers and their cognate TCR ligand (Denkberg et al., 2001). This highlights the importance of sequential staining with tetramer complex prior to anti-CD8 antibody.

The tetramer approach has also been used to stain CD8<sup>+</sup> T cells in both frozen and lightly fixed tissue sections, extending the method to archival specimens. The technique required amplification of the tetramer stain by using rabbit anti-FITC antibodies and Cy3-conjugated goat anti-rabbit antibodies. Moreover, the blocking effect of some anti-CD8 antibodies on tetramer staining was again found (Skinner et al., 2000).

### **5.2.5 Therapeutic potential**

With the potential to isolate antigen-specific CTLs, the therapeutic potential of MHC class I tetramers has also been keenly investigated (Reviewed in (Xu and Screaton, 2002)). The primary approach has investigated the utility of using this technology to identify antigen-specific CTLs in order to adoptively transfer them for therapeutic purposes. The second approach has investigated the use of antigen-MHC Class I tetramers as a form of antigen-specific immunotherapy.

Yee *et al* (Yee et al., 1999) formed an array of CTL clones from human HLA-A2 donor PBMCs reactive with one of two human melanoma antigens, MART-1 and gp100. Having formed these clones HLA-A2 tetramers were loaded with one of two epitopes from these antigens and used to identify high and low avidity T cell subpopulations from both the T cell clones and heterogeneous cultures of bulk stimulated CTLs. They concluded that it would be possible to isolate tumour-reactive CTLs for adoptive therapy. Of interest to the above discussion, Echchakir *et al* (Echchakir et al., 2002) used HLA-A2 tetramers loaded with a mutated  $\alpha$ -actinin-4 peptide (an antigenic peptide isolated from non-small cell lung cancer) to show a higher functional avidity of tumour-infiltrating CTLs compared to those isolated from PBMCs. The suggestion of selective *in situ* expansion of functionally higher avidity anti-tumour CTLs may have a bearing on such immunotherapy.

Another group has taken a further step towards peptide-specific immunotherapy by targeting tumour lysis using MHC class I tetramers (Robert et al., 2000). Specific anti-tumour marker monoclonal antibody Fab fragments were chemically coupled to the streptavidin molecules that were used to tetramerise biotinylated HLA-A2-influenza matrix peptide monomers. These conjugates were able to specifically bind cell lines expressing the relevant tumour antigen (*e.g.* CEA) and were specifically lysed by influenza matrix peptide-specific CTLs. Although an entirely *in vitro* experiment, targeting of tumour cells using similar techniques is feasible if a similar but smaller conjugate could be constructed to improve *in vivo* targeting.

A different approach to anti-tumour therapy would be to isolate and generate peptide-specific alloreactive T cells against a synthetic peptide bound to nonself-MHC molecules. The sensitivity of the tetramer approach in identifying such allorestricted T cells from a population of alloreactive T cells was demonstrated by Moris *et al* (Moris et al., 2001). This group suggested that such an approach could be also be used to generate donor allorestricted CTLs specific for a leukaemia tumour antigen to enhance graft-vs-leukemia reaction at the time of allogeneic bone marrow transplantation.

Maile *et al* (Maile *et al.*, 2001) investigated the possibility of immune response modulation using MHC class I tetramers as direct immune modulators. Using H-2D<sup>b</sup> tetramers loaded with HY peptide (male antigen), they were able to identify male-antigen-reactive CTLs in two sets of female mice (wild-type C57BL/6 and HYTCR transgenic mice). Moreover, they noted that although a single dose of the tetramer resulted in priming of the T cell response to male skin grafts, repeated intraperitoneal doses of the peptide-loaded tetramer resulted in reduced T cell responsiveness to male skin grafts. This was noted to be associated with reduced levels of CD8, and may well be due to activation-induced cell death of the more responsive CTLs. This work not only raised the possibility of antigen-specific immunotherapy, but also highlighted the utility of the tetramer approach in identifying antigen-specific T cells in naïve animals.

### **5.2.6 Utility of the tetramer approach**

From the above discussion it can be seen that this new approach has seen a revolution in our understanding of the CTL response. The technique is exquisitely specific and sensitive, detecting antigen-specific CD8<sup>+</sup> T cells down to a level of 0.02% (Dunbar *et al.*, 1998), although it may not be as sensitive as initially thought in identifying naïve antigen-specific T cells (DrakeIII and Braciale, 2001). However, the approach has enabled improved CTL cloning and has been shown to provide a possible alternative approach to assessing TCR functional avidity (Dutoit *et al.*, 2002, Lim *et al.*, 2000). The door has also been opened to peptide-specific immunotherapy. The discrepancies with the well established LDA reveal that the latter is able to detect only those T cells with long term growth potential, rather than the true antigen-reactive pool (Kuroda *et al.*, 1998, McMichael and O'Callaghan, 1998). Moreover, there is no evidence that this tetrameric approach overestimates the number of antigen-specific T cells (McMichael and Kelleher, 1999).

Although this technique is able to detect antigen-specific T cells independent of survival, expansion or effector function, its one major drawback is that the antigenic epitope must be known in the context of a particular MHC class I. Thus,



the reagents must be custom made for each individual TCR ligand specificity. However, the success of this new technique is highlighted by the establishment of a tetramer synthesis facility by the National Institute of Health in the United States (<http://www.niaid.nih.gov/reposit/tetramer/index.html>). This facility not only provides for custom synthesis of MHC class I tetramers, but also offers information on tetramer synthesis and staining protocols (Dunbar and Ogg, 2002).

### 5.3 Development of MHC class II Multimers

The development of MHC class I multimers offered the potential for enormous advances in other research areas involving not only MHC class II-restricted CD4<sup>+</sup> T cells, but also NK cells and glycolipid-specific T cells restricted by CD1 isoforms (Dunbar and Ogg, 2002). However, these other avenues have required the development of new techniques to form the monomeric building blocks of the final functional oligomers. Indeed, the inertia experienced in developing MHC class II oligomers led to the convening of a workshop at the US National Institute of Allergy and Infectious Diseases in September 2002 to address the problems faced. The consensus reached was that whereas many pMHC class II tetramers have been proven to be effective, why others have been less than useful remains “an inexact science” (Hackett and Sharma, 2002).

Fundamental differences between MHC class I and class II molecules have certainly hindered the engineering of stable MHC class II protein constructs (McMichael and Kelleher, 1999). One of the most fundamental differences is the essentially monomeric nature of the MHC class I peptide binding groove, with the single MHC class I heavy chain being stable in solution complexed with its essentially invariant light chain,  $\beta$ 2-microglobulin. In stark contrast, the MHC class II peptide-binding groove is formed by two heterodimeric heavy chains that tend to dissociate if not associated with a cell membrane or high-affinity peptide. Moreover, whereas the MHC class I peptide-binding groove is enclosed so limiting the size and position of bound peptides, the MHC class II peptide-binding groove is open-ended



so accommodating peptides of considerably different lengths (Chicz et al., 1992, Rudensky et al., 1992). The peptides bound to MHC class II can, therefore, bind in two or more frames making the definition of a peptide-binding motif a unique challenge to MHC class II (Buus, 1999, Chiciz et al., 1993, Godkin et al., 2001, Kasson et al., 2000). Although many of these differences and their associated problems can and have been overcome, the remaining issues in this field have hindered further development. These issues include circulating CD4<sup>+</sup> T cell frequency, TCR avidity, T cell activation state and staining properties (Cameron et al., 2001, Kwok et al., 2002).

### **5.3.1 The generation of peptide-MHC class II complexes**

One of the first hurdles in the formation of MHC class II oligomers is the formation of the monomeric subunits. Initially soluble MHC class II proteins were prepared by proteolytic cleavage of the extracellular domains from B cell lines (Gorga et al., 1987). However, the complexes purified had a high degree of endogenous peptide occupancy making homogenous loading with a defined peptide difficult (Dornmair and McConnell, 1990). Such MHC class II proteins would also require further modification to enable their oligomerisation. Two alternative techniques for the consistent production of homogenous MHC class II proteins were developed: expression of MHC class II subunits in *E.coli* followed by *in vitro* refolding, and secretion of soluble folded MHC class II protein from insect cells.

The bacterial expression system has had limited success, with several human and murine MHC class II proteins being produced, but has been hampered by the intrinsic structural instability of soluble MHC class II proteins. The murine MHC class II protein I-E<sup>k</sup> was one of the first to be produced using this expression system. The basic technique involves the separate formation of the  $\alpha$  and  $\beta$  chains within bacterial inclusion bodies followed by purification of the separate chains. The purified chains are then refolded by rapid dilution into a refolding buffer with or without the antigenic peptide of interest. The proteins formed were demonstrated to be conformationally correct and able to stimulate antigen-specific T-cells,

demonstrating that glycosylation was not necessary for these properties (Altman et al., 1993). The I-E<sup>k</sup> proteins formed by this group have since been used in the formation of tetramers by the addition of a BSP at the carboxy-terminal of the truncated I-E<sup>k</sup>α chain allowing tetramerisation through the avidin-biotin interaction (Gütgemann et al., 1998). The bacterial expression system has been used to form only a few other MHC class II proteins to date, namely HLA-DR1 (Frayser et al., 1999), HLA-DR2 (Arimilli et al., 1995, Nag et al., 1994, Nag et al., 1996), and HLA-DR5 (Stöckel et al., 1997, Stöckel et al., 1994). Of these, only HLA-DR1 has been used in the formation of oligomers (Cameron et al., 2001, Cochran et al., 2000). One of the main drawbacks of this technique is the need for *in vitro* refolding of the subunits that requires optimisation for each MHC class II protein expressed. This optimisation is highlighted by the finding that the design of a linker peptide between an antigenic peptide and the amino terminus of the β chain can significantly affect the yield and stability of an expressed MHC class II protein (Cunliffe et al., 2002, Wyer et al., 2001). This has meant that although the principles of this expression system could be applicable to other MHC class II proteins, difficulties have been encountered in their expression and/or refolding (Frayser et al., 1999). This variation in refolding is in contrast to the relatively standardised production of MHC class I proteins using the same expression system.

In order to overcome the *in vitro* refolding problems inherent in the bacterial expression system, insect cell expression systems have been used with a greater degree of success by several research groups, yielding several recombinant MHC class II proteins. The expression systems used have been based on either a baculovirus vector or a metallothionein-inducible *Drosophila* vector. Both systems lead to the production of soluble, correctly folded MHC class II subunits which are variably associated with or without peptide, depending upon the exact expression system used. The added benefit of insect expression is that it leads to a degree of glycosylation (Stern and Wiley, 1992), although this is unlikely to replicate the naturally expressed protein.

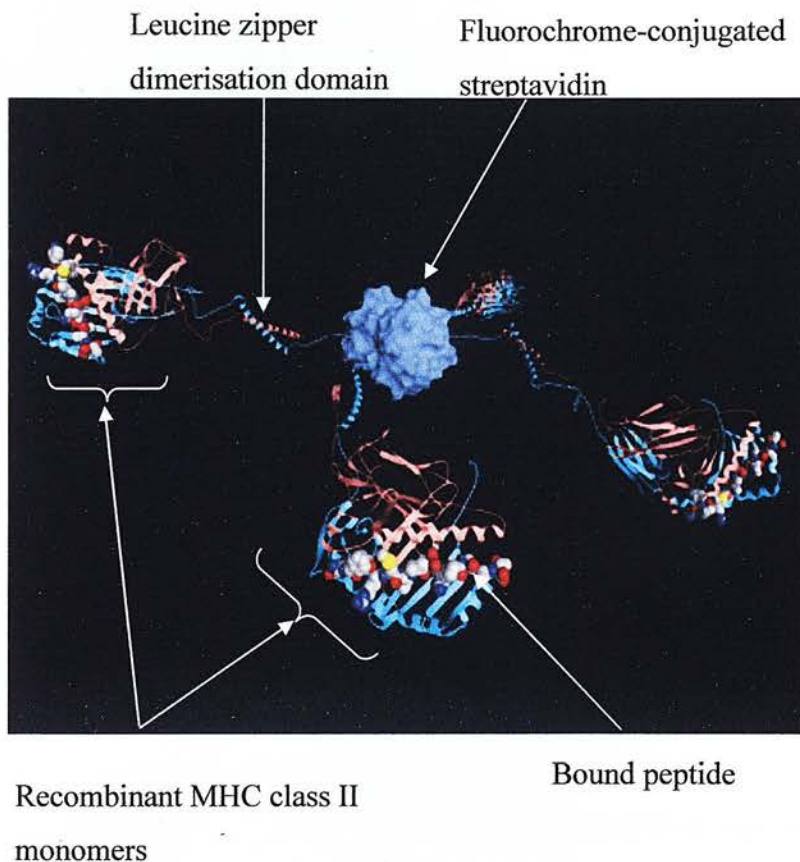
The baculovirus system was the first to be utilised. Soluble HLA-DR1 extracellular domains were expressed using baculovirus vectors containing the separate  $\alpha$  and  $\beta$  chains co-transfected into Sf9 cells. The HLA-DR1 protein was secreted into the growth medium and was found to be conformationally correct using a variety of biophysical methods, including peptide binding which was also seen to stabilise the HLA-DR1 protein (Stern and Wiley, 1992). The HLA-DR1 protein was also noted to be essentially empty of endogenous peptides allowing the generation of homogenous peptide/MHC complexes by the addition of the appropriate peptide (Stern et al., 1994). In an attempt to improve the yield, stability, and homogeneity of expressed MHC class II proteins Kozono *et al* (Kozono et al., 1994) engineered a flexible peptide linker onto the amino terminus of the  $\beta$  chain of I-E<sup>k</sup> and I-A<sup>d</sup> murine class II proteins. This linker enabled the covalent attachment of various peptides to the class II proteins in a manner that allowed their uniform occupation of the class II peptide-binding groove to which they were linked. This linker was noted not to significantly affect T cell recognition (Fremont et al., 1996, Kozono et al., 1994). This development acted as the spring board for a series of MHC class II proteins with linked peptides including I-A<sup>d</sup> and I-E<sup>k</sup> (Crawford et al., 1998), I-A<sup>b</sup> (Rees et al., 1999), I-A<sup>g7</sup> (Liu et al., 2000), and HLA-DR4 (Kotzin et al., 2000, Meyer et al., 2000). All of these MHC class II proteins have been used to form tetramers through the engineering of a site-specific biotinylation sequence at the carboxy terminus of the  $\beta$  chain.

Earlier work had indicated the importance of the transmembrane domain to heterodimeric chain pairing (Cosson and Bonifacino, 1992), and so attempts were made to improve heterodimeric chain pairing and thus the stability and solubility of the heterodimeric complex by the addition of leucine zipper dimerisation domains to the carboxy termini of the extracellular  $\alpha$  and  $\beta$  chains (O'Shea et al., 1993). These dimerisation domains have either been adapted from the Fos - Jun transcription factors in the case of HLA-DR15 (Gauthier et al., 1998, Smith et al., 1998), HLA-DQ2 (Quarsten et al., 2001) and I-A<sup>g7</sup> (Latek et al., 2000), or engineered acid – base leucine zipper motifs (Chang et al., 1994, O'Shea et al., 1993) in the case of I-A<sup>u</sup> (Anderton et al., 2001, Radu et al., 2000, Radu et al., 1998).

Many researchers have, however, found the erratic virus production step required in the baculovirus system too labour-intensive. Protein expression using stably transfected *Drosophila melanogaster* S2 Schneider cells has been found to provide equivalent protein yield with much less effort (Bunch et al., 1988, Cameron et al., 2002, Ivey-Hoyle, 1991). This system was initially used to produce soluble empty I-E<sup>d</sup> by co-transfection of S2 cells with separate  $\alpha$  and  $\beta$  chain constructs in the expression vector pRmHa3. The I-E<sup>d</sup> expressed in this system was free of bound endogenous peptides, and up to 90% of the purified I-E<sup>d</sup> could be homogeneously loaded with peptide resulting in functionally active pMHC complexes (Wallny et al., 1995). However, it became apparent that not all MHC class II proteins could be formed as easily using this system due to a failure of assembly of certain MHC class II proteins and/or their tendency to aggregate despite the presence of a peptide ligand. Leucine zipper motifs were used to improve this system. Using the Fos – Jun leucine zipper domains, HLA-DR15 was initially expressed empty in the yeast *Pichia pastoris* (Kalandadze et al., 1996) before being expressed in S2 cells using the vector pRmHa3 with the MBP peptide 85-99 being covalently attached to the amino terminus of the  $\beta$  chain by a linker peptide (Appel et al., 2000). This system has recently been used to produce both HLA-DR2 and HLA-DR7 tetramers with a series of covalently linked peptide ligands (Yang et al., 2002). Concurrently, acid-base leucine zipper dimerisation domains have been used in the expression of soluble empty I-A<sup>d</sup> (Scott et al., 1996), as well as I-A<sup>d</sup> covalently linked via the  $\beta$  chain amino terminus to an ovalbumin peptide (Scott et al., 1998). With the success of this modification, the group lead by William Kwok have successfully produced non-peptide loaded tetramers of HLA-DQ6 (Kwok et al., 2000, Reichstetter et al., 2000) and HLA-DR4 (Buckner et al., 2002, Gebe et al., 2001, Novak et al., 2001a, Novak et al., 1999, Novak et al., 2001b). The tetramers formed were based on the MHC class II heterodimer containing a BSP at the carboxy terminus of the  $\beta$  chain resulting in the addition of a single biotin to each MHC class II monomer before tetramerisation using avidin (Figure 1.7). The formation of such soluble, yet empty, heterodimers opens the way for loading a variety of peptide ligands to the expressed

MHC class II proteins without the added effort of genetically engineering individual linked peptides.

**Figure 1.7 – Leucine zipper associated MHC Class II tetramer**



Molecular model of the complete MHC class II tetramer taken from (Nepom et al., 2002). Streptavidin (in blue) anchors the long, flexible linker arms that contain the leucine zipper dimerisation domains. These linker arms form the anchors for the MHC class II units that are recognized by the antigen-specific T cell receptor.

### 5.3.2 Novel MHC class II oligomer systems

Despite the success of the “classical” tetramer design based upon the avidin biotin interaction (Figure 1.8), several groups have designed other strategies to produce multivalent peptide/MHC complexes (reviewed in (Hugues et al., 2002)). Indeed, some have suggested that the rigidity of the avidin-biotin scaffold in



“standard” tetramers may impede the optimal interaction of these with TCRs (Casares et al., 2001a).

**Figure 1.8 – “Classical” tetramer design**

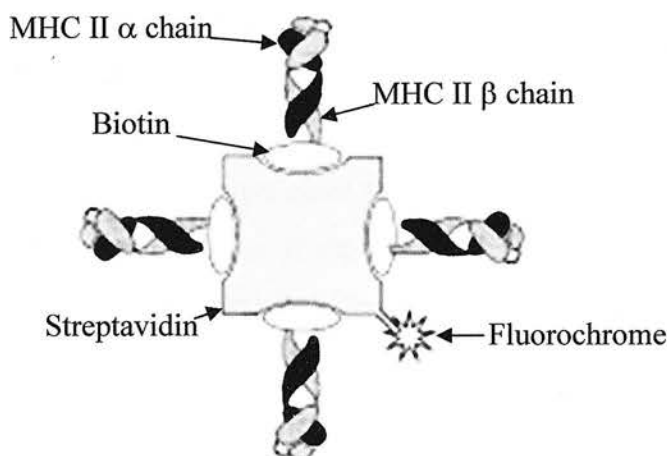


Illustration of the “classical” tetramer design based on the archetypal MHC class I tetramer taken from (Hugues et al., 2002). The MHC II  $\alpha$  and  $\beta$  chains are non-covalently linked. The carboxy terminus of the extracellular MHC II  $\beta$  chain is directly biotinylated without an intervening linker sequence.

The first multivalent peptide/MHC complex linked the immunoglobulin heavy chain IgG1 to the carboxy terminus of the extracellular portion of MHC class I H-2K<sup>b</sup> resulting in a dimeric MHC class I complex (Porto et al., 1993). This immunoglobulin scaffold was used in the formation of I-E<sup>k</sup>, linking the  $\alpha$  and  $\beta$  chains to IgG light and heavy chains respectively (Figure 1.9a). The dimeric I-E<sup>k</sup> proteins were covalently linked to moth cytochrome C peptide (MCC 91-103) and were expressed in a baculovirus system. The dimeric peptide-I-E<sup>k</sup> complexes were able to specifically bind to and activate their cognate antigen-specific T cell (Hamad et al., 1998). Using a variation of the IgG scaffold idea, Casares *et al* have linked the carboxy terminus of I-E<sup>d</sup>  $\beta$  chain to the hinge region of murine IgG2a heavy chain (Figure 1.9b). The influenza virus hemagglutinin peptide (HA110-120) was linked to the amino terminus of the same I-E<sup>d</sup>  $\beta$  chain. Both the I-E<sup>d</sup>  $\alpha$  and modified  $\beta$  chains were expressed using a baculovirus system leading to the formation of dimeric I-E<sup>d</sup>

proteins. These proteins were noted to be conformationally correct and able to stain HA antigen-specific T cells (Casares et al., 2001a, Casares et al., 1997), as well as being able to alter T cell activation (Casares et al., 2002) and differentiation (Casares et al., 1999). However, and once again, this scaffold idea could not be readily extended to other MHC class II proteins without further modification. Malherbe *et al* (Malherbe et al., 2000) modified the carboxy termini of I-A<sup>d</sup> extracellular  $\alpha$  and  $\beta$  chains by adding acid and base leucine zipper sequences respectively, linking the carboxy terminus of the resulting  $\alpha$  chain to the Fc portion of murine IgG2a (Figure 1.9c). The amino terminus of the  $\beta$  chain was covalently linked to a *Leishmania* LACK peptide antigen. The resulting dimer was expressed in *Drosophila* S2 cells using the vector pRmHa3. The dimers were noted to bind LACK-specific T cells. A similar system has been used to produce HLA-DR15 and HLA-DR4 (Appel et al., 2000, Appel et al., 2001).

**Figure 1.9 – Immunoglobulin scaffold based oligomers (Figure adapted from (Hugues et al., 2002))**

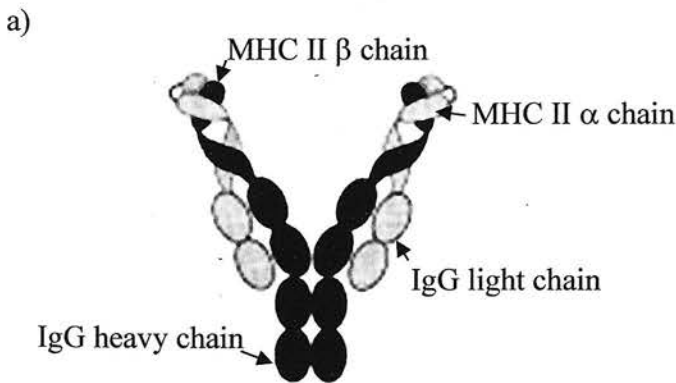


Illustration of the archetypal immunoglobulin-based scaffold used to both aid in the MHC class II  $\alpha\beta$  chain association, and also in the formation of MHC class II dimers.



b)

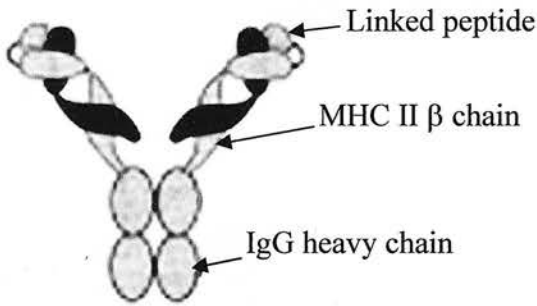


Illustration of the modified immunoglobulin scaffold structure linking the carboxy-terminus of the MHC Class II  $\beta$  chain to the hinge region of the IgG2a heavy chain.

c)

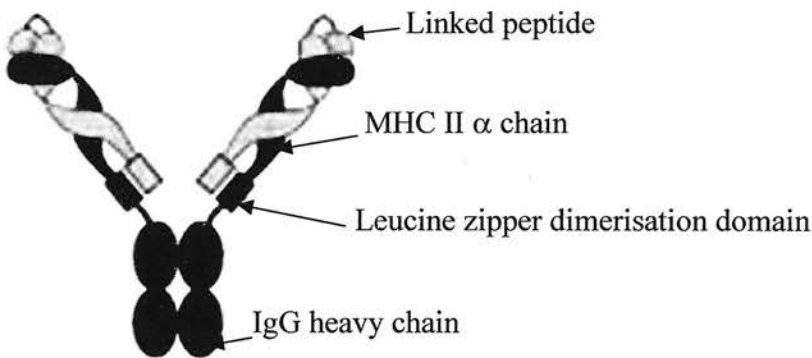
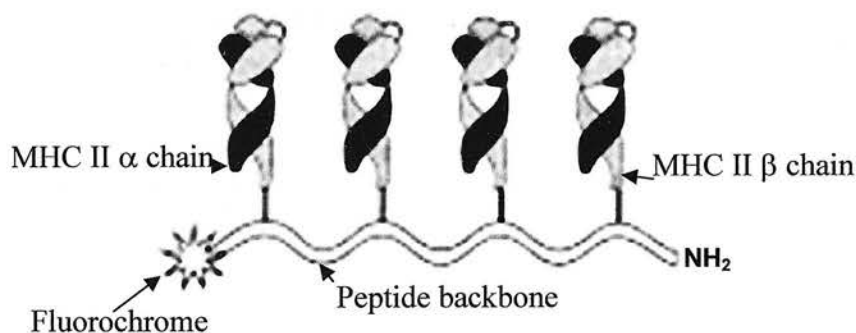


Illustration of the additional modifications of the immunoglobulin scaffold using leucine zipper domains to aid  $\alpha\beta$  chain association.

An innovative oligomerisation technique has been engineered by Cochran *et al* (Cochran *et al.*, 2000) using thiol-reactive maleimide groups linked to a defined number of lysine residues spaced along a flexible non-repeating peptide backbone containing glycine, serine and glutamic acid (Figure 1.10). HLA-DR1 was modified by the addition of a cysteine residue at the carboxy terminus of the  $\beta$  chain before being expressed in *E.coli* and folded *in vitro*. The refolded HLA-DR1 heterodimer could then be formed into dimers, trimers and tetramers by chemical linkage to the peptide backbone that also contained a fluorescent label. This system not only

allowed assessment of antigen-specific T cells, but also the molecular requirements in terms of TCR binding for T cell activation.

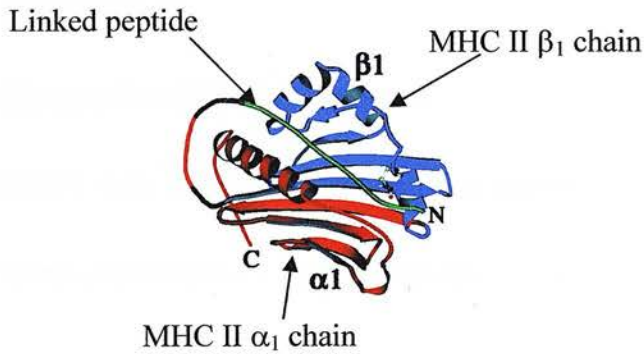
**Figure 1.10 – Peptide backbone oligomerisation (Figure adapted from (Hugues et al., 2002))**



Given the problem of the heterodimeric nature of MHC class II proteins, methods are needed to improve chain pairing. The above has highlighted two techniques, namely the addition of a molecular scaffold and the addition of leucine zipper dimerisation domains, the latter possibly being more effective (Scott et al., 1996). A novel way around the problem was first developed by Rhode *et al* (Rhode et al., 1996) who linked the carboxy terminus of the I-A<sup>d</sup> extracellular  $\beta$  chain to the amino terminus of the I-A<sup>d</sup>  $\alpha$  chain by a 24 amino acid flexible linker. The construct was expressed using a baculovirus system and found to be conformationally correct as evidenced by antigen-specific T cell stimulation. This technique was extended by Burrows *et al* (Burrows et al., 1998) who have constructed a two-domain single chain MHC class II peptide, linking the  $\beta 1$  domain directly to the  $\alpha 1$  domain (Figure 1.11). The  $\alpha 2$  and  $\beta 2$  domains of MHC class II appear to be involved in TCR signalling through their interaction with CD4 (Cammarota et al., 1992, Huang et al., 1997a, König, 2002, König et al., 1995). Studies have, however, shown that although CD4 is required for T cell signalling it is not required for pMHC-TCR binding stability (Boniface et al., 1998, Hamad et al., 1998, König, 2002, Radu et al., 2000). This group has engineered these single chain MHC class II peptides for rat RT1.B (Burrows et al., 2000a, Burrows et al., 1998, Burrows et al., 1999) and human HLA-DR15 (Chang et al., 2001). These constructs were expressed in *E.coli* inclusion bodies and required less complicated refolding compared to the

heterodimeric constructs previously expressed in *E.coli*. Moreover, the constructs could be covalently linked to antigenic peptides through the amino terminus of the  $\beta 1$  domain, improving their stability. The constructs have been shown to be functionally correct through antigen-specific T cell binding and inhibition, but have not yet been oligomerised into an antigen-specific multimeric T cell staining reagent.

**Figure 1.11 – Single chain MHC class II (Figure adapted from (Burrows et al., 1999))**



## 6 Concluding Remarks

### 6.1 Utility of the tetramer approach

The above discussion highlights the various difficulties that are being overcome from the seminal work on MHC class I multimers to the work currently in progress on MHC class II multimers. MHC class I multimers are now readily produced and have been successfully utilised in a number of studies to date. MHC class II multimers have also been produced, but their synthesis has not been as uniformly successful. Indeed, at the inception of this thesis few MHC class II multimers had been described, and these were mainly produced using either the bacterial expression systems previously used for MHC class I multimer production, or the baculovirus system. Consistent production of MHC class II multimers only began at the turn of the millennium, but multiple strategies were being used, with no

one strategy being clearly pre-eminent. Nevertheless, the promising clinical utility of this approach remains a major driving force to its continued development. Possible uses include (Nepom et al., 2002):

- Ability to identify antigen-specific T cells
- Define intermediate phenotypes involved in disease progression
- Distinguish responder versus non-responder status for different therapeutics
- Characterize clinical heterogeneity
- Mark T cells for studies of novel genes and molecular pathways
- Screen peptide libraries for epitope identification

## 6.2 Aims of the study

With the emerging developments in the MHC class II multimer approach to characterising CD4<sup>+</sup> T cells came the possibility of developing such a reagent to study an archetypal human autoimmune disease, Goodpasture's disease. The building blocks of MHC Class II tetramers are recombinant MHC Class II peptides that have been modified to allow both expression in a soluble form and multimerisation to form the final tetrameric units. These form the **Tetramer Building Blocks (TBB)**.

The aim of this project was to develop TBBs that could be used to examine autoreactive T cells in patients and/or mice with Goodpasture's Disease and mice with autoimmune anaemia. At the commencement of the study, the three most promising techniques for TBB construction were taken as templates for further development towards the formation of three MHC Class II multimers: I-E<sup>d</sup>, HLA-DR7 and HLA-DR15. HLA-DR7 and HLA-DR15 were chosen for their negative

and positive associations respectively with Goodpasture's Disease, whilst I-E<sup>d</sup> was chosen for its association with autoimmune anaemia.

As a technology that, even now, is still in relatively early development, it was recognised from the outset that the generation of TBBs would be a major challenge in its self, and most likely the most that I could achieve in the time available. This would leave others to evaluate these TBBs as agents for investigating the autoimmune response in both Goodpasture's Disease and autoimmune anaemia.

### 6.3 Outline of approaches

The first approach built on work performed by Wallny *et al* (Wallny et al., 1995), and employed an insect expression system based in *Drosophila melanogaster* S2 cells (Ivey-Hoyle, 1991) (Figure 1.12a). The copper inducible vectors containing the separate extracellular alpha and beta chains of the murine I-E<sup>d</sup> were kindly donated by Wallny *et al*. This group had successfully produced soluble I-E<sup>d</sup> heterodimers. The heterodimers formed were devoid of bound endogenous peptide, and were capable of being extrinsically loaded with peptide following their purification from the -induced supernatant. The heterodimers demonstrated conformational change upon peptide binding and were noted to be functionally active after this by antigen-specific T cell stimulation (Wallny et al., 1995). The above work had not made use of techniques to enhance the heterodimeric association of the produced alpha and beta chains. Given the importance of peptide binding for the correct association of native MHC Class II alpha and beta chains, the amino terminus of the beta chain was engineered to contain a covalently attached peptide-binding cassette based on the work of Kozono *et al* (Kozono et al., 1994). Such a construct could, therefore, be formed with or without a covalently attached peptide. The latter construct would not only allow ease of changing the associated peptide, but would for example, allow for extrinsic loading of a panel of peptides to more rapidly probe T cell epitopes (Kwok et al., 2001). The possibility of using this covalently attached peptide-binding cassette was made available for all three approaches, although not

necessarily utilised at all times. The plan was to use the “classical” tetramer foundation of the avidin-biotin interaction, and so a site-specific biotinylation sequence was engineered onto the carboxy-terminus of the I-E<sup>d</sup> beta chain.

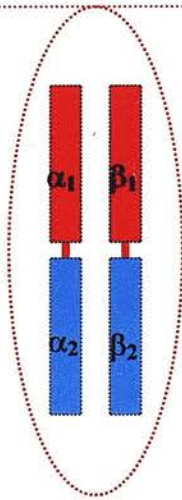
The second approach is an enhancement of the above system and employs two leucine zipper domains at the carboxy terminus of the extracellular domains of both alpha and beta chains (Figure 1.12b). These leucine zipper domains would be intended to maintain the heterodimeric chain association of the alpha and beta chains (Kalandadze et al., 1996, Scott et al., 1996) with or without a covalently linked peptide. Such an approach should also theoretically improve the yield of correctly associated heterodimeric protein.

The final approach circumvents the heterodimeric association by hybridising the  $\alpha 1$  and  $\beta 1$  domains into a single chain construct that maintains the peptide-binding groove in this cooperative unit (Braunstein et al., 1990) (Figure 1.12c). This hybrid molecule was initially developed by Burrows *et al* (Burrows et al., 1998) using rat RT1.B class II molecules with great success. This final approach was the most innovative of the three and had not been used for MHC multimer formation. Protein refolding techniques would have to be developed for these bacterially expressed recombinant proteins.

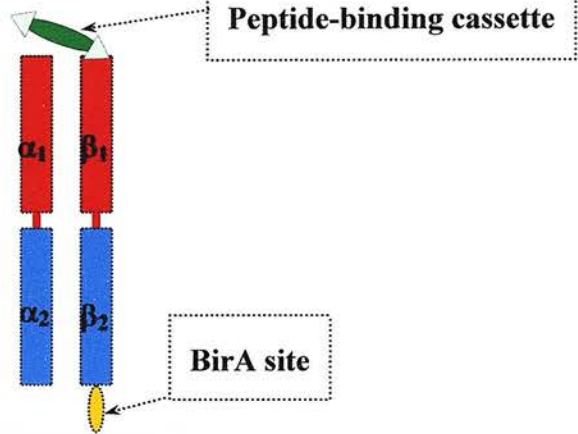


Figure 1.12 – Diagram of TBB Approaches

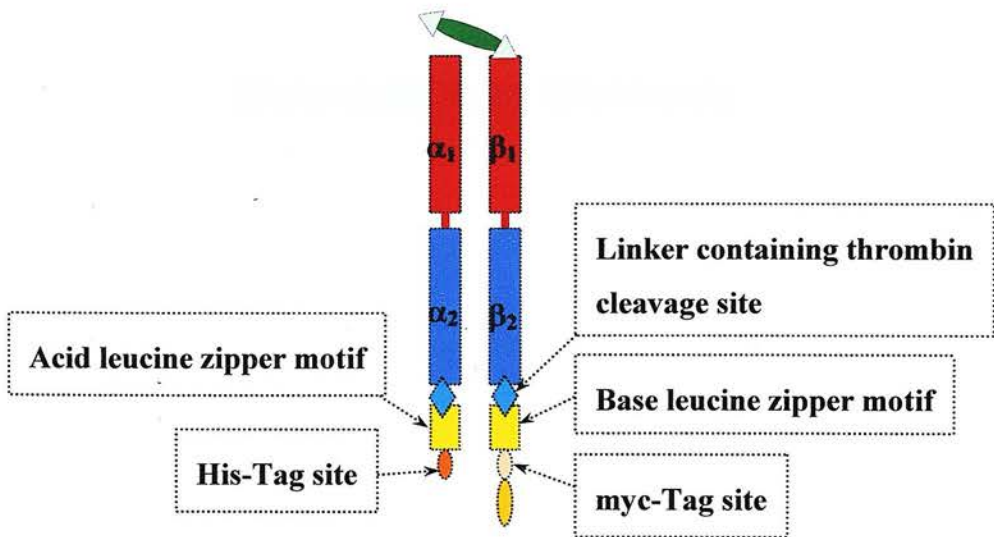
**Heterodimer of Wallny *et al***



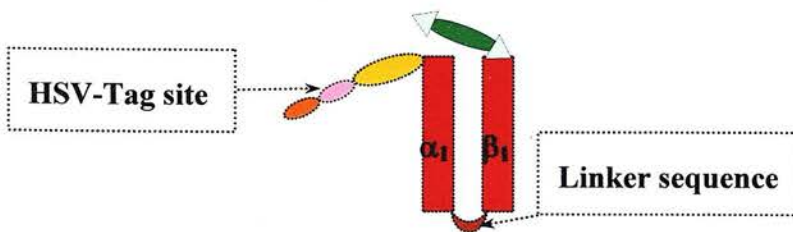
a) I-E<sup>d</sup> heterodimer



b) Leucine-zipper associated HLA-DR heterodimers



c) Single-chain TBBs





## **Chapter 2**

### **Materials and Methods**

# Chapter 2

## Materials and Methods

### Contents

1	MATERIALS.....	49
2	NUCLEIC ACID METHODS.....	52
3	HYBRIDOMA CELL CULTURE.....	58
4	INSECT CELL CULTURE AND PROTEIN PRODUCTION METHODS.....	61
5	BACTERIAL PROTEIN PRODUCTION METHODS.....	65
6	CELL LYSATE PREPARATION.....	70
7	PROTEIN IDENTIFICATION METHODS.....	71

## 1 Materials

### 1.1 General Chemicals

All materials, with the exception of those mentioned, were obtained from either Sigma-Aldrich Company Limited, UK; Fisher Scientific, UK; BDH Laboratory Supplies (VWR International); or Scientific Laboratory Supplies Ltd, UK.

## 1.2 Molecular biology additive stock solutions

The following stock solutions were formed and stored at -20°C:

Ampicillin	50mg/ml in dH <sub>2</sub> O
Carbenicillin ( <i>CN Bioscience</i> )	50mg/ml in dH <sub>2</sub> O
Chloramphenicol ( <i>Transgenomic Limited</i> )	34mg/ml in 100% ethanol
IPTG ( <i>Transgenomic Limited</i> )	1M in dH <sub>2</sub> O
Tetracycline ( <i>Transgenomic Limited</i> )	12.5mg/ml in 50% ethanol in dH <sub>2</sub> O
X-gal ( <i>Transgenomic Limited</i> )	2% solution in dimethylformamide

## 1.3 Tissue Culture

### 1.3.1 Plastics / Glassware

All materials, with the exception of those mentioned, were obtained from either Nalge Nunc International (Denmark), Sarstedt Inc. (USA), or Techne (Cambridge) Ltd (UK).

### 1.3.2 Media

All media, with the exception of those mentioned, were obtained from either Invitrogen Life Technologies (Holland) or PAA Laboratories (UK).

### 1.3.3 Cell Lines

All cell lines, with the exception of those mentioned, were obtained from either Invitrogen Life Technologies (Holland), or American Type Culture Collection (Table 1).

Table 1 – Cell lines

Cell Line	Utility	Source	Reference
<b>HL-60</b>	Source of human c-myc onco-protein as a positive control.	Dr K. Britton, Royal Dick Veterinary School, Edinburgh	(Evan et al., 1985)
<b>BE1</b>	Source of HLA-DR as a positive control.	European Collection of Cell Cultures	
<b>A20</b>	Source of I-E <sup>d</sup> as a positive control	Dr L. Bowie, University of Aberdeen	(Glimcher et al., 1982)
<b>DR2-LUM</b>	Source of HLA-DRB*1501	European Collection of Cell Cultures	(Young and Darke, 1994)
<b>DA6.147</b>	Source of murine IgG <sub>1</sub> monoclonal antibody directed against the $\alpha$ chain human MHC Class II antigens.	European Collection of Cell Cultures	(Guy et al., 1982)
<b>DA6.231</b>	Source of murine IgG <sub>1</sub> monoclonal antibody directed against the $\beta$ chain human MHC Class II antigens.	European Collection of Cell Cultures	(Guy et al., 1982)
<b>L243</b>	Source of murine monoclonal antibody directed against conformationally correct HLA-DR complexes		(Lampson and Levy, 1980, Nepom et al., 1996)

## 2 Nucleic Acid Methods

### 2.1 Ligation of DNA fragment into a plasmid vector

The relevant plasmid and DNA insert were digested with the required restriction enzymes (*Promega Corporation*) at 37°C for between 2-3 hours. The optimal buffer for each enzyme combination was utilised for each restriction enzyme digest.

The plasmid was dephosphorylated by incubating with Calf Intestinal Alkaline phosphatase (CIP) in CIP buffer (*Promega Corporation*) for 1 hour at 37°C as per the manufacturer's instructions. Dephosphorylation was terminated by inactivating the enzyme through the addition of 0.5M EDTA and incubation at 65°C for 20 minutes. The plasmid was then purified using the QIAEX II<sup>®</sup> protocol for desalting and concentrating DNA solutions (*Qiagen*) as per the manufacturer's instructions. This protocol is based on the adsorption of DNA to silica gel that is then washed to remove impurities including salts. The adsorbed and purified DNA can then be eluted using a low salt alkaline eluant such as 10mM Tris.Cl (pH 8.5).

The DNA insert was separated by agarose gel electrophoresis prior to excising the relevant insert band and purifying using the QIAEX II<sup>®</sup> gel extraction protocol (*Qiagen*) as per the manufacturer's instructions. This protocol utilises an optimised buffer containing a high concentration of chaotrophic salt to disrupt the hydrogen bonds within the agarose polymer, allowing solubilisation of gel slice. In addition, the high salt concentration dissociates DNA binding proteins from the DNA fragments, allowing the DNA to be adsorbed to a silica gel as above.

The concentration of the purified products was assessed roughly by agarose gel electrophoresis using a 1:4 ratio of cut plasmid to cut insert.

The following ligation mixtures were prepared and incubated at 16°C overnight in a thermal cycler (Genius – *Techne (Cambridge) Ltd.*): To 1µl of cut plasmid was added 0, 1, 4, and 7µl of prepared insert prior to adding 1µl of T4 ligase buffer (*Promega Corporation*) and 1µl of T4 ligase (*Promega Corporation*). The

mixture was adjusted to 10µl with sterile water. The ligated products could be transformed into competent cells as noted below.

## 2.2 Making and transforming competent cells

The following protocol is based on the work of Hanahan (Hanahan, 1983) and was adapted from Sambrook *et al* (Sambrook et al., 1989).

SOB/LB agar plates were prepared using 1.5% agar autoclaved in the bacterial growth medium prior to pouring into 90mm plates (*Bibby Sterilin Ltd.*). Magnesium sulphate was added, as well as any antibiotics required, prior to pouring the plates. Subcloning Efficiency<sup>TM</sup> DH5α<sup>TM</sup> *E.coli* (*Life Technologies*) were streaked onto a prepared agar plate (without antibiotic) using a sterile applicator (*Nalge Nunc International*) prior to incubating overnight in a 37°C incubator (*Sanyo Gallenkamp*).

A 50ml baffled flask was sterilised by adding 50ml dH<sub>2</sub>O and boiling in a microwave (Program 1050 - *ProLine*) for 3 minutes prior to discarding the water and adding 50ml sterile complete SOB/LB medium. Using a sterile applicator, approximately 20 bacterial colonies were taken and placed into the prepared flask before incubating in an orbital shaker (Orbital Incubator – *Sanyo Gallenkamp*) at 37°C until the optical density at 550nm (OD<sub>550</sub>) was between 0.3–0.4 (Unicam UV1 – *Thermo Spectronic, USA*). The cell suspension was decanted into a pre-cooled 50ml Falcon tube prior to centrifuging at 2000g at 4°C for 10 minutes. The supernatant was discarded prior to re-suspending in 10–15ml ice-cold transforming buffer and leaving on ice for 10 minutes. The suspension was centrifuged as before prior to re-suspending in 2–5ml ice-cold transforming buffer and adding 140µl of DD solution, swirling immediately. The solution was incubated for 10 minutes prior to adding a further 140µl of DD solution and swirling as before, incubating for a further 20 minutes on ice.



5µl of plasmid (1:10 dilution) or ligation mixture was added to a 1.5ml epindorf tube prior to placing on ice. 50µl of the above cell suspension was added to each epindorf tube prior to mixing and leaving on ice for 30 minutes. The bacteria were heat shocked by placing into a 42°C water-bath for 90 seconds, then returning to ice for 2 minutes. 200µl of pre-warmed SOC medium (EKIT-B1 – *ThermoHybaid Ltd.*) was then added to each epindorf prior to incubating at 37°C for 1 hour. The cell suspension was spread onto dried SOB agar plates containing 100µg/ml ampicillin, incubating inverted overnight in a 37°C incubator.

### 2.3 Small-scale preparation of plasmid DNA (“Mini-prep”)

The success of plasmid ligation was assessed by performing small-scale DNA preparations of a selected number of colonies from agar plates predicted to contain the desired insert. These plates were those having the greatest colony count above the background (cut plasmid alone) plate. The method of DNA preparation was adapted from Sambrook *et al* (Sambrook et al., 1989).

Each of the selected colonies was taken from the agar plate using separate sterile applicators and placed into 2ml of sterile bacterial medium containing 100µg/ml ampicillin in a 15ml Falcon tube. The tubes were placed in a 37°C orbital shaker overnight at 200rpm. The following morning, 1.5ml of the cell suspension was poured into a clean epindorf tube, with the remaining suspension being stored at 4°C. The epindorf tube was centrifuged at 18000g at room temperature (Sigma 1-15 – *Sigma (Germany)*) for 3 minutes prior to discarding the medium. The pellet was re-suspended in 100µl of GTE by vigorous vortexing, adding 200µl of sodium hydroxide/SDS solution to each suspension and mixing by inversion prior to incubating on ice for 5 minutes. 150µl of ice-cold 3M/5M potassium acetate solution was then added, mixing the resulting solution by gentle vortexing prior to incubating on ice for a further 15 minutes. The solution was then centrifuged at 18000g at room temperature for 5 minutes to remove cellular debris and precipitated proteins, transferring the supernatant to a fresh epindorf tube. The supernatant was vortexed

with 200µl of buffered phenol (*Severn Biotech Ltd.*) and centrifuged at 18000g for 2 minutes to remove any remaining protein. The upper phase of the resulting solution was removed and the DNA precipitated by adding an equal volume of 100% isopropanol and vortexing prior to centrifuging at 18000g for 5 minutes at room temperature. The supernatant was aspirated and 1ml of 70% ethanol added prior to centrifuging for 1 minute as above. The ethanol was then removed and the pellet allowed to air-dry prior to re-dissolving in 50µl 10mM Tris.Cl pH8.5.

Once re-dissolved the DNA was assessed by performing a panel of restriction enzyme digests in the presence of RNase. The digests were assessed by agarose gel electrophoresis. The DNA was stored at -20°C if required for further analysis at a later point in time.

## 2.4 Larger scale DNA preparation (“Midi-prep”)

Once colonies containing the correctly ligated DNA had been provisionally established as above, further clarification and sequencing was performed on larger scale and purer DNA preparations.

100µl of the stored bacterial suspension was inoculated into 50ml of bacterial culture medium containing 100µg/ml ampicillin in a 250ml microwave-sterilised baffled flask. The bacteria were allowed to grow overnight in a 37°C orbital shaker at 250rpm prior to preparing the DNA using the QIAGEN® Plasmid Midi Kit (*QIAGEN*) as per the manufacturer’s instructions. This plasmid purification protocol is based on a modified alkaline lysis procedure, binding the plasmid DNA to an anion-exchange resin at a low-salt concentration. RNA, proteins, dyes and low molecular weight impurities are removed by a medium-salt concentration buffer prior to eluting the plasmid DNA in a high-salt buffer. The DNA is concentrated and desalted by isopropanol precipitation. The DNA is precipitated by centrifugation at 15000g for 30 minutes at 4°C before washing in 70% ethanol. The washed DNA is centrifuged at 15000g for 10 minutes at room temperature. The resulting DNA pellet can either be stored at -20°C under ethanol in order to keep sterile, or re-dissolved in

10mM Tris.Cl pH8.5 for use in restriction digests to confirm or refute the presence of the correct insert sequence prior to storing at -20°C.

## 2.5 Agarose gel electrophoresis

Agarose mini gels were formed to analyse the DNA products of PCR, restriction enzyme digests or plasmid production. In general, 1.5% agarose gels were formed using 0.5% TBE buffer by heating the agarose in the TBE buffer until it dissolved to form a clear solution using a microwave. 5µl of 10mg/ml ethidium bromide was added to each 50ml agarose gel prior to pouring into the mini gel apparatus (*Scie-Plas Ltd.*) and allowing to solidify at room temperature. Once solidified 50ml of 0.5% TBE buffer was poured over the gel and 5µl of a 1:10 dilution of Hae III digest DNA ladder (*Kramel Biotech International*) was loaded into one well after mixing with a small drop of DNA loading buffer (roughly 1/6<sup>th</sup> volume).

Samples were loaded after mixing with a small amount of DNA loading buffer as above. The gel was electrophoresed at 100V, 75mA for 30 minutes to obtain adequate separation. The DNA bands were visualised under UV light.

## 2.6 Assessment of nucleic acid concentration

Assessment of DNA and RNA concentration was made spectrophotometrically (Unicam UV1 – *Thermo Spectronic, USA*) after the nucleic acid sample was diluted in Milli-Q H<sub>2</sub>O (*Millipore UK Ltd*). DNA solutions were diluted at 1:800 in Milli-Q H<sub>2</sub>O, whilst RNA solutions were diluted at 1:100. Milli-Q H<sub>2</sub>O was used to zero the instrument before the ODs of the solutions were analysed at 260nm ( $A_{260nm}$ ) and 280nm ( $A_{280nm}$ ). Actual nucleic acid concentrations were then calculated as follows:

$$[RNA] = (A_{260nm} \times 40 \times \text{dilution factor}) \mu\text{g/ml}$$

$$[\text{DNA}] = (A_{260\text{nm}} \times 50 \times \text{dilution factor}) \mu\text{g/ml}$$

The ratio of  $A_{260\text{nm}}:A_{280\text{nm}}$  should be roughly 1.8-2.0:1 indicating a low level of protein contamination.

## 2.7 DNA Sequencing and sequence analysis

All DNA sequencing was performed by DNAShef at the Royal Infirmary of Edinburgh using fluorescence-based dideoxy chain-termination cycle sequencing (ABI Prism® BigDye™ Terminator – *Applied Biosystems*).

The sequencing data was viewed using Edit View v1.0.1 (*Perkin-Elmer Corp.*). Sequences were compared using ClustalX (Thompson et al., 1997) and DNA Strider v1.2 (*CEA, France*).

## 2.8 Extraction of mRNA and RT-PCR

Extraction of mRNA was carried out on *Drosophila melanogaster* S2 as well as DR2Lum cells. All procedures were undertaken under RNase-free conditions at all times. The cell suspension was centrifuged at 500g for 5 minutes at 15°C, before removing the supernatant and re-suspending in 2ml of fresh medium. A cell count was performed, with approximately  $1 \times 10^7$  cells being taken for mRNA extraction. The extraction of mRNA was carried out using the QuickPrep™ *Micro* mRNA Purification Kit (*Amersham Pharmacia Biotech*). The kit combines extraction of RNA in a buffered solution containing guanidinium thiocyanate to ensure rapid inactivation of endogenous RNases with separation of the poly(A)<sup>+</sup> RNA using oligo(dT) attached to cellulose. The separated poly(A)<sup>+</sup> RNA is washed in high and low salt buffers before eluting from the oligo(dT) cellulose. The separated poly(A)<sup>+</sup> RNA is composed of both heterogeneous nuclear RNA (hnRNA) and mRNA. Once eluted, the RNA was concentrated by precipitation using the supplied glycogen and potassium acetate solutions combined with pre-chilled 95% ethanol at -20°C for 1

hour. The precipitated RNA was then stored as a pellet under ethanol at  $-80^{\circ}\text{C}$  following centrifugation at  $15000g$  at  $4^{\circ}\text{C}$  for 5 minutes.

RT-PCR was carried out using Ready-To-Go<sup>®</sup> RT-PCR beads (*Amersham Pharmacia Biotech*) as per the manufacturer's two-step protocol using pd(N)<sub>6</sub> as the first-strand primer in a thermal cycler (*Genius – Techne (Cambridge) Ltd.*). Each bead is optimised to allow cDNA synthesis and PCR to occur sequentially within the same tube, and contains the correct quantities of Moloney Murine Leukemia Virus (M-MuLV) reverse transcriptase and *Taq* DNA polymerase together with buffer,  $\text{MgCl}_2$ , nucleotides and RNAGuard. For one bead reaction,  $10\mu\text{l}$  of RNA suspension was used as the template RNA, with  $5\mu\text{l}$  of  $0.5\mu\text{g}/\mu\text{l}$  pd(N)<sub>6</sub> random primer being used as the first strand primer. To this  $25\mu\text{l}$  of MilliQ  $\text{H}_2\text{O}$  was added and the bead incubated at  $42^{\circ}\text{C}$  for 30 minutes prior to inactivating the reverse transcriptase by heating to  $95^{\circ}\text{C}$  for 5 minutes. The cDNA formed by this process was then amplified by PCR using gene-specific primers. Where DNA contamination might affect the interpretation of results, for example in the assessment of DNA transcription in transfected S2 cells, DNase I pre-treatment of the RNA was used. This was performed by incubating the RNA with RNase-free DNase I (*Promega*) in DNase Buffer ( $\times 10$ ) for 1 hour at  $37^{\circ}\text{C}$  before using the resulting solution containing RNA as the template for first-strand cDNA synthesis.

### 3 Hybridoma Cell Culture

#### 3.1 Routine culture

All hybridoma cell lines were cultured in RPMI 1640 supplemented with a final concentration of  $2\text{mM}$  L-glutamine/ $100\text{U}/\text{ml}$  penicillin/ $0.1\text{mg}/\text{ml}$  streptomycin and 10% heat-inactivated foetal calf serum. Cells were maintained at a concentration of between  $10^5 - 10^6$  cells/ml by re-suspending in fresh media on passaging. Cells were maintained at  $37^{\circ}\text{C}$  and 5%  $\text{CO}_2$  in a WTC Binder (Germany) incubator.

L243 hybridoma cells were initially grown in Modified Dulbecco's medium with 10% heat-inactivated foetal calf serum prior to gradually transferring to RPMI 1640 as above.

### 3.2 Cryopreservation

Hybridoma cells were cryopreserved at passaging. A 10ml cell suspension was taken and centrifuged at 500g for 5 minutes at 20°C. The supernatant was discarded to leave 1.5ml of conditioned medium. To this, an equal quantity of a 10% DMSO in heat-inactivated foetal calf serum was added, thus re-suspending in a final concentration of 5% DMSO. The resulting cell suspension was placed into a cryovial prior to placing in Mr Frostie<sup>®</sup> (*Nalge Nunc International*), which was then placed at -80°C (*Sanyo Ultra Low*) overnight. The cryovials were then transferred to a liquid nitrogen store (*Cryosystem 2000 - MVE Cryogenics, USA*) for prolonged storage.

### 3.3 Recovery of cells

Cryopreserved cells were defrosted rapidly by placing the cryovial in a 37°C water-bath. Just prior to complete defrosting, the cryovial was sprayed with a 70% ethanol solution and placed in a sterile safety cabinet. The cell suspension was removed and 10ml of fresh medium added to the suspension. The suspension was centrifuged at 500g for 5 minutes at 20°C prior to discarding the supernatant and re-suspending the cell pellet in 10mls fresh medium. The cell suspension was placed into a sterile 25cm<sup>2</sup> flask prior to maintaining as above. The cells were passaged initially 48 hours later, using a 1:2 dilution with fresh medium, prior to following the normal routine outlined above.



### 3.4 Cell lysis

The required cell suspension (at least  $10^7$  cells/ml) was initially centrifuged at 750g at 4°C for 5 minutes to pellet the cells, which could then be stored at -20°C until required. To the cell pellet, 1ml of cell lysis solution was added, prior to vortexing and placing on ice for at least 3 hours. The suspension was then centrifuged at 20000g for 30 minutes prior to removing the supernatant and storing this at -20°C until required.

### 3.5 Antibody purification

Supernatant was collected from antibody-producing hybridoma cells when they were passaged. The supernatant was centrifuged at 2000g for 5 minutes at 4°C before decanting the cell-free supernatant into a sterile bottle containing a final concentration of 0.1% sodium azide. The bottle was stored at 4°C until full, then placed at -20°C for long-term storage.

When purifying, 1l of frozen supernatant was defrosted at room temperature before precipitating the antibody with 40% ammonium sulphate at 4°C overnight prior to centrifuging at 5500g for 30 minutes at 4°C. The pellet was dissolved in PBS to 20% of the starting volume. The resulting solution was placed into prepared Seamless Cellulose dialysis tubing and dialysed extensively at 4°C against sodium phosphate loading buffer containing 0.05% sodium azide. The final solution was filtered through a 0.45µm filter prior to storing at 4°C.

A 2ml anti-mouse IgG sepharose column was packed and equilibrated with 20 column volumes of sodium phosphate wash buffer using a Biocad 700E Workstation. The antibody solution was then loaded at 2ml/minute onto the column in 100ml aliquots, eluting each time with 10 column volumes of 0.1M glycine buffer (pH2.5) containing 0.15M NaCl, collecting the eluate in a neutralising volume of 1M sodium phosphate buffer pH8.0. The final eluate was then concentrated by loading onto a 1.7ml Poros® A column (*PerSeptive Biosystems*) which had been equilibrated

with sodium phosphate wash buffer as above, eluting with glycine buffer as above. Sodium azide was added to the final eluate to a concentration of 0.1% prior to aliquoting and storing at -20°C.

## 4 Insect Cell Culture and Protein Production Methods

### 4.1 Routine culture

*Drosophila melanogaster* Schneider 2 (S2) cells were used throughout this study for the production of MHC Class II heterodimers.

The S2 cells were grown in either serum supplemented media (Schneider's *Drosophila* Medium), or serum-free media (Insect Express Sf9-S2). Serum supplementation was carried out by the addition of 10% heat-inactivated insect-qualified foetal calf serum. Penicillin and streptomycin were added to all media to give a final concentration of 100U/ml and 0.1mg/ml respectively.

The S2 cell lines were passaged twice weekly by gently tapping the flask and removing about 80% of the resulting cell suspension, prior to replacing with an equal volume of fresh medium. Although transfected cell lines were maintained primarily within the same flask, untransfected cells were transferred into a fresh flask at each passage.

All insect cell work was carried out under sterile conditions in a Baker Sterilgard Class II biological safety cabinet (*Baker Corporation*). This was cleaned with a 2% Virkon (*Antec International Ltd.*) solution before and after use.

Cell lines were maintained at 26°C either in tissue culture flasks within a cooled incubator (*LMS*), or in magnetic spinner flasks maintained at 26°C within a magnetic, thermostatically controlled water bath (*MCS-104L* and *MWB-12L–Technique*).

## 4.2 Cryopreservation

S2 cell lines were cryopreserved when required at passaging. A 10ml cell suspension was taken and centrifuged at 500g for 5 minutes at 20°C (4K15 - *Sigma Laboratory Centrifuges*). The supernatant was discarded to leave 1.5ml of conditioned medium. To this, an equal quantity of a 15% DMSO solution was added. This solution was formed in either heat-inactivated foetal calf serum or serum-free medium, depending upon the growing medium. The resulting cell suspension was placed into a cryovial prior to placing in Mr Frostie® as described above.

## 4.3 Recovery of cells

Cryopreserved S2 cells were defrosted rapidly by placing the cryovial in a 37°C water-bath. Just prior to complete defrosting, the cryovial was sprayed with a 70% ethanol solution and placed in a sterile safety cabinet. The cell suspension was removed and 10ml of fresh medium (serum-free or serum-supplemented as required) was added to the suspension. The suspension was centrifuged at 500g for 5 minutes at 20°C prior to discarding the supernatant and re-suspending the cell pellet in 10mls fresh medium. The cell suspension was placed into a sterile 25cm<sup>2</sup> flask prior to maintaining as above. The cells were passaged initially 48 hours later, using a 1:2 dilution with fresh medium, prior to following the normal routine outlined above.

## 4.4 Transfecting S2 cells

S2 cells were stably transfected as per manufacturer's protocol using calcium phosphate (*Drosophila Expression System Version A - Invitrogen Life Technologies*). S2 cells were initially seeded into six-well plates 24 hours prior to transfection, with the plates being placed within a humidified box within the cooled incubator. The ethanol covering the sterile DNA pellets was first removed before

allowing the pellets to air-dry. The dried pellets were re-suspended in 20µl of Milli-Q H<sub>2</sub>O before assessing the DNA concentration as per Methods. Transfection was carried out using a total of 19µg of DNA per transfection, with 1µg being the resistance vector. Therefore, where two DNA sequences require co-transfection, 9µg of each sequence is transfected with the resistance vector. Selection was carried using hygromycin-B at 500µg/ml, with selection being carried out within the six-well plates for 4 weeks prior to transfer to larger culture flasks for continued selection. A negative transfection control without DNA was used in parallel with a positive transfection control. The latter was in the form of a previously successful plasmid encoding for the α3(NC1) domain of Type IV collagen – pMT/BiP/V5His/A/P<sup>+</sup> (Chopra, 1999). The vector encoding for hygromycin-B resistance, pCoHYGRO, was kindly donated by Dr S. Chopra (Chopra, 1999).

#### 4.5 Production of recombinant protein

Following at least 6 weeks of selection in serum-supplemented medium containing 500µg/ml hygromycin-B, the stably transfected cells were transferred to hygromycin-B-free serum-supplemented medium by using this medium on passaging. The cells were then seeded either into tissue culture flasks or into spinner flasks at a density of  $2 \times 10^6$ /ml and allowed to grow until a density of  $4-6 \times 10^6$ /ml was reached. Cell viability was assessed by Trypan Blue exclusion using the following formula:

$$\text{Total viable cells} \div \text{Total cell number} \times 100\%$$

The cells were induced at this point with 100mM 0.2µm filter-sterilised CuSO<sub>4</sub> solution to give a final concentration of 1mM Cu<sup>2+</sup>. The supernatant was harvested after 4-5 days or when the cell density had reached  $10-20 \times 10^6$ /ml. The supernatant was harvested by centrifuging the cell suspension at 1500g for 5 minutes at 20°C prior to removing the supernatant and processing as noted below.

Cells were also transferred to serum-free medium after transferring to hygromycin-B-free medium by a gentle weaning process involving reducing quantities of serum-supplemented medium at each passage.

Growth in spinner flasks as suspension cultures was aided by the addition of filter sterilised 10% Pluronic F-68 to the medium to give a final concentration of 0.1%. This surfactant helps reduce shear stress.

## 4.6 Purification of recombinant protein

The recombinant protein was precipitated by mixing with ammonium sulphate at a final concentration of 40% w/v (Kuroda et al., 2000) at 4°C overnight. The precipitated proteins were harvested by centrifugation at 5500g for 30 minutes at 4°C, re-suspending the precipitate in 20% of the initial volume of PBS (*Diagnostics Scotland*) with 0.05% sodium azide. The resuspended protein was then placed into a prepared cellulose dialysis tube and dialysed extensively against PBS/0.05% sodium azide at 4°C. The dialysis membrane was prepared by boiling in dH<sub>2</sub>O for 20 minutes three times. Once dialysed, the solution was filtered through a 0.45µm filter prior to adding a 1:10<sup>3</sup> dilution of protease inhibitor cocktail (Cocktail for use in purification of poly(Histidine)-tagged proteins). Dialysis should remove the copper ions used to induce the cells that may interfere with the nickel chelation step below. The solution was stored for a short period at 4°C prior to further purification.

Further purification was carried out by metal chelation affinity chromatography using Poros<sup>®</sup>20MC medium (1.7ml bed volume) and a Biocad 700E workstation (*PerSeptive Biosystems Inc.*). The column was stripped, regenerated and loaded with nickel as per the manufacturer's instructions before being equilibrated in the column wash buffer. The sample solution was mixed in a 50:50 ratio with the column wash solution prior to loading onto the prepared Poros<sup>®</sup>20MC column at 3ml/minute. The column was washed for 10 column volumes in column wash buffer prior to eluting with the column elution solution over 20 column volumes at

3ml/minute. The eluate was then dialysed extensively into PBS containing 0.1% sodium azide.

## 5 Bacterial Protein Production Methods

### 5.1 Transforming BL21 (DE3) Cells

BL21(DE3) (*CN Bioscience*) cells were transformed as per above method using the single-chain constructs for HLA-DR15, HLA-DR7 or IE<sup>d</sup> (Figure 5.14) ligated into pET25b (*CN Bioscience*) as per above method. The transformed bacteria were plated onto LB agar plates containing 100µg/ml of carbenicillin prior to placing in a 37°C incubator overnight.

### 5.2 Small scale protein production and analysis

Five single colonies from the above transformation were taken using a sterile loop and placed into 10ml LB medium containing 200µg/ml carbenicillin allowing the bacteria to grow at 37°C in an orbital shaker at 250rpm for up to 6 hours. The bacterial suspension was centrifuged at 5000g at 4°C for 5minutes before re-suspending the cell pellet in 20ml fresh LB medium containing 300µg/ml carbenicillin and storing at 4°C for a maximum period of 72 hours.

500µl of the stored suspension was taken and placed in 10ml LB medium containing 400µg/ml of carbenicillin before incubating in an orbital shaker at 37°C and 250rpm. The optical density at 600nm (OD<sub>600</sub>) was measured and the cell suspension was induced with 1M IPTG to give a final concentration of 1mM once an OD<sub>600</sub> of 0.5 had been attained. The induced cells were kept in the orbital shaker at 37°C and 250rpm for 4 hours before centrifuging at 5000g for 10minutes at 4°C, storing the cell pellet at -80°C overnight.



The use of high concentrations of carbenicillin helps to prevent the overgrowth of cells that have lost the transformed plasmid that might otherwise occur due to bacterial  $\beta$ -lactamase production.

The stored pellets were defrosted at room temperature with 10ml PBS being added to each pellet before sonicating for 60seconds with a 50% duty cycle on ice (Ultrasonic Processor – *Jenkons Scientific Ltd.*). The suspension was centrifuged at 10000g for 20minutes at 4°C, discarding the supernatant before sonicating in a further 10ml PBS as previously. After further centrifugation, the pellet was resuspended in 1ml Inclusion body re-suspension solution by further sonication followed by shaking on ice overnight. The suspension was centrifuged at 15000g for 20minutes at 4°C and the soluble fraction collected and analysed using SDS-PAGE and Coomassie Brilliant Blue stain.

The monomeric scTBB proteins have the following predicted molecular weights (inclusive of the BirA recognition sequence, HSV-Tag<sup>®</sup> and His-Tag<sup>®</sup>):

HLA-DR15sc – 26.4kD

HLA-DR7sc – 26.3kD

IE<sup>d</sup>sc – 26.4kD

### 5.3 Cryopreservation of transformed cells

Once the colony having the greatest protein production had been identified above, a glycerol stock was formed as follows:

The stored cell suspension was centrifuged at 5000g for 5 minutes at 4°C resuspending the cell pellet in 10ml fresh LB containing 400 $\mu$ g/ml carbenicillin. 500 $\mu$ l of the resulting suspension was taken and added to 10ml fresh LB containing 400 $\mu$ g/l carbenicillin and incubated at 37°C in an orbital shaker at 250rpm until an OD<sub>600</sub> of 0.5 had been attained. 4.5ml of the cell suspension was then added to 0.5ml

of 80% glycerol in LB medium that had been previously sterilised by autoclaving. Carbenicillin was added to the resulting mixture to give a final concentration of 100µg/ml. The resulting cell suspension was aliquoted into sterile cryovials before snap freezing in an ethanol/dry ice bath and storing the frozen vials at -80°C.

In order to make use of this stored colony, a sterile applicator was scraped over the glycerol surface before streaking across an LB-agar plate containing 200µg/ml of carbenicillin. The plate was incubated inverted overnight in a 37°C incubator to allow bacterial growth. Single colonies were then assessed for protein production as above before proceeding to large-scale protein production using the colony with the highest protein yield.

## 5.4 Large scale production of recombinant protein

Once the colony with the highest protein yield had been chosen from the small-scale preparation above, a larger scale culture of the bacterial colony was made. The stored cell suspension was centrifuged at 5000g for 5 minutes before removing the supernatant and resuspending the cell pellet in 10ml of fresh LB medium containing 400µg/ml carbenicillin by gentle vortexing. The resulting suspension was then divided between two 1l samples of LB medium containing 300 µg/ml carbenicillin contained in 2l baffled flasks. The bacterial suspensions were incubated at 37°C in an orbital shaker at 250rpm until the OD<sub>600</sub> was between 0.6 and 0.8. The cell suspension was induced with 1M IPTG to give a final concentration of 1mM, and the resulting suspension continued to be incubated in the orbital shaker for 4 hours at 37°C. The cell suspensions were centrifuged at 5000g for 10 minutes prior to discarding the supernatant and storing the pellet at -20°C until required.

Once required, the pellet was defrosted and resuspended in 35ml ice-cold PBS using an Ultra-Turrax T8 (*IKA Labortechnik, Germany*) prior to placing into Oakridge tubes at -80°C for five hours. The suspension was defrosted prior to sonicating on ice for 120 seconds using a 50% duty cycle. Lysozyme was added at a

final concentration of 0.2mg/ml prior to incubating at 4°C on a rolling platform for 1 hour. The aim of this step was to improve overall bacterial cell lysis efficiency. To this suspension was added deoxycholic acid to a final concentration of 0.1%, magnesium chloride to a final concentration of 2mM, and DNase I to a final concentration of 2µg/ml prior to replacing on the roller platform at 4°C overnight. This step was used to solubilise cellular membranes and destroy bacterial DNA so aiding downstream purification. The suspension was then centrifuged at 20000g at 4°C for 10 minutes prior to discarding the supernatant and resuspending the pellet in 25ml ice cold PBS using an Ultraturex and sonication for 60s with a 50% duty cycle before centrifuging once more as above. This was repeated three times. The pellet was then resuspended in 25ml of a solution of 0.5% TritonX100 and 1mM EDTA using the Ultraturex and sonication on ice as previous. This suspension was incubated at 4°C on a roller platform for 30 minutes before centrifuging as above. Finally, the pellet was resuspended in 30ml ice cold PBS using the Ultraturex and sonication as previously, before centrifuging as above. This was also repeated three times. Such washing has been shown to improve the purity of the final inclusion body preparation (Fischer et al., 1992, Kuhelj et al., 1995). This final proteinaceous pellet was resuspended in 10ml 6M Urea with 50mM HEPES pH 8.0 and 1M sodium chloride using a combination of Ultraturex and sonication on ice as above. The resulting suspension was incubated on a roller platform overnight at 4°C. This final suspension was centrifuged at 20000g at 4°C for 15 minutes prior to removing and storing the supernatant at 4°C, adding 0.25ml of a protease inhibitor cocktail adapted for nickel-chelation chromatography.

The above inclusion body isolation technique was based on a documented method (Sambrook et al., 1989), with adaptations based on a combination of other methodologies following various trial isolation attempts (Altman et al., 1991, Altman et al., 1993, Fischer et al., 1992, Frayser et al., 1999, Rudolph, 1996, Rudolph and Lilie, 1996).

## 5.5 Purification and refolding of recombinant protein

A 1.7ml POROS®20MC perfusion chromatography® column was packed using the POROS® Self Pack® packing device on a Biocad 700E (*PerSeptive Biosystems Inc.*) as per manufacturer's instructions. The packed column was initially stripped and regenerated as per the manufacturer's instructions prior to saturating the column with nickel ions. The nickel ions were loaded using 400ml of the nickel loading buffer past over the column at 3ml/minute using a Biocad 700E, removing any unbound nickel using 10 column volumes of 0.5M sodium chloride. The prepared column was equilibrated in 20 column volumes of the wash solution for single chain. The protein suspension was passed through a 0.45µm filter before loading onto the equilibrated column at 3ml/minute in 5ml aliquots, each aliquot being separated by a 10 column volume wash step using the wash solution for single chain. The column was eluted using 10 column volumes of the elution solution for single chain. The eluted protein solution was stored at 4°C after adding 0.25ml of Bacterial Protease Inhibitor Cocktail.

Based on the work of several authors (Burrows et al., 1998, Frayser et al., 1999, Rudolph, 1996, Stöckel et al., 1997), slow refolding of the purified single chain protein construct was undertaken using serial dialysis at 4°C. A Seamless Cellulose dialysis membrane was prepared by boiling three times for 20 minutes each time in Milli-Q water. 20ml aliquots of the purified single chain protein construct were placed into the prepared membrane before dialyzing at 4°C against 2l of a solution containing 6M Urea, 150mM NaCl, 5mM reduced glutathione, 0.5% NP40, and 0.1% sodium azide in 20mM ethanolamine pH10. Dialysis was continued for 48 hours, changing the dialysate after 24 hours for a fresh solution. Dialysis was then continued in 48-hour stages using 2l of the following solutions:

- 150mM NaCl with 5mM reduced glutathione, 0.5% NP40, and 0.1% sodium azide in 20mM ethanolamine pH10
- 150mM NaCl with 5mM reduced glutathione, and 0.1% sodium azide in 20mM ethanolamine at pH10

- 150mM NaCl with 5mM reduced glutathione, 0.5mM oxidised glutathione and 0.1% sodium azide in 20mM ethanolamine at pH10
- PBS with 0.1% sodium azide
- PBS with 0.05% sodium azide

Once in PBS the refolded single chain construct was removed from the dialysis membrane and stored at 4°C with 0.25ml of Bacterial Protease Inhibitor Cocktail.

## 6 Cell Lysate Preparation

### 6.1 A20/HL60/BE1 Cell lysate

A20/HL60/BE1 cells were cultured in RPMI until at least  $10^7$  cells were available for lysis. The cell suspension was centrifuged at 2000g for 5 minutes at 5°C before discarding the media and resuspending the cell pellet by vortexing in 1ml PBS containing 2% NP40 and 75µl of Protease Inhibitor Cocktail (for mammalian cell extracts - *Sigma-Aldrich Company Limited*). The cells were vortexed frequently over a 1-hour period of storage on ice. The cell suspension was centrifuged at 3000g for 5 minutes at 0°C and the supernatant harvested. The supernatant was stored at -20°C until required.

### 6.2 Balb/c spleen lysate

The Balb/c spleen lysate was prepared using two methods. Initial work used a method adapted from Marrack *et al* (Marrack et al., 1993). The spleen was removed from a freshly killed Balb/c mouse and crushed between two frosted slides, placing the contents into 1ml PBS containing 2% NP40 and Protease Inhibitor Cocktail (for mammalian cell extracts - *Sigma-Aldrich Company Limited*) at 1ml per 20g wet weight of tissue. The spleen extract was sonicated on ice for 30 seconds three times 1 hour apart before centrifuging at 18000g at 0°C for 30 minutes. The resulting mixture was sonicated on ice before centrifuging as above. The supernatant

was removed and 200µl sterile water added to lyse any remaining red cells before centrifuging at 20000g for 10 minutes at 0°C. The supernatant containing the cell membrane suspension was removed and stored at -20°C until needed. Later work used an adaptation of this method in order to improve yield. The spleen pulp was initially homogenised using a Teflon-coated glass homogeniser on ice in the presence of the Protease Inhibitor Cocktail. The resulting suspension was centrifuged at 500g for 10 minutes at 4°C to remove nuclei and organelles. The supernatant was removed and centrifuged at 100000g for 2 hours at 4°C in a Beckman T70i ultracentrifuge (*Beckman Coulter (UK) Ltd.*) in order to pellet the membranes. The resulting pellet was resuspended in ice-cold PBS, 1% NP40, 0.05% Sodium azide, and Protease Inhibitor Cocktail before storing at -20°C until required.

## 7 Protein Identification Methods

### 7.1 SDS-PAGE

SDS-PAGE gels were prepared in the usual manner as laid out in Sambrook *et al* (Sambrook *et al.*, 1989). Once set, the gels were placed into an electrophoresis tank before being loaded with samples. Samples were mixed in a 50:50 ratio with SDS sample buffer prior to running at 120V, 20mA (per gel) for 1.5hours (*Consort E834*). 10µl of Perfect Protein™ Markers (*CN Bioscience*) was loaded in one well of each gel.

### 7.2 Western Blot

Proteins from the above gels were transferred onto a nitrocellulose membrane (*Schleicher & Schuell*) by blotting at 30V, 40mA in a wet blotting tank overnight. This enabled further analysis by antibody probing of the resulting membrane.

All procedures were carried out at room temperature. The membrane was initially stained with Ponceau S working solution for approximately 10 minutes prior



to developing the stain with three washes in 1% acetic acid solution. The stained marker lane was then excised from the membrane prior to blocking the membrane in a solution of 0.5% TWEEN 20 in PBS for 30 minutes. The nitrocellulose was then washed for 5 minutes (x3) in a solution of 0.1% TWEEN 20 in PBS, before exposing the membrane to the primary antibody diluted to the desired concentration in 0.1% TWEEN 20/PBS for 2 hours at room temperature on a rocking platform. The nitrocellulose was then washed in 0.1% TWEEN 20/PBS as before prior to exposing the membrane to the secondary antibody diluted in 0.1% TWEEN 20/PBS for 2 hours at room temperature.

At this juncture, two separate approaches were taken depending upon the nature of the proteins being assessed:

In the majority of cases, particularly for bacterially derived proteins, a two-layer approach was taken whereby the secondary antibody was conjugated to alkaline phosphatase. Following exposure to the secondary antibody, the membrane was washed with 0.1% TWEEN/PBS as previously prior to washing with alkaline phosphatase buffer for 5 minutes. Detection was carried out by adding solutions of both NBT and BCIP in a 1:400 dilution in alkaline phosphatase buffer. The colour was allowed to develop prior to stopping the reaction by washing in dH<sub>2</sub>O, allowing the membrane to air dry.

The alternative approach utilised a three-layer approach whereby the secondary antibody was conjugated to biotin (*Diagnostics Scotland*) with a tertiary layer composed of streptavidin-peroxidase (*Diagnostics Scotland*). Detection was carried out by adding either Sigma Fast<sup>TM</sup> 3,3'-Diaminobenzidine hydrochloride or 3-amino-9-ethylcarbazole as per the manufacturer's instructions.

See Table 2 for complete list of antibodies used.

Table 2 – Antibodies used

Antibody	Specificity	Isotype	Supplier	Working Dilution	Reference
<b>2G9</b>	Anti-mouse I-A <sup>d</sup> /I-E <sup>d</sup>	Rat IgG <sub>2a</sub> , $\kappa$	PharMingen	1:2000 (0.5mg/ml stock)	(Becker et al., 1992)
<b>14-4-4S</b>	Anti-mouse I-E <sup>k</sup> /I-E <sup>d</sup>	Murine IgG <sub>2a</sub> , $\kappa$	Hybridoma – Protein A purified supernatant	1:100	(Ozato et al., 1980, Ozato and Sachs, 1982)
<b>DA6.231</b>	Anti-human HLA-DR $\beta$	Murine IgG <sub>1</sub>	Hybridoma – Protein A purified supernatant	1:100	(Gorga et al., 1987, Guy et al., 1982, Stern and Wiley, 1992)
<b>DA6.147</b>	Anti-human HLA-DR $\alpha$	Murine IgG <sub>1</sub>	Hybridoma – Protein A purified supernatant	1:10	(Guy et al., 1982)
<b>L243</b>	Anti-human HLA-DR $\alpha\beta$ complex	Murine IgG <sub>2a</sub>	Hybridoma – Protein A purified supernatant	1:100	(Gorga et al., 1987, Lampson and Levy, 1980)
<b>YD1/63.4.10</b>	Anti-human HLA-DR	Rat IgG <sub>2a</sub>	Abcam Ltd.	1:400 (1mg/ml stock)	(Pawelec et al., 1982)

Antibody	Specificity	Isotype	Supplier	Working Dilution	Reference
<b>9E10</b>	Anti-human c-myc (carboxy terminus sequence - <i>EQKLISEEDL</i> )	Murine IgG <sub>1</sub>	Hybridoma – Protein A purified supernatant	1:100	(Campbell et al., 1992, Evan et al., 1985)
<b>His-Tag</b>	Anti-histidine tag (five consecutive histidine residues)	Murine IgG <sub>1</sub>	Novagen Inc.	1:500  (0.2mg/ml stock)	
<b>HSV-Tag</b>	Anti-Herpes Simplex Virus glycoprotein D sequence <i>GPELAPEDPED</i>	Murine IgG <sub>1</sub>	Novagen Inc.	1:10000	
<b>Anti-rat IgG AP</b>	Whole molecule of rat IgG	Goat IgG	Sigma- Aldrich	1:10000  (0.5-8mg/ml stock)	(Avrameas, 1969)
<b>Anti-mouse IgG AP</b>	Whole molecule of mouse IgG	Goat IgG	Sigma- Aldrich	1:10000	(Avrameas, 1969)
<b>Biotin anti- mouse IgG</b>	Whole molecule of mouse IgG	Biotin- sheep IgG	Diagnostics Scotland	1:1000	

### 7.3 Coomassie Brilliant Blue

Proteins from the above gels were also stained overnight using GelCode<sup>®</sup> Blue Stain Reagent (*Perbio Science*) as per the manufacturer's instructions. Although utilising the colloidal properties of Coomassie G-250, this system was not only more

convenient to use, but also yielded clearer results due to reduced background staining.

## 7.4 Silver Stain

For greater sensitivity in protein detection, a silver stain was adapted from Sambrook *et al* (Sambrook et al., 1989). All procedures were carried out at room temperature. The proteins were fixed by incubating overnight in five gel volumes of a solution of 30% ethanol, 10% glacial acetic acid and 60% Milli-Q water. The fixative solution was discarded and the gel washed twice in 10 gel volumes of 30% ethanol for 30 minutes each time. The gel was then washed three times in Milli-Q water for 10 minutes each time. The water was discarded and five gel volumes of freshly prepared 0.1% silver nitrate was added for 30 minutes. The gel was washed rapidly in Milli-Q water prior to developing in five gel volumes of a freshly prepared solution of 2.5% sodium carbonate and 0.02% formaldehyde in Milli-Q water. The developing reaction was quenched by washing the gel in 1% acetic acid prior to washing in dH<sub>2</sub>O.

All solutions were prepared using Milli-Q water in clean glass containers to reduce leaching from plastics. A rocking platform was used throughout to circulate the solutions around the gel, and all incubations were performed at room temperature.

## 7.5 Drying SDS-PAGE gels

SDS-PAGE gels were dried using a gel drying kit (*Promega Corporation*) following the manufacturer's instructions. In essence, the SDS-PAGE gels are washed in dH<sub>2</sub>O prior to placing between 2 sheets of Gel Drying Film that had been moistened in a solution of 40% methanol, 10% glycerol and 7.5% acetic acid. The films are clamped between two drying frames and allowed to dry at room temperature for 48hrs.

## 7.6 Immunoprecipitation

The immunoprecipitation method was adapted from that laid out in Sambrook *et al* (Sambrook *et al.*, 1989). The antigen/antibody mixture volume was adjusted using NET-gel buffer before incubating at 4°C on a rocking platform for 5 – 6 hours. The Protein A-sepharose was equilibrated in NET-gel buffer prior to adding 100µl of the suspension to the antigen/antibody mixture and continuing to incubate overnight. The Protein A-sepharose mixture was passed through a Mobicol® 1ml microcolumn (*MoBiTec GmbH*) with a 10µm pore filter to collect the sepharose beads. The beads were then washed twice with NET-gel buffer at room temperature for 20 minutes each time before washing once with 10mM Tris.Cl (pH 7.5)/0.1% NP40 for 30 minutes at room temperature. The beads were dried by centrifuging the column at 2000g at room temperature for 5 minutes. The antibody/antigen were eluted from the protein A-sepharose by incubating with 100µl 100mM glycine (pH 2.95) / 0.15M NaCl for 2 minutes at room temperature prior to centrifuging at 2000g for 10 minutes at room temperature. The eluate was collected in a microcentrifuge tube containing a neutralising quantity of 1M Tris (pH 8.0). The eluate was stored at -20°C until analysis.

## 7.7 Cytospin

Cytospins were prepared from cell suspensions of both induced and non-induced *Drosophila* S2 cells. 100µl of cell suspension was taken and centrifuged at 300g for 3 minutes onto Superfrost Plus® (*BDH Laboratory Supplies*) slides using a Shandon Cytospin 2® cytocentrifuge (*Thermo Shandon Inc.*). The slides were allowed to air-dry for 10 minutes prior to fixing in a solution of 90% chemically dry acetone and 10% methanol for 10 minutes at room temperature. The now fixed slides were then allowed to air-dry at room temperature before being stored at room temperature for a maximum of 48 hours. Slides were also stored at -20°C following the initial 10 minute period of air-drying at room temperature.

The fixed cells were first demarcated by encircling using an ImmEdge Pen<sup>®</sup> (*Vector Laboratories Inc.*). In order to stain the fixed cells, the slides were first washed in PBS +/- 0.1% saponin for two 5-minute washes at room temperature before blocking for non-specific protein binding. Blocking was achieved by sequentially washing with a solution of 1% BSA in PBS +/- 0.1% saponin for 30 minutes at room temperature followed by 1% serum (homologous to the secondary antibody to be applied) in PBS +/- 0.1% saponin for 30 minutes at room temperature. The slides were then washed twice for 5 minutes in PBS +/- 0.1% saponin prior to incubating flat with a 1:50 dilution of the primary antibody in PBS +/- 0.1% saponin for 1 hour at room temperature. The slides were then washed twice for 5 minutes in PBS +/- 0.1% saponin before incubating flat, hidden from light and at room temperature, with a 1:50 dilution of the relevant FITC-conjugated secondary antibody in PBS +/- 0.1% saponin. The slides were then washed 3 times for 5 minutes in PBS +/- 0.1% saponin prior to air-drying at room temperature. The stained slides were mounted in VectorShield with DAPI<sup>®</sup> (*Vector Laboratories Inc.*) under a coverslip before sealing with clear nail varnish.

The stained slides were viewed using an Axiovert S100<sup>®</sup> microscope (*Carl Zeis*) with a CoolSNAP<sup>®</sup> camera (*PhotoMetrics*) and Openlab 3.0<sup>®</sup> software (*Improvision*). In general, exposure times were as follows:

DAPI – 0.03s at x63(oil-immersion) and 1.00s at x32

FITC – 1.50s at x63(oil-immersion) and 8.00s at x32

The photographs were collated using Adobe<sup>®</sup> Photoshop<sup>®</sup> 6.0 (*Adobe Systems Inc.*), overlaying the FITC image onto the DAPI background image set at 45% opacity.

See Appendix 3 for list of solutions used.

## **Chapter 3**

### **Results (I)**



## Chapter 3

### Results (I)

## Formation of Soluble Recombinant I-E<sup>d</sup> Heterodimers Suitable for Tetramer formation

### 1 Introduction

Preliminary investigations were undertaken using murine I-E<sup>d</sup> for two main reasons. First, there was the prospect of undertaking interesting experiments aimed at studying important questions in collaboration with Dr R.N. Barker's group at the University of Aberdeen. Second, constructs and a working expression system were available locally that required relatively minor degrees of alteration to allow their theoretical viability.

Dr Barker's group have been investigating spontaneous autoimmune haemolytic anaemia (AIHA) that occurs in NZB mice. The target antigen for this is known to be the Band 3 anion channel protein found on red blood cells, and the process is known to be I-E<sup>d</sup> restricted (Elson and Barker, 2000, Perry et al., 1996). Therefore, this collaboration would enable any I-E<sup>d</sup> tetramer constructs to be tested *in vivo* within a working disease model, and would form the basis for the development of human MHC class II tetramer work within a developing disease model of Goodpasture's Disease.

Soluble recombinant I-E<sup>d</sup> devoid of its transmembrane domains (I-E<sup>d</sup>t) had been successfully produced using insect cell expression systems. Kozono *et al* (Kozono et al., 1994) had used a baculovirus based system to form soluble murine MHC class II proteins (I-E<sup>dk</sup> and I-A<sup>d</sup>) with covalently bound peptides, whilst Wallny *et al* (Wallny et al., 1995) had used the simpler *Drosophila melanogaster* Schneider cell expression system to form soluble I-E<sup>d</sup>t devoid of associated peptide. Given the success of the latter system as well as its relative ease of use, the

*Drosophila melanogaster* Schneider line 2 (S2) cell expression system was chosen. The rapidity of selection using hygromycin B and the ease of expression using the inducible metallothionein promoter adds to the systems favourability. Moreover, the cell lines are capable of growth in serum-free medium without a significant loss of protein expression, and in large-scale reactors so improving production and purification steps. The majority of proteins produced to date using this system have been functionally indistinguishable from their native counterparts, and have not required further refolding (Ivey-Hoyle, 1991).

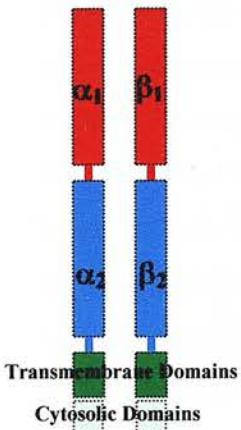
## 2 Construction of Recombinant I-E<sup>d</sup>tPCBirA

### 2.1 The I-E<sup>d</sup>βtBirA construct

Wallny *et al* (Wallny et al., 1995) had demonstrated the functionality of the expressed I-E<sup>d</sup>t in terms of peptide binding and T cell activation. They had exogenously loaded the soluble recombinant I-E<sup>d</sup>t proteins and used the resulting complexes to coat ELISA plates and show T cell activation by the formed complexes. Adapting this established functional system for TBB formation required modification of the construct (Figure 3.1). The necessary adaptations to I-E<sup>d</sup>t had largely been completed when I joined the laboratory and these will be briefly described here because my work built upon these constructs in general, specifically pRmHa3 I-E<sup>d</sup>βtBirA. Wallny *et al* (Wallny et al., 1995 15) kindly donated the constructs pRmHa-3 I-E<sup>d</sup>αt and I-E<sup>d</sup>βt. Two modifications to the I-E<sup>d</sup>βt were undertaken to enable its further use in tetramer formation:

Figure 3.1 – I-E<sup>d</sup> construct comparison

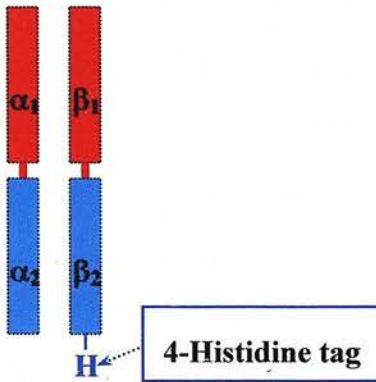
a) Natural murine I-E<sup>d</sup>



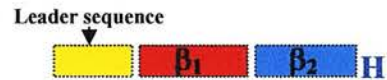
I-E<sup>d</sup> $\beta$  cDNA:



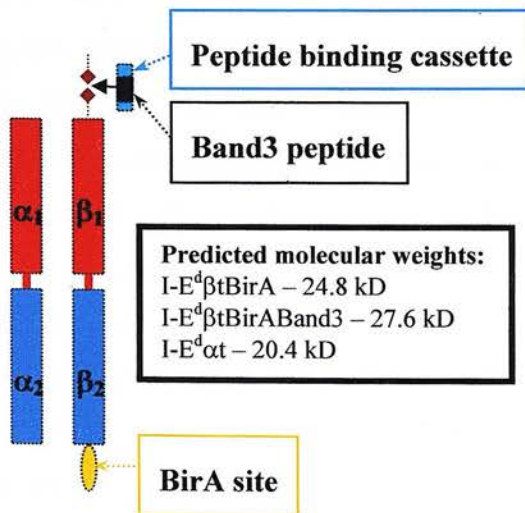
b) Recombinant truncated murine I-E<sup>d</sup>t (Wallny *et al* (Wallny et al., 1995))



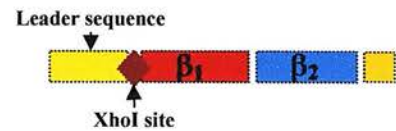
I-E<sup>d</sup> $\beta$ t cDNA:



c) Planned recombinant murine I-E<sup>d</sup>tBirA and I-E<sup>d</sup>tBand3



I-E<sup>d</sup> $\beta$ tBirA cDNA:



I-E<sup>d</sup> $\beta$ tPCBirA-Band3 cDNA:



The first modification was the addition of the BirA biotinylation consensus sequence to the carboxy terminus of the extracellular I-E<sup>d</sup> beta chain. This consensus sequence results in the covalent attachment of biotin, through the action of the *E.coli* biotin holoenzyme synthetase BirA, to a unique lysine residue (**K**) within the 13 amino acid consensus sequence domain (LxxILDAQKMVWx) (Beckett et al., 1999, Schatz, 1993). The consensus sequence used is the same as that used by Altman *et al* (Altman et al., 1996) and is based upon the work of Schatz (Schatz, 1993). The addition of this sequence to the carboxy terminus of I-E<sup>d</sup>βt permits enzymatic site-specific biotinylation of the recombinant I-E<sup>d</sup> beta chain. Such single-site biotinylation is important in order to ensure that later mixing with avidin results in four recombinant I-E<sup>d</sup>tBirA molecules being bound to each avidin molecule so forming a tetramer without interfering with T cell TCR binding. This modification was performed using the two oligonucleotides BirA1 and BirA2 (See Appendix 1) that were annealed to create the BirA adapter sequence. This sequence was inserted into the KpnI/BamHI site of pUC19, so forming pUC19BirA.

The second modification was the addition of a covalently linked peptide-binding domain to the amino terminus of the I-E<sup>d</sup> beta chain following on from the work of Kozono *et al* (Kozono et al., 1994). This would allow relatively easy insertion of cDNA encoding different peptides into the recombinant I-E<sup>d</sup>tBirA. This involved the insertion of an XhoI restriction site between the leader sequence and the start of the β<sub>1</sub> domain of I-E<sup>d</sup>βt (*vide infra*). The insertion of this site involved the separate PCR amplification of the I-E<sup>d</sup>βt leader sequence using the oligonucleotide pair IE1 and IE2 (See Appendix 1) and the I-E<sup>d</sup>βt sequence itself using oligonucleotide pair IE3 and IE4 (See Appendix 1). This amplification introduces an EcoRI site 5' of the leader sequence, an XhoI site 3' of the leader sequence and 5' of the I-E<sup>d</sup>βt sequence, and a KpnI Site 3' of the I-E<sup>d</sup>βt sequence. These two separate products were combined using the intervening XhoI site prior to expanding with the two outside oligonucleotides IE1 and IE4. This final product was inserted into pUC19BirA using the EcoRI and KpnI restriction sites so forming pUC19-I-E<sup>d</sup>βtBirA (Figure 3.2)

Figure 3.2 – Nucleotide and amino acid Sequences of I-E<sup>d</sup>βtBirA

a) Nucleotide sequence:

1	<b>GAATTC</b> GAGC	TCCTGCAGCA	<b>TGGTGTGGCT</b>	<b>CCCCAGAGTT</b>	<b>CCCTGTGTGG</b>
	<b>EcoRI</b>	<b>START</b>		<b>LEADER</b>	<b>SEQUENCE</b>
51	<b>CAGCTGTGAT</b>	<b>CCTGTTGCTG</b>	<b>ACAGTGCTGA</b>	<b>GCCCTCCAGT</b>	<b>GGCTTTGGTC</b>
101	<b>AGAGACACTC</b>	<b>GAG</b> GGCCACG	GTTTTTGGAA	TACGTTACAT	CTGAGTGTCA
	<b>XhoI</b>				
151	TTTCTACAAC	GGGACGCAGC	ACGTGCGGTT	TCTGGAGAGA	TTCATCTACA
201	ACCGGGAGGA	GAACCTGCGC	TTCGACAGCG	ACGTGGGCGA	GTACCGCGCG
251	GTGACAGAGC	TGGGGCGGCC	AGACCCGAG	AACTGGAACA	GCCAGCCGGA
301	GATCCTGGAG	GATGCGCGGG	CCTCGGTGGA	CACGTACTGC	AGACACAACT
351	ATGAGATCTC	GGATAAATTC	CTTGTGCGGC	GGAGAGTTGA	GCCTACGGTG
401	ACTGTGTACC	CCACAAAGAC	GCAGCCCCTG	GAACACCACA	ACCTCCTGGT
451	CTGCTCTGTG	AGTGACTTCT	ACCCTGGCAA	CATTGAAGTC	AGATGGTTCC
501	GGAATGGCAA	GGAGGAGGAA	ACAGGAATTG	TGTCCACGGG	CCTGGTCCGA
551	AATGGAGACT	GGACCTTCCA	GACACTGGTG	ATGCTGGAGA	CGGTTCTCTCA
601	GAGTGGAGAG	GTTTACACCT	GCCAGGTGGA	GCATCCCAGC	CTGACCGACC
651	CTGTCACGGT	CGAGTGGAAA	GCACAGTCCA	CATCTAGGGG	<b>TACCGCTAGC</b>
				<b>KpnI</b>	
701	<b>GGCGGTGGAC</b>	<b>TGCATCATAT</b>	<b>TCTGGATGCA</b>	<b>CAGAAAATGG</b>	<b>TGTGGAATCA</b>
751	TCGT <b>TAAGGA</b>	<b>TCC</b>		<b>Bir A</b>	<b>SEQUENCE</b>
	<b>STOP</b>	<b>BamHI</b>			

b) Protein sequence:

1	<b>RDTRG</b>	PRFLE	YVTSE	CHFYN	GTQHV	RFLER	FIYNR	EENLR
	<b>Peptide cassette link</b>							
41	FDSDV	GEYRA	VTELG	RPDAE	NWNSQ	PEILE	DARAS	VDTYC
81	RHNYE	ISDKF	LVRRR	VEPTV	TVYPT	KTQPL	EHHNL	LVCSV
121	SDFYP	GNIEV	RWFRN	GKEEE	TGIVS	TGLVR	NGDWT	FQTLV
161	MLETV	PQSGE	VYTCQ	VEHPS	LTDPV	TVEWK	AQSTS	RGTAS
201	<b>GGGLH</b>	<b>HILDA</b>	<b>QKMWV</b>	<b>NHR</b>				
	<b>BirA Sequence</b>							



Once formed in pUC19, the I-E<sup>d</sup>βtBirA construct was sequenced to confirm its accuracy before cloning into the expression vector pRmHa-3 using the EcoRI and BamHI restriction sites. Based on the murine model of AIHA, the linked peptide chosen was a Band 3 peptide previously shown to stimulate a vigorous T cell response.

The pRmHa3-I-E<sup>d</sup>αt construct required no modification from that described by Wallny *et al* (Wallny *et al.*, 1995).

## 2.2 The Peptide binding cassette construct

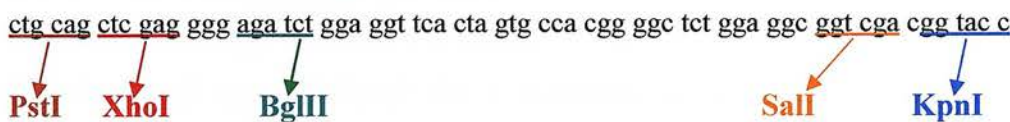
Peptide binding is an important component in the maintenance of MHC Class II heterodimeric stability and association (Germain and Hendrix, 1991). Therefore, a peptide-binding cassette was constructed in order to enable different peptides to be covalently linked to the N-terminus of I-E<sup>d</sup>βtBirA. In order to allow relatively easy insertion of cDNA encoding these different peptides we designed a cassette containing two insertion sites suitable to accept adapters for the desired peptides. The covalently linked peptides should thus occupy the peptide-binding groove of I-E<sup>d</sup>βtBirA, improving overall peptide-binding groove occupancy and stability. The peptide-binding cassette was modelled on the successful construct described by Kappler and Marrack's group (Kozono *et al.*, 1995, Kozono *et al.*, 1994, Liu *et al.*, 1997).

The cassette was generated by annealing the oligonucleotides PCTop and PCBottom (See Appendix 1) to generate a double-stranded adapter cDNA which was cloned into the XhoI/BglII sites of pUC19, forming pUC19pepcas. This plasmid was used to assemble and sequence the cDNAs encoding the desired peptide inserted into the cassette using the BglII site. The complete cassette could then be excised using XhoI/SalI prior to insertion into the XhoI site of I-E<sup>d</sup>βtBirA (Figure 3.3). The correct insertion of the cassette would require clarification through restriction enzyme digestion. Once the recombinant peptide had been formed linked to the I-

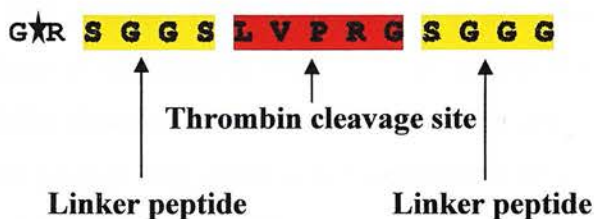
E<sup>d</sup>βtBirA construct, the linked peptide could, if desired, be released from its covalent linkage by thrombin enzymatic cleavage.

**Figure 3.3 – The peptide-binding cassette**

a) Nucleic acid sequence:



b) Amino acid sequence:



The diagram shows the nucleic acid sequence of the planned peptide-binding cassette, including its intrinsic unique restriction enzyme sites. The expected amino acid of the cassette is outlined, and the site of peptide linkage is asterisked.

I felt that it was necessary to assess the accuracy of the DNA sequences of I-E<sup>d</sup>αt and I-E<sup>d</sup>βtBirA within the pRmHa3 vector, particularly with respect to the reading frame of the sequences, prior to assessing the presence of inducible protein. Samples of both pRmHa3-I-E<sup>d</sup>αt and pRmHa3-I-E<sup>d</sup>βtBirA were sequenced using the metallothionein promoter oligonucleotide (pMT) as the sequencing primer. Analysis of the DNA sequences revealed that they were correct and in frame.



### 3 Expression of Recombinant I-E<sup>d</sup>tBirA - Preliminary work

#### 3.1 Transfection and selection of S2 cells

*Drosophila melanogaster* S2 cells were transfected by calcium phosphate precipitation with a mixture of 1µg pCoHYGRO (Hygromycin-resistance vector), 9µg I-E<sup>d</sup>αt, and 9µg of either I-E<sup>d</sup>βtBirA or I-E<sup>d</sup>βtPCBirA-Band3. Selection with Hygromycin-B was continued for a minimum of six weeks. Induction was performed with 1mM copper sulphate. Initial protein induction was carried out in the presence of Hygromycin-B, although the later work was carried out in its absence.

The selection of the Hygromycin-B concentration used was based upon an assessment of the concentration of Hygromycin-B needed to kill untransfected S2 cells whilst allowing the survival of transfected cells. Two six well plates were taken and each seeded with either a cell suspension of untransfected S2 cells or S2 cells transfected with the pCoHYGRO vector. Hygromycin-B was then added to the medium in each of the two plates in increasing concentrations per well (300, 500, 600, 700, 800 and 1000µg/ml), before incubating the plates in the cooled incubator at 25°C. After 72 hours incubation all of the transfected cells were found to be viable, however, the untransfected cells were only viable at the lowest Hygromycin-B concentration. After a further 72 hours, none of the untransfected cells were viable, whilst all of the transfected cells remained viable. Following from this brief experiment a concentration of 500µg/ml of Hygromycin-B was used as the selection concentration for all further experiments.

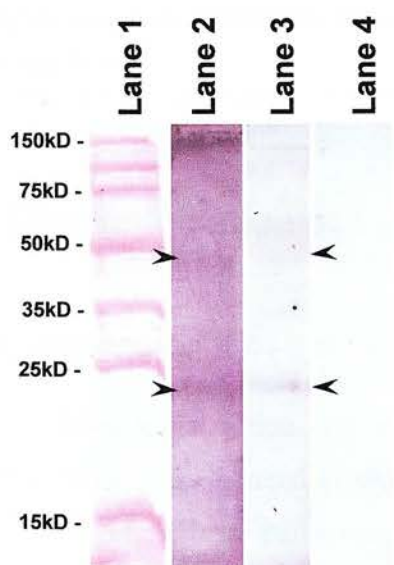
#### 3.2 Assessment of I-E<sup>d</sup> controls using monoclonal antibodies

In order to assess the formation of recombinant heterodimeric I-E<sup>d</sup> using the *Drosophila* expression system, positive controls needed to be established and antigen-specific monoclonal antibodies needed to be evaluated.

Two different protein controls were formed: an A20 cell lysate and a Balb/c spleen preparation. Each of these was assessed by Western blotting using the monoclonal antibodies 14-4-4S and 2G9 (Figure 3.4 & Figure 3.5).

2G9 identifies the I-E<sup>d</sup> $\alpha\beta$  heterodimeric band at approximately 50kD, as well as the monomeric  $\alpha$  band at approximately 25kD, within both the Balb/c spleen and the A20 cell lysates (Becker et al., 1992). 14-4-4S does not appear to bind to I-E<sup>d</sup> as well as 2G9 during Western blotting. The 14-4-4S antibody normally binds to a conformational epitope formed by both I-E<sup>d</sup>  $\alpha$  and  $\beta$  chains, which is altered during SDS-PAGE (Ozato and Sachs, 1982). However, the antibody does appear to bind weakly to I-E<sup>d</sup> $\alpha\beta$  heterodimeric band and an I-E<sup>d</sup> monomer band within the A20 lysate. Later work suggests that 14-4-4S may be specific to an I-E<sup>d</sup>  $\alpha$ -chain epitope (Spencer et al., 1993, Spencer and Kubo, 1989).

**Figure 3.4 – A20 cell lysate samples with I-E<sup>d</sup>-specific monoclonal antibodies**



**Key:**

**Lane 1** – Perfect Protein<sup>®</sup> marker

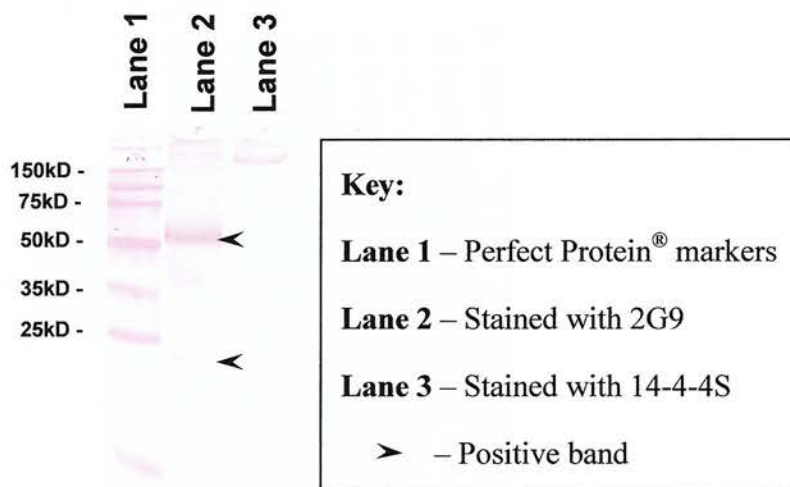
**Lane 2** – Stained with 14-4-4S

**Lane 3** – Stained with 2G9

**Lane 4** – Stained with anti-mouse IgG alone

➤ – Positive band

A20 cell lysate samples were separated by SDS-PAGE and transferred onto nitrocellulose by Western blotting. The nitrocellulose was probed using both I-A/I-E – specific monoclonal antibodies. A faint band at about 25kD is identified by both monoclonal antibodies, and represents the separate I-E<sup>d</sup> $\alpha$  chain. This is more clearly defined with 2G9. A faint band is also seen at 50kD with both monoclonal antibodies representing the heterodimeric I-E<sup>d</sup>. No non-specific staining is seen with secondary antibody alone.

**Figure 3.5 – Balb/c spleen lysate samples with I-E<sup>d</sup>-specific monoclonal antibodies**

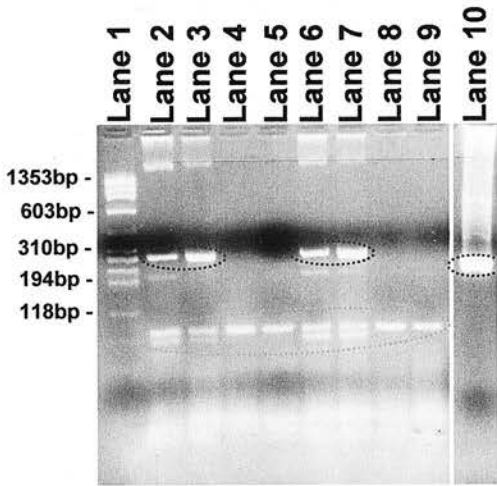
Balb/c spleen lysate samples were separated by SDS-PAGE and transferred onto nitrocellulose by Western blotting. The nitrocellulose was probed using both I-A/I-E – specific monoclonal antibodies. A definite band at about 50kD is identified by 2G9 representing the heterodimeric I-E<sup>d</sup>αβ. Fainter bands are seen at about 25kD that represent the monomeric α chain of I-E<sup>d</sup>. No definite staining is seen with 14-4-4S.

## 4 Characterisation of Expression of Recombinant I-E<sup>d</sup>

### 4.1 Assessment of transcription

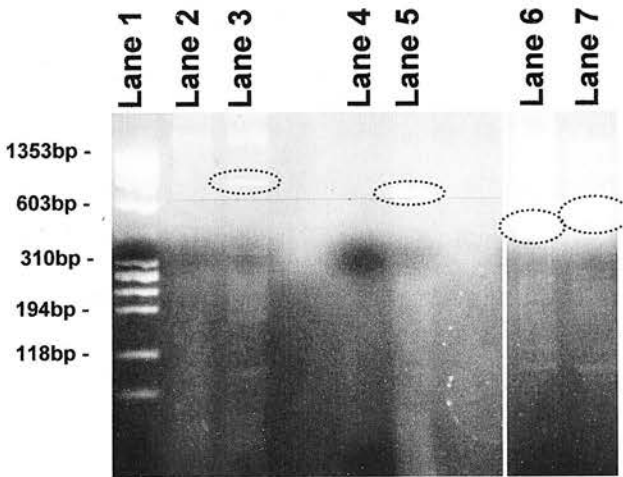
DNA transcription was assessed in duplicate using RT-PCR of extracted mRNA from both induced (1mM CuSO<sub>4</sub>) and non-induced S2 cells (Figure 3.6). The following primer pairs were used for gene-specific amplification following cDNA synthesis:

- For IE<sup>d</sup>αt – SC3 and SCm4 (See Appendix 2)
- For IE<sup>d</sup>βtBirA - IE1 and IE4 (See Appendix 1)

**Figure 3.6 - I-E<sup>d</sup> transcription assessed by RT-PCR**a) Transcription of I-E<sup>d</sup>  $\alpha$ -chain assessed by RT-PCR**Key:****Lane 1** – Hae III DNA digest ladder**Lane 2** – I-E<sup>d</sup>tBirA – non-induced S2 cells**Lane 3** - I-E<sup>d</sup>tBirA – induced S2 cells**Lane 4** – I-E<sup>d</sup>tBirA – non-induced S2 cells (Reverse transcriptase inactivated)**Lane 5** – I-E<sup>d</sup>tBirA – induced S2 cells (Reverse transcriptase inactivated)**Lane 6** - I-E<sup>d</sup>tBand3 – non-induced S2 cells**Lane 7** - I-E<sup>d</sup>tBand3 – induced S2 cells**Lane 8** - I-E<sup>d</sup>tBand3 – non-induced S2 cells (Reverse transcriptase inactivated)**Lane 9** - I-E<sup>d</sup>tBand3 – induced S2 cells (Reverse transcriptase inactivated)**Lane 10** – pRmHa3-I-E<sup>d</sup> $\alpha$ t plasmid

– Positive bands

– Primer dimers/trimers

b) Transcription of I-E<sup>d</sup>  $\beta$ -chain assessed by RT-PCR**Key:**

**Lane 1** – Hae III DNA digest ladder

**Lane 2** – I-E<sup>d</sup>tBirA – non-induced S2 cells

**Lane 3** – I-E<sup>d</sup>tBirA – induced S2 cells

**Lane 4** – I-E<sup>d</sup>tBand3 – non-induced S2 cells

**Lane 5** – I-E<sup>d</sup>tBand3 – induced S2 cells

**Lane 6** – pRmHa3-I-E<sup>d</sup> $\beta$ tBirA plasmid

**Lane 7** – pRmHa3-I-E<sup>d</sup> $\beta$ tPCBirABand3 plasmid

 – Positive bands

mRNA was extracted and treated with RNase-free DNase I (*Promega Corporation, USA*) prior to first strand synthesis to reduce DNA cross-contamination. A concurrent control was also performed as per manufacturer's instructions to assess DNA cross-contamination by inactivating the M-MuLV reverse transcriptase. Separate micro-tubes were used for cDNA synthesis intended for assessment of IE<sup>d</sup> alpha chain and beta chain mRNA using gene-specific primers. First strand cDNA was generated by M-MuLV reverse transcriptase and PCR was used to amplify the cDNA using the gene specific primers (32 cycles, denature at 95°C for 30 seconds and anneal at 55°C for 30seconds). Positive controls for the PCR step were formed using the plasmids pRmHa3-IE<sup>d</sup> $\alpha$ t, pRmHa3-IE<sup>d</sup> $\beta$ tBirA and pRmHa3-IE<sup>d</sup> $\beta$ tPCBirABand3. The PCR products were analysed by agarose gel electrophoresis. The above is a representative gel from three experiments.

RT-PCR shows the production of the I-E<sup>d</sup>βt chain mRNA only in the induced cells (Figure 3.6b). In terms of the I-E<sup>d</sup>αt chain, it would appear that some mRNA is present in the uninduced cells, although this is increased upon induction (Figure 3.6a). This does not appear to be secondary to DNA contamination as there are no bands in the negative control lanes. The above experiment indicates that DNA transcription of pRmHa3-IE<sup>d</sup>αt, pRmHa3-IE<sup>d</sup>βtBirA and pRmHa3-IE<sup>d</sup>βtPCBirABand3 plasmids was taking place upon induction of the cells with copper.

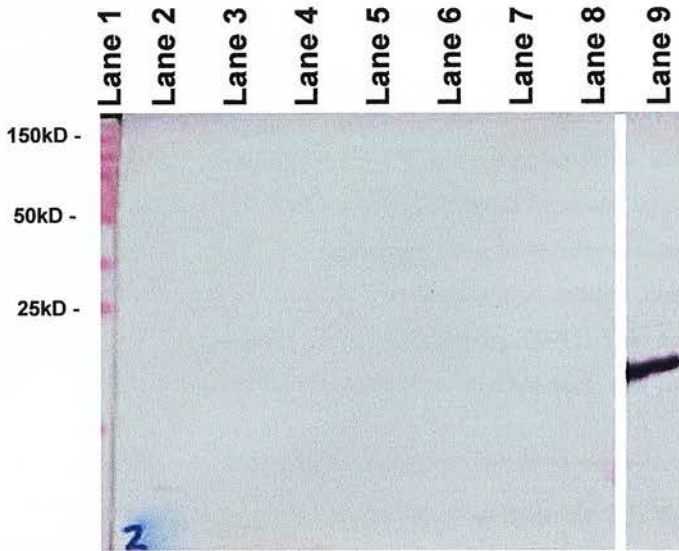
## 4.2 Assessment of protein production within induced S2 cell supernatant

Preliminary work using S2 cells stably transfected with pRmHa3-human α3 Type (IV) collagen NC1 domain had shown protein production after 2 days of copper induction, continuing for at least 16 days. S2 cells stably transfected with pRmHa3-IE<sup>d</sup>α and pRmHa3-IE<sup>d</sup>βtBirA (+/- covalently linked Band3 peptide) were induced using 1mM copper sulphate for 10 days. The supernatant from the induced cells was analysed by Western blot probed with I-A/E<sup>d</sup> specific monoclonal antibody 2G9 (Figure 3.7). No identifiable I-E<sup>d</sup>tBirA was detected in this preliminary induction using 1mM copper ions in the presence of Hygromycin-B. The possibility of low-level production was assessed by repeating the above induction. S2 cells stably transfected pRmHa3-IE<sup>d</sup>α and pRmHa3-IE<sup>d</sup>βtBirA were induced as above and a larger volume of cell supernatant concentrated by immunoprecipitation using the 14-4-4S monoclonal antibody (Figure 3.8). This revealed faint bands at around 30kD in lanes 1 and 2, at a similar level to the bands seen in the control lane 3. The predicted molecular weights of I-E<sup>d</sup>βtBirA, I-E<sup>d</sup>αt and native I-E<sup>d</sup>α and I-E<sup>d</sup>β being 24.8kD, 20.4kD, and about 34kD and 29kD respectively. No similar bands are seen in the antibody alone lane (Lane 4). The dual banding may represent differential I-E<sup>d</sup>αt and βt chain SDS-PAGE mobilities. 2G9 certainly competes with the I-Aβ chain specific monoclonal antibody MK-D6 (Ruberti et al., 1992), although the paper



describing the development of 2G9 implies recognition of the I-A/I-E $\alpha$  chain rather than a conformational epitope *per se* (Becker et al., 1992). The yield of I-E<sup>d</sup>tBirA, therefore, appears to be at a low level using the current induction regimen, although the formed protein appears to be “conformationally correct” given its immunoprecipitation using 14-4-4S. However, the disparity between the expected molecular weights of the immunoprecipitated proteins and their apparent weights is difficult to explain other than to consider the result a spurious one.

**Figure 3.7 – Assessment of I-E<sup>d</sup>tBirA production by stably transfected S2 cells**



**Key:**

**Lane 1** – Perfect Protein® marker

**Lane 2** – Supernatant from untransfected S2 cells

**Lane 3** – Supernatant from S2 cells transfected with human  $\alpha 3(\text{IV})$  collagen

**Lane 4** – Supernatant from S2 cells transfected with I-E<sup>d</sup>tBand3

**Lane 5** – Supernatant from S2 cells transfected with I-E<sup>d</sup>tBirA

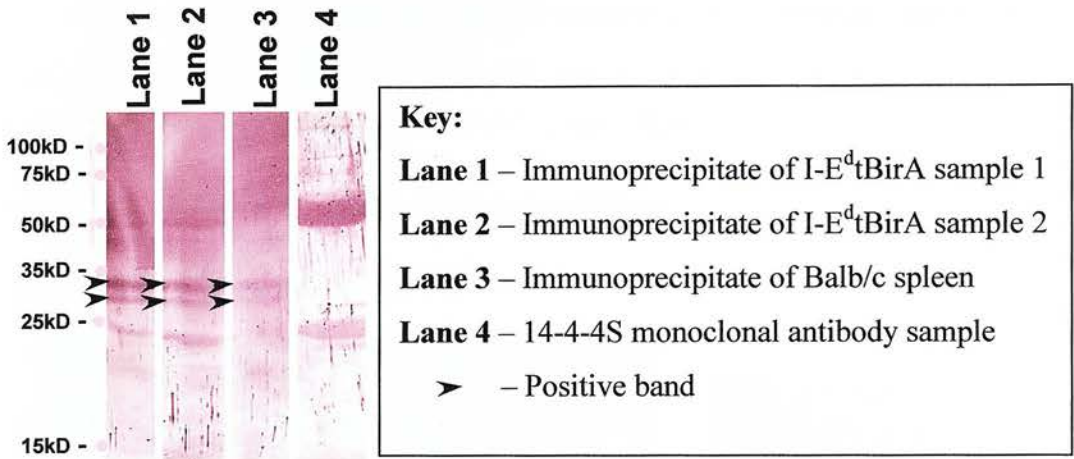
**Lane 6** – Supernatant from S2 cells transfected with murine  $\alpha 3(\text{IV})$  collagen

**Lane 7 & 8** – Supernatant from S2 cells transfected with human  $\alpha 5(\text{IV})$  collagen

**Lane 9** – Concentrated recombinant I-E<sup>d</sup>t from I-E<sup>d</sup>t transfected S2 cell supernatant

2G9 immunoblot of supernatant taken from induced S2 cells transfected with constructs coding for one of five different protein sequences. The only positive band seen is in the positive control Lane 9. This is representative of five separate protein induction experiments.



Figure 3.8 - Immunoprecipitation of I-E<sup>d</sup>tBirA

S2 cells stably transfected with pRmHa3-IE<sup>d</sup>βtBirA and pRmHa3-IE<sup>d</sup>αt were induced using 1mM copper sulphate. The supernatant was harvested after 72 hours by centrifuging the cell suspension at 500g for 5 minutes at 15°C. 40ml of supernatant was immunoprecipitated using the 14-4-4S monoclonal antibody. Balb/c spleen was used as the positive antigen control. The elution was performed using 100μl SDS gel-loading buffer (containing DTT). The immunoprecipitates were separated by SDS-PAGE gel electrophoresis before a Western blot was performed using 2G9 as previous.

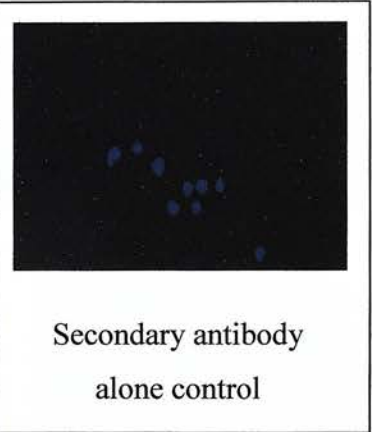
The results indicated possible expression of soluble I-E<sup>d</sup>tBirA complexes that bound 14-4-4S, but at much lower levels than expected from previous reports {Wallny, 1995 #15}. Possible causes for the disappointing results could have included the concentration of copper used at induction, the length of the induction period, as well as the presence of hygromycin at induction. These factors were separately assessed on at least two occasions each, but the results remained disappointingly unchanged, with a consistent lack of identifiable I-E<sup>d</sup>tBirA protein in induced S2 cell supernatants. Although previous work using pRmHa3-human α3 Type (IV) collagen NC1 domain had shown variations in expressed protein production between stably transformed cell populations, this could not be a feasible explanation for the consistent lack of identifiable I-E<sup>d</sup>tBirA protein. Therefore, the possibility of intracellular sequestration of the induced protein due to poor secretion was investigated.

### 4.3 Assessment of protein production within induced S2 cells

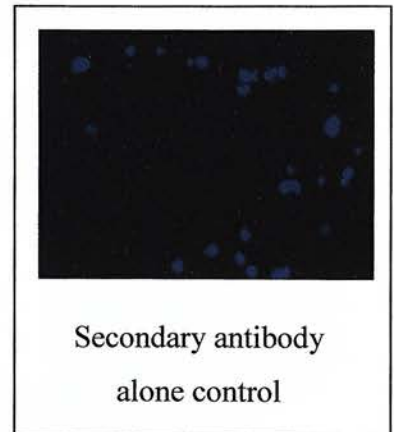
In order to investigate the possible sequestration of proteins within induced cells, cytopins of both the induced and non-induced S2 cells were made. The cytopins were stained using either 2G9 (Figure 3.9) or 1444S.

**Figure 3.9 – Cytopin of S2 cells transfected with I-E<sup>d</sup>tBirA (+/- Band3) stained using 2G9**

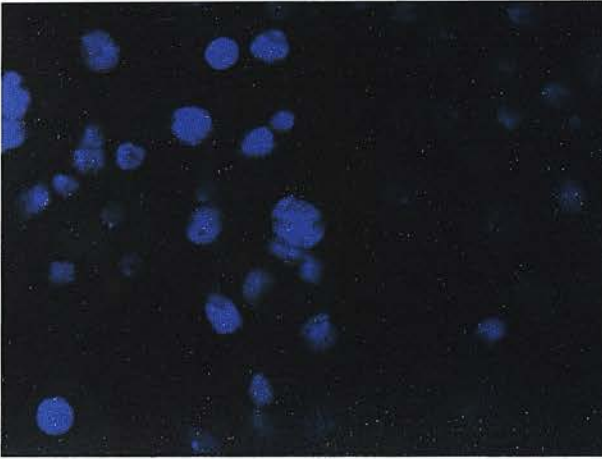
a) Induced S2 cells with I-E<sup>d</sup>tBirA (No saponin used) – X400 magnification



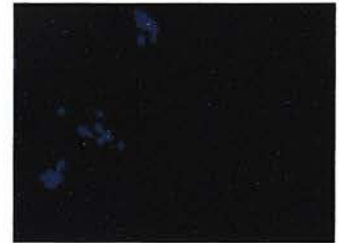
b) Induced S2 cells with I-E<sup>d</sup>tBirA (Saponin used) – X400 magnification



c) Uninduced S2 cells with I-E<sup>d</sup>tBirA (Saponin used) – X630 magnification



d) Induced S2 cells with I-E<sup>d</sup>tBirABand3 (No saponin used) – X400 magnification

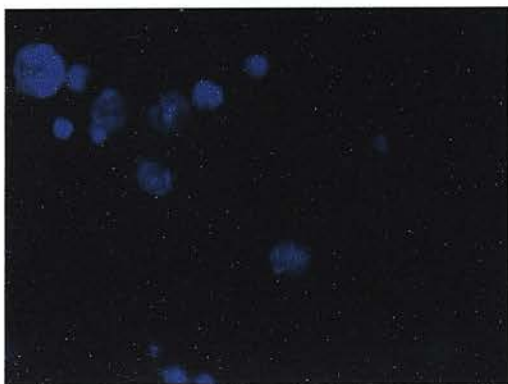


Secondary antibody  
alone control

e) Induced S2 cells with I-E<sup>d</sup>tBirABand3 (Saponin used) – X400 magnification



Secondary antibody  
alone control

f) Uninduced S2 cells with I-E<sup>d</sup>tBirABand3 (Saponin used) – X630 magnification

The S2 cells were washed and probed in the presence and absence of saponin. Saponin was utilised in order to permeabilise the S2 cell membranes and allow intracellular protein identification. 2G9 was used at a 1:50 dilution for 2 hours at room temperature before washing and developing using FITC-conjugated goat-anti-rat IgG at a 1:50 dilution for 1 hour at room temperature. Uninduced S2 cells were used as negative controls for the primary antibody, whilst the secondary antibody alone was used to assess for non-specific staining. The above are representative cytopins from three experiments.

The cytopins stained with 2G9 reveal low-level I-E<sup>d</sup>tBirABand3 and I-E<sup>d</sup>tBirA protein production. The staining pattern appears to be cytoplasmic, whether with or without saponin, indicating that the cytopin process may have permeabilised the cells. There is no clear indication of excessive intracellular protein sequestration (Figure 3.9). Non-specific staining is not seen in the secondary antibody alone control slides, and there is no evidence of protein production in the uninduced cells. There does not appear to be any subjective difference between transfectants carrying the linked Band 3 peptide and those simply carrying the empty peptide-binding cassette. Similar results were seen when using 14-4-4S. These results are in keeping with the findings of both supernatant immunoprecipitation and RT-PCR of probable low-level protein production.



## 5 Discussion

Attempts at producing the modified murine I-E<sup>d</sup>tBirA +/- linked Band3 peptide resulted in poor protein yield. Although nucleic acid work had shown the accuracy of the DNA sequences and their transcription on copper induction, translational problems appear to have occurred preventing significant protein production. The system was tested in the absence of selection agent to minimise cellular toxicity at induction with no real difference in outcome. Certainly difficulties had been experienced with yield by other groups using eukaryotic expression of 'empty' MHC Class II molecules (McMichael and Kelleher, 1999), and this had led to the use of covalently linked peptide to the amino terminus of the  $\beta$ 1 chain of MHC Class II molecules using a flexible linker (Crawford et al., 1998, Kozono et al., 1994). One drawback to this approach is that separate constructs would have to be engineered for each peptide being analysed. However, the presence of covalently linked peptide did not appear to improve protein production in my system, highlighting that such modifications are not always successful. It is possible that the relatively minor modifications to the I-E<sup>d</sup> $\beta$ t resulted in a reduction of expression efficiency, however the reasons for this remain unclear.

It was clear that changes to the construct and/or expression system would be necessary to obtain sufficient protein to form tetramers. I considered exploring further the reasons for the poor yield, but reports from other groups clearly indicated that efficient production required careful enhancement of  $\alpha\beta$  association either through non-covalent or covalent binding. Two techniques were beginning to emerge in the literature:

Work by Cosson *et al* (Cosson and Bonifacino, 1992) identified the importance of the transmembrane domains of MHC Class II molecules in facilitating their heterodimeric association, although not necessarily their peptide-binding ability. The importance of chain pairing is further highlighted by reports that separate MHC Class II chains may bind peptide (Dornmair and McConnell, 1990, Rothenhausler et al., 1990), and indeed that this binding may induce antigen-specific apoptosis of T cells (Nag et al., 1996). Acid-base leucine zipper dimerisation

domains had been successfully used to replace the transmembrane domains and lead to the production of recombinant soluble MHC Class II heterodimers (Novak et al., 1999, Radu et al., 1998, Scott et al., 1998). Following discussions with Dr E. Sally Ward's group, they made their acid-base leucine zipper motif available to me for further modification to enable its use in my constructs (See Chapter 4).

The second technique used bacterial expression to improve yield, and radically altered the way in which the heterodimeric peptide-binding domain of MHC Class II was formed. Burrows *et al* (Burrows et al., 1998, Burrows et al., 1999) had developed a single chain construct linking the rat RT1.B  $\beta_1$  to the  $\alpha_1$  domain in such a way that they could be refolded into an active and functional peptide binding domain (See Chapter 5).

As both techniques were evolving and not yet of proven utility, I decided to utilise both in a twin-pronged attack on the generation of murine and human MHC Class II multimers.

## **Chapter 4**

### **Results (II)**



## Chapter 4

### Results (II)

## Formation of Leucine Zipper-associated Recombinant Heterodimeric HLA-DR Tetramer Building Blocks

### 1 Introduction

I decided to adapt a technique that has been successfully used by other groups to facilitate the heterodimeric pairing between two protein chains. The leucine zipper motif mediates dimerization of a number of different proteins, classically DNA-binding proteins. The motif is a sequence of leucine residues spaced every seventh amino acid residue along an alpha helix, and as a result, all the leucine residues of the motif are placed along one side of the alpha helix. According to the zipper model, the leucine side chains extending from the leucine repeats are able to interdigitate with the leucine side chains of a second polypeptide chain that contains the same motif. Therefore, the hydrophobic surfaces of two leucine repeating sequences of the protein molecules interact to form homo or heterodimers (Landschulz et al., 1988). Based on the Fos-Jun leucine zipper interaction O'Shea *et al* (O'Shea et al., 1993) engineered an acid-base leucine zipper coiled-coil structure that had additional unfavourable electrostatic interactions in the homodimeric state, so further favouring heterodimeric association. This strategy was used to enhance the heterodimeric pairing of a TCR  $\alpha$  and  $\beta$  chain (Chang et al., 1994), and was developed further by Dr E. Sally Ward's group to improve the heterodimeric association and stability of recombinant I-A<sup>u</sup> and I-A<sup>q</sup> expressed using the baculovirus insect cell expression system (Radu et al., 1998). Dr W. Kwok's group also developed the same strategy for the formation of recombinant HLA-DR4 using the *Drosophila* S2 expression system (Novak et al., 1999).

Other groups have successfully used such a chain-pairing strategy. Scott *et al* (Scott et al., 1996, Scott et al., 1998) used leucine zippers to improve the yield and

stability of ‘empty’ functional I-A<sup>d</sup> expressed in *Drosophila melanogaster* SC2 cells using the pRmHa3 vector. Wucherpfennig’s group have used the Fos/Jun transcription factor leucine zipper motifs to aid in the formation of secreted HLA-DR2 using both a yeast (Kalandadze et al., 1996) and a baculovirus expression system (Gauthier et al., 1998, Smith et al., 1998).

Following a presentation by Dr Radu (Radu, 1999), I approached his group regarding the use of their acid-base leucine zipper construct in my own work. As we were working on different disease models, Dr Ward kindly donated cDNA encoding the zipper motifs. This chapter describes my design, production and characterisation of HLA-DR15 and HLA-DR7 heterodimers utilising acid-base leucine zippers to promote heterodimer formation.

## **2 Design of Acid-Base Leucine Zipper-associated HLA-DR15 and HLA-DR7 Molecules**

The aim of this strategy is to promote both the association and stability of the HLA-DR  $\alpha\beta$  heterodimeric complex by replacing the transmembrane domains of the  $\alpha$  and  $\beta$  chains with acidic and basic leucine zipper sequences respectively. The use of these zipper motifs would fix the alignment of the alpha and beta chains, so correct design was imperative. Therefore, I modelled my construct design on that successfully used by Dr Ward’s group (Radu et al., 1998) by aligning the sequence of the I-A<sup>d</sup> molecule they adapted with the sequences of HLA-DR15 and DR7 using Clustal X (Thompson et al., 1997). The alignments shown in Figure 4.1 identified the positions in the sequence of HLA-DR $\alpha$  and  $\beta$  where insertion of the leucine zipper sequences would most closely resemble the successful construct produced by Dr Ward’s group.

Figure 4.1 - Alignment of I-A and HLA-DR peptide sequences

**Alignment of MHC Class II alpha chain peptide sequences**I-A<sup>q</sup> alpha chain -    **I E A D H V--E L T E T - *Linker sequence***HLA-DRA\*0101 -    **I E E K H V--E T T E N - *Transmembrane*****Alignment of MHC Class II beta chain peptide sequences**I-A<sup>q</sup> beta chain -    **H F V A Q L--E S A L S K - *Linker sequence***HLA-DRB1\*1501 -    **R F L W Q P--E S A Q S K - *Transmembrane***HLA-DRB1\*0701 -    **R F L W Q G--E S A Q S K - *Transmembrane***

The sequences for I-A<sup>q</sup> were provided with the constructs donated by Dr Ward's group (C.G. Radu, personal communication). The HLA-DR sequences were obtained from the GenBank sequence database. The figure shows extracts of the alignments taken at the commencement of the I-A<sup>q</sup> alpha and beta sequences and the junction site with the transmembrane domain.

The design features of the construct were (Figure 4.2):

- An acidic and basic leucine zipper sequence at the carboxy terminus of the extracellular alpha and beta chain domains respectively to enhance heterodimer formation and the yield of conformationally correct HLA-DR molecules.
- A polyhistidine tail at the carboxy terminus of the alpha chain acidic leucine zipper to aid identification of the alpha chain and protein purification by metal chelation chromatography (Kuroda et al., 2000, Scott et al., 1998).

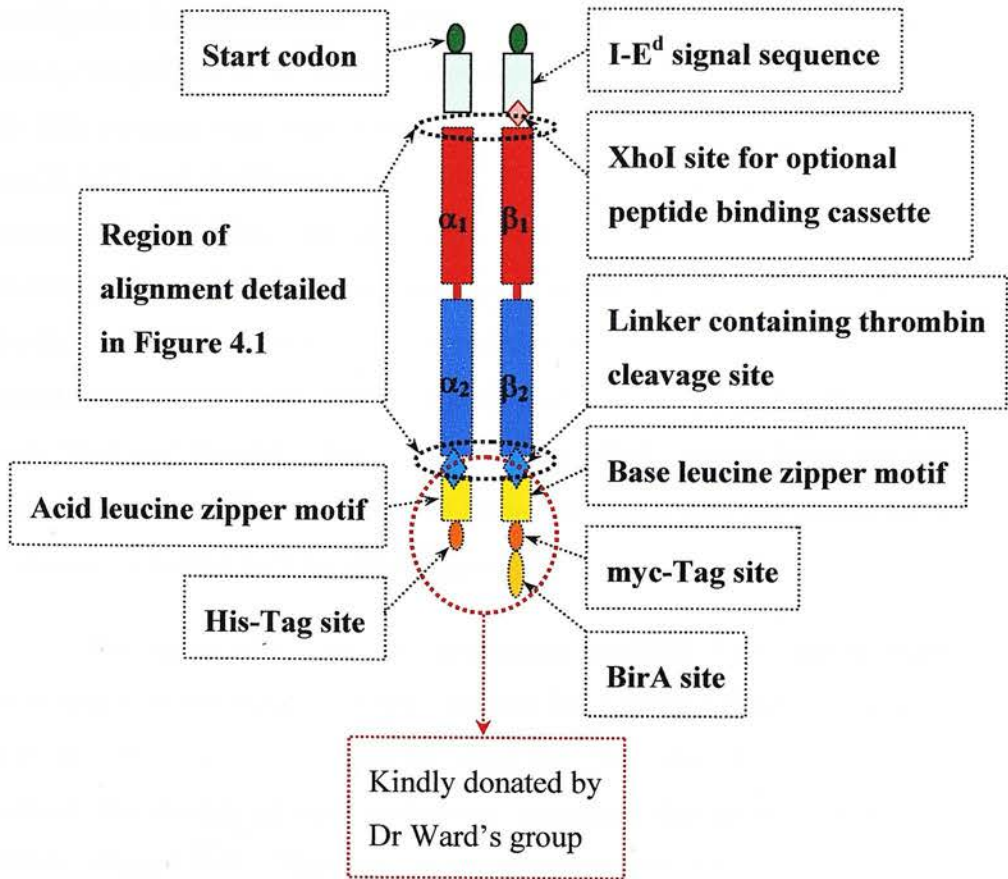
- c) A human c-myc tag at the carboxy terminus of the beta chain basic leucine zipper to aid beta chain identification.
- d) A linker sequence between the  $\alpha$  and  $\beta$  chains and their relevant tail sections that not only allows for greater flexibility of the final heterodimer, but also contains a thrombin cleavage site which can be used to release each chain from its tail. The flexibility afforded by these linker sequences may allow or even facilitate clustering of the MHC – peptide – TCR complex on the surface of an antigen-specific T cell. Such flexibility might also compensate for any errors in chain alignment.
- e) A site-specific biotinylation sequence at the carboxy terminus of the beta chain construct. This sequence would permit site-specific biotinylation of the beta chain and enable multimerisation of the resulting  $\alpha\beta$  heterodimer using the avidin-biotin interaction as per “classical” tetramer design.
- f) No covalently attached peptide was specified in order to allow different peptides to be associated. This would enable various reagents to be formed in order to analyse T cells (Kwok et al., 2001, Novak et al., 2001a). Provision was made for later insertion of covalently attached peptide should problems arise with poor heterodimeric association, yield, or peptide loading by the introduction of the peptide-binding cassette described previously via the preserved XhoI site at the N-terminus of the  $\beta$  chains (Figure 4.3).

Construction of the design involved the following:

- a) Formation of the extracellular portions of HLA-DRA1\*0101, HLA-DRB1\*1501, and HLA-DRB1\*0701 using PCR based upon the alignment above.
- b) Ligation of the above sequences into a modified pUC19 vector containing the murine I-E<sup>d</sup> signal sequence (Figure 3.2). The murine signal sequence was used for logistical reasons as it was readily available and was known to be functionally successful (see Results (I)).

- c) Excision of acidic and basic zipper and associated sequences from the I-A<sup>q</sup> constructs provided by Dr Ward's group and ligation of these 3' of the above.
- d) Transfer of the above to the expression vector pRmHa3

Figure 4.2 – HLA-DR zipper-associated construct



### 3 Construction of Leucine Zipper Associated HLA-DR $\alpha$ Chain

#### 3.1 Construction of extracellular alpha chain

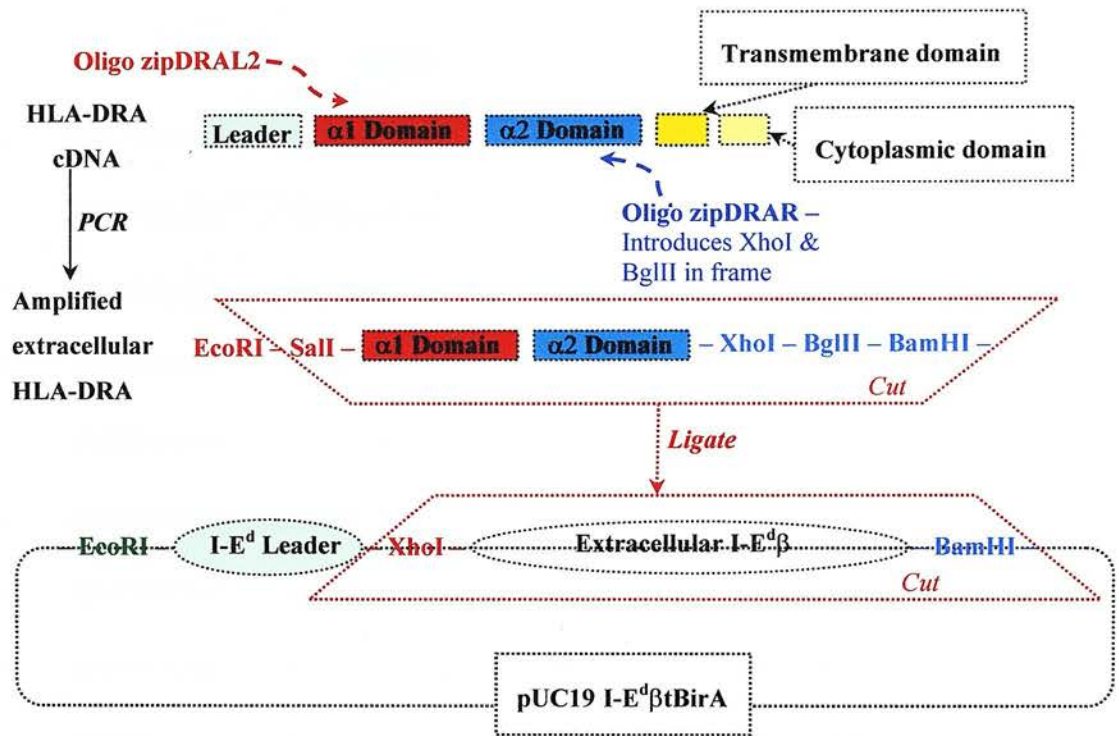
The extracellular HLA-DRA1\*0101 cDNA sequence was obtained by RT-PCR of mRNA from DR2Lum cells extracted using the QuickPrep<sup>TM</sup> Micro mRNA purification kit (*Amersham Pharmacia Biotech*). RT-PCR was performed using Ready-To-Go<sup>®</sup> RT-PCR beads (*Amersham Pharmacia Biotech*). The cDNA formed by this process was then amplified by PCR using the oligonucleotide primers zipDRAL2 and zipDRAR (Appendix 1). The PCR was carried out over 30 cycles (Denature at 95°C for 1 minute, anneal at 56°C for 1 minute, extend at 72°C for 90 seconds). The 603bp DNA product was separated by agarose gel electrophoresis and purified using the QIAEX II<sup>®</sup> gel extraction protocol. This DNA product was then restricted with Sall and BamHI, and ligated into the pUC19-I-E<sup>d</sup> $\beta$ tBirA restricted with XhoI and BamHI. This resulted in the DNA product being ligated in-frame with the murine I-E<sup>d</sup> start codon and leader sequence, with the loss of the I-E<sup>d</sup> $\beta$ tBirA sequence including its XhoI site (Figure 4.3).

The ligated construct was transformed into DH5 *E.coli* and the transformants were tested for the presence of the expected DNA using a panel of restriction enzyme digests. DNA sequencing using the using pUC19 primer 'M13 forward' was used to confirm the identity of the transformant containing the desired plasmid sequence – WSA1 (Figure 4.4). This part of the construct was relatively straight forward to produce, only requiring two attempts for a successful outcome.

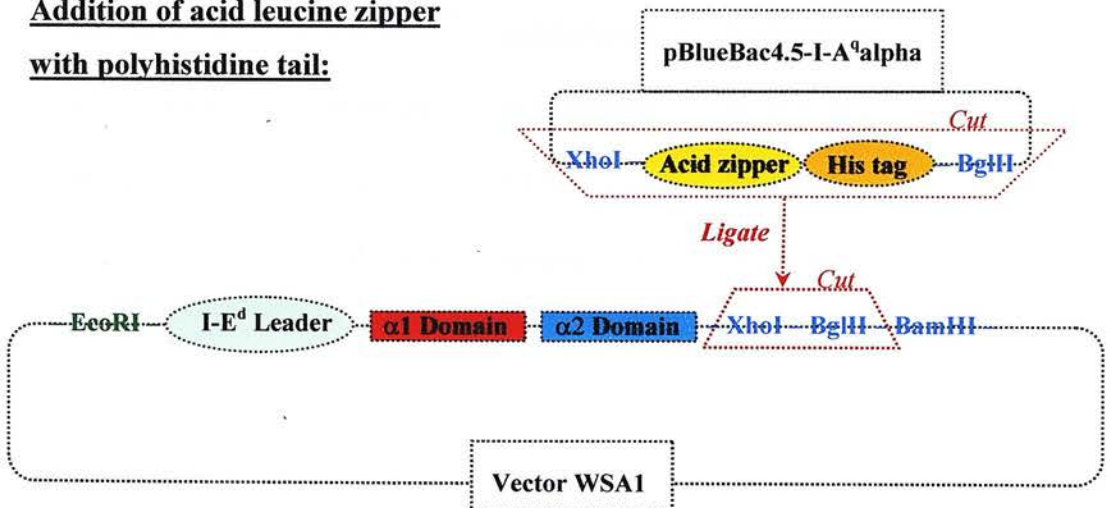


Figure 4.3 – Construction of HLA-DRA with acidic leucine zipper

### Formation of WSA1:



### Addition of acid leucine zipper with polyhistidine tail:



### Final construct (WSA2):



NB: Restriction enzyme sites of importance marked



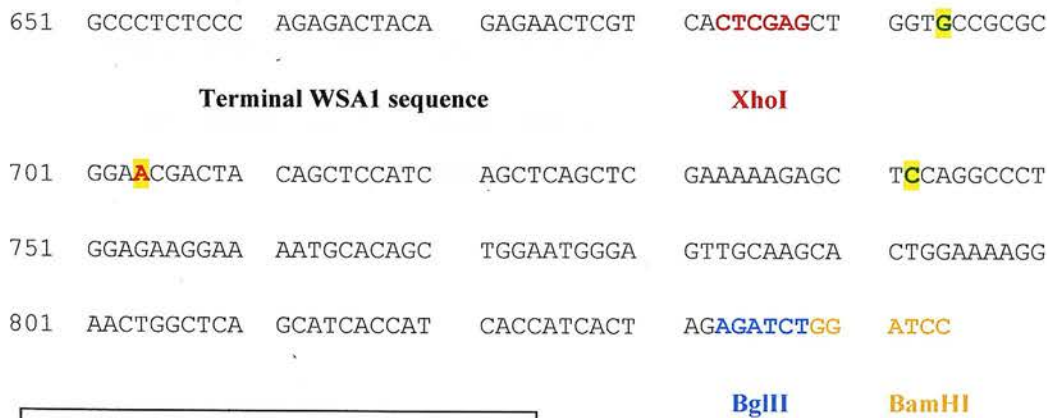
Figure 4.4 – WSA1 nucleotide sequence

1	GAATTCGAGC	TCCTGCAGCA	TGGTGTGGCT	CCCCAGAGTT	CCCTGTGTGG
	EcoRI	START			
51	CAGCTGTGAT	CCTGTTGCTG	ACAGTGCTGA	GCCCTCCAGT	GGCTTTGGTC
101	AGAGACACTC	GACATGTGAT	CATCCAGGCC	GAGTTCTATC	TGAATCCTGA
151	CCAATCAGGC	GAGTTTATGT	TTGACTTTGA	TGGTGATGAG	ATTTTCCATG
201	TGGATATGGC	AAAGAAGGAG	ACGGTCTGGC	GGCTTGAAGA	ATTTGGACGA
251	TTTGCCAGCT	TTGAGGCTCA	AGGTGCATTG	GCCAACATAG	CTGTGGACAA
301	AGCCAACCTG	GAAATCATGA	CAAAGCGCTC	CAACTATACT	CCGATCACCA
351	ATGTACCTCC	AGAGGTAACT	GTGCTCACGA	ACAGCCCTGT	GGAAGTGAGA
401	GAGCCCAACG	TCCTCATCTG	TTTCATCGAC	AAGTTCACCC	CACCAGTGGT
451	CAATGTCACG	TGGCTTCGAA	ATGGAAAACC	TGTCACCACA	GGAGTGTGAG
501	AGACAGTCTT	CCTGCCCAGG	GAAGACCACC	TTTTCCGCAA	GTTCCACTAT
551	CTCCCCCTTC	TGCCCTCAAC	TGAGGACGTT	TACGACTGCA	GGGTGGAGCA
601	CTGGGGCTTG	GATGAGCCTC	TTCTCAAGCA	CTGGGAGTTT	GATGCTCCAA
651	GCCCTCTCCC	AGAGACTACA	GAGAACTCGT	CAC <b>TCGAGAG</b>	<b>ATCTGGATCC</b>
				XhoI	BglIIBamHI

3.2 Addition of acid leucine zipper to extracellular alpha chain

The acid leucine zipper and polyhistidine tag sequence was excised from the vector provided by Dr Ward’s group (pBlueBac4.5 with I-A<sup>q</sup>Alpha (Radu et al., 1998)) by restricting with XhoI and BglII. Concomitantly, WSA1 was restricted with Xho I and Bgl II and dephosphorylated prior to ligation with the above. The ligated construct was then transformed into DH5 *E.coli* and the transformants were tested for the presence of the expected DNA using restriction enzyme digestion. DNA sequencing with the pUC19 primer ‘M13 reverse’ was used to confirm the identity of the transformant containing the desired plasmid sequence - WSA2. Sequencing showed three base changes compared to the expected sequence resulting in a single conservative amino acid change of a threonine to a serine near the beginning of the acid leucine zipper motif and far removed from the peptide-binding groove (Figure 4.5). This part of the construct was relatively straight forward to produce, only requiring two attempts for a successful outcome.

Figure 4.5 – Acid leucine zipper and polyhistidine sequence of WSA2



Key:

- C** – No amino acid change resulting
- A** – Leads to Ser rather than Thr

### 3.3 Transfer of $\alpha$ -chain construct to pRmHa3 expression vector

The  $\alpha$ -chain construct (HLA-DRAz) was excised from WSA2 using BamHI and EcoRI, and ligated into pRmHa3-I-E<sup>d</sup> $\alpha$ t (see Chapter 4) restricted with the same enzyme pair. The ligated construct was then transformed into DH5 *E.coli* and the transformants tested for the presence of the expected DNA using a panel of restriction enzyme digests. This part of the construct was straight forward to produce, only requiring one attempt for a successful outcome. DNA was purified from a “midi-prep” of the transformant containing the expected DNA bands. This DNA was used for transfecting *D.melanogaster* S2 cells (*vide infra*). The expected translated protein sequence is seen in Figure 4.6.

**Figure 4.6 – HLA-DRAz protein sequence**

1	HVIIQ	AEFYI	NPDQS	GEFMF	DFDGD	EIFHV	DMAKK	ETVWR
41	LEEFQ	RFASF	EAQGA	LANIA	VDKAN	LEIMT	KRSNY	TPITN
81	VPPEV	TVLTN	SPVEL	REPNV	LICFI	DKFTP	PVVNV	TWLRN
121	GKPVT	TGVSE	TVFLP	REDHL	FRKFH	YLPFL	PSTED	VYDCR
161	VEHWG	LDEPL	LKHWE	FDAPS	PLPET	TENSS	LLEVP	RGSTT
						<b>Linker Thrombin site</b>		
181	APSAQ	LEKEL	QALEK	ENAQL	EWELQ	ALEKE	LAQHH	HHHH
	<b>Linker</b>	<b>Acidic leucine zipper</b>				<b>Polyhistidine tag</b>		

## 4 Construction of Leucine Zipper Linked HLA-DR $\beta$ Chains

### 4.1 Construction of extracellular beta chains

The extracellular HLA-DRB1\*1501 cDNA sequence was obtained by RT-PCR of mRNA from DR2Lum cells as noted above. The cDNA formed by this process was then amplified by PCR using the oligonucleotide primers zipDRBL and zipDRBR (Appendix 1) in the same manner as their  $\alpha$ -chain counterparts noted above. The 615bp DNA product was separated by agarose gel electrophoresis and purified using the QIAEX II<sup>®</sup> gel extraction protocol. This DNA product was then restricted with XhoI and HindIII, and ligated into the vector pUC19-I-E<sup>d</sup>tBirA restricted with the same enzyme pair. This resulted in the DNA product being ligated in-frame with the murine I-E<sup>d</sup> start codon and leader sequence. The ligated construct was transformed into DH5 *E.coli* and the transformants were tested for the presence of the expected DNA using a panel of restriction enzyme digests. DNA sequencing using the using pUC19 primer 'M13 forward' was used to confirm the integrity of the transformant containing the desired plasmid sequence – WSB1-15 (Figure 4.7).

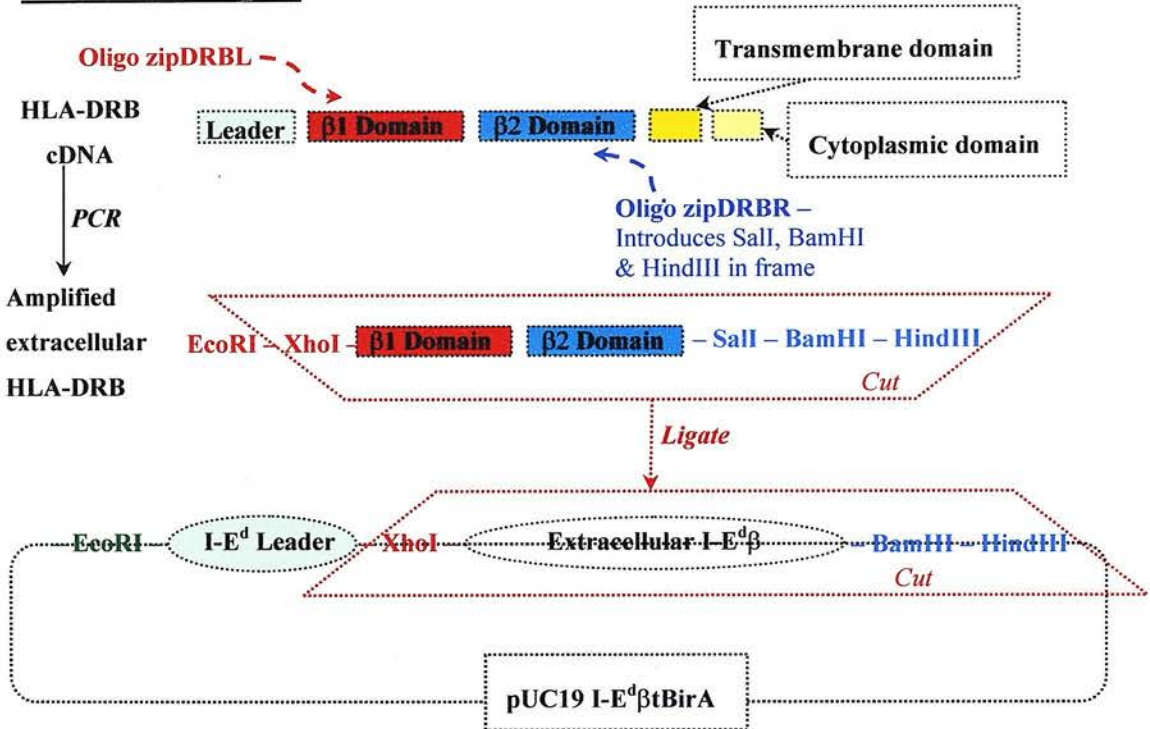
The extracellular HLA-DRB1\*0701 DNA sequence was obtained by PCR using the oligonucleotide primers zipDRBL and zipDRBR on HLA-DR7 cDNA cloned from HLA-DR7 positive B cells by Mrs D. Wojtacha. This template was shown by DNA sequencing to contain exon 2 of HLA-DRB1\*0701. The PCR was carried out over 30 cycles (Denature at 95°C for 1 minute, anneal at 55°C for 90 seconds, extend at 72°C for 90 seconds). The single 615bp DNA product was separated by agarose gel electrophoresis and purified using the QIAEX II<sup>®</sup> gel extraction protocol. This DNA product was then restricted with XhoI and HindIII, and ligated into the vector pUC19-I-E<sup>d</sup>tBirA as above. DNA sequencing using the using pUC19 primer 'M13 forward' was used to confirm the identity of the transformant containing the desired plasmid sequence – WSB1-7 (Figure 4.8).

This section of construct formation was relatively straight forward, only requiring two attempts for a successful outcome in each case.

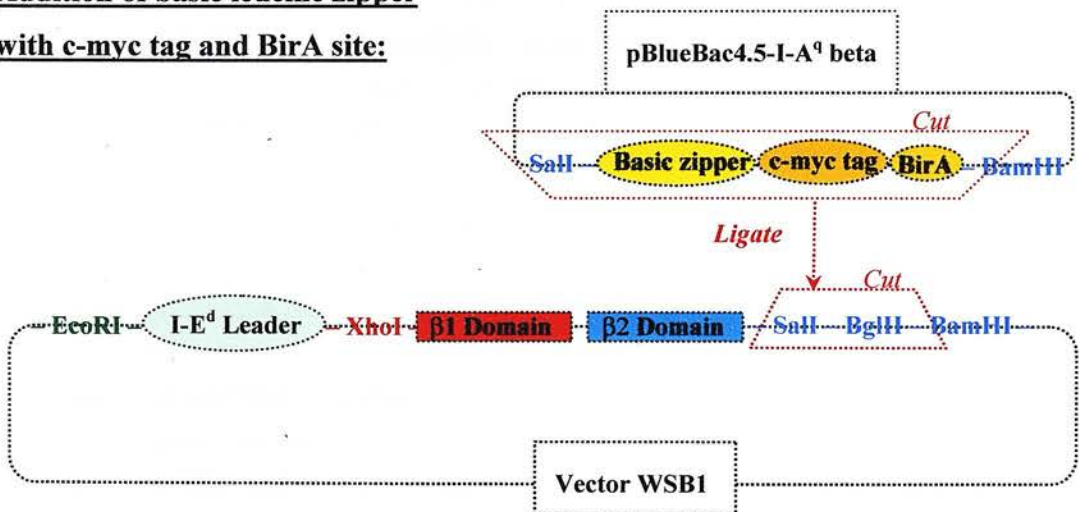


Figure 4.7 - Construction of DRB with zipper

### Formation of WSB1:



### Addition of basic leucine zipper with c-myc tag and BirA site:



### Final construct (WSB2):



NB: Restriction enzyme sites of importance marked

Figure 4.8 – WSB1-07 and WSB1-15 nucleotide sequences

15		<b>GAATTC</b> GAGC	TCCTGCAGCA	TGGTGTGGCT	CCCCAGAGTT	CCCTGTGTGG
07	1	-----	-----	-----	-----	-----
		<b>EcoRI</b>				
15	51	CAGCTGTGAT	CCTGTTGCTG	ACAGTGCTGA	GCCCTCCAGT	GGCTTTGGTC
07		-----	-----	-----	-----	-----
15		AGAGACA <b>CTC</b>	<b>GAG</b> CCCCACG	TTTCCTGTGG	CAGCCTAAGA	GGGAGTGTCA
07	101	-----	-----	-----	---GG---T	ATA-----
		<b>XhoI</b>				
15	151	TTTCTTCAAT	GGGACGGAGC	GGGTGCGGTT	CCTGGACAGA	TACTTCTATA
07		-----C	-----	-----A---	-----A---	CT-----
15	201	ACCAGGAGGA	GTCCGTGCGC	TTCGACAGCG	ACGTGGGGGA	GTTCCGGGCG
07		-----	--T-----	-----	-----	--A-----
15	251	GTGACGGAGC	TGGGGCGGCC	TGACGCTGAG	TACTGGAACA	GCCAGAAGGA
07		-----	-A-----	--T---C---	-C-----	-----
15	301	CATCCTGGAG	CAGGCGCGGG	CCGCGGTGGA	CACCTACTGC	AGACACAAC
07		-----	G-CAG-----	G-CA-----	----GTG---	-----
15	351	ACGGGGTTGT	GGAGAGCTTC	ACAGTGACAGC	GGCGAGTCCA	ACCTAAGGTG
07		-----G	T-----	-----	-----	T---G-----
15	401	ACTGTATATC	CTTCAAAGAC	CCAGCCCCTG	CAGCACCACA	ACCTCCTGGT
07		-----G----	--G-C-----	T-----	-----	-----
15	451	CTGCTCTGTG	AGTGGTTTCT	ATCCAGGCAG	CATTGAAGTC	AGGTGGTTCC
07		-----	-----	-----	-----	-----
15	501	TGAACGGCCA	GGAAGAGAAG	GCTGGGATGG	TGTCCACAGG	CCTGATCCAG
07		G-----	-----	-----G---	-----	-----
15	551	AATGGAGACT	GGACCTTCCA	GACCCTGGTG	ATGCTGGAAA	CAGTTCCTCG
07		-----	-----	-----	-----	-----
15	601	AAGTGGAGAG	GTTTACACCT	GCCAAGTGGA	GCACCCAAGC	GTGACAAGCC
07		G-----A	-----	-----	-----T	----TG----
15	651	CTCTCACAGT	GGAATGGAGA	GCACGGTCTG	AATCTGCACA	GAGCAAGTCG
07		-----	-----	-----	-----	-----
15		TCAG <b>TCGACG</b>	<b>GATCCAAGCT</b>	<b>T</b>		
07	701	-----	-----	-		
		<b>Sall</b>	<b>BamHI</b>	<b>HindIII</b>		



## 4.2 Addition of basic leucine zipper to extracellular beta chains

The basic leucine zipper sequence with its c-myc tag and BirA site-specific biotinylation sequence was excised from the vector provided by Dr Ward's group (pBlueBac4.5 with I-A<sup>q</sup>Beta (Radu et al., 1998)) by restricting with SalI and BamHI. Concomitantly, the WSB1 vectors were restricted with same enzyme pair and dephosphorylated prior to ligation with the above. The ligated constructs were then transformed into DH5 *E.coli* and the transformants tested for the presence of the expected DNA using restriction enzyme digestion. DNA sequencing with 'M13 reverse' was used to confirm the identity of the transformants containing the desired plasmid sequences - WSB2-07 and WSB2-15 (Figure 4.9). The sequencing showed no changes from the expected. This part of the construction process was relatively straight forward, only requiring one attempt for a successful outcome.

**Figure 4.9 – Basic leucine zipper, c-myc tag and BirA sequence for WSB2**

15		AATCTGCACA	GAGCAAGTCG	TCAG <b>TCGACC</b>	TGGTTCCGCG
7	681	-----	-----	-----	-----
				<b>SalI</b>	
15	721	CGGATCGACT	ACAGCTCCAT	CAGCTCAGTT	GAAAAAGAAA
7		-----	-----	-----	-----
15	761	TTGCAAGCAC	TGAAGAAAAA	GAACGCTCAG	CTGAAGTGGA
7		-----	-----	-----	-----
15	801	AACTTCAAGC	CCTCAAGAAG	AAACTCGCCC	AGGTCACCGT
7		-----	-----	-----	-----
15	841	CTCCTCAGAA	CAAAACTCA	TCTCAGAAGA	GGATCTGAAT
7		-----	-----	-----	-----
15	881	AGTGGCGGTG	GCCCAGGTGG	CCTGGTTTCT	ATCTTCGAAG
7		-----	-----	-----	-----
15		CTCAGAAAAT	CGAATGGCAC	TAAG <b>GGATCCA</b>	AGCTT
7	921	-----	-----	-----	-----
				<b>BamHI</b>	

### 4.3 Transfer of $\beta$ -chain constructs to pRmHa3 expression vector

The  $\beta$ -chain constructs (HLA-DRB15z and HLA-DRB7z) were separately transferred to the vector pRmHa3-I-E<sup>d</sup> $\alpha$ t as noted for the  $\alpha$ -chain constructs. The ligated constructs were then transformed into DH5 *E.coli* and the transformants tested for the presence of the expected DNA using a panel of restriction enzyme digests. DNA was purified from a “midi-prep” of the transformant containing the expected DNA bands. The restriction enzyme digests of the pRmHa3-DR $\beta$ 15z transformant were found to contain all the expected DNA bands, whilst that of pRmHa3-DR $\beta$ 7z was less clear. Sequencing performed using the pMT promoter primer later revealed that both vectors contained the expected sequence. This DNA was used for transfecting *D.melanogaster* S2 cells *vide infra*. The expected translated peptide sequences are seen in Figure 4.10.

**Figure 4.10 – HLA-DRB15z and -DR7z peptide sequences**

15	1	DTRGP	RFLWQ	PKREC	HFFNG	TERVR	FLDRY	FYNQE
07		-----	-----	G-YK-	-----	----Q	--E-L	-----
		<b>Leader end</b>						
15	36	ESVRF	DSDVG	EFRAV	TELGR	PDAEY	WNSQK	DILEQ
07		-F----	-----	-Y----	-----	-V--S	-----	-----D
15	71	ARAAV	DTYCR	HNYGV	VESFT	VQRRV	QPKVT	VYPSK
07		R-GQ-	--V--	-----	G----	-----	H-E--	---A-
15	106	TQPLQ	HHNLL	VCSVS	GFYPG	SIEVR	WFLNG	QEEKA
07		-----	-----	-----	-----	-----	--R--	-----
15	141	GMVST	GLIQN	GDWTF	QTLVM	LETVP	RSGEV	YTCQV
07		-V----	-----	-----	-----	-----	-----	-----
15		EHPSV	TSPLT	VEWRA	RSESA	QSKSS	VDLVP	RGSTT
07	176	-----	M-----	-----	-----	-----	-----	-----
						<b>Linker</b>		
						<b>Thrombin site</b>		
15/07	211	APSAQ	LKKKL	QALKK	KNAQL	KWKLQ	ALKKK	LAQVT
		<b>Linker</b>		<b>Base zipper sequence</b>				
15/07	246	VSSEQ	KLISE	EDLNS	GGGPG	GLVSI	FEAQK	IEWH
			<b>c-myc Tag</b>		<b>Linker</b>		<b>BirA sequence</b>	

## 5 Expression of Leucine Zipper-Associated Heterodimeric HLA-DR15 Construct

### 5.1 Establishment of stable S2 cell transfectants

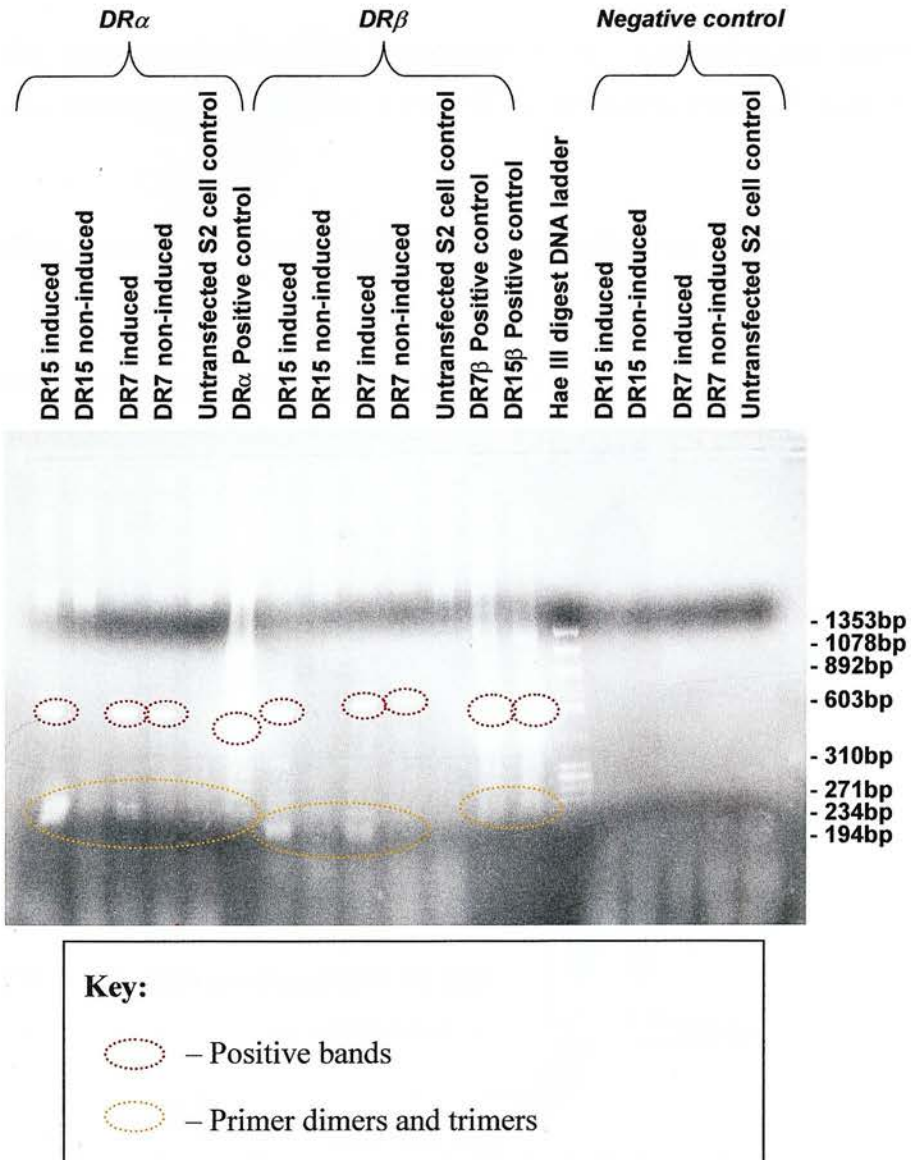
S2 cells were stably transfected with pRmHa3-DRAz and pRmHa3-DRB15z by calcium phosphate precipitation as per Methods. Selection was carried out using Hygromycin-B for at least eight weeks before induction was attempted. Prior to induction the medium was changed in order to remove the Hygromycin-B in order to improve the protein production as noted previously (W. Kwok, *personal communication*).

Appropriate transcription of pRmHa3-DRAz and pRmHa3-DRB15z was tested in duplicate by RT-PCR of mRNA extracted from stable transfectants with or without prior induction with copper sulphate. The following gene-specific primer pairs were used:

- For DRAz – zipDRAL2 and zipDRAR (Appendix 1)
- For DRB15z – zipDRBL and zipDRBR (Appendix 1)

The resulting DNA was analysed by agarose gel electrophoresis. As shown in Figure 4.11, the relevant mRNA is only expressed upon induction of the transfected S2 cells for both the DRAz and DRB15z chains. There is no DNA contamination using the methods outlined as seen by the lack of bands in the negative control wells. The untransfected S2 cells do not have the relevant DNA transcript upon induction.

Figure 4.11 – DR15 and DR7 mRNA RT-PCR



mRNA from S2 cells stably transfected with pRmHa3-DRAz and pRmHa3-DRB15z or pRmHa3-DRB7z was extracted and treated with RNase-free DNase I (*Promega Corporation, USA*) prior to first strand synthesis to reduce DNA cross-contamination. A concurrent control was also performed as per manufacturer's instructions to assess DNA cross-contamination by inactivating the M-MuLV reverse transcriptase. Separate micro-tubes were used for cDNA synthesis intended for assessment of alpha chain and beta chain mRNA using gene-specific primers. First strand cDNA was generated by M-MuLV reverse transcriptase and PCR was used to amplify the cDNA using the gene specific primers. Positive controls for the PCR step were formed using the plasmids pRmHa3-DRAz, pRmHa3-DRB15z and pRmHa3-DRB7z. The PCR products were analysed by agarose gel electrophoresis. The above is a representative gel from three experiments.

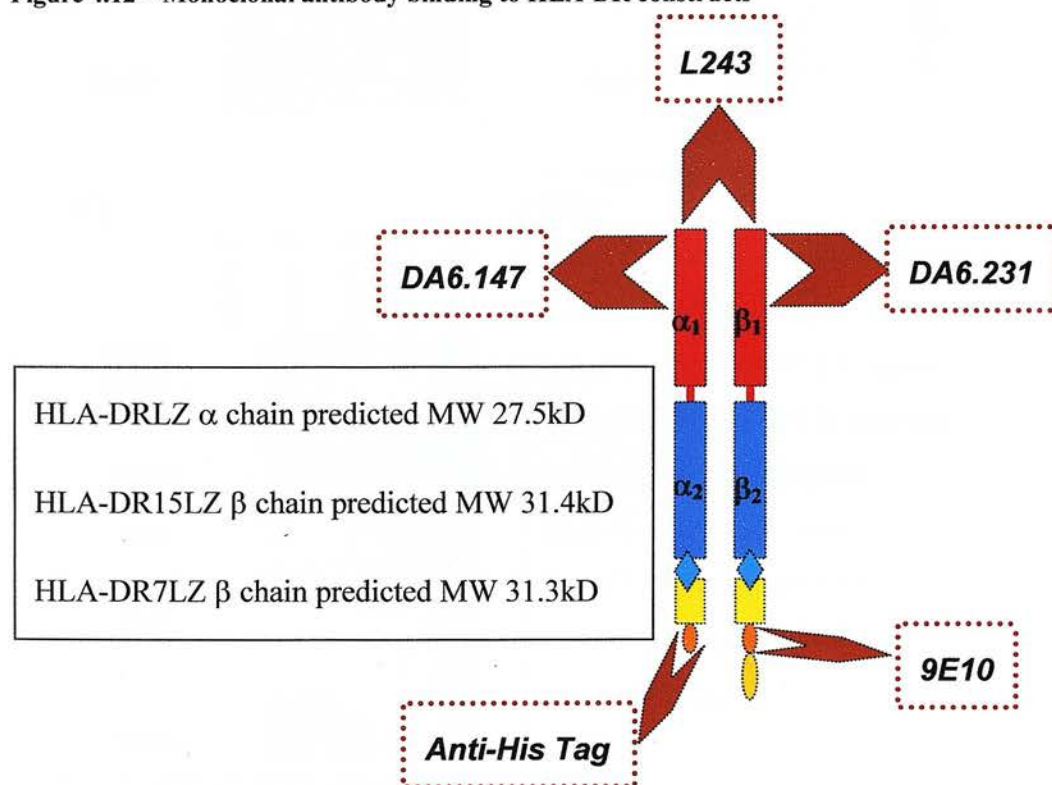


## 5.2 Characterisation of HLA-DR15LZ in post-induction supernatant

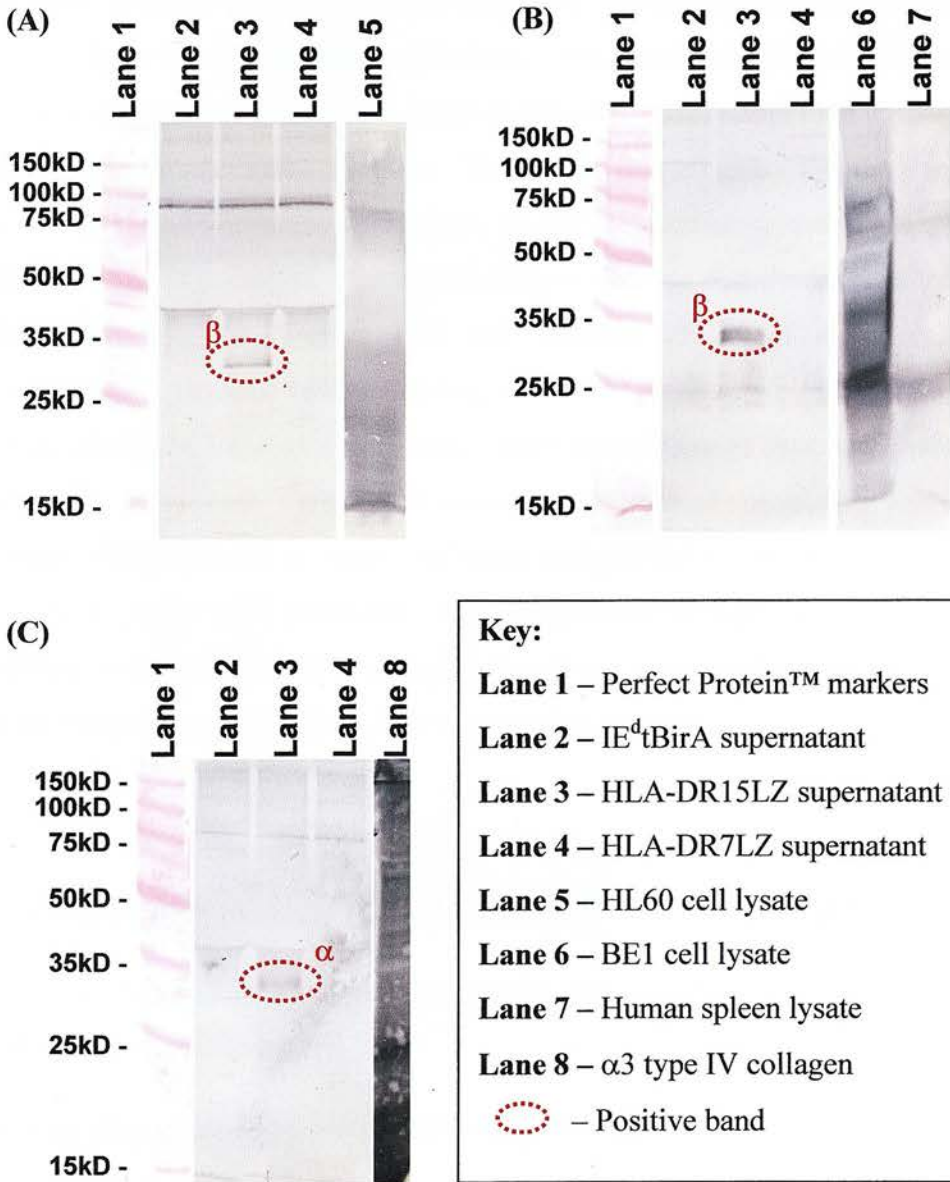
The assessment of protein production within post-induction supernatant utilised five monoclonal antibodies: L243; 9E10; DA6.231; DA6.147; and anti-His tag.

The binding pattern of each of these monoclonal antibodies is depicted in Figure 4.12.

**Figure 4.12 – Monoclonal antibody binding to HLA-DR constructs**



Small-scale assessment of protein production was initially performed in 25cm<sup>2</sup> flasks using 20ml of medium. Induction was carried out using 1mM copper sulphate, collecting the supernatant after 96hours. The pre-induction viable cell count was  $5.9 \times 10^6$  cells/ml (85% viability), whilst the post-induction cell count was  $8.7 \times 10^6$  cells/ml (73% viability). The cell suspension was centrifuged at 2000g for 10 minutes at 4°C before collecting the supernatant (Figure 4.13).

**Figure 4.13 – HLA-DR15LZ & HLA-DR7LZ supernatant assessment**

S2 cells transfected with I-Ed, HLA-DR15LZ, and HLA-DR7LZ were induced using 1mM copper sulphate. 20µl samples of the post-induction supernatants were separated by SDS-PAGE and electroblotted onto nitrocellulose. Concurrently 20µl of the following positive control preparations were also separated: HL60 cell lysate (c-myc control); BE1 cell lysate (HLA-DR control); a human spleen lysate, prepared as per Balb/c spleen (HLA-DR control); and a sample of a His-tag labelled human α3 type IV collagen kindly provided by Dr J. Zou (University of Edinburgh). The preparation of these is outlined in Chapter 2. The nitrocellulose membranes were then separately probed with the following monoclonal antibodies: 9E10 (A), DA6.231 (B), and anti-His tag (C). The blots were developed using the three-layer approach and Sigma Fast™ 3,3'-Diaminobenzidine hydrochloride. The above is representative of four protein induction experiments.



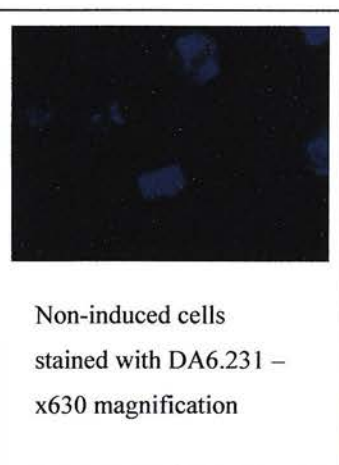
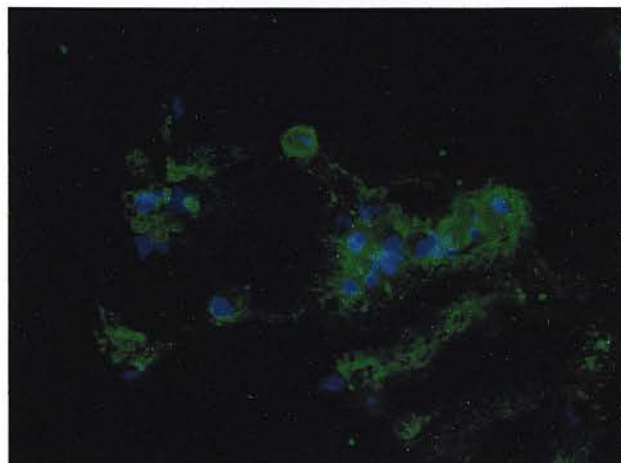
The presence of both the HLA-DR15 $\beta$  and  $\alpha$  chains within the induced supernatant is clearly seen in Lane 3 of the above immunoblots at approximately the expected size of 31kD and 28kD respectively. The bands identified within the blots are seen to be at that expected of a single monomeric chain rather than at that of the heterodimerically associated  $\alpha\beta$  dimer. This would suggest either that the chains are already dissociated within the supernatant, or that the conditions within the gel have resulted in their dissociation. Further assessment showed that the latter is the most likely explanation, in keeping with the findings of Kwok *et al* (personal communication), as noted below. Having shown the presence of the separate  $\alpha$  and  $\beta$  chains within the induced supernatant, further assessment of their association and functionality is required. Larger scale production of induced supernatant was carried in spinner flasks in order to obtain sufficient material for further analysis. Neither the  $\alpha$  or  $\beta$  chain were detectable within the induced supernatant of S2 cells transfected with the HLA-DR7 construct *vide infra*. The monoclonal antibodies used were seen to correctly identify the relevant positive controls.

### 5.3 Characterisation of cell-associated HLA-DR15LZ protein

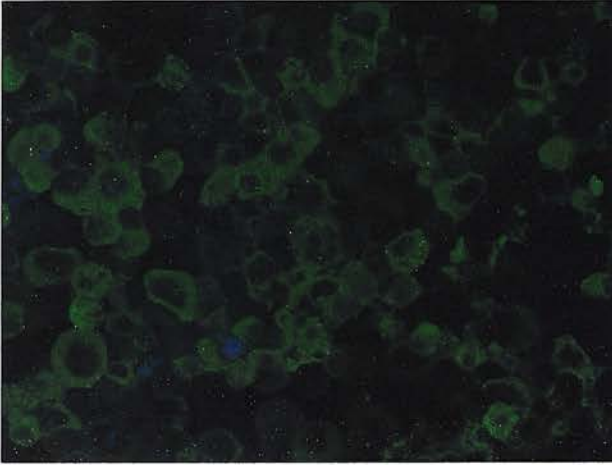
The presence of cell-associated protein was assessed using cytopspins from the above experiment (Figure 4.14).

**Figure 4.14 – Assessment of cell-associated HLA-DR15LZ TBB**

a) Stained with DA6.231 (Saponin used) – X400 magnification

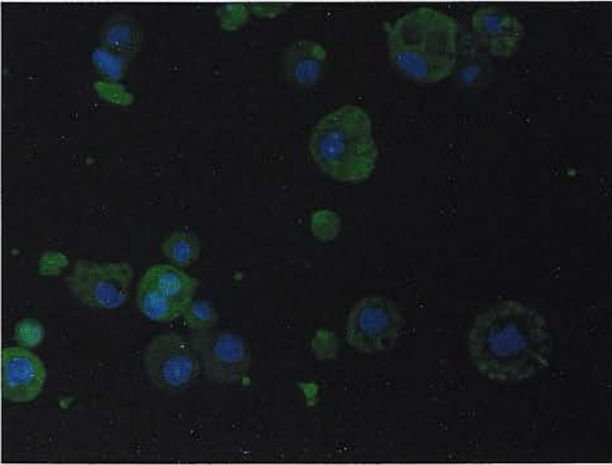


b) Stained with anti-His Tag (Saponin used) – X 400 magnification



Non-induced cells  
stained with anti-His Tag  
– x630 magnification

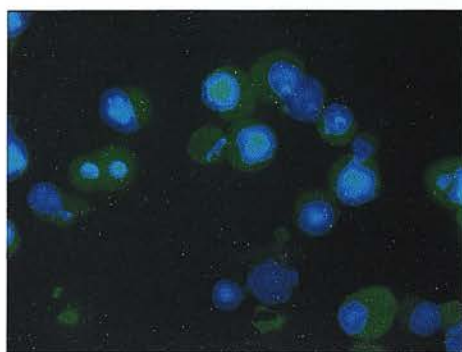
c) Stained with L243 (Saponin used) – X 400 magnification



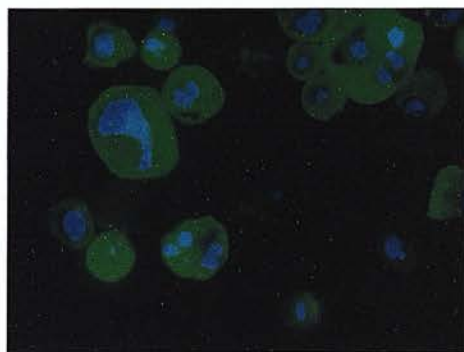
d) Stained with secondary antibody alone (Saponin used) – X 400 magnification



## e) Stained with L243 – Oil Immersion magnification



Saponin used



Saponin not used

Cell suspensions from induced and non-induced transfected S2 cell cultures used in (Figure 4.13) were used to form cytopins. The cytopins were probed using the beta chain-specific monoclonal antibody DA6.231, the alpha chain-specific anti-His tag monoclonal antibody, and the conformational sensitive L243 monoclonal antibody only in the case of induced cells. Controls for non-specific staining with the secondary antibody alone were also prepared. Saponin was used to enhance intracellular penetration of the antibodies. Uninduced S2 cells were used as negative controls for the primary antibody, whilst the secondary antibody alone was used to assess for non-specific staining. The above is representative of three cytopins.

The presence of the separate HLA-DR $\alpha$  and HLA-DR $\beta$ 15 chains is seen within the induced S2 cells (Figure 4.14a&b), but not the non-induced cells (Figure 4.14a&b inset). Indeed, conformationally correct heterodimeric HLA-DR15LZ also appears to be present associated with these cells (Figure 4.14c). The staining seen certainly does not appear to be non-specific as there is no fluorescence seen using the secondary antibody alone (Figure 4.14d). Saponin was used in the hope that it would help to differentiate between intracellular and cell surface protein. The results with and without saponin appear to be similar (Figure 4.14e), and would either indicate that induced proteins can be found both within cells and surface associated, or that in preparing the cells the membrane is sufficiently damaged to negate any differentiation that saponin could make.

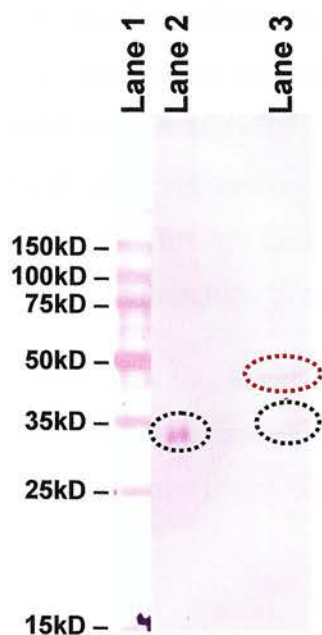


## 5.4 Utility of serum-free medium

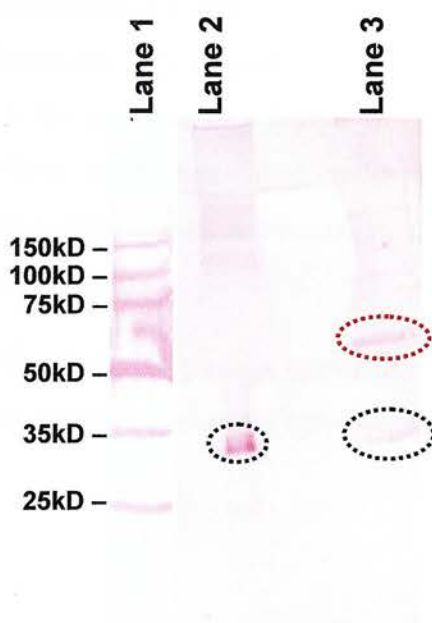
Growth in serum-free media would ease further purification of recombinant proteins by minimising contamination by serum proteins. However, it was important to assess whether the successfully transfected S2 cells were able to grow in this medium, and whether protein production was still feasible. Therefore, HLA-DR15LZ transfected S2 cells were sequentially adapted to serum-free growth over a series of five passages. Once growing in serum-free medium, a test induction using 1mM copper sulphate was performed (Figure 4.15).

Figure 4.15 – Assessment of HLA-DR15LZ production in serum-free medium

a) Anti-His tag



b) 9E10



### Key:

**Lane 1** – Perfect Protein<sup>®</sup> markers; **Lane 2** – Standard media; **Lane 3** – Serum-free media

○ – Monomeric HLA-DR $\alpha$  or  $\beta$  band      ○ – Heterodimeric HLA-DR $\alpha\beta$  band

Post-induction supernatant was collected after 5 days. The pre-induction viable cell count was  $2.5 \times 10^6$  cells/ml (91% viability), whilst the post-induction cell count was  $2.4 \times 10^6$  cells/ml (59% viability). The cell suspension was centrifuged at 2000g for 10 minutes at 4°C. 20µl samples of the post-induction supernatant were separated by SDS-PAGE and electro-blotted onto nitrocellulose. The blots were probed with anti-His Tag and 9E10 monoclonal antibodies, developing the blot using the three-layer approach utilising Sigma Fast™ 3,3'-Diaminobenzidine hydrochloride. The above is representative of 3 protein induction experiments.

The blots clearly show the presence of both the DR $\alpha$  band (Figure 4.15a) and the DR $\beta$  band (Figure 4.15b) at their expected size (28kD and 31kD respectively). However, the amount of protein induced using the serum-free media (Lane 3) is substantially less than that from the serum-containing media (Lane 2) in Figure 4.15. This would be in keeping with the poorer cell growth noted in the serum-free media. One possible solution to this would be the addition of a reduced amount of serum, *eg* 1%, that would improve cell growth without hindering downstream purification (Malherbe et al., 2000). One intriguing finding is the presence of a higher weight band that represents heterodimeric HLA-DR15 $\alpha\beta$  units that have remained associated through their leucine zipper motifs. This may have been masked by the heavy albumin band present in serum-supplemented medium.

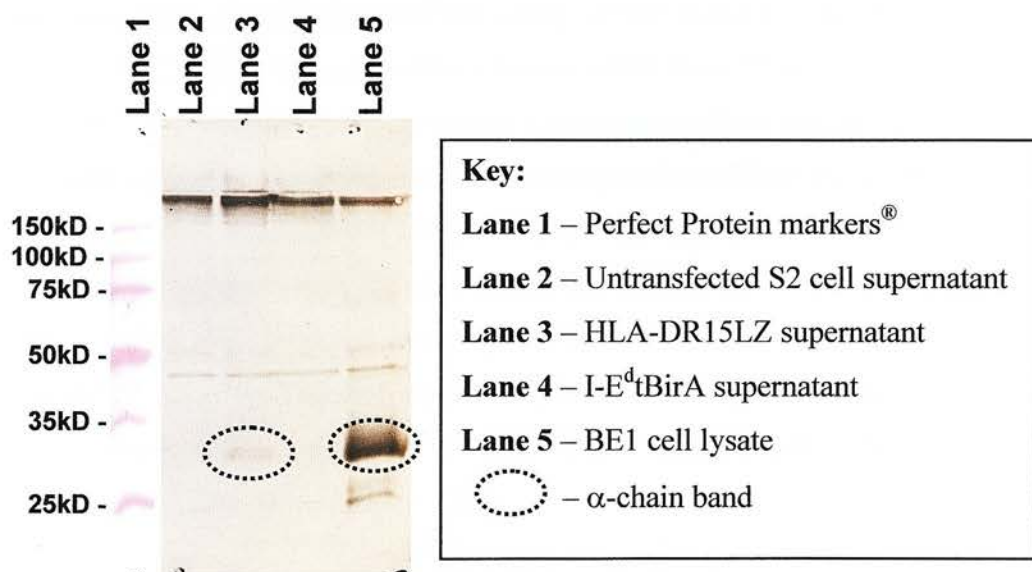
The functional heterodimeric nature of the induced protein under these conditions was assessed in parallel with that of the induced protein in serum-based medium below (See Chapter 6).

## 5.5 Assessment of heterodimeric nature of induced protein

For the recombinant HLA-DR15  $\alpha$  and  $\beta$  proteins to be functionally useful as tetramer building blocks (TBB) they must be in a heterodimeric association. Although heterodimeric association was seen, the majority of the proteins were separate  $\alpha$  and  $\beta$  chains as expected in SDS-PAGE (Kwok *et al*, personal communication). Therefore, to determine the proportion of induced protein occurring as  $\alpha\beta$  heterodimer complexes in post-induction supernatant I used two different techniques. In the first, the  $\beta$  chain-specific monoclonal antibody DA6.231

was used to precipitate the HLA-DR15LZ  $\beta$  chain and the precipitate probed for HLA-DR15LZ  $\alpha$  chain co-precipitation (Figure 4.16). In the second, the HLA-DR15LZ  $\alpha$  chain was immobilised via the His tag using nickel-chelation chromatography, and the immobilised protein examined for HLA-DR15LZ  $\beta$  chains (Figure 4.17).

**Figure 4.16 –Western blot stained with DA6.147 following DA6.231 immunoprecipitation**



Immunoprecipitation was carried out using 12ml of the following copper-induced supernatants: S2 cells transfected with HLA-DR15LZ construct grown in serum-containing medium; S2 cells transfected with the I-E<sup>d</sup>tBirA grown in serum-containing medium (this was used as a negative control); and untransfected S2 cells grown in serum-containing medium (this was used as a further negative control). To each of the above 10ml of DA6.231 hybridoma supernatant was added, and the resulting solution made up to 30ml with NET-gel buffer. 1ml of BE1 lysate was used as a positive control for HLA-DR immunoprecipitation. The immunoprecipitation was performed as per Methods. The eluates were separated by SDS-PAGE gel electrophoresis, before electro-blotting onto nitrocellulose overnight. The nitrocellulose membrane was probed with the DA6.147 (HLA-DR $\alpha$  chain-specific monoclonal antibody) monoclonal antibody. The blot was developed using the three-layer approach with Sigma Fast™ 3,3'-Diaminobenzidine hydrochloride.

Immunoprecipitation of the DR $\beta$  chain with the DR $\beta$  chain-specific monoclonal antibody DA6.231 brought down DR $\alpha$  chains detected with the DR $\alpha$  chain-specific monoclonal antibody DA6.147. This is consistent with the S2 cell



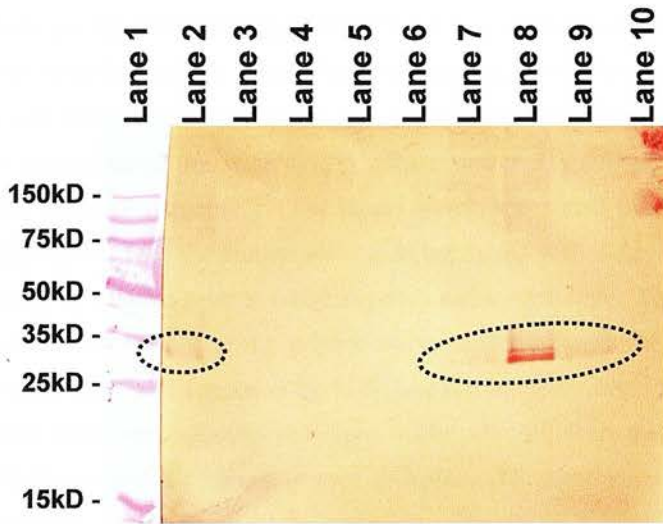
supernatants containing  $\alpha\beta$  heterodimeric complexes sufficiently stably associated to persist through immunoprecipitation.

In order to further assess the proportion of HLA-DR15LZ  $\beta$  chain that was associated with  $\alpha$  chain as against free, I took advantage of the His-tag at the carboxy terminus of the  $\alpha$  chain to extract all the free  $\alpha$  chains as well as those in  $\alpha\beta$  heterodimers by metal chelation chromatography of the induced supernatant. This would also allow an assessment of the utility of the method in the purification of HLA-DR15LZ. 30ml of copper-induced supernatant from S2 cells transfected with HLA-DR15LZ construct grown in serum-containing medium was precipitated with ammonium sulphate, dissolving the precipitated protein in PBS/0.05% sodium azide. This step not only concentrates the protein, but also allows for removal of copper ions that may interfere with the nickel-histidine interaction. A small-scale nickel affinity column was prepared using a 3ml bed-volume of iminodiacetic acid – Sepharose 6B Fastflow<sup>®</sup> beads formed in an Econo-Pac<sup>®</sup> disposable chromatography column (*BioRad Laboratories*). A small-scale nickel-affinity chromatography purification was carried out (Figure 4.17).

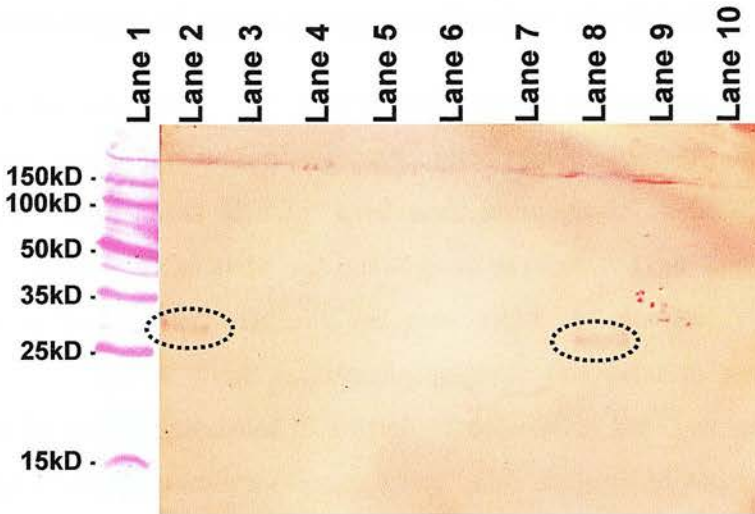
After passage over the nickel-IDA column, there were no detectable recombinant protein losses seen by the lack of either detectable HLA-DR $\alpha$  or HLA-DR $\beta$  chains in the column post-load or wash steps. This would indicate that the vast majority of  $\beta$  chains were associated with  $\alpha$  chains, and that any protein losses are small. The  $\beta$  chains were recovered with the  $\alpha$  chains upon elution of the nickel-IDA column with EDTA. The recombinant protein also appears to be concentrated by the elution process (as seen in Lanes 8 of Figure 4.17). The presence of detectable HLA-DR $\beta$  in the eluate (Lane 8 of Figure 4.17a) indicates that HLA-DR15LZ TBB can withstand ammonium sulphate precipitation and that nickel-chelation chromatography could be used in larger-scale purification. Furthermore, this finding confirms the heterodimeric association of the recombinant HLA-DR15LZ TBB.

Figure 4.17 – Metal chelation extraction of  $\alpha$  chain pulls down  $\beta$  chain

a) 9E10 – Probes for  $\beta$  chain



b) Anti-His tag – Probes for  $\alpha$  chain



**Key:**

**Lane 1** – Perfect Protein<sup>®</sup> markers

**Lane 2** – Column pre-load

**Lane 3** – Column post-load

**Lane 4** – Column wash 1

**Lane 5** – Column wash 2

**Lane 6** – Column wash 3

**Lane 7** – Column eluate 1

**Lane 8** – Column eluate 2

**Lane 9** – Column eluate 3

**Lane 10** – Column eluate 4

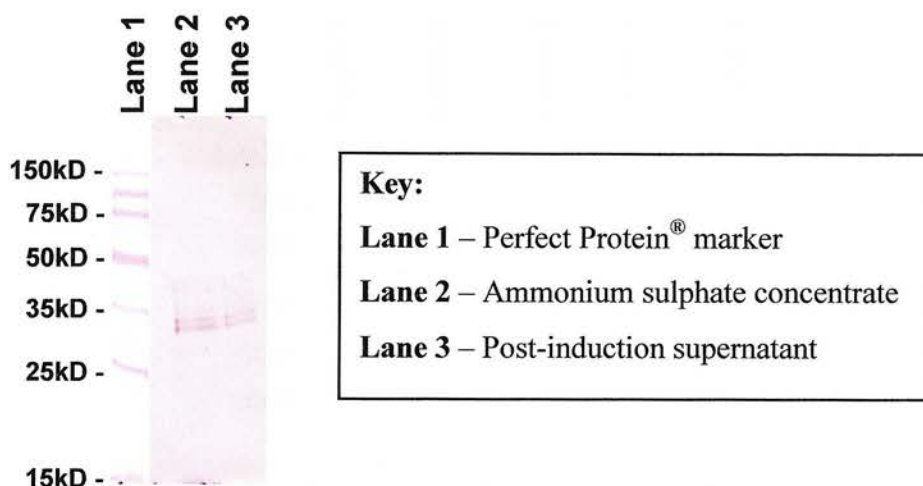
○ – Positive  $\alpha$  and  $\beta$  chain bands

The small IDA column was equilibrated in 80ml of PBS by gravity flow before stripping the column of any bound metal ions using 20ml PBS/100mM EDTA. The stripped column was equilibrated with 130ml PBS before loading with nickel ions using 20ml 0.1M nickel chloride/10mM sodium acetate pH 5.0. The column was equilibrated using 30ml PBS and 50ml PBS/10mM imidazole to remove any unbound nickel ions from the column. 10ml of the crude protein solution prepared above with 10mM imidazole added was loaded onto the column by gravity flow, collecting the resulting post-load. Unbound protein was removed by washing the column using 3 x 10ml PBS/10mM imidazole, collecting the three wash steps separately. The bound protein was eluted from the column using 4 x 2.5ml PBS/100mM EDTA, with the elution solution being mixed with the column beads and left at room temperature for 10 minutes prior to collecting each eluate separately. The column was washed and regenerated using PBS/100mM EDTA prior to storing under 30% ethanol at 4°C. 10µl samples of each fraction were taken and separated by SDS-PAGE electrophoresis. The separated proteins were electro-blotted onto nitrocellulose overnight. The nitrocellulose membranes were probed separately using 9E10 and anti-His tag monoclonal antibodies. The membranes were developed using the three-layer approach with 3-amino-9-ethylcarbazole. The above is representative of two small scale metal chelation experiments.

## 5.6 Assessment of large-scale production of HLA-DR15LZ TBB

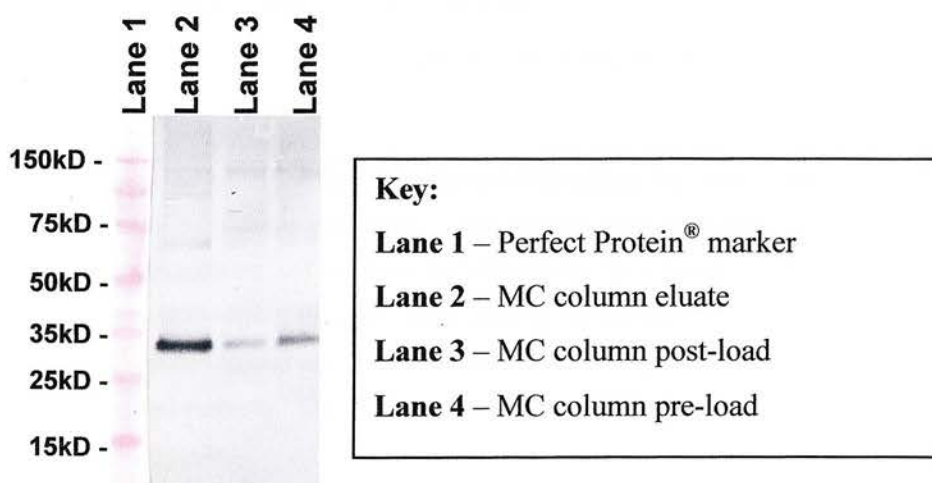
Given the successful small-scale production and purification of HLA-DR15LZ TBB, larger scale production was attempted using spinner flasks. Serum-supplemented media was initially tried and, although HLA-DR15LZ TBB was successfully produced, the yield was not as good as predicted due to poor cell growth within the spinner flasks. Despite the poor yield, the possibility of large-scale production was proven. The ammonium sulphate precipitation step was seen to concentrate the protein produced to a small extent, raising the issue of protein losses at this stage of the preparation (Figure 4.18). This suggestion was not born out on further analysis (Figure 4.20). Large-scale nickel-chelation chromatography was also performed using a Biocad 700E<sup>®</sup> workstation (*PerSeptive Biosystems Inc.*) (Figure 4.19). Unfortunately, the column did not appear to completely bind all the recombinant protein at the first pass. Therefore, this post-load was loaded onto the column once more, and a further assessment made (Figure 4.20). This second passage appeared to minimise the protein losses. Furthermore, minimal losses were noted at the ammonium sulphate precipitation step, as there was no detectable protein in the non-precipitated supernatant (Lane 2 of Figure 4.20). However, this does not take into account any irretrievably aggregated protein.

**Figure 4.18 – Concentration of large-scale production of HLA-DR15LZ TBB**

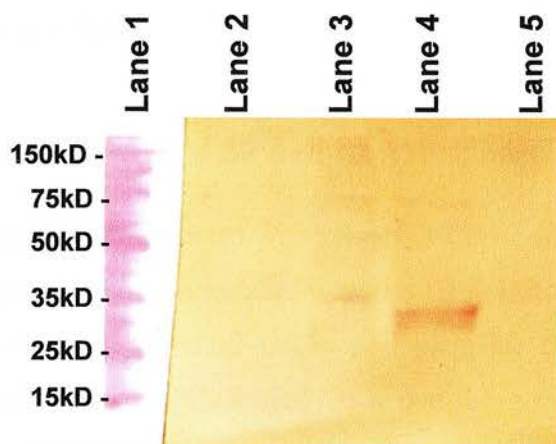


20µl samples of post-induction supernatant from HLA-DR15LZ transfected S2 cells before and after ammonium sulphate precipitation were separated by SDS-PAGE. The gels were electro-blotted prior to probing with DA6.231 (β-chain specific) monoclonal antibody. The membranes were developed using the three-layer approach with Sigma Fast<sup>™</sup> 3,3'-Diaminobenzidine hydrochloride.

**Figure 4.19 – Protein losses using a Poros<sup>®</sup> MC column**



Nickel-chelation affinity chromatography purification was carried out using a 1.7ml bed volume column packed with Poros<sup>®</sup> 20MC medium and a Biocad 700E workstation (PerSeptive Biosystems Inc.). 20µl samples of the pre-load, post-load and eluate were separated by SDS-PAGE and electro-blotted onto nitrocellulose. The membrane was probed with 9E10 (anti-c-myc tag, β-chain specific) monoclonal antibody and developed using the three layer approach with Sigma Fast<sup>™</sup> 3,3'-Diaminobenzidine hydrochloride. The above was replicated on two occasions.

**Figure 4.20 – Final purification of HLA-DR15LZ TBB****Key:****Lane 1** – Perfect Protein<sup>®</sup> marker**Lane 2** – Ammonium sulphate precipitate supernatant**Lane 3** – MC column pre-load**Lane 4** – MC column eluate**Lane 5** – MC column post-load

The post-load from the initial loading of the Poros<sup>®</sup> MC column was loaded again onto the prepared column and affinity purification carried out. 20 $\mu$ l samples were taken from the pre-load, post-load and eluate of this experiment and separated by SDS-PAGE. In conjunction with this, a 20 $\mu$ l sample from the supernatant overlying the ammonium sulphate precipitate was also separated on the same gel. The gel was electro-blotted onto nitrocellulose before probing with 9E10 (anti-c-myc tag,  $\beta$ -chain specific) monoclonal antibody. The membranes were developed using the three-layer approach with 3-amino-9-ethylcarbazole.



## 6 Expression of Leucine Zipper-Associated Heterodimeric HLA-DR7 Construct

### 6.1 Establishment of stable S2 cell transfectants

S2 cells were stably transfected with pRmHa3-DR1 $\alpha$  and pRmHa3-DR7 $\beta$  by calcium phosphate precipitation in parallel with the HLA-DR15 transfection above. Appropriate transcription of pRmHa3-DRAz and pRmHa3-DRB7z was tested in duplicate by RT-PCR as for pRmHa3-DRB15z above using the same gene-specific primer pairs. The resulting DNA was analysed by agarose gel electrophoresis (Figure 4.11). Unlike the HLA-DR15LZ transfected S2 cells, it would appear that mRNA is transcribed in both un-induced and copper-induced cells transfected with the HLA-DR7LZ construct. This finding is somewhat difficult to explain given that both constructs are contained within the same vector, and indeed the HLA-DRAz vector is identical in both cases. This phenomenon is not due to contamination by genomic DNA, as the negative control lanes contain no nucleotide bands.

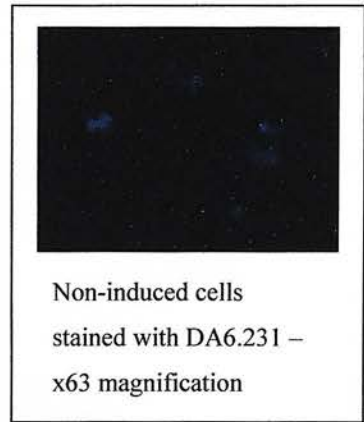
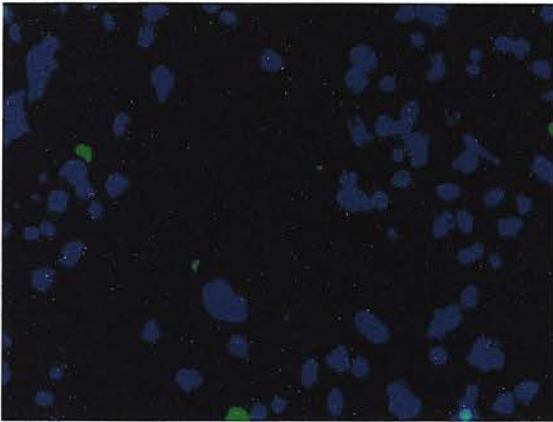
### 6.2 Assessment of protein production

A small-scale induction was carried out using 1mM copper sulphate, collecting the induced supernatant after 96hours. The pre-induction viable cell count was  $3 \times 10^6$  cells/ml (83% viability), whilst the post-induction cell count was  $15.7 \times 10^6$  cells/ml (90% viability). The supernatant was collected and samples analysed (Figure 4.13). No detectable HLA-DR7LZ  $\alpha$ -chain or  $\beta$ -chain were identified on the Western blot. Therefore, although transfection was apparently successful in terms of cell selection and DNA transcription, there appeared to be a translational or post-translational problem. To define this further, cytopspins were formed as above in order that cell-associated proteins could be identified. Once again, no specific proteins were detectable (Figure 4.21). Furthermore, these cytopspins show a lack of significant non-specific binding by the primary antibodies to the cell preparations.

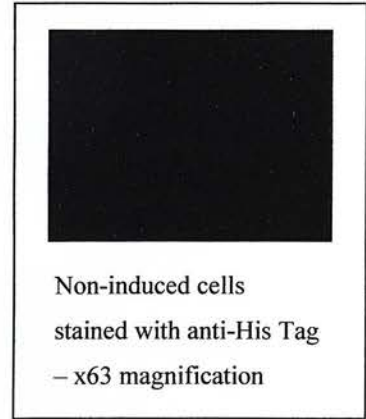
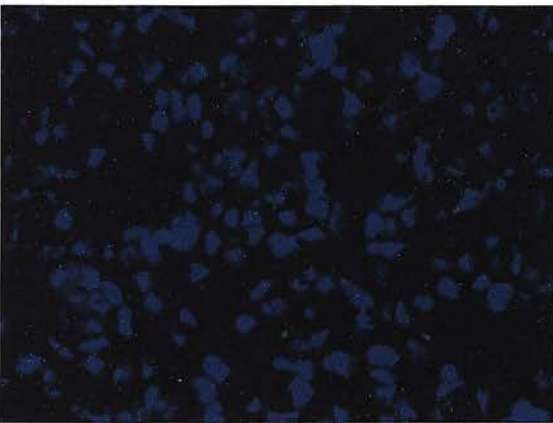


**Figure 4.21 – Assessment of cell-associated HLA-DR7LZ TBB**

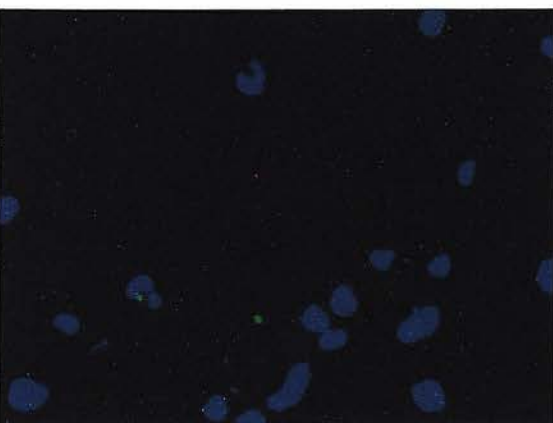
a) Stained with DA6.231 (Saponin used) – X40 magnification



b) Stained with anti-His Tag (Saponin used) – X 40 magnification



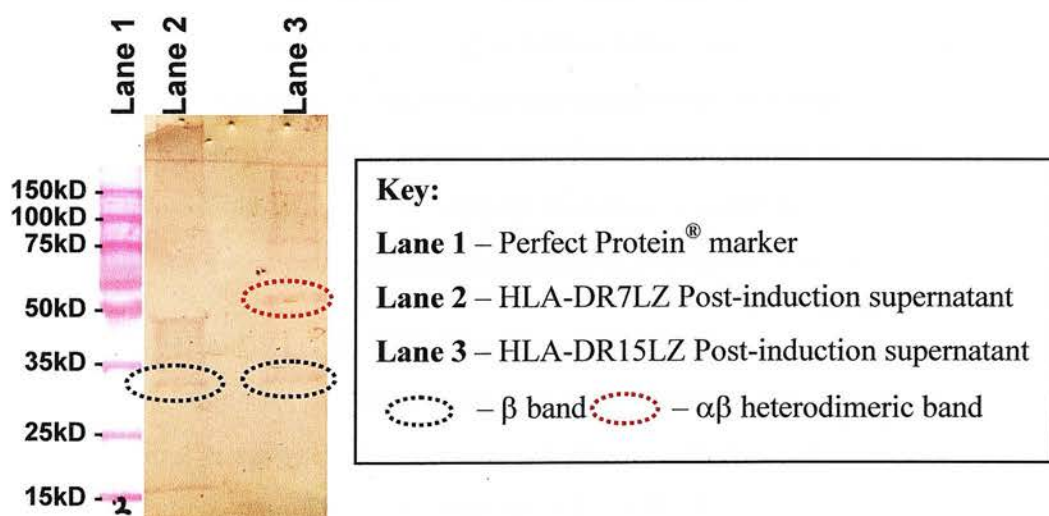
c) Stained with L243 (Saponin used) – X 40 magnification



As Figure 4.14

One possible factor was that of DNA quantity and quality. With this in mind, a further transfection was carried out using double and treble the standard DNA quantities previously used. Selection was carried out as per Methods. Only those cells transfected with double the standard DNA quantities survived the selection process. A small-scale induction was carried out as above, collecting the induced supernatant after 7 days (Figure 4.22). A faint band was detectable using 9E10 in the HLA-DR7LZ supernatant as well as the serum-free supernatant from the HLA-DR15LZ-transfected S2 cells. This band was at the expected molecular size for the  $\beta$ -chain. This result may suggest that the possible problem was related RNA translation factors such as RNA ‘hairpins’. Supplementary transfections will need to be carried out in order to assess the HLA-DR7LZ construct further.

**Figure 4.22 – Western blot showing weak HLA-DR7LZ expression**



A 20 $\mu$ l sample of the HLA-DR7LZ post-induction supernatant was separated using SDS-PAGE prior to electro-blotting onto nitrocellulose overnight. Post-induction supernatant from HLA-DR15LZ transfected cells grown in serum-free medium was used as a positive control for the Western blot. The nitrocellulose membrane was probed with 9E10 (anti-c-myc tag,  $\beta$ -chain specific) monoclonal antibody and developed using the three-layer approach with 3-amino-9-ethylcarbazole.

## 7 Discussion

In this chapter, I have described the successful construction of the nucleic acid sequences for both HLA-DR15LZ TBB and HLA-DR7LZ TBB. HLA-DR15LZ TBB has been successfully expressed in *Drosophila* S2 cells and has been shown to assemble as  $\alpha\beta$  heterodimers in solution having the correct protein tags attached. Moreover, the protein expressed has been easily identified using standard SDS-PAGE techniques indicating that the yield using this system is consistently greater than that previously found using the initial I-E<sup>d</sup> construct (Chapter 3). The heterodimeric nature of the HLA-DR15LZ TBB protein in both liquid phase and cell-associated forms has been established, with provisional purification techniques also being confirmed in the form of nickel-chelation chromatography. Indeed, the functional heterodimeric nature of HLA-DR15LZ TBB has been alluded to through the finding of L243 antibody staining in both solution and the cell-associated phase. In an attempt to minimise extraneous protein contamination, serum-free medium was used with a degree of success. Indeed, one viable option would be to use serum-free media supplemented with a small amount of serum in order to improve yield whilst still minimising extraneous protein contamination (Malherbe et al., 2000).

The HLA-DR15LZ TBB formed appears to be in a consistently stable heterodimeric state as evidenced by the data above. This together with the conformational integrity of the recombinant protein, alluded to by L243 monoclonal antibody binding, would indicate that the HLA-DR15LZ TBB is also likely to be functionally correct. The lack of covalently bound peptide allows for greater flexibility in peptide loading, with the leucine zipper domains providing the necessary stability as suggested in the literature, notably by William Kwok's group (Mallone and Nepom, 2004). Certainly, the consistency of recombinant protein production using the *Drosophila* S2 cell system highlights its ease of use compared to the baculovirus based system that has been previously used to form recombinant HLA-DR15 (Gauthier et al., 1998, Smith et al., 1998). Furthermore, the polyhistidine tag allows for ease of purification without any apparent loss of conformational integrity, as has been found by other groups (Kuroda et al., 2000). A further purification step using antibody-based affinity chromatography remains a

possibility using the L243 monoclonal antibody. The main problems were faced upon increasing the scale of production.

Large-scale production of HLA-DR15LZ TBB was initiated although with limited success in terms of protein yield. The problems encountered are easily surmountable in terms of improved cell growth through the use of different flasks such as bubbling spinner flasks (Kuroda et al., 2000), or roller flasks (Appel et al., 2000). The ammonium sulphate concentration step, although cumbersome, is effective, and has been used by other groups for the same purpose (Kuroda et al., 2000). However, it maybe worth trying to load the post-induction supernatant directly onto the nickel-loaded column as has been used in small-scale production by other groups (Kuroda et al., 2000) in order to assess whether the copper ions in the large-scale supernatant do actually affect protein binding to the affinity column. Should there be no effect, it would be then reasonable to omit the extra step of ammonium sulphate precipitation with its attendant risks of protein losses. The purification step using nickel chelation was successful, but column losses required multiple loading and elution steps. In order to circumvent this a larger column could be used and/or the column resin could also be changed. The resin used at present is based on the tridentate iminodiacetic acid (IDA). Nickel may be released from its interaction with this resin during chromatography, so reducing the resin binding capacity. The quadridentate resin nitrilotriacetic acid (NTA) has improved nickel ion retention and is therefore potentially a more stable adsorbent, with improved binding capacity (Hochuli et al., 1987). Using this resin may mean an alteration to the automation process as the NTA columns currently available are for use in low pressure systems and not HPLC systems such as the Biocad 700E<sup>®</sup> workstation (*PerSeptive Biosystems Inc.*).

Despite the success of the HLA-DR15LZ TBB expression, difficulty was experienced in expressing HLA-DR7LZ TBB. Analysis of these difficulties indicated that the problem was likely to be at the RNA translation stage of the HLA-DRB7z construct. Should further work using HLA-DR15LZ TBB prove successful, these problems may be remediable, allowing the formation and assessment of HLA-DR7LZ TBB.

## **Chapter 5**

### **Results (III)**

## Chapter 5

### Results (III)

## Formation of Recombinant MHC Class II Single-chain constructs

### 1 Introduction

Bacterial expression was developed in parallel with the insect cell expression system outlined in the previous chapter. The impetus behind this diversification was the anticipated problem with the eukaryotic expression system in terms of protein yield. This problem was realised in the initial attempts to form I-E<sup>d</sup>tBirA as noted in Chapter 4. Although *Drosophila* S2 cell expression leads to the formation of secreted and essentially correctly folded protein, the yield of this can be quite low and appears to depend upon the protein being expressed (Ivey-Hoyle, 1991, Stern and Wiley, 1992, Wallny et al., 1995).

Altman *et al* (Altman et al., 1993) were one of the first groups to demonstrate production and *in vitro* refolding of MHC class II proteins produced in *E.coli*. This group also demonstrated that glycosylation of MHC class II proteins is not an absolute requirement for functional TCR recognition. Refolding was performed in the presence an excess of antigenic peptide. Other groups have since used bacterial expression to produce functional HLA-DR molecules with and without antigenic peptide in the refolding solution. There appears to be a consensus that the former leads to a greater refolding yield (Arimilli et al., 1995, Stöckel et al., 1994) in keeping with earlier work suggesting the importance of peptide in stabilising the correct conformation of MHC Class II (Sadegh-Nasseri and Germain, 1991). However, refolding naturally expressed  $\alpha$  and  $\beta$  chains into functional class II molecules has proven a difficult and inefficient process, particularly in the absence of antigenic peptide (Frayser et al., 1999, McMichael and Kelleher, 1999). Although



the leucine zipper approach could have been tried to enhance yields from prokaryotic expression, I felt that the problems previously encountered with bacterial expression of MHC class II (See Introduction) warranted a different strategy. It is striking that MHC class I, where the peptide-binding domain is formed within the same polypeptide chain by an intramolecular disulphide bond between the  $\alpha 1$  and  $\alpha 2$  domains of that chain, folds much more efficiently into a functional unit following bacterial expression. Therefore, an attractive strategy for the formation of recombinant MHC class II proteins using a bacterial expression system was the formation of MHC class II  $\alpha$ - $\beta$  chain fusion proteins. The attractions of such a strategy would include the inherently correct ratio of  $\alpha$  and  $\beta$  chains covalently bound together in a similar manner to the MHC class I peptide-binding domain. Furthermore, the nature of the construct would allow the use of a single plasmid within the context of a simpler expression system as compared to the *Drosophila* S2 system outlined in the previous chapter.

Fusion protein approaches have been used successfully to circumvent the problems of heterodimeric association and improve functional yield for both MHC class I and II proteins. Kourilsky's group at the Pasteur Institute engineered a recombinant single-chain murine MHC Class I molecule by linking the carboxy-terminus of the murine H-2K<sup>d</sup> ectodomain to the amino terminus of murine  $\beta_2$ -microglobulin through a 15 amino acid linker. This construct was expressed in a eukaryotic system and found to bind synthetic peptides with the same specificity as the native molecule, and trigger antigen-specific T cells (Abastado et al., 1995, Mottez et al., 1991). Moreover, this group used the immobilised construct to successfully enrich for antigen-specific T cells (Bousso et al., 1997). Denkberg *et al* adapted this approach by linking the amino terminus of HLA-A2 to the carboxy terminus of human  $\beta_2$ -microglobulin, adding the peptide sequence for site-specific biotinylation by BirA biotin ligase to the carboxy terminus of HLA-A2. This construct was expressed using a bacterial expression system and, after peptide loading and biotinylation, was tetramerised using phycoerythrin-conjugated streptavidin. These MHC Class I tetramers were able to stain antigen-specific CD8<sup>+</sup> T cell lines (Denkberg et al., 2000). The fusion protein approach has also been used

to form a functional murine MHC Class II I-A<sup>d</sup> construct where the carboxy terminus of the I-A<sup>d</sup>  $\beta_2$  domain is linked by a 24 amino acid linker to the amino terminus of the I-A<sup>d</sup>  $\alpha$ -chain extracellular domain. The construct was expressed using a baculovirus expression system in Sf9 insect cells and found to be functionally correct in terms of both peptide binding and antigen-specific T cell activation (Rhode et al., 1996). As predicted, the functional protein yield and heterodimeric association was greatly improved using this method of enforced chain association. A similar construct has been successfully produced for HLA-DR1 (Zhu et al., 1997).

Taking this fusion protein approach one step further, Burrows *et al* (Burrows et al., 1998) were the first to engineer a functional fusion protein consisting of solely of the peptide binding ‘superdomain’. They linked the carboxy terminus of the  $\beta_1$  domain to the amino terminus of the  $\alpha_1$  domain of rat RT1.B MHC Class II. The construct was produced in a bacterial expression system and was found to be functionally correct in terms of peptide binding following *in vitro* refolding. The peptide-loaded construct was found to bind antigen-specific T cells *in vitro* and lead to antigen-specific inhibition of T cells both *in vitro* and *in vivo*. Given the effectiveness of this approach, I used it as the template in designing both murine and human two-domain single-chain MHC Class II constructs (scTBB – single-chain Tetramer Building Blocks).

## 2 Construction of Single-chain MHC Class II Molecules

### 2.1 Design

In order to generate single-chain murine I-E<sup>d</sup> and human HLA-DR molecules we examined the alignment of these with rat RT1.B in relation to the x-ray crystallographic structure of HLA-DR1 (Stern et al., 1994). This analysis suggested that a short linker sequence could be used to join the  $\beta_1$  and  $\alpha_1$  domains of both murine I-E<sup>d</sup> and human HLA-DR in an analogous manner to that successfully used to form the RT1.B fusion protein. Using Burrows’ RT1.B peptide sequence (Burrows

et al., 1998) and the published sequences for I-E<sup>d</sup>, HLA-DRB1\*1501 and HLA-DRB1\*0701, an alignment of the relevant sequences was made using ClustalX (Thompson et al., 1997) (Figure 5.1).

**Figure 5.1 – Alignment of HLA-DR, I-E<sup>d</sup> and RTB**

### Alignment of MHC Class II chains with RT1B sequence

RT1B	( $\beta_1$ ) -----TSLRRL <b>GGQD</b> DIEADH ----- ( $\alpha_1$ )
I-E <sup>d</sup>	( $\beta_1$ ) -----LVRRRV <b>GAQD</b> AIKEEH ----- ( $\alpha_1$ )
HLA-DR	( $\beta_1$ ) -----TVQRRV <b>GAQD</b> AIKEEH ----- ( $\alpha_1$ )

Alignments of HLA-DRA1\*0101 and I-E<sup>d</sup>  $\alpha$ -chain with rat RT1B  $\alpha$ -chain, and of HLA-DRB1\*0701, HLA-DRB1\*1501 and I-E<sup>d</sup>  $\beta$ -chain with rat RT1B  $\beta$ -chain in the vicinity of the linker used to fuse the rat  $\alpha_1$  and  $\beta_1$  domains (**GGQD**) in the construct made by Burrows *et al* (Burrows et al., 1998) were performed with the aid of the Clustal X software package (Thompson et al., 1997). The sequences for RT1B were taken from the two-domain single-chain construct of Burrows *et al* (Burrows et al., 1998). The HLA-DR and I-E<sup>d</sup> sequences were obtained from the SWISS-PROT sequence database. A similar short amino acid linker sequence (**GAQD**) was engineered into our two-domain construct to link the  $\beta_1$  and  $\alpha_1$  domains.

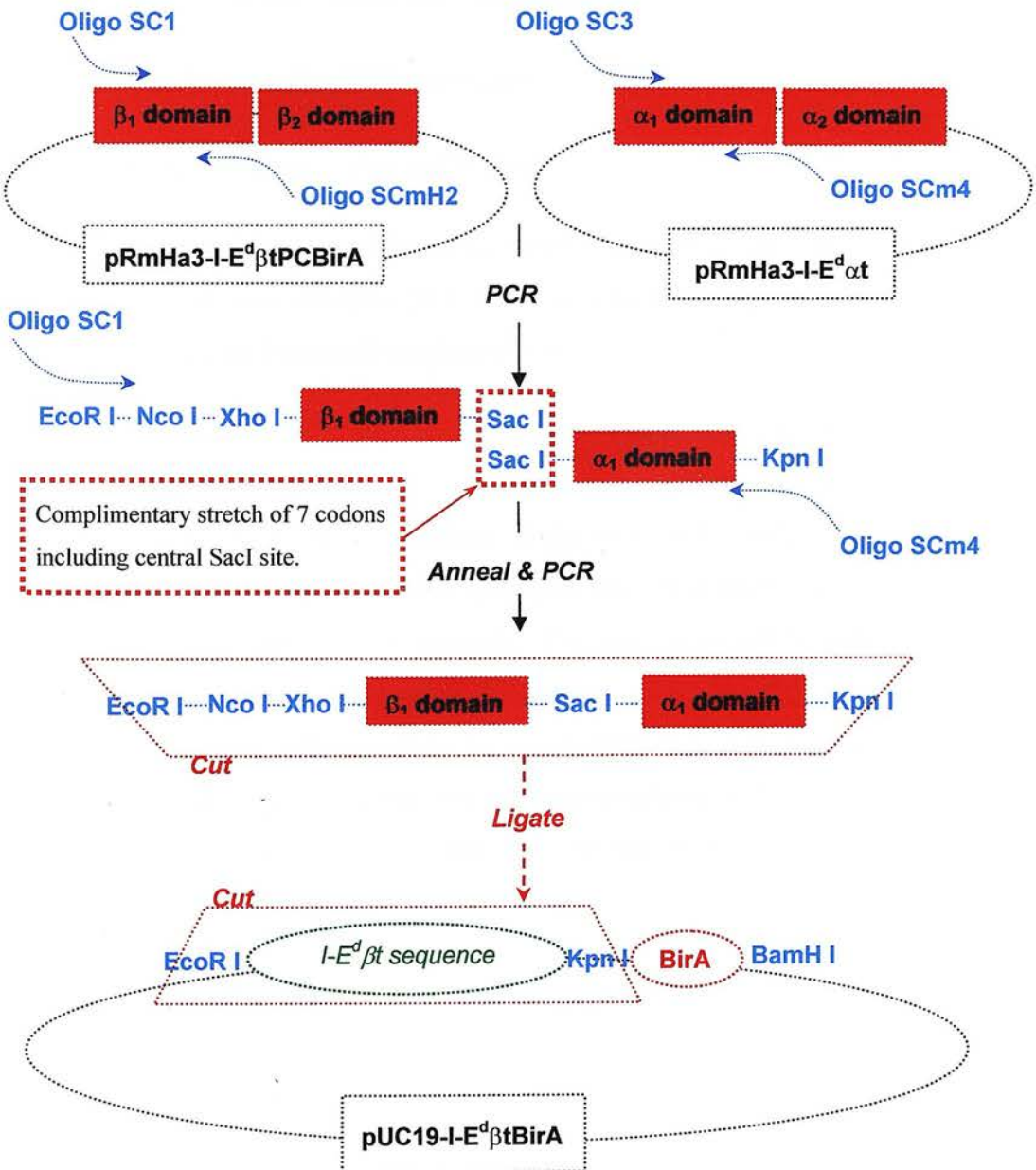
Having identified how HLA-DR and I-E<sup>d</sup>  $\alpha$  and  $\beta$  chains could be joined in a similar manner to the recombinant RT1B construct, oligonucleotides were designed to add suitable restriction and junctional sites to the 5' and 3' ends of the  $\beta_1$  and  $\alpha_1$  domains by PCR. Each  $\beta_1$  and  $\alpha_1$  domain was then joined together by overlap extension PCR (Horton et al., 1990) prior to ligating into pUC19I-E<sup>d</sup> $\beta$ tBirA containing in frame the cDNA sequence encoding the BirA biotinylation consensus

sequence (Figure 5.2). The option to covalently link a peptide to the amino-terminus of the construct was generated by the insertion of an XhoI into the construct at a suitable location to be compatible with the peptide-binding cassette strategy discussed in Chapter 3 (Figure 3.3).

The major risk in adopting this approach was its extreme novelty. At the time, it had only been shown to work for RT1B. Although RT1B had refolded readily into a functional protein, it was anticipated that this could be a major obstacle in adaptation to HLA-DR15, HLA-DR7 and I-E<sup>d</sup>. The protein formed would need to be purified from other bacterial proteins, although the bacterial inclusion bodies in which the protein is expected to accumulate are primarily composed of the expressed protein. The protein would also require *in vitro* refolding which presents its own set of challenges (Lilie et al., 1998).

## 2.2 Formation of murine single-chain MHC Class II construct

Figure 5.2 – Outline of I-E<sup>d</sup> single-chain construct formation



NB: Restriction enzyme sites of importance marked

The first stage in the formation of this construct was the expansion of the I-E<sup>d</sup>  $\alpha_1$  and  $\beta_1$  domains using PCR. Vectors pRmHa3-I-E<sup>d</sup> $\beta$ tBirA and pRmHa3-I-E<sup>d</sup> $\alpha$ t were used as the source of I-E<sup>d</sup> $\beta_1$  and I-E<sup>d</sup> $\alpha_1$  respectively. PCR was set up using the following oligonucleotide primer pairs (Appendix 2):

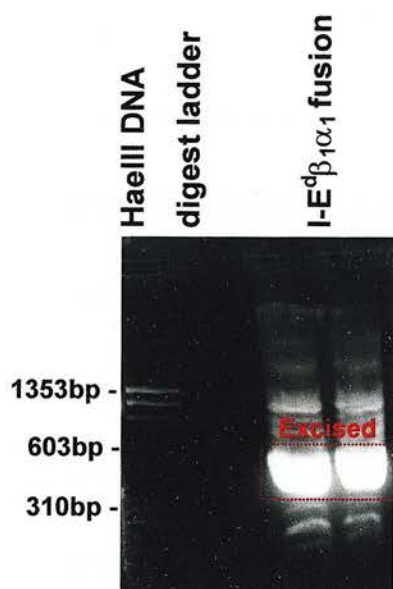
For I-E<sup>d</sup> $\alpha_1$  domain – SC3 and SCm4

For I-E<sup>d</sup> $\beta_1$  domain – SC1 and SCmH2

The PCR was carried out over 25 cycles (Denature at 95°C for 1 minute, anneal at 52°C for 1 minute, and extend at 72°C for 90 seconds). A single well-defined 300bp product was purified from each reaction mixture.

The  $\alpha_1$  and  $\beta_1$  PCR products were heated, annealed and any  $\alpha_1\beta_1$  pairings extended using DNA polymerase. Unsatisfactory results were obtained on five occasions before the relative quantities of the two PCR products were carefully adjusted to 1:1 comparing the concentrations by sequential dilution and densitometry of the agarose gel separated PCR products. The yield of the 600bp  $\alpha_1\beta_1$  pairing was very low at this stage, and PCR using the terminal primer pair (SC1 and SCm4) was employed to generate sufficient DNA for purification from an agarose gel (Horton et al., 1990) (Figure 5.3). Once the relative concentrations of the two PCR products had been adjusted, a successful outcome was achieved on the second attempt.



Figure 5.3 – Formation of I-E<sup>d</sup>sc fusion protein

Two cycles of overlap extension PCR were carried out following an initial denature step at 94.5°C for 5 minutes. Each cycle consisted of the following: denature at 94.5°C for 1 minute, anneal at 60°C for 2 minutes, and extend at 72°C for 5 minutes. The annealed and extended product then underwent a further 26 cycles of PCR using the primers SC1 and SCm4 (Denature at 94.5°C for 20 seconds, anneal at 60°C for 1 minute, and extend at 72°C for 1 minute). The defined band of approximately 600bp was excised as indicated. The PCR regimen was based upon the work of Burrows *et al* (Burrows *et al.*, 1998).

Next, the 600bp I-E<sup>d</sup>β<sub>1</sub>α<sub>1</sub> fusion product was restricted with EcoRI and KpnI and cloned into pUC19-I-E<sup>d</sup>βtBirA (See Chapter 3 figure 3.2). Transformants were tested for the presence of the expected DNA using a panel of restriction enzyme digests. One transformant was found to contain the expected DNA bands and was sequenced using the ‘M13’ primers. This part of the construction process required five attempts for a successful outcome. The sequencing revealed four base pair changes from the expected sequence. These changes are due to degeneracy in oligonucleotide primers SC1 and SCmH2 and likely variations of the I-E<sup>d</sup> sequence given that none had translational effects (Mengle-Gaw *et al.*, 1984) (Figure 5.4).

Figure 5.4 – IE<sup>d</sup>sc DNA sequence

1	GAATTCATG	GGCTCTCGAG	GCCCACGGTT	TCTGGAATAC	GTTACATCTG
	EcoRI	XhoI		T	
51	AGTGTCATTT	CTACAACGGG	ACGCAGCACG	TACGGTTTCT	GGAGAGATTC
101	ATCTACAACC	GGGAGGAGAA	CCTGCGCTTC	GACAGCGACG	TGGGCGAGTA
β1	151	CCGCGCGGTG	ACAGAGCTGG	GGCGGCCAGA	CGCCGAGAAC
	201	AGCCGGAGAT	CCTGGAGGAT	GCGCGGGCCT	CGGTGGACAC
	251	CACAACTATG	AGATCTCGGA	TAAATTCCTT	GTGCGGCGGC
				A	G
					SacI
α1	301	TCAAGACGCT	ATCAAAGAGG	AACACACCAT	CATCCAGGCA
				A	G
	351	TTTTACCAGA	CAAACGTGGA	GAGTTTATGT	TTGACTTTGA
	401	ATTTTCCATG	TAGACATTGA	AAAGTCAGAG	ACCATCTGGA
	451	ATTTGCAAAG	TTTGCCAGCT	TTGAGGCTCA	GGGTGCACTG
	501	CTGTGGACAA	AGCTAACCTG	GATGTCATGA	AAGAGCGTTC
	551	CCAGATGCCA	ACGGTACCGC	TAGCGGCGGT	GGACTGCATC
		KpnI			
	601	TGCACAGAAA	ATGGTGTGGA	ATCATCGTTA	AGGATCC
				BamHI	
					BirA

**KEY:**

★ – Sites of base pair changes

C – Changes secondary to oligonucleotide primer degeneracy

## 2.3 Formation of HLA-DR15 $\beta$ 1 $\alpha$ 1 DNA fusion construct

The formation of the HLA-DR15 $\beta$ 1 $\alpha$ 1 DNA fusion construct was performed in parallel with the formation of the I-E<sup>d</sup> $\beta$ 1 $\alpha$ 1 fusion DNA construct above. HLA-DR15 $\beta$ 1 and HLA-DR $\alpha$ 1 domains were amplified from full length cDNAs for HLA-DRB1\*1501 and HLA-DRA1\*0101 kindly donated by Dr K. Dornmair (Stöckel et al., 1994). PCR amplification was performed using the following oligonucleotide primer pairs (Appendix 2):

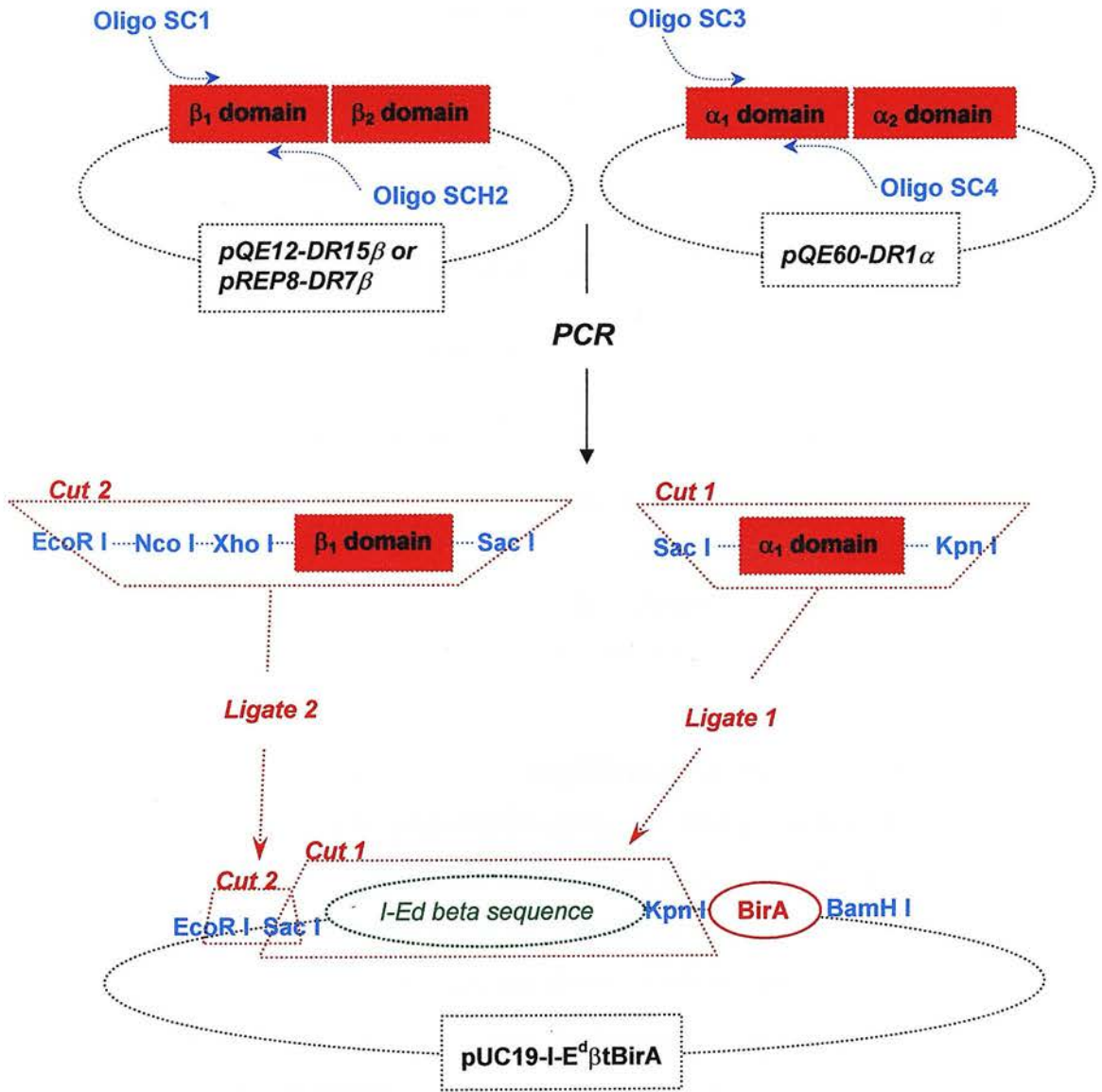
For DR $\alpha$ 1 domain – SC3 and SC4

For DR $\beta$ 1 domain – SC1 and SCH2

PCR was carried out as for the I-E<sup>d</sup> $\beta$ 1 $\alpha$ 1 fusion DNA construct above. Both PCR reactions yielded the approximate 300bp products as expected. This part of the construct formation was straightforward requiring only one attempt for a successful outcome. Attempts to join the products by overlap extension PCR yielded the expected approximate 600bp product, but this, on two separate occasions, was determined to have a sequence unacceptably altered by presumed PCR errors. Therefore, a two-stage approach sequentially ligating the  $\alpha$ 1 and  $\beta$ 1 sequences into pUC19-I-E<sup>d</sup> $\beta$ tBirA was employed (See Figure 5.5).

First the 300bp product of the amplification of the  $\alpha$ 1 domain of HLA-DRA1\*0101 was restricted using SacI and KpnI and cloned into pUC19BirA. Transformants were tested for the presence of the expected DNA using a panel of restriction enzyme digests. One transformant was found to contain the expected DNA bands. This required two attempts for a successful outcome. The DNA from this transformant was sequenced and revealed two base pair changes within the expected sequence that are likely to be variations of the HLA-DR $\alpha$ 1 sequence or as a result of degeneracy within the oligonucleotide primer SC3 and are without translational effects (Figure 5.6).




Figure 5.5 – Outline of human single-chain formation





NB: Restriction enzyme sites of importance marked



**Figure 5.6 – Sequence of HLA-DR $\alpha$ 1 DNA**

1	<b>GAGCTC</b> AAGA	CGCTATCAAA	GAGGAACATG	TGATCATCCA	GGCCGAGTTC
	<b>SacI</b>		  <b>A</b>		
51	TATCTGAATC	CTGACCAATC	AGGCGAGTTT	ATGTTTGACT	TTGATGGTGA
101	TGAGATTTTC	CATGTGGATA	TGGCAAAGAA	GGAGACGGTC	TGGCGGCTTG
151	AAGAATTTGG	ACGATTTGCC	AGCTTTGAGG	CTCAAGGTGC	ATTGGCCAAC
201	ATAGCTGTGG	ACAAAGCCAA	CCTGGAAATC	ATGACAAAGC	GCTCCAAC TA
			 <b>T</b>		
251	TACTCCGATC	ACCAAT <b>GGTA</b>	<b>CC</b>		
		<b>KpnI</b>			

**KEY:**

-  – Sites of base pair changes
-  – Change as a result of SC3 degeneracy

Next, the 300bp products of the amplification of the  $\beta_1$  domains from HLA-DRB1\*1501 and HLA-DRB1\*0701 using the oligonucleotide primers SC1 and SCH2 (Appendix 2) were purified from agarose gels. The right hand oligonucleotide primer (SCH2) was modified to be specific for the human DR $\beta$  sequences in response to the problems encountered above. Each purified  $\beta_1$  domain fragment was restricted with SacI and EcoRI prior to ligating into pUC19 $\alpha_1$ BirA. The ligated constructs were transformed into DH5 *E.coli*. Transformants were tested for the presence of the expected DNA using a panel of restriction enzyme digests. Two transformants for each of HLA-DR7 and –DR15 single-chain constructs were sequenced using the ‘M13’ primers. Only one of the transformants for each construct was found to contain the correct DNA sequence (Figure 5.7). This part of construct formation also required two attempts for a successful outcome. The HLA-DR15sc construct was noted to have a single base pair change compared to the expected sequence that is as a result of degenerate base in the oligonucleotide primer SC1. This is without translational effect.

Figure 5.7 – Sequence for HLA-DR7sc and DR15sc

		<b>Start</b>		<b>β1 sequence</b>	
15		<b>GAATTCCATG</b>	<b>GGCTCTCGAG</b>	GCCACGTTT	★TCTGTGGCAG
7	1	-----	-----	-----	-----
		<b>EcoRI</b>	<b>NcoI</b>	<b>XhoI</b>	
15	41	CCTAAGAGGG	AGTGTCATTT	CTTCAATGGG	ACGGAGCGGG
7		GG----TATA	-----	-----C---	-----
15	81	TGCGGTTCCT	GGACAGATAC	TTCTATAACC	AGGAGGAGTC
7		---A-----	---A---CT-	-----	-----T
15	121	CGTGCGCTTC	GACAGCGACG	TGGGGGAGTT	CCGGGCGGTG
7		-----	-----	-----A	-----
15	161	ACGGAGCTGG	GGCGGCCTGA	CGCTGAGTAC	TGGAACAGCC
7		-----A-	-----T	---C---C-	-----
15	201	AGAAGGACAT	CCTGGAGCAG	GCGCGGGCCG	CGGTGGACAC
7		-----	-----G-C	AG-----G-C	A-----
15	241	CTACTGCAGA	CACAACACTACG	GGGTGTGGA	GAGCTTCACA
7		-GTG-----	-----	-----GT--	-----
15		GTGCAGCGGC	GAGTCG <b>GAGC</b>	<b>TCAAGACGCT</b>	<b>α1 sequence</b> ATCAAAGAGG
7	281	-----	-----	-----	-----
			<b>SacI</b>		
15	321	AACATGTGAT	CATCCAGGCC	GAGTTCTATC	TGAATCCTGA
7		-----	-----	-----	-----
15	361	CCAATCAGGC	GAGTTTATGT	TTGACTTTGA	TGGTGATGAG
7		-----	-----	-----	-----
15	401	ATTTTCCATG	TGGATATGGC	AAAGAAGGAG	ACGGTCTGGC
7		-----	-----	-----	-----
15	441	GGCTTGAAGA	ATTTGGACGA	TTTGCCAGCT	TTGAGGCTCA
7		-----	-----	-----	-----
15	481	AGGTGCATTG	GCCAACATAG	CTGTGGACAA	AGCCAACCTG
7		-----	-----	-----	-----
15	521	GAAATCATGA	CAAAGCGCTC	CAACTATACT	CCGATCACCA
7		-----	-----	-----	-----
15		AT <b>GGTACC</b>	<b>Start of BirA sequence -&gt;</b>		
7	561	-----			
		<b>KpnI</b>			

**KEY:**

★– Site of C to T base pair change



### 3 Expression of Single-chain Tetramer Building Blocks in *E.Coli*

#### 3.1 Selection of expression vector

A T7-based vector was desirable to achieve high level expression in *E.coli* (Studier and Moffatt, 1986). The pET prokaryotic expression system (CN Biosciences (UK) Ltd.) was utilised because of its range of vector-host combinations and its proven efficiency by Burrows *et al.* Expression was piloted using the I-E<sup>d</sup>sc construct ligated into pET14b as this vector/construct combination was readily available in the laboratory and mirrored the successful expression of RT1.B single-chain fusion protein by Burrows *et al.* (Burrows *et al.*, 1998, Burrows *et al.*, 1999). The pilot study demonstrated I-E<sup>d</sup>sc expression, but purification and identification was initially hampered by the absence of a tag that was identifiable on the denatured single-chain fusion protein. To gain suitable tags, initial expression of HLA-DR15sc was attempted using the expression vector pETBlue2 that had both HSV<sup>®</sup> and His<sup>®</sup> tags. Frustratingly, this proved a very unsatisfactory choice of vector, probably as a result of secondary structure formation in the mRNA (Dr B. Morris, Senior Scientist, Novagen<sup>®</sup> product applications – *personal communication*). A third T7 vector, pET25b, containing both C-terminal HSV<sup>®</sup> and His<sup>®</sup> tags was identified and HLA-DR15sc inserted using a different ligation strategy. HLA-DR15sc and HLA-DR7sc expression using pET25b proved efficient for both HLA-DR single-chain fusion proteins.

#### 3.2 Expression of I-E<sup>d</sup>sc TBB using the pET14b vector

The I-E<sup>d</sup>sc TBB construct was formed before either of the HLA-DRsc TBB constructs and was thought suitable to pilot single-chain fusion protein expression because a monoclonal antibody (2G9 (Becker *et al.*, 1992)) was available capable of recognising I-E<sup>d</sup> on a Western blot. The I-E<sup>d</sup> $\beta_1\alpha_1$ BirA construct was cloned into pET14b using the NcoI and BamHI cloning sites which had the consequence of

cutting out the His-Tag<sup>®</sup> sequence inherent in the pET14b vector. Transformants were identified by restriction enzyme digests and the purified plasmid transformed into the bacterial expression host BL21(DE3), a strain of *E.coli* that contains the T7 RNA polymerase gene required for high efficiency expression.

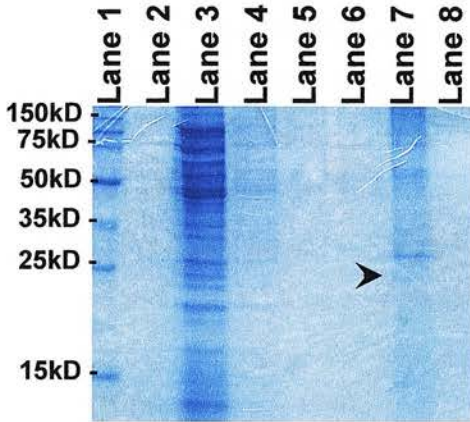
An assessment of protein production was made by inducing 2ml cultures of I-E<sup>d</sup>sc pET14b BL21(DE3) and analysing the cultures in order to detect expression of I-E<sup>d</sup>sc TBB (Figure 5.8). The I-E<sup>d</sup>sc TBB product was found to be confined to inclusion bodies, from which it could be solubilised using urea (AmershamBiosciences, 1997, Williams et al., 1982). There was minimal loss during cell lysis as indicated by the presence of a small amount of 2G9 positive staining in Lane 3 of Figure 5.8b. This figure also shows that a proportion of the I-E<sup>d</sup>sc TBB bound the I-E<sup>d</sup>-specific monoclonal antibody 2G9.

Following the detection of I-E<sup>d</sup>sc TBB within induced I-E<sup>d</sup>sc pET14b BL21(DE3), the experiment was adjusted in order to test the impact on expression of various parameters. It was found that the highest level of expression was achieved by:

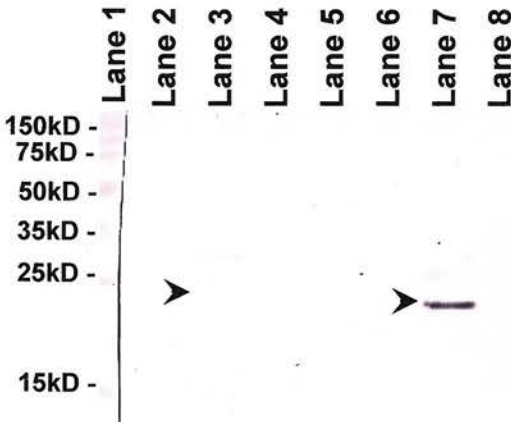
- Selecting the colony to be used in large-scale induction from a subjective assessment of protein production in small-scale culture.
- Use of LB medium which was found to be the most versatile and effective medium.
- Use of carbenicillin as opposed to amoxicillin in order to reduce bacterial overgrowth.
- Use of 1mM IPTG for induction over 4 hours once the OD<sub>600</sub> was between 0.6 and 0.8.

Figure 5.8 – Assessment of I-E<sup>d</sup>sc TBB protein production

## a) Coomassie stain



## b) 2G9-probed Western blot

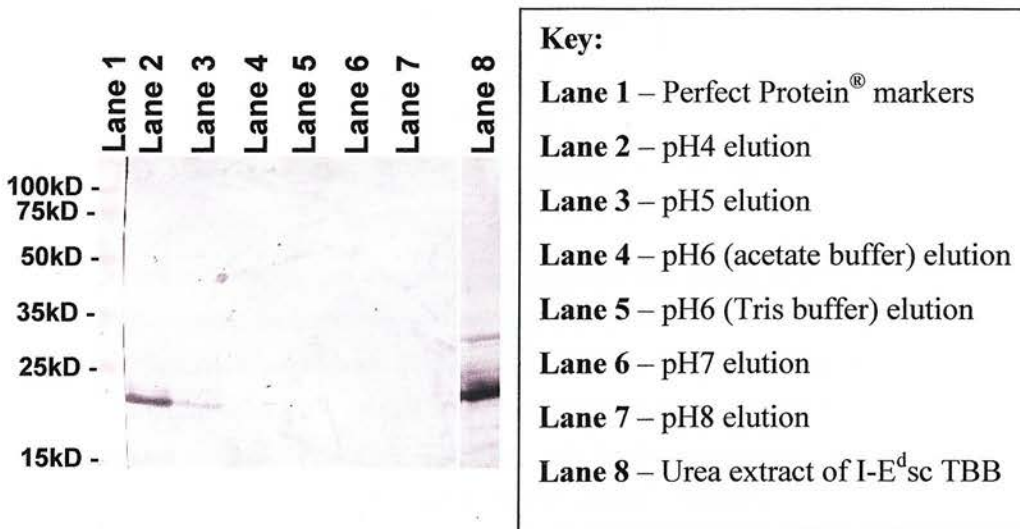
**Key:****Lane 1** – Perfect Protein® markers**Lane 2** – Bacterial supernatant**Lane 3** – Bacterial cell lysate**Lane 4** – Wash I**Lane 5** – Wash II**Lane 6** – Wash III**Lane 7** – Urea extract I**Lane 8** – Urea extract II➤ – I-E<sup>d</sup>sc TBB protein

2ml cultures of I-E<sup>d</sup>sc pET14b BL21(DE3) were induced using IPTG. The presence of I-E<sup>d</sup>sc TBB was assessed at each stage of the purification process of the induced bacterial culture by taking samples and separating these by SDS-PAGE. The gels were analysed using both Coomassie staining and Western blotting in parallel. The Western blot was probed using 2G9. This is representative of three protein induction experiments.

### 3.3 Pilot study purification of I-E<sup>d</sup>sc TBB

The I-E<sup>d</sup>sc TBB extracted from inclusion bodies contained considerable quantities of contaminating proteins and so required further purification. Ion-exchange chromatography was used initially as described by Burrows *et al* (Burrows *et al.*, 1999). The pI of the extracted IE<sup>d</sup>sc TBB was first roughly measured as being about pH5 (Figure 5.9). The results suggested that anion exchange resins should bind the fusion protein in buffers more alkaline than pH5, and cation exchange resins in buffers more acidic than pH5. I chose anion exchange using basic buffers as these were noted to improve the functional purification of the rat single-chain fusion protein (Burrows *et al.*, 1999).

Figure 5.9 – pI of I-E<sup>d</sup>scTBB

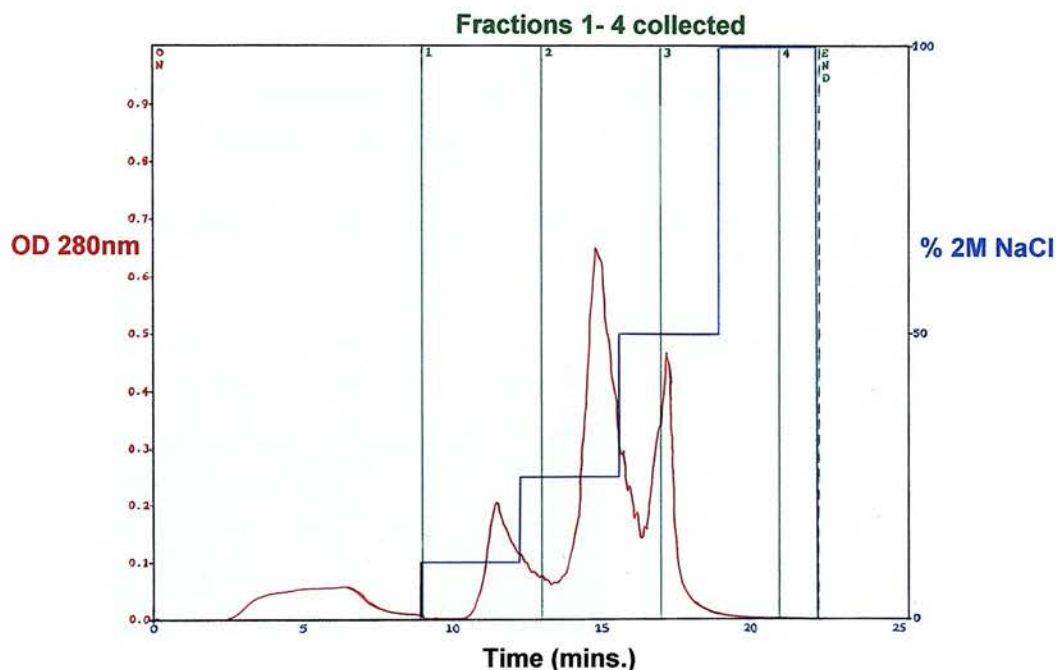


The pI of the extracted I-E<sup>d</sup>sc TBB was first roughly calculated by equilibrating samples of the protein extract in a series of buffer solutions of 8M urea with either 50mM Tris.Cl (pH6, 7, 8 &9) or 50mM sodium acetate (pH4, 5 & 6). The above samples were combined with S-Sepharose Fast cation exchange beads equilibrated with the appropriate buffer. The beads were washed twice with the appropriate buffer before eluting any bound protein using an elution buffer (8M urea, 0.25M sodium chloride & 50mM Tris.Cl pH10). The eluates were separated by SDS-PAGE gel electrophoresis before transferring onto nitrocellulose by Western blotting. The resulting blot was probed with 2G9 monoclonal antibody using the two-layer approach. The IE<sup>d</sup>sc TBB protein appears to have bound S-Sepharose at pH5 but not pH6 suggesting a pI of about 5. This is in agreement with the theoretical pI of the construct using the ExPASy Compute pI/MW tool ([http://us.expasy.org/tools/pi\\_tool.html](http://us.expasy.org/tools/pi_tool.html))



Anion exchange chromatography was performed using Poros® 20HQ medium (Figure 5.10).

**Figure 5.10 – Anion exchange of IE<sup>d</sup>sc TBB**



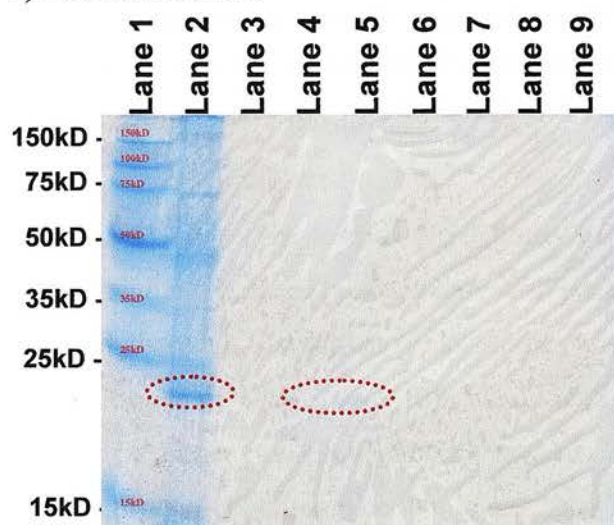
A 4.6mm diameter/50mm length chromatography column was packed with Poros® 20HQ medium (*PerSeptive Biosystems Inc.*) forming a 0.8ml bed volume as per manufacturer's instructions. The column was first equilibrated with 20 column volumes of 6M urea/50mM Tris.Cl pH8.5. The previously extracted IE<sup>d</sup>sc TBB solution was filtered through a 0.45µm filter before loading onto the prepared column in 10ml aliquots per separation. The loaded column was washed with 10 column volumes of the above equilibration buffer, before adding increasing salt concentrations to the equilibration buffer in 10 column volume steps at 0.2M, 0.5M, 1M and 2M sodium chloride. 10ml fractions were collected at each step. The separation process was carried out using a Biocad 700E (*PerSeptive Biosystems Inc.*). The separation process was repeated ten times with identical chromatograms.

The chromatogram highlights the problems encountered during the purification process. Although three distinct elution peaks are seen only the first contains the IE<sup>d</sup>sc TBB, while the other two higher optical density peaks do not appear to contain any protein Figure 5.11a. These later peaks are only seen after loading the extracted

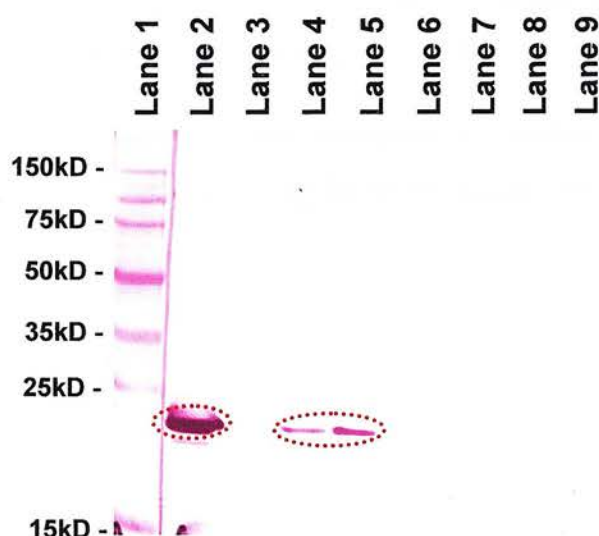
IE<sup>d</sup><sub>sc</sub> TBB, and were not present during “dummy” separations using buffers alone. It was also noted that the column used was unable to accommodate more than 10ml of crude extract without increasing post-load losses. These later peaks may well, therefore, represent impurities which led to column “fouling” and a loss of column efficiency. This is a well recognised problem encountered with inclusion body purification due to hydrophobic lipoprotein contaminants, particularly with anion resins (AmershamPharmaciaBiotech, 2001).

Figure 5.11 – Assessment of anion exchange separation of IE<sup>d</sup><sub>sc</sub> TBB


a) Coomassie stain



b) 2G9-probed Western blot





**Key:****Lane 1** – Perfect Protein markers**Lane 2** – Pre-load**Lane 3** – Post-load**Lane 4** – Peak 1 from 2<sup>nd</sup> separation**Lane 5** – Peak 1 from 9<sup>th</sup> separation**Lane 6** – Peak 2 from 2<sup>nd</sup> separation**Lane 7** – Peak 2 from 9<sup>th</sup> separation**Lane 8** – Peak 3 from 2<sup>nd</sup> separation**Lane 9** – Peak 3 from 9<sup>th</sup> separation – I-E<sup>d</sup>sc TBB band

Samples from each stage of the anion exchange separation were taken and separated by SDS-PAGE using two gels in parallel. One gel was stained with Coomassie Blue, whilst the other was electroblotted onto nitrocellulose overnight and probed with 2G9 monoclonal antibody. Separations 2 and 9 were used as representative samples of the ten separations performed.

Figure 5.11 shows the loss of the majority of impurities upon passage through the anion column (compare pre-load lane with peak 1 lanes in Figure 5.11a). Moreover, although there are two further peaks on the chromatogram, these do not stain positive using Coomassie Blue stain. This would tend to suggest that these latter peaks are formed by either non-proteinaceous material or small amounts of high molecular weight protein-containing contaminants that have been diluted in the separation process. The reduced intensity of the I-E<sup>d</sup>sc TBB in the eluates reflects at least three-fold dilution of the crude I-E<sup>d</sup>sc TBB preparation demonstrated by the reduced 2G9 stain in the eluate lane (Figure 5.11b).

The difficulties encountered with this particular expression system made its further development for the human single-chain fusion proteins unattractive.

### 3.4 Expression of single-chain proteins using the pET25b vector

#### 3.4.1 Cloning of single-chain proteins into pET25b vector

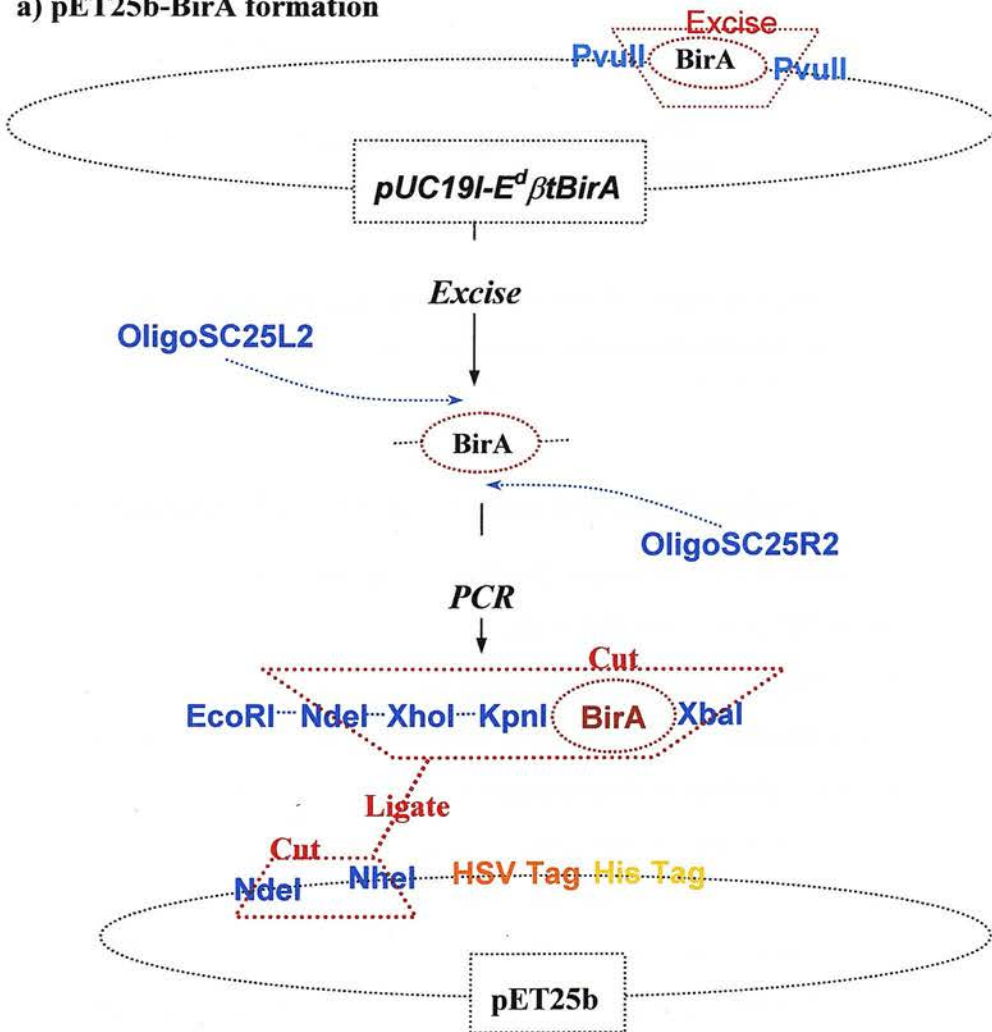
In order to overcome the purification difficulties, a different pET vector was utilised that would place both an HSV-Tag<sup>®</sup> and a His-Tag<sup>®</sup> at the C-terminus of the single-chain fusion protein. Tagging would not only enhance recombinant protein identification, but would also allow alternative purification strategies to be used. These issues are of particular relevance to the two human HLA-DR single-chain constructs that currently do not have a monoclonal antibody akin to 2G9 with which to identify them in their unfolded form. pET25b was chosen as the vector for its HSV-Tag<sup>®</sup> and His-Tag<sup>®</sup> as well as its T7 promoter. However, cloning of the single-chain constructs into pET25b in order to utilise the C-terminal tags was not straightforward because of unsuitable restriction enzyme sites and the presence of a stop-codon after the C-terminal BirA sequence within the single-chain constructs (See Figure 5.4 & Figure 5.7). A two-step strategy was adopted that first cloned in a modified BirA sequence before cloning in the separate single-chain construct sequences.

The first stage in this process was the adaptation of the BirA DNA sequence. The BirA DNA sequence was excised from the vector pUC19I-E<sup>d</sup>βtBirA (See Chapter 3) using the restriction enzyme PvuII. The DNA fragment of interest was initially excised in order to reduce any non-specific binding of the rather long oligonucleotide primers. The excised and purified DNA sequence was expanded and modified using the oligonucleotide primer pair SC25L2 and SC25R2 (See Appendix 2). Thirty cycles of PCR were carried out (denature at 95°C for 60 seconds, anneal at 52°C for 30 seconds, and extend at 72°C for 60 seconds). The resulting DNA fragment was purified by agarose gel electrophoresis and restricted with NdeI and XbaI before cloning into the pET25b vector restricted with NdeI and NheI and dephosphorylated (Figure 5.12a). This part of the construct formation was difficult, requiring six attempts to achieve a successful outcome. Transformants were assessed by restriction enzyme digests. A plasmid from a suitable transformant was

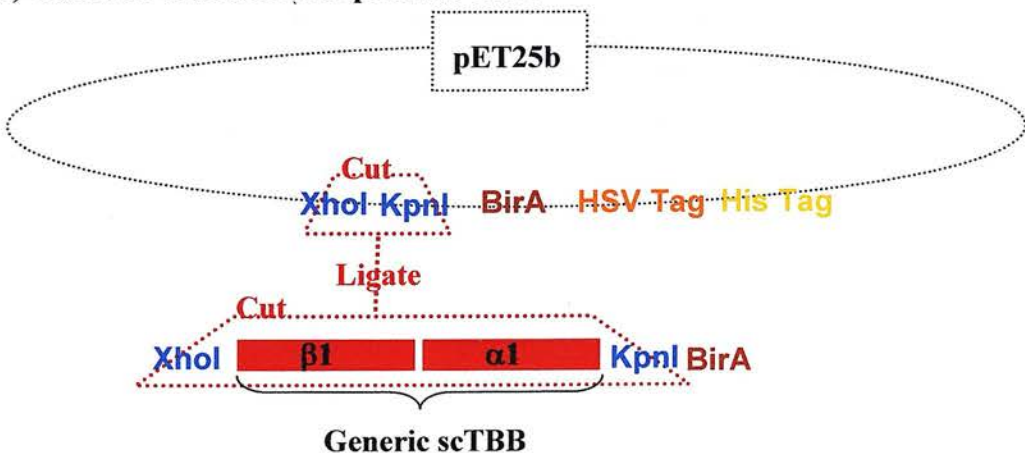
sequenced using the 'T7 promoter' primer and shown to have the expected sequence (Figure 5.13). This modified vector was named pET25b (BirA).

Figure 5.12 – Outline of pET25b-BirA scTBB formation

a) pET25b-BirA formation



b) Insertion of scTBB into pET25b-BirA



**Figure 5.13 – Sequence pET25b(BirA) using T7 promoter primer**

```

1   CATATGTCCTC  GAGGGGTACC  AGCGGCGGTG  GACTGCATCA
    NdeI        XhoI KpnI

41  TATTCTGGAT  GCACAGAAAA  TGGTGTGGAA  TCATCGTTCC
      BirA Sequence

81  TCTAGCCAGC  CAGAACTCGC  CCCGGAAGAC  CCCGAGGATG
      HSV Tag

121 TCGAGCACCA  CCACCACCAC  CACTGAGAT
      His Tag      STOP
    
```

The above shows the nucleic acid sequence of the modified vector, pET25b(BirA). The His and HSV tags are in frame with the 'stop' codon. Important restriction enzyme sites are also marked.

### 3.4.2 Cloning of scTBB sequences into pET25b(BirA)

Having formed the pET25b(BirA) vector the DNA sequences for the three single-chain fusion protein constructs (HLA-DR15sc, HLA-DR7sc and I-E<sup>d</sup>sc) could be cloned into the vector. Each of the three scTBB DNA sequences were cloned into the XhoI/KpnI site in pET25b(BirA) (Figure 5.12b). Transformants were assessed by restriction enzyme digests and a plasmid from a suitable transformant sequenced for each of the three cloned constructs using the 'T7 promoter' primer. This part of the construct formation only required one attempt for a successful outcome. The sequence of pET25b-IE<sup>d</sup>sc contained two base pair changes, that of pET25b-HLADR15sc contained a single base pair change, whilst pET25b-HLADR7sc matched the expected sequence (Figure 5.14). In the case of I-E<sup>d</sup>sc, these base pair changes may represent primer degeneracy, whilst for HLA-DR15sc the changes may represent variations of the nucleotide sequence as none were predicted to result in any amino acid changes. Translations of the DNA sequences of the three scTBB proteins are shown in Figure 5.15.



**Figure 5.14 – Nucleotide sequences of pET25b-IE<sup>d</sup>sc TBB, -DR15sc TBB & -DR7sc TBB**

scTBB(IE <sup>d</sup> )		<b>CATATGTC</b> TC	<b>GAG</b> GCCCACG	GTTTTTGGAA	TACGTTACAT
scTBB(DR15)	1	-----	-----	T--CC--TGG	C-GCC-AGA
scTBB(DR7)		-----	-----	T--CC--TGG	C-GGG--AG-
		<b>NdeI</b>	<b>XhoI</b>		
scTBB(IE <sup>d</sup> )		CTGAGTGTCA	TTTCTACAAC	GGGACGCAGC	ACGTGCGGTT
scTBB(DR15)	41	GG-----	-----T---T	-----G---	GG-----
scTBB(DR7)		A-A-----	-----T----	-----G---	GG-----A---
scTBB(IE <sup>d</sup> )		TCTGGAGAGA	TTCATCTACA	ACCGGGAGGA	GAACCTGCGC
scTBB(DR15)	81	C-----C---	-A-T-----T-	---A-----	-TC-G-----
scTBB(DR7)		C-----A---	C--T-----T-	---A-----	-TT-G-----
scTBB(IE <sup>d</sup> )		TTCGACAGCG	ACGTGGGCGA	GTACCGCGCG	GTGACAGAGC
scTBB(DR15)	121	-----	-----G--	--T---G---	-----G----
scTBB(DR7)		-----	-----G--	-----G---	-----G----
scTBB(IE <sup>d</sup> )		TGGGGCGGCC	AGACGCCGAG	AACTGGAACA	GCCAGCCGGA
scTBB(DR15)	161	-----	T-----T---	T-----	-----AA---
scTBB(DR7)		-A-----	T-T-----	TC-----	-----AA---
scTBB(IE <sup>d</sup> )		GATCCTGGAG	GATGCGCGGG	CCTCGGTGGA	CACGTACTGC
scTBB(DR15)	201	C-----	C-G-----	--G-----	---C-----
scTBB(DR7)		C-----	--CAG-----	G-CA-----	---CGTG---
scTBB(IE <sup>d</sup> )		AGACACAAC	ATGAGATCTC	GGATAAATTC	CTTGTGCGGC
scTBB(DR15)	241	-----	-C-G-G-TGT	---G-GC---	ACA----A--
scTBB(DR7)		-----	-C-G-G-TGG	T--G-GC---	ACA----A--
scTBB(IE <sup>d</sup> )		GG <sup>C<sup>A</sup></sup> GAGTCGG	AGCTCAAGAC	GCTATCAAAG	AGGAACACAC
scTBB(DR15)	281	--C-----	-----	-----	-A-----TGT
scTBB(DR7)		--C-----	-----	-----	-A-----TGT
scTBB(IE <sup>d</sup> )		CATCATCCAG	GCA <sup>G</sup> GAGTTCT	ATCTTTTACC	AGACAAACGT
scTBB(DR15)	321	G-----	--C-----	----GAAT--	T---C-TCA
scTBB(DR7)		G-----	--C-----	----GAAT--	T---C-TCA
scTBB(IE <sup>d</sup> )		GGAGAGTTTA	TGTTTGA	TGACGGCGAT	GAGATTTTCC
scTBB(DR15)	361	--C-----	-----	---T--T---	-----
scTBB(DR7)		--C-----	-----	---T--T---	-----
scTBB(IE <sup>d</sup> )		ATGTAGACAT	TGAAAAGTCA	GAGACCATCT	GGAGACTTGA
scTBB(DR15)	401	----G--T--	G-C----AAG	----GG---	--C-G-----
scTBB(DR7)		----G--T--	G-C----AAG	----GG---	--C-G-----
scTBB(IE <sup>d</sup> )		AGAATTTGCA	AAGTTTGCCA	GCTTTGAGGC	TCAGGGTGCA
scTBB(DR15)	441	-----G-	CGA-----	-----	---A-----
scTBB(DR7)		-----G-	CGA-----	-----	---A-----

scTBB(IE <sup>d</sup> )		CTGGCTAATA	TAGCTGTGGA	CAAAGCTAAC	CTGGATGTCA
scTBB(DR15)	481	T----C--C-	-----	-----C---	C <sup>T</sup> ----AA---
scTBB(DR7)		T----C--C-	-----	-----C---	-----AA---
scTBB(IE <sup>d</sup> )		TGAAAGAGCG	TTCCAACAAC	ACTCCAGATG	CCAACGGTAC
scTBB(DR15)	521	---C-A----	C-----T-T	-----GATCA	----T-----
scTBB(DR7)		---C-A----	C-----T-T	-----GATCA	----T-----
					KpnI
scTBB(IE <sup>d</sup> )		CAGCGGCGGT	GGACTGCATC	ATATTCTGGA	TGCACAGAAA
scTBB(DR15)	561	-----	-----	-----	-----
scTBB(DR7)		-----	-----	-----	-----
scTBB(IE <sup>d</sup> )		ATGGTGTGGA	ATCATCGTTC	CTCTAGCCAG	CCAGAACTCG
scTBB(DR15)	601	-----	-----	-----	-----
scTBB(DR7)		-----	-----	-----	-----
scTBB(IE <sup>d</sup> )		CCCCGGAAGA	CCCCGAGGAT	GTCGAGCACC	ACCACCACCA
scTBB(DR15)	641	-----	-----	-----	-----
scTBB(DR7)		-----	-----	-----	-----
scTBB(IE <sup>d</sup> )		CCACTGA			
scTBB(DR15)	681	-----			
scTBB(DR7)		-----			
		STOP			

**Key:**  
A<sup>G</sup> – A is determined base sequence & G is the expected base sequence.



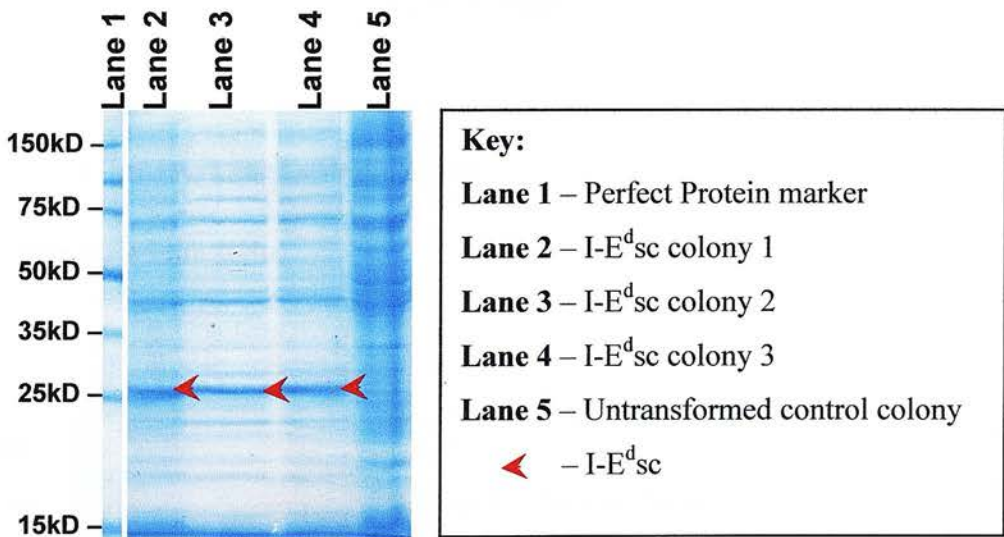
Figure 5.15 – Protein sequences of scTBB constructs

IE <sup>dsc</sup>		MSRGP	RFLEY	VTSEC	HFYNG	TQHVR	FLERF	IYNRE
DR15sc	1	-----	---WQ	PKRE-	--F--	-ER--	--D-Y	F--Q-
DR7sc		-----	---WQ	GKYK-	--F--	-ER-Q	----L	F--Q-
<b>Natural disulphide bond</b>								
IE <sup>dsc</sup>		ENLRF	DSDVG	EYRAV	TELGR	PDAEN	WNSQP	EILED
DR15sc	36	SV---	-----	-F---	-----	----Y	----K	D---Q
DR7sc		FV---	-----	-----	-----	-V--S	----K	D----
IE <sup>dsc</sup>		ARASV	DTYCR	HNYEI	SDKFL	VRRRV	GAQDA	IKEEH
DR15sc	71	---A-	-----	---GV	VES-T	-Q---	-----	-----
DR7sc		R-GQ-	--V--	---GV	GES-T	-Q---	-----	-----
<b>β1-α1 Junction</b>								
IE <sup>dsc</sup>		TIIQA	EFYLL	PDKRG	EFMFD	FDGDE	IFHVD	IEKSE
DR15sc	106	V----	----N	--QS-	-----	-----	-----	MA-K-
DR7sc		V----	----N	--QS-	-----	-----	-----	MA-K-
IE <sup>dsc</sup>		TIWRL	EEFAK	FASFE	AQGAL	ANIAV	DKANL	DVMKE
DR15sc	141	-V---	---GR	-----	-----	-----	-----	EI-TK
DR7sc		-V---	---GR	-----	-----	-----	-----	EI-TK
IE <sup>dsc</sup>		RSNNT	PDANG	TSGGG	LHHIL	DAQKM	VWNHR	SSSQP
DR15sc	176	---Y-	-IT--	-----	-----	-----	-----	-----
DR7sc		---Y-	-IT--	-----	-----	-----	-----	-----
<b>BirA sequence</b>								
IE <sup>dsc</sup>		ELAPE	DPEDV	EHHHH	HH			
DR15sc	211	-----	-----	-----	--			
DR7sc		-----	-----	-----	--			
<b>HSV Tag</b>								
<b>His Tag</b>								

### 3.4.3 Assessment of recombinant scTBB protein production

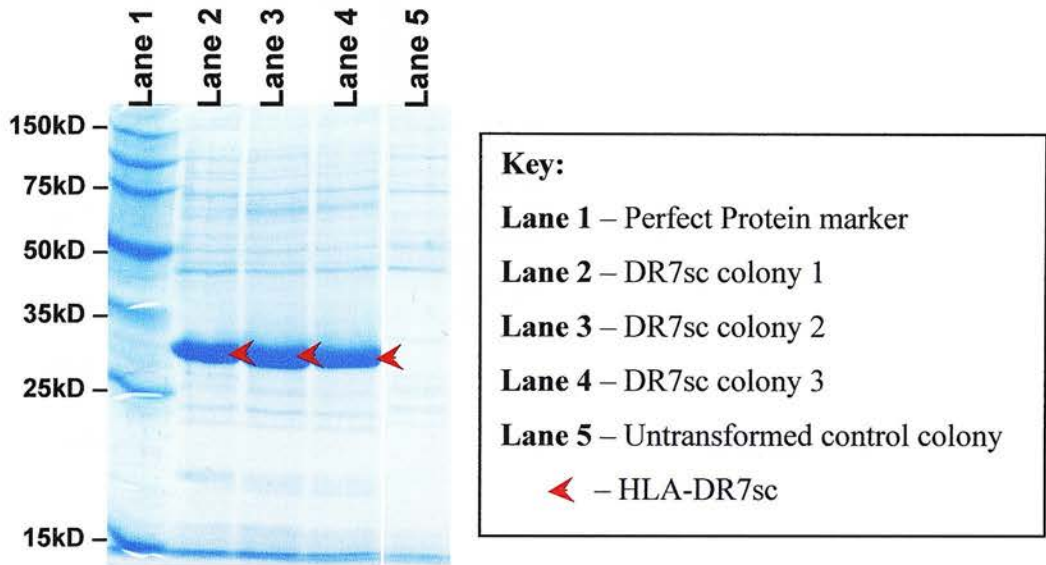
Sequenced plasmids (pET25b(BirA)-DR15sc TBB, -DR7sc TBB and -I-E<sup>d</sup>sc TBB) were transformed into the bacterial expression host BL21(DE3) *E.coli*. Cultures were induced and analysed as previously (Figure 5.16, Figure 5.17, and Figure 5.18). A protein of the predicted 26kD size was identified in all transformed colonies using the Coomassie stain. Immunoblotting identified DR15sc TBB as having a polyhistidine tag as expected. The additional bands seen in the anti-His Tag immunoblots may represent dimers (50kD bands) and breakdown products of the scTBB as the untransformed control colony had few polyhistidine tagged elements identified. Of note is the high expression and greater purity of the single-chain fusion proteins using this vector in comparison to pET14b, particularly the two human HLA-DR proteins.

Figure 5.16 – I-E<sup>d</sup>sc TBB peptide production



The above shows test cultures of three pET25b BL21(DE3) I-E<sup>d</sup>sc colonies induced using IPTG. The crude urea-extracted inclusion body preparation was separated by SDS-PAGE. The gel was analysed using Coomassie staining. A band of the expected size is seen in each of the three test colonies but not in the untransformed control colony. This is representative of three protein induction experiments.

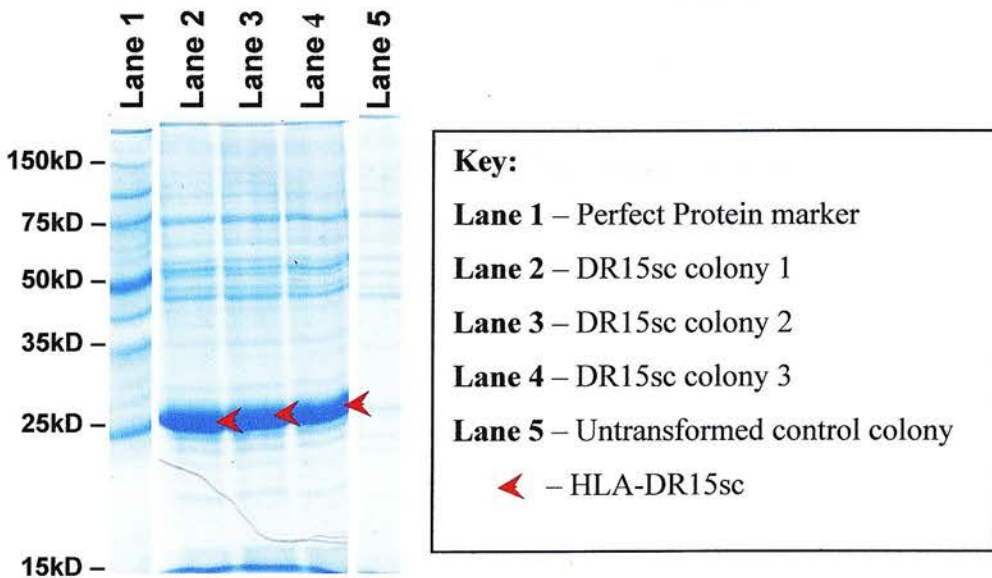
Figure 5.17 – DR7sc TBB peptide production

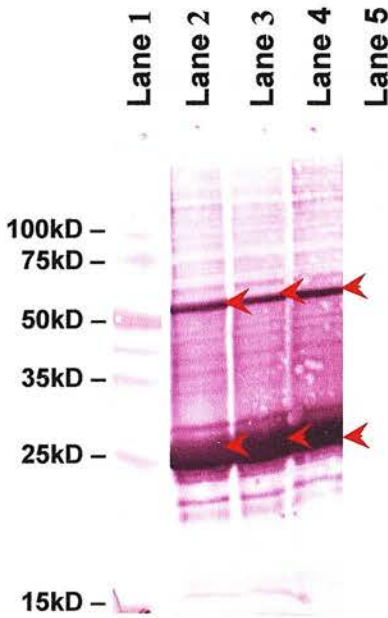


Legend as Figure 5.16

Figure 5.18 – DR15sc TBB peptide production

a) Coomassie blue stain



**b) Anti-His tag immunoblot****Key:****Lane 1** – Perfect Protein marker**Lane 2** – DR15sc colony 1**Lane 3** – DR15sc colony 2**Lane 4** – DR15sc colony 3**Lane 5** – Untransformed control colony

◀ – HLA-DR15sc

The above shows test cultures of three pET25b BL21(DE3) DR15sc colonies induced using IPTG. The crude urea-extracted inclusion body preparations were separated by SDS-PAGE. The gels were analysed using Coomassie staining, or electroblotted onto nitrocellulose overnight prior to probing with anti-His tag monoclonal antibody and developing using the two-layer approach. A band of the expected size is seen in each of the three test colonies but not in the untransformed control colony. The higher weight band identified using the monoclonal antibody may represent dimerization of the DR15sc TBB. This is representative of three protein induction experiments.

Having now established that all three scTBB constructs could be induced using this expression system, the next step involved the assessment of purification strategies.

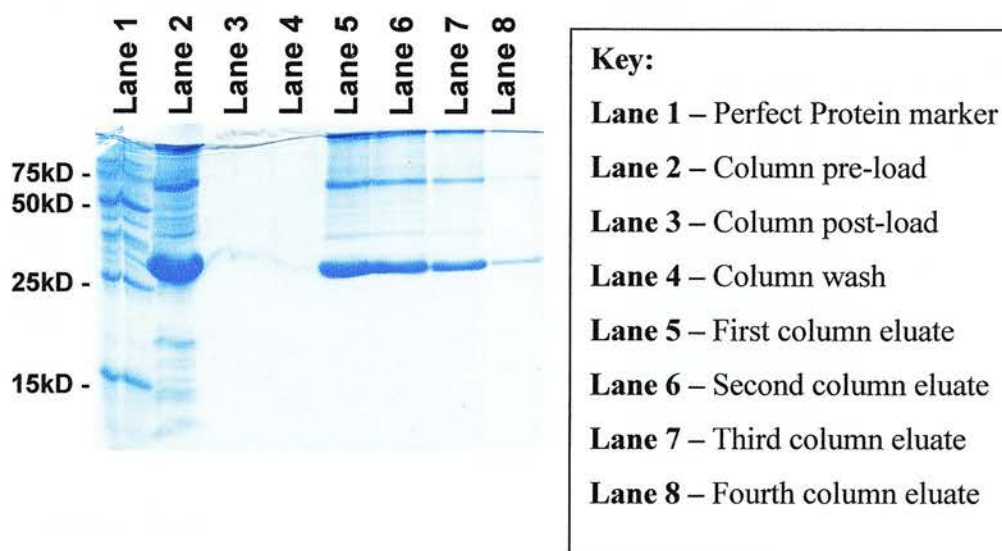


## 4 Purification of scTBB proteins

### 4.1 Assessment of nickel chelation chromatography

The above series of results show that proteins of the expected size are being produced with the expected His-Tag<sup>®</sup> sequence. The next stage was to utilise this His-Tag<sup>®</sup> as a means of purification. A pilot purification was undertaken using HLA-DR7scTBB as this protein had been the first to be successfully expressed.

A large-scale protein induction was performed utilising the bacterial clone identified in the small-scale induction above as producing the highest protein yield. 5ml of the chosen bacterial colony suspension was taken and placed in 100ml of LB medium containing 200µg/ml carbenicillin in a 250ml baffled flask. The resulting suspension was incubated at 37°C, induced using IPTG and processed as per Methods. In this pilot purification, the inclusion body pellet was solubilised using 6M guanidine hydrochloride (GnHCl) buffered with 50mM Tris.Cl pH 7.5. The resulting suspension was filtered through a 0.45µm filter before storing at 4°C overnight. Subsequent inclusion body preparations were successfully solubilised using the inclusion body re-suspension solution which utilises 6M urea and a HEPES buffer (*vide infra*). The HLA-DR7scTBB suspension was purified using a 3ml bed-volume Iminodiacetic acid (IDA)-Sepharose 6B Fastflow<sup>®</sup> column (Figure 5.19). The nickel chelation column results in loss of low molecular weight contaminants, although their absence from the post-load is difficult to explain other than for a dilutional effect or breakdown. There are some losses during the purification process, but the majority of the HLA-DR7sc TBB protein is eluted from the nickel column, although still having some impurities. There is a higher weight band seen in all the gels (at around 50kD) which may represent dimerization of the HLA-DR7sc TBB protein through intermolecular disulphide bond formation.

**Figure 5.19 – His-Tag<sup>®</sup> purification of DR7sc TBB**

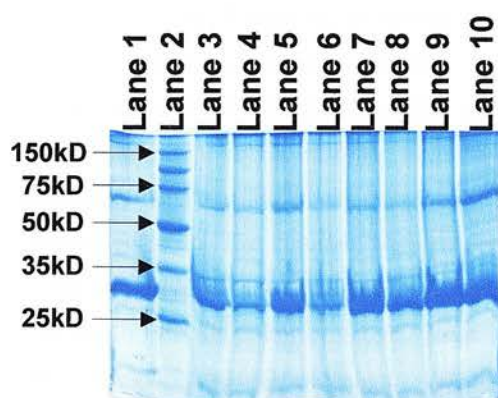
A 3ml bed-volume IDA-Sepharose 6B Fastflow<sup>®</sup> column was formed in an Econo-Pac<sup>®</sup> disposable chromatography column (Bio-Rad Laboratories Inc.). The prepared column was washed twice with 20ml of 50mM Tris.Cl pH7.5 before loading with nickel ions. 30ml of column metal ion loading solution was passed over the column before washing twice with 20ml 50mM Tris.Cl pH7.5 and three times with 10ml 6M GnHCl/50mM Tris.Cl pH 7.5/10mM imidazole. The imidazole was added in an attempt to prevent non-specific low-level interactions between non-His Tag<sup>®</sup> histidine containing peptides and the nickel loaded column during purification. 1ml of HLA-DR7scTBB suspension was loaded onto the prepared column after adding 10mM imidazole to the suspension. The column was washed three times with 10ml 6M GnHCl/50mM Tris.Cl pH 7.5/10mM imidazole, before eluting the column four times with 10ml 6M GnHCl/50mM Tris.Cl pH 7.5/100mM EDTA. In order to assess the above purification samples from each stage were precipitated using four volumes of 100% ethanol at -20°C for 72 hours. The precipitated solutions were centrifuged at 20000g for 30minutes at 4°C, suspending the precipitated protein in 8M urea/20mM ethanolamine pH10/PMSF/ EDTA. Samples were separated by SDS-PAGE gel electrophoresis before staining with Coomassie Blue. The majority of impurities appear to have been removed during this purification. This is representative of two purification experiments.

One way of improving separation and reducing non-specific protein binding to the nickel-loaded column would be to increase the imidazole concentration in the loading and wash buffers. However, this may result in increased losses, and so a pilot study was carried out to determine the optimum imidazole concentration (Figure 5.20).

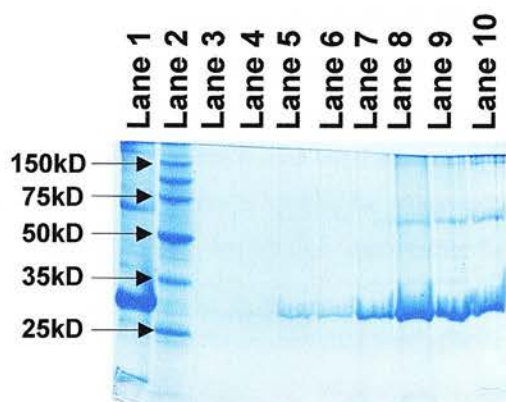


Figure 5.20 – Assessment of imidazole concentration for His-Tag purification

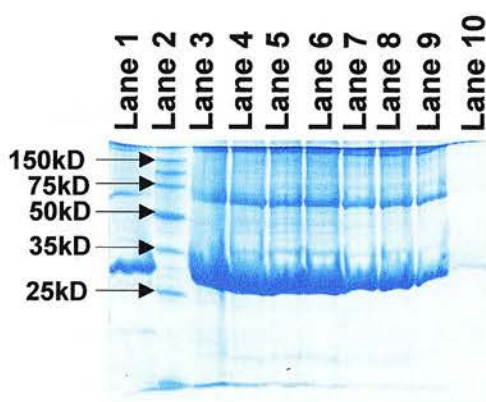
a) Column post-load



b) Column wash



c) Column eluate



**Key:**

**Lane 1** – Column pre-load

**Lane 2** – Perfect Protein marker

**Lane 3** – 0mM imidazole

**Lane 4** – 10mM imidazole

**Lane 5** – 20mM imidazole

**Lane 6** – 30mM imidazole

**Lane 7** – 50mM imidazole

**Lane 8** – 75mM imidazole

**Lane 9** – 100mM imidazole

**Lane 10** – 200mM imidazole

Eight 60µl bed-volume IDA-Sepharose 6B Fastflow<sup>®</sup> columns were formed using Mobicol<sup>®</sup> 1ml microcolumns (*MoBiTec GmbH*) with a 10µm pore filter to collect the sepharose beads. These columns were each loaded with 1ml of column metal ion loading solution before being equilibrated with 300µl of one of eight wash buffers. The buffers were composed of 6M GnHCl/0.1M Tris.Cl pH7.5 and one of eight imidazole concentrations (0mM, 10mM, 20mM, 30mM, 50mM, 75mM, 100mM, and 200mM). 20µl of HLA-DR7sc TBB inclusion body solution was added to each column together with 80µl of the relevant wash buffer. The columns were mixed for 1.5hours at room temperature before collecting the post-load by centrifuging each column at 18000g for 30 seconds into a microfuge tube. The columns were washed twice with 100µl of the relevant wash buffer before eluting with 100µl of 6M GnHCl/0.1M Tris.Cl pH8/100mM EDTA. The wash steps and eluates were collected by centrifugation as above. Each sample collected was precipitated with four volumes of 100% ethanol at -20°C overnight. The precipitates were collected and re-suspended in 8M urea/20mM ethanolamine pH10/PMSF/ EDTA before separating by SDS-PAGE gel electrophoresis and staining with Coomassie Blue.

As can be seen in Figure 5.20a&b the increasing imidazole concentrations resulted in increasing post-load losses particularly evident beyond 50mM imidazole, with increasing losses during the column wash step beyond 20mM imidazole. Moreover, there would appear to be little to gain in terms of eluate purity by altering the imidazole concentration (Figure 5.20c). On balance, I decided to continue to use 10mM imidazole in order to achieve the optimum balance between the reduction of non-specific binding and increasing protein losses.

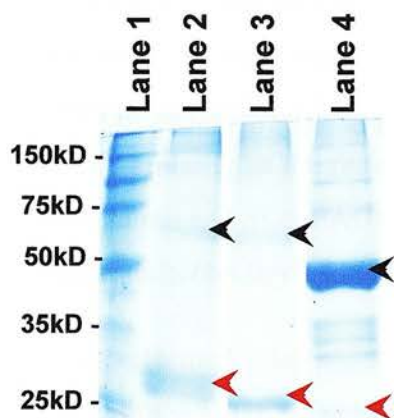
As a result of the difficulty in directly analysing the GnHCl prepared samples, I used 6M urea as the chaotroph in later inclusion body preparations together with 1M NaCl to maintain the ionic strength of the buffer and reduce non-specific column interactions. Large-scale purification used Poros<sup>®</sup> MC medium (*PerSeptive Biosystems*) packed into a HPLC column. Having reviewed the manufacturer's literature regarding the Poros<sup>®</sup> MC medium, I opted to use HEPES buffer rather than Tris, as there is a theoretical weakening of metal ion binding to the Poros<sup>®</sup> MC medium in the presence of primary amines as found in Tris buffer.

## 4.2 Assessment of scTBB refolding

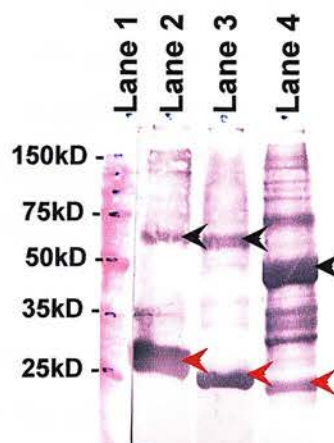
The incorporation of the recombinant scTBBs into insoluble bacterial inclusion bodies simplifies the preliminary isolation steps as seen above. However, the difficulties encountered during purification are shifted downstream in terms of functionally correct protein refolding and disulphide bond formation.

Figure 5.21 – SDS-PAGE gel mobilities of the scTBBs

### a) Coomassie Blue



### b) Anti-His Tag



#### Key:

**Lane 1** – Perfect Protein marker<sup>®</sup>

**Lane 2** – HLA-DR7sc (26.3kD)

**Lane 3** – I-E<sup>d</sup>sc (26.4kD)

**Lane 4** – HLA-DR15sc (26.4kD)

◀ – Expected monomer sc TBB

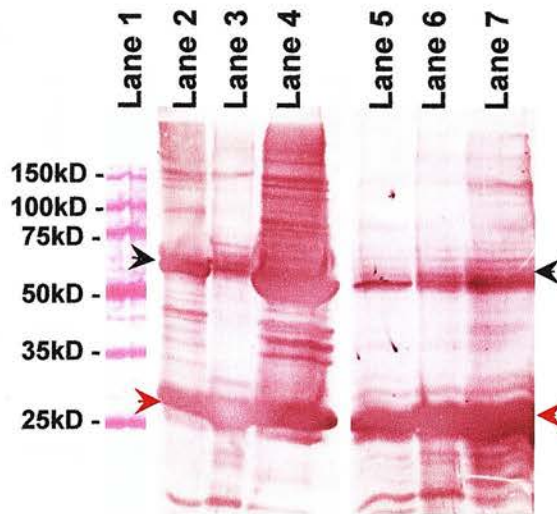
◀ – Apparent dimeric sc TBB

SDS-PAGE separation of urea-extract of inclusion body preparation from each of the three fusion-protein constructs. One gel is stained with Coomassie Blue, whilst the other was electro-blotted onto nitrocellulose before probing with anti-His tag monoclonal antibody and developing using the two-layer approach. The variable mobility of the three constructs is seen. There is also a variable proportion of each construct dimerised. The expected molecular weight of each construct is shown in brackets. This is representative of the SDS-PAGE separation of four separate inclusion body preparations.

The scTBBs are very similar in their amino acid sequences and predicted molecular weights, but their SDS-PAGE gel mobilities are very different as demonstrated in Figure 5.21. The proportion of each scTBB at an apparently dimeric mobility is also very different, being greater for HLA-DR15sc. Furthermore, the greater frequency of protein fragments within the HLA-DR15sc separation possibly suggests a more disorganised refolding permitting greater cleavage by proteases. This dimerization is probably occurring through interchain disulphide bond formation given the presence of two cysteine residues within the  $\beta_1$  domain of each scTBB protein. Nonetheless, this was a surprising finding given that Burrows *et al* did not seem to experience this dimerization with either of their two constructs (Burrows et al., 1999, Chang et al., 2001). Therefore, although there is a large degree of similarity in the primary structure of the three scTBB proteins, the degree of dimerization and SDS-PAGE gel mobility is seen to vary between them indicating differences in secondary and tertiary structure.

I performed pilot studies to ascertain the optimum folding regimen for the scTBBs formed. HLA-DR15sc was used as the pilot refolding target given its apparently greater dimeric constitution. Monomer formation in the absence of reducing conditions was used as a surrogate marker for correct refolding. The initial refolding strategy was based upon that of Burrows *et al* (Burrows et al., 1999) (Figure 5.22). The aliquot removed after the addition of DTT showed a considerable reduction in the content of the 55kD band compared with that pre-treatment (compare lanes 2 and 3 in Figure 5.22) confirming that the band was due to dimer formation as a result of inter-chain disulphide bonds. Unfortunately, considerable dimer reformation occurred following the removal of the DTT (lane 4 Figure 5.22). The majority of dimers could be broken by the addition of DTT (compare lanes 2-4 and 5-7 Figure 5.22). This result suggested that refolding should be undertaken with more dilute protein solutions to reduce inter-chain disulphide bond formation, and use a glutathione reoxidation system to facilitate disulphide bond shuffling during refolding (Altman et al., 1993, Frayser et al., 1999, Rudolph and Lilie, 1996). A subsequent pilot study was performed using this system (Figure 5.23).



**Figure 5.22 – DR15sc TBB refolding without redox shuffle (anti-HSV Tag)****Key:****Lane 1** – Perfect Protein® markers**Lane 2 & 5** – Urea sample -/+ DTT reduction**Lane 3 & 6** – DTT sample -/+ DTT reduction**Lane 4 & 7** – PBS sample -/+ DTT reduction

◀ – Monomer scTBB

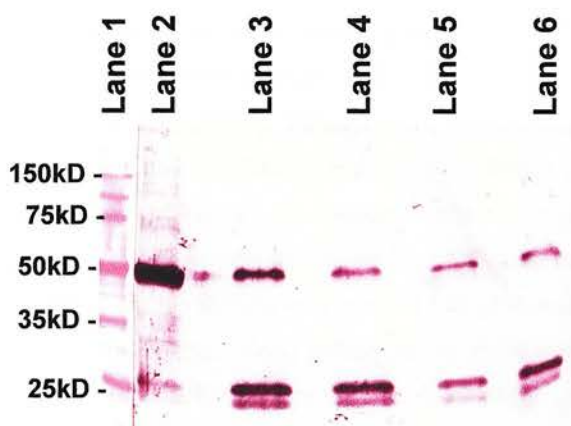
◀ – Dimeric scTBB

A 6ml sample of His-Tag® purified HLA-DR15sc in its elution buffer was placed into prepared Seamless Cellulose® dialysis tubing and dialysed against 5x400ml 6M urea/20mM ethanolamine pH10 at 4°C over a 48hour period ('urea sample'). This was primarily performed to remove the nickel ions from the purified protein which may prevent cysteine residue oxidation during downstream renaturation (Rudolph and Lilie, 1996). Following this DTT was added to a final concentration of 50mM and the resulting solution placed at 37°C for 1 hour in order to reduce any disulphide bonds (Fischer et al., 1992) ('DTT sample'). The protein solution was then dialysed against 2 x 1l 20mM ethanolamine pH10 at 4°C for 72hours and finally 3x1l PBS/0.05% sodium azide at 4°C over 24hours ('PBS sample'). 10µl samples of each stage was taken and separated by SDS-PAGE gel electrophoresis before and after further reduction with 100mM DTT at 95°C for 10 minutes. The SDS-PAGE gel was electro-blotted onto nitrocellulose before being probed with anti-HSV Tag monoclonal antibody and developed using the two layer technique.

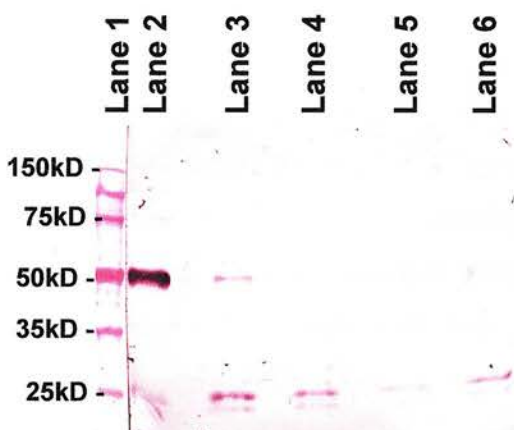


Figure 5.23 – Refolding scTBB(DR15) using redox shuffle

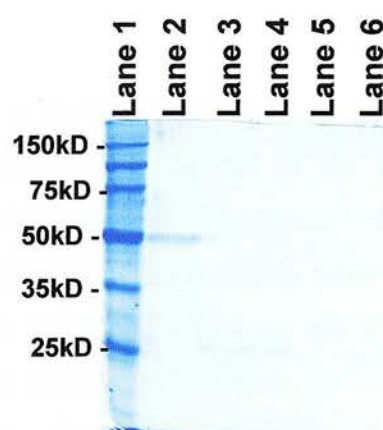
a) Anti-HSV Tag



b) Anti-His Tag



c) Coomassie Blue stain



**Key:**

**Lane 1** – Perfect Protein<sup>®</sup> marker

**Lane 2** – Pre-refolding

**Lane 3** – Urea & reduced glutathione

**Lane 4** – Ethanolamine & reduced glutathione

**Lane 5** – Ethanolamine & oxidised glutathione

**Lane 6** – PBS

A 15ml sample of His-Tag® purified scTBB(DR15) in its elution buffer was first dialysed into 6M urea/20mM ethanolamine pH10 as above. To this 10mM reduced glutathione was added and the resulting solution gently mixed at 4°C overnight. This solution was then dialysed against 2l 20mM ethanolamine pH10/10mM reduced glutathione at 4°C overnight. Such slow dialysis should reduce the urea concentration gradually and so theoretically reducing the risk of aggregation (Rudolph, 1996, Rudolph and Lilie, 1996). Following this step, the solution was removed from the dialysis tubing and oxidised glutathione added to a final concentration of 1mM together with sodium azide to a final concentration of 0.05%. The resulting solution was gently mixed at 4°C for 48hours before dialysing against 2x4l PBS/0.05% sodium azide at 4°C for a further 48hours. The final refolded solution was removed from the dialysis tubing and 0.1ml of Protease Inhibitor Cocktail for Bacterial Cell extracts (Sigma-Aldrich Inc.) added before storing the solution at 4°C. Samples taken over the refolding process were taken and separated by SDS-PAGE gel electrophoresis. One gel was stained with Coomassie Blue whilst two were electro-blotted onto nitrocellulose overnight. The blots were probed with anti-His-Tag® and anti-HSV-Tag® monoclonal antibodies

This refolding strategy resulted in a greater proportion of the HLA-DR15scTBB protein remaining in monomeric form at the end of the refolding process, although dilution of the protein had also occurred. The amount of protein remaining in the dimeric state was minimised through this refolding process. The dilution process itself may well have had a beneficial effect on the refolding-aggregation equilibrium. The dual band seen at around 25kD (Figure 5.23a&b) may represent the HLA-DR15scTBB protein with either altered mobility or relative biotinylation.

The refolding strategy was also successfully used for both IE<sup>d</sup>scTBB and HLA-DR7scTBB. Further refolding attempts resulted in minor additions to the refolding solutions. NP40 was used in the initial stages of the refolding process as a non-ionic detergent in an attempt to reduce aggregation further (Labeta et al., 1988, Stöckel et al., 1997). In order to reduce ionic variation over the refolding process, the salt concentration was kept constant at 150mM NaCl.

## 5 Discussion

In this chapter, I have described the successful construction of three two-domain MHC Class II fusion proteins. The initial construction work was performed using murine I-E<sup>d</sup> through overlap-extension PCR, but this could not be extrapolated for use with either HLA-DR7 or HLA-DR15. Their construction required a successful revision of the previous method. Incorporation into a viable bacterial expression system ultimately yielded abundant fusion proteins.

The pET14b vector system was initially utilised due to its availability in the laboratory and its similarity to the pET21d vector used by Burrows *et al* (Burrows *et al.*, 1998). The murine construct I-E<sup>d</sup>scTBB was successfully ligated into this expression vector, and the recombinant fusion protein found to be produced in bacterial inclusion bodies. Unfortunately, further development of this system was hindered because of a number of factors including poor yield and difficulties with downstream purification using anion exchange chromatography that proved more troublesome than encountered by other groups (Burrows *et al.*, 1998, Burrows *et al.*, 1999, Chang *et al.*, 2001). The main problem with this technique was that of non-proteinaceous column fouling that could not be removed by thorough washing of the inclusion bodies prior to their re-suspension. This resulted in a marked reduction in column capacity and increased dilution of the resulting purified I-E<sup>d</sup>scTBB protein. In order to open up other purification avenues, as well as improve the chances of incorporating the human scTBB constructs into a bacterial expression vector, a different pET vector was sought.

The vector pET25b was chosen due to its two C-terminal tags and the accessibility of its cloning sites. The basic vector was successfully modified to allow ligation of the three scTBB constructs in such a way that two C-terminal tags could be utilised, whilst removing the pelB leader sequence that would otherwise facilitate the export of the recombinant proteins into the periplasmic space. All three recombinant scTBB proteins were produced using this expression system. Nickel chelation chromatography was successfully optimised in the purification of each construct, with each construct having the expected C-terminal tags. However, as

predicted, protein refolding and disulphide bond formation of these recombinant proteins proved challenging. Despite the similarities between each of the three recombinant constructs, there was a varying degree of dimerization of the scTBB proteins. This suggested differences in secondary and tertiary protein structure between the three scTBB proteins that may have occurred due to subtle differences in their production conditions, out with those already accounted for. Burrows' group reported no such problems with either anion exchange or protein refolding, experiencing no such disulphide dimerization problems (G. Burrows, *personal communication*). Based on modifications of a number of techniques (Arimilli et al., 1995, Kuhelj et al., 1995, Lilie et al., 1998, Rudolph, 1996, Rudolph and Lilie, 1996, Stöckel et al., 1997), and using Burrows' methodology as a base line (Burrows et al., 1998), I developed a reproducible refolding strategy that minimised the degree of dimerization using a redox-shuffle technique. Although this strategy did not completely remove the dimeric scTBB forms, the hope is that the improved refolding achieved would enhance functionality beyond these dimeric forms.

One possible improvement to the current purification and refolding strategy would be to utilise on-column purification followed by refolding (AmershamPharmaciaBiotech, 2001, Colangeli et al., 1998). This technique is feasible, but would require some modification to the strategy used above in order to reduce possible nickel oxidation on the chromatography column during refolding. Moreover, further purification steps may well be required to improve protein homogeneity and purity in the form of size-exclusion chromatography +/- anion exchange chromatography (Burrows et al., 1998, Colangeli et al., 1998). Before further purification was undertaken, I felt that it would be prudent to assess the functionality of the scTBB proteins as described in the following chapter.

## **Chapter 6**

### **Results (IV)**



## Chapter 6

### Results (IV)

## Functional Evaluation of Tetramer Building Blocks

### 1 Introduction

Within the preceding chapters, I have described the design, construction, expression and purification of recombinant murine and human MHC Class II proteins. These recombinant proteins have the expected molecular size on SDS-PAGE and the expected affinities for certain monoclonal antibodies. In this chapter, I will describe experiments that evaluate the conformational and functional nature of the purified constructs. In particular, I demonstrate that both HLA-DR15LZ TBB and HLA-DR15sc TBB specifically bind peptide ligands. Initial work used the HLA-DR15 TBBs to develop appropriate assays that were then applied to the other recombinant proteins.

### 2 Leucine Zipper-associated Heterodimeric HLA-DR Tetramer Building Blocks

#### 2.1 Conformational Nature of the Purified HLA-DR15LZ TBB

It was not straightforward to demonstrate that the HLA-DR15LZ  $\alpha$  and  $\beta$  chains co-expressed in S2 cells associated to form HLA-DR15LZ  $\alpha\beta$  heterodimers because, in the absence of proper peptide loading, recombinant HLA-DR15LZ  $\alpha\beta$  heterodimers dissociated under the conditions of SDS-PAGE (Figure 4.13). Therefore, I chose two approaches to demonstrate the heterodimeric nature of the recombinant HLA-DR15LZ. First, immunoprecipitation using the monoclonal antibody L243. This monoclonal antibody binds to the HLA-DR  $\alpha$  chain of HLA-

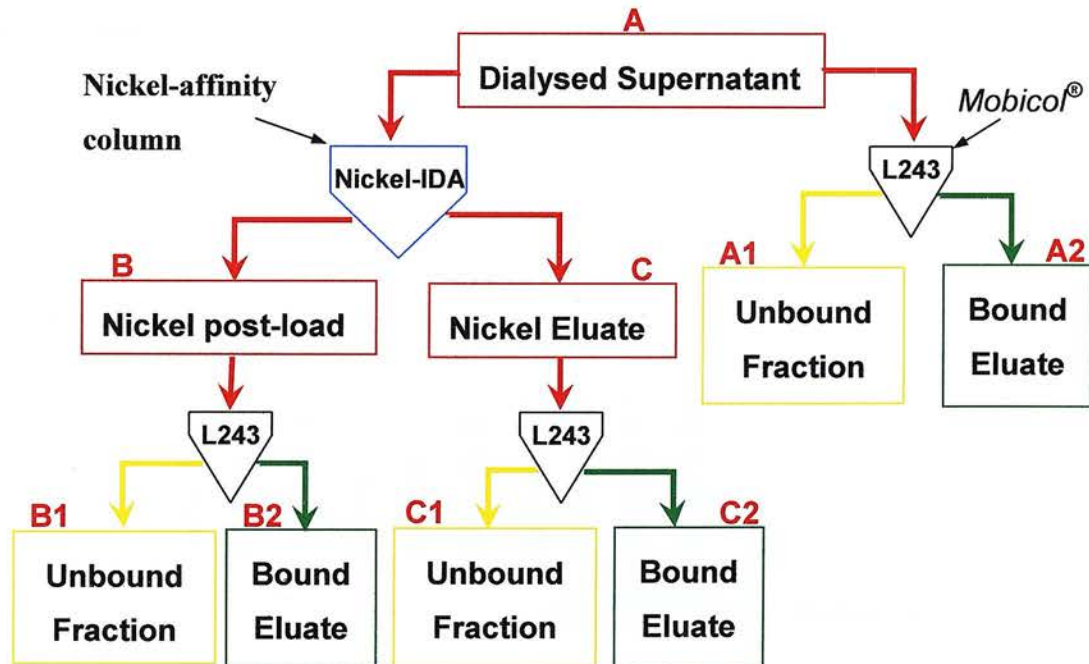
DR  $\alpha\beta$  heterodimers but not to isolated HLA-DR  $\alpha$  chains (Fu and Karr, 1994). Immunoprecipitation of HLA-DR15LZ by L243 would, therefore, bring down the ‘conformationally’ correct fraction of the recombinant HLA-DR15LZ and confirm the existence of  $\alpha\beta$  heterodimers (Gorga et al., 1987, Lampson and Levy, 1980, Stöckel et al., 1994). Second, I captured total  $\alpha$  chain (both free  $\alpha$  and  $\alpha\beta$  heterodimers) onto Nickel-resin by exploiting the His-tag on the carboxy terminus of the recombinant  $\alpha$  chain. The aim was to demonstrate  $\alpha\beta$  heterodimers in solution by detecting co-precipitating  $\beta$  chain. These two approaches are shown in Figure 6.1. The results are shown in Figure 6.2. The key observations from the above analysis are as follows:

- a) A large proportion of the total HLA-DR15LZ alpha chain within the dialysed supernatant is captured by the L243 monoclonal antibody indicating their occurrence as ‘conformationally correct’  $\alpha\beta$  heterodimers (compare samples A, A1 and A2).
- b) Extraction of the HLA-DR15LZ alpha chain by nickel-chelation chromatography results in almost complete extraction of the HLA-DR15LZ beta chain (very little  $\beta$  chain staining in sample B1 and C1 compared to A1), indicating that almost all  $\beta$  chains are associated with  $\alpha$  chains.
- c) The more evident alpha-chain staining in B1 and C1 would suggest that there might be a greater production of free alpha than beta chain.
- d) The nickel-chelation chromatography column maintains the  $\alpha\beta$  heterodimeric association of HLA-DR15LZ TBB (compare C2 to A2).
- e) The column size, and hence protein over-loading of the column, has resulted in protein losses from the nickel-chelation column (B), with a proportion of this being conformationally correct (B2).

- f) The presence of the acid-base leucine-zipper motif is able to maintain a significant proportion of HLA-DR15LZ TBB in  $\alpha\beta$  heterodimeric association (see samples A2 and C2).

In summary, this elaborate experiment has confirmed the occurrence of HLA-DR15LZ  $\alpha\beta$  heterodimers in the induced S2 cell supernatant and their survival following nickel-chelation affinity chromatography.

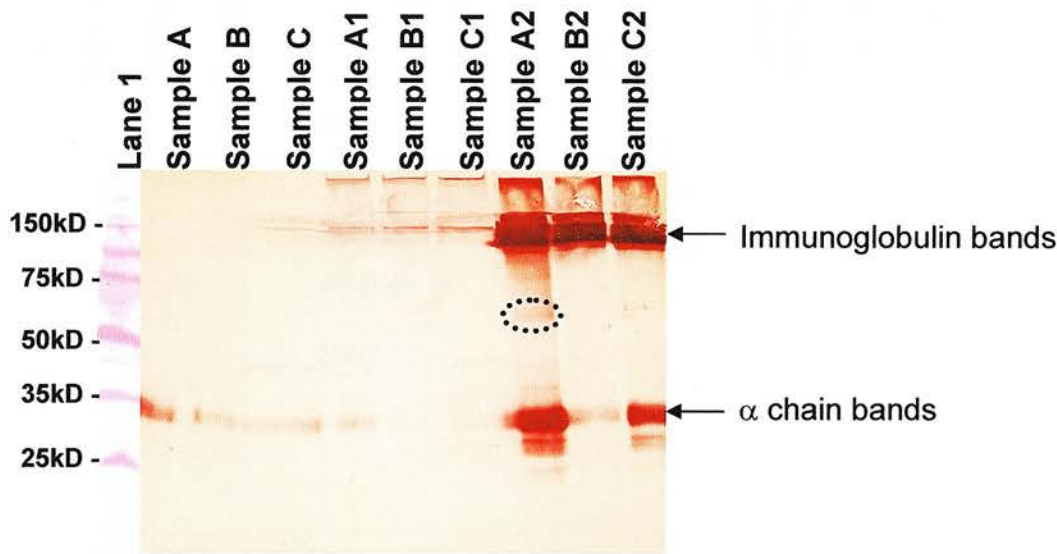
**Figure 6.1 - Immunoprecipitation with L243 to investigate the occurrence of  $\alpha\beta$  heterodimers**



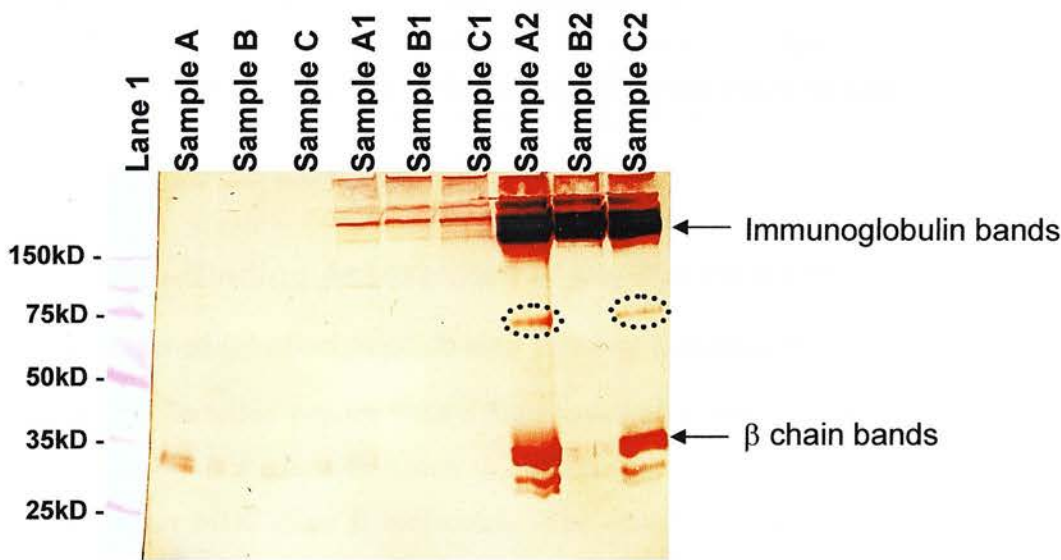
The small-scale nickel-chelation chromatography column and method has been described in Chapter 5. 10ml of dialysed supernatant containing HLA-DR15LZ in PBS prior to nickel affinity purification (A) was purified using the nickel-IDA column and eluted with 10ml of elution buffer forming sample C (Eluted fraction from affinity column). The volumes of samples A, B and C were therefore equivalent. 10ml of A, B (Unbound fraction from nickel-affinity column), and C, and 100 $\mu$ l BE1 cell lysate as a positive control were immunoprecipitated using L243. The immunoprecipitate was eluted into a final volume of 250 $\mu$ l. This represents approximately a 40 fold concentration of A, B and C. Samples were collected from both the bound (A2, B2 and C2) and unbound (A1, B1 and C1) fractions of the antigen-L243 combinations above. The nickel-affinity column is expected to bind the histidine-tagged HLA-DR15LZ alpha chain. L243 is expected to bind conformationally correct HLA-DR15LZ  $\alpha\beta$  heterodimers. All samples were separated by SDS-PAGE prior to blotting onto nitrocellulose and probing with DA6.231, 9E10 and anti-His tag monoclonal antibodies (Figure 6.2).

Figure 6.2 - L243 immunoprecipitation analysis of HLA-DR15LZTBB

a) Anti-His Tag monoclonal – Stains alpha chain



b) DA6.231 monoclonal – Stains beta chain



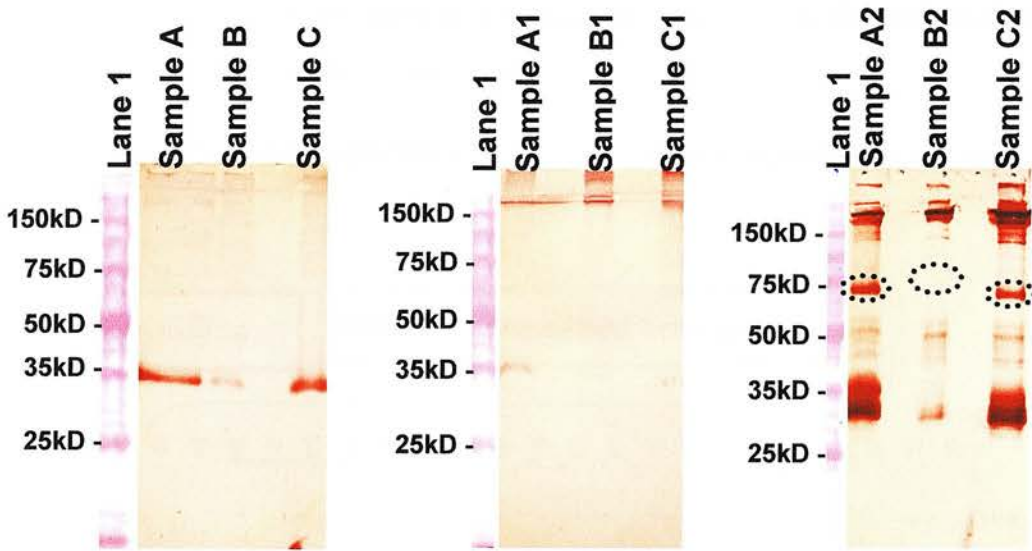
**Key:**

**Lane 1** – Perfect Protein<sup>®</sup> markers

⊙ – αβ heterodimer band



## c) 9E10 monoclonal – Stains beta chain



Samples from the immunoprecipitation analysis were separated by SDS-PAGE prior to electroblotting onto nitrocellulose. The blots were probed using anti-His tag, DA6.231 and 9E10 monoclonal antibodies. The former is expected to bind to HLA-DR15LZ alpha chain, whilst the latter two antibodies are expected to bind to HLA-DR15LZ beta chain. The blots were developed using the three-layer approach with 3-amino-9-ethylcarbazole. The HLA-DR15LZ alpha chain appears to be running heavier than the expected 28kD, whilst the beta chain is found close to the expected 31kD.

## 2.2 Peptide-Binding Assessment of Purified HLA-DR15LZ TBB

### 2.2.1 Design of labelled peptide and binding conditions

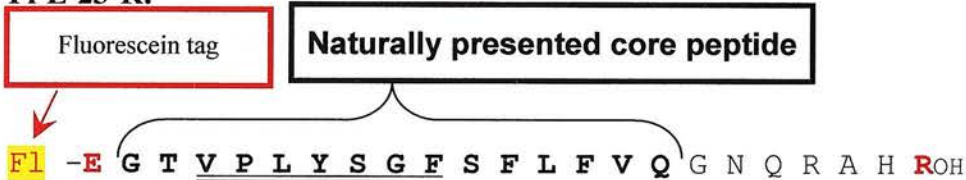
A FITC-labelled peptide with a high predicted affinity for both HLA-DR15 and HLA-DR7 was made with which to examine the peptide-binding properties of the recombinant MHC class II molecules. The choice of peptide was based upon work previously undertaken on the Goodpasture antigen (Phelps et al., 2000, Phelps et al., 1998, Phelps et al., 1996), and the reported peptide-binding characteristics of HLA-DR7 and HLA-DR15 (Chicz et al., 1993, Marsh et al., 2000, Vogt et al., 1994, Wucherpfennig et al., 1994). A synthetic peptide was manufactured containing the  $\alpha 3(\text{IV})$  collagen sequence between amino acid position 26-47 (p26-47), the numbering being relative to the sequence 'SPAT' at the beginning of the NC1



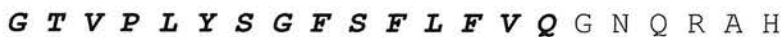
domain. In order to minimise alterations to the peptide conformation, yet allow ease of peptide detection, the peptide was manufactured with an N-terminal fluorescein tag (*BACHEM (UK) Ltd.*) (Figure 6.3).

**Figure 6.3 – Fluorescein-tagged peptide (FI-E-23-R) compared to peptide p3b** (Phelps et al., 2000)

**FI-E-23-R:**



**Peptide p3b:**



The fluorescein-tagged synthetic peptide (FI-E-23-R) was based upon peptide p3b that is known to bind both HLA-DR15 and HLA-DR7 with medium to high affinity (Phelps et al., 2000, Phelps et al., 1998). Peptides FI-E23-R and p3b differ only by the additional residues (in red) in order to improve the predicted solubility of the former. Both the additional residues and the fluorescein tag were designed not to be close to the predicted residues involved in the HLA-DR15 peptide-binding pockets (underlined) (Marsh et al., 2000).

Recombinant and native purified MHC class II molecules are usually obtained in complex with peptides within their peptide-binding domain. In the former case the peptides presumably complex during refolding of the recombinant structure, and are likely to be of relatively low affinity given the non-physiological nature of their production. Therefore, in order to demonstrate the peptide-binding capacity of MHC class II molecules it is necessary to test these molecules using a labelled peptide under conditions that favour peptide exchange. Although exact binding conditions vary between MHC class II types, several studies have identified general principles such as:

- pH 5-7 (Coligan et al., 2001, Scheirle et al., 1992, Sette et al., 1992);

- The presence of certain detergents, *e.g.* NP40, that increase the rate of association of added peptide and the percent occupancy of the recombinant MHC class II molecule, presumably because the dissociation of endogenous peptide is the rate-limiting step in binding (Buelow et al., 1994);
- The presence of hydroxyl groups, *e.g.* in alcohols, that are able to disrupt the hydrogen bonds between peptide ligands and MHC class II molecules and so catalyse ligand exchange even at neutral pH (Falk et al., 2002).

I chose binding conditions based upon these principles of pH 5.0 using a citrate buffer, in the presence of 0.5% NP40 and 5% ethanol. Two approaches were utilised to examine fluorescein-tagged peptide/HLA-DR15LZ TBB interactions. Capture ELISA and a novel approach using bead capture and FACS analysis.

### **2.2.2 Capture ELISA approach**

In order to examine the association of the fluorescein-tagged peptide with MHC class II complexes I first developed a capture ELISA using monoclonal antibodies to trap the MHC class II complexes onto the surface of an ELISA plate, analysing the test plate using a fluorescent plate reader.

Native HLA-DR15 from HLA-DR15-expressing B cell lysates was captured onto flat-bottomed ELISA plates coated with either DA6.231 or L243 monoclonal antibodies in carbonate buffer (35mM NaHCO<sub>3</sub>/15mM Na<sub>2</sub>CO<sub>3</sub> pH9.6). The presence of captured MHC class II complexes was assessed by using the rat anti-Human MHC class II monoclonal antibody YD1/63.4.10 (Pawelec et al., 1982), an alkaline phosphatase-conjugated anti-rat IgG and p-nitrophenyl phosphate. The plate was viewed at 405nm using an *Anthos ht2* plate reader (*Anthos Labtec Instruments, Salzburg*), and revealed the presence of MHC class II complexes in the wells. Native HLA-DR15 was then incubated with serial dilutions of either Fl-E-23-R or a biotin-labelled MBP peptide (MBP<sub>85-108</sub>) at 25°C for 90hours in citrate buffer pH5.0. Fl-E-23-R was formed into a 1mM solution using 2% DMSO/5% acetonitrile in dH<sub>2</sub>O. Fluorescence associated with the MHC complexes was measured by analysing

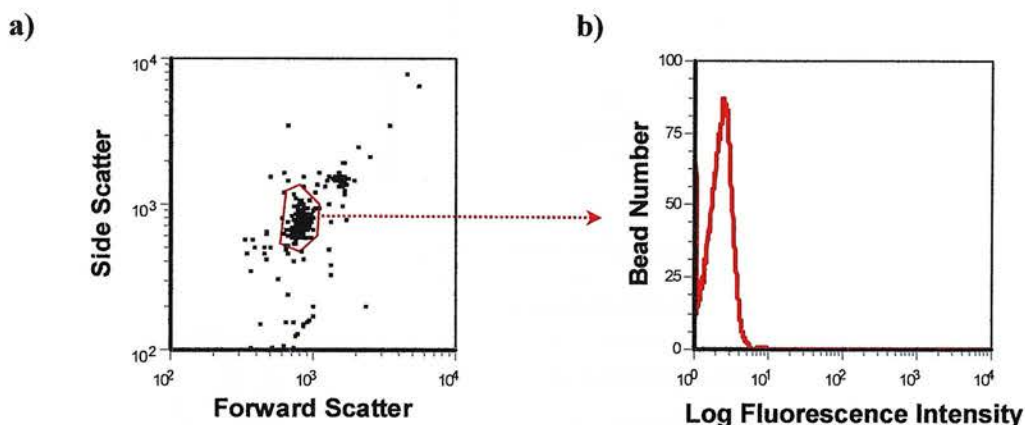
emissions at 535nm following excitation at 485nm using a *Wallac™ 1420 Victor<sup>2</sup>* Multilabel Counter (*PerkinElmer Analytical Instruments (UK)*). The presence of biotin-labelled peptide was detected by developing the wells with Extravidin<sup>®</sup> alkaline phosphatase and p-nitrophenyl phosphate, viewing the plate at 405nm using an *Anthos ht2* plate reader (*Anthos Labtec Instruments, Salzburg*). Although there was no increase in fluorescence above background using FI-E-23-R indicating a lack of peptide binding, the presence of biotin-labelled peptide was detected at the highest concentration after prolonged colour development.

The results indicated that FI-E-23-R had a much lower affinity than expected, and certainly lower than the biotin-labelled peptide our laboratory previously used for HLA – peptide binding assays. Moreover, the results revealed a troublesome tendency for FI-E-23-R to precipitate out of solution in aqueous buffers giving rise to high levels of non-specific binding.

A limited investigation of FI-E-23-R – HLA-DR15LZ interaction using this assay was, unsurprisingly, uninformative. The difficulties encountered above, and the prohibitive expense of manufacturing another tagged peptide, led me to try another technique to assess peptide binding.

### **2.2.3 Bead capture and FACS analysis approach**

I reasoned that coating HLA-DR15LZ onto cell-sized beads would enable me to exploit the sensitivity and versatility of FACS instruments. I used CELlection<sup>™</sup> Dynabeads<sup>®</sup> (*Dynal Biotech UK*) pre-coated with a human IgG<sub>4</sub> that recognises the Fc portion of all murine IgG subclasses. FACS analysis of these beads showed a well defined forward- and side-scatter profile with minimal auto-fluorescence. Experimental analysis could be performed by gating the main population of beads to reduce interference from non-bead bound fluorescent material (Figure 6.4).

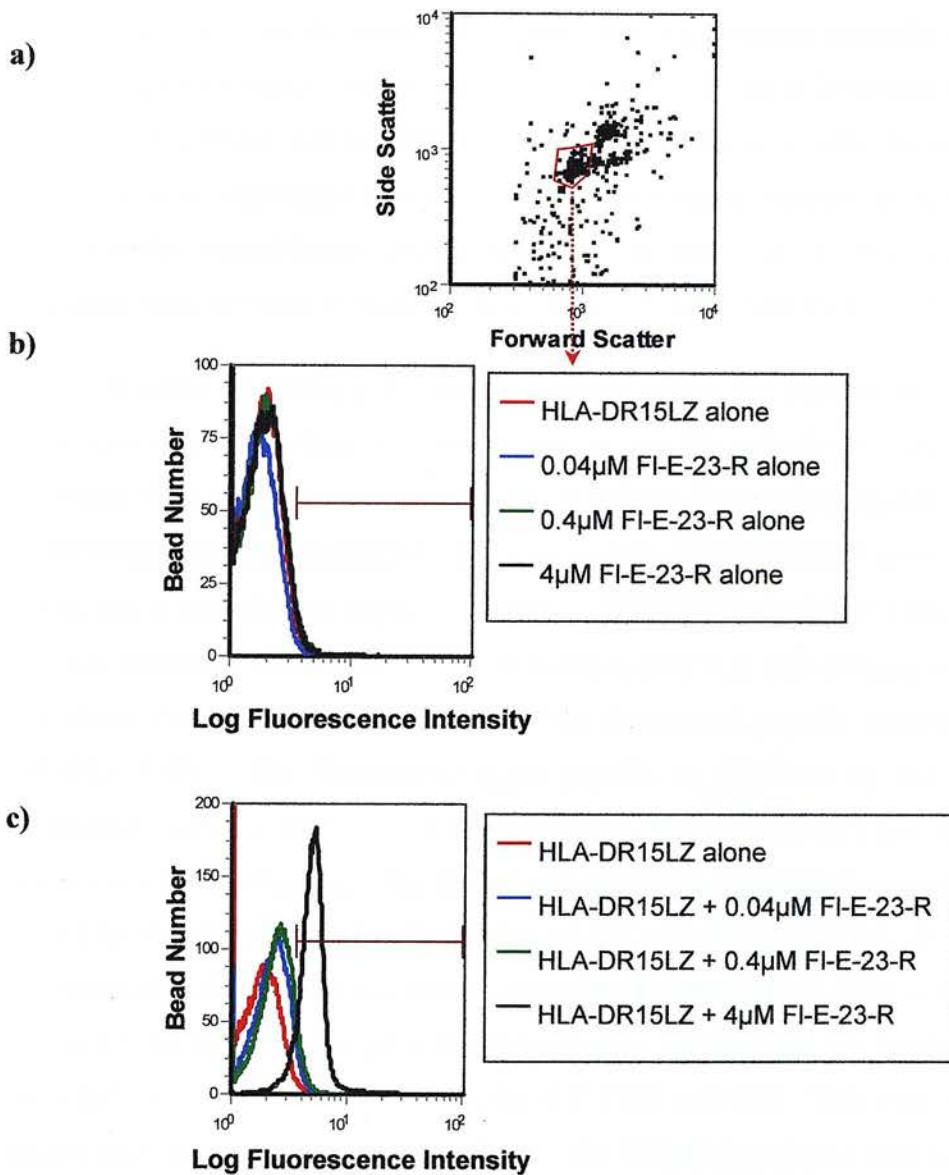
**Figure 6.4 – Gating on Dynal® beads**

CELLlection™ Dynabeads® were coated with 9E10 by mixing 5µl of bead suspension with 0.5ml of affinity purified 9E10 solution in PBS/1% BSA for 1.5 hours at room temperature. The beads were washed in PBS/1% BSA using a magnetic particle concentrator (Dynal MPC®). The beads were assessed by FACS using a Coulter Epics XL-MCL (*Beckman Coulter (UK) Ltd*). The major population of beads was gated as shown and 10000 events within the gate used as the stopping point. There was no significant difference in the fluorescence chromatogram using non-gated events. FACS data was analysed using FCS Express2® software (*De Novo Software (Canada)*). This is representative of five separate FACS analyses.

The 9E10-coated beads could, therefore, be used to capture the recombinant HLA-DR15LZ TBB via the myc-tag and act as the framework for peptide-binding assessment. An initial series of peptide-binding experiments were performed in order to ascertain whether HLA-DR15LZ TBB could bind Fl-E-23-R and whether such binding could be detected within this assay system (Figure 6.5). Peptide binding was performed at 37°C overnight in an attempt to strike a balance between improving binding kinetics and worsening peptide degradation.



Figure 6.5 – HLA-DR15LZ TBB binds to FI-E-23-R

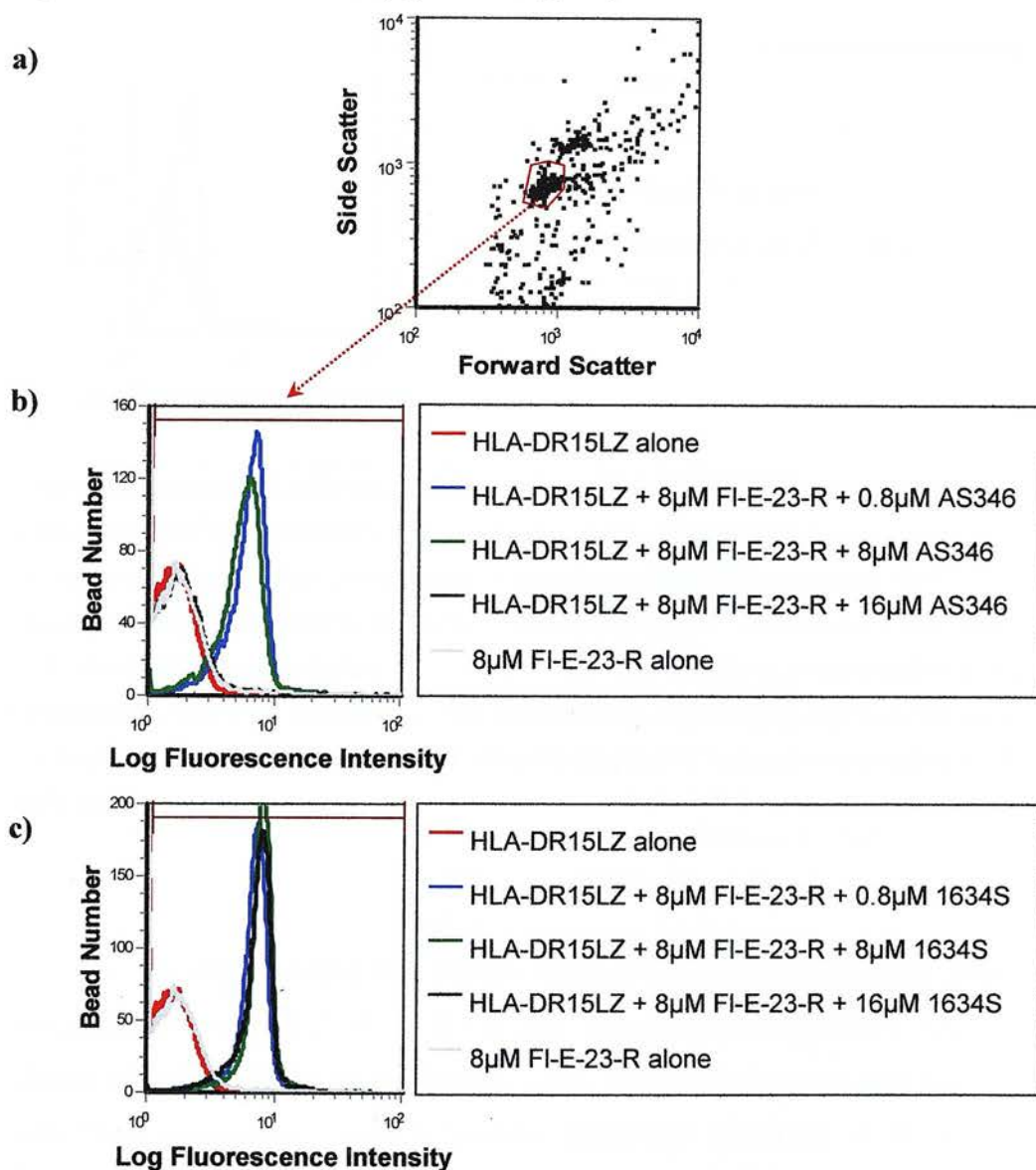


250μl of concentrated HLA-DR15LZ TBB in PBS was added to 1ml of citrate buffer pH5.0 containing Protease Inhibitor Cocktail® (for polyhistidine-tagged proteins – *Sigma-Aldrich Inc.*), 0.5% NP40 and 5% ethanol. FI-E-23-R was added such that the final concentration of peptide was 4μM, 0.8μM, 0.4μM or 0.08μM. The resulting mixtures were incubated at 37°C overnight with gentle shaking. A similar series of peptide concentrations were incubated without HLA-DR15LZ TBB. The mixtures were neutralised to pH7 with 80μl 1M phosphate buffer pH8 prior to adding 80μl of 9E10 coated-beads (about  $5 \times 10^5$  beads) and incubating at RT for 4 hours using the Dynal Sample Mixer®. The beads were washed twice in 1ml PBS. The beads were gated and analysed as previously. The beads combined with peptide alone (b) were used to define the limit of background fluorescence within the gated beads as shown by the positive marker region. This is representative of three peptide loading experiments.

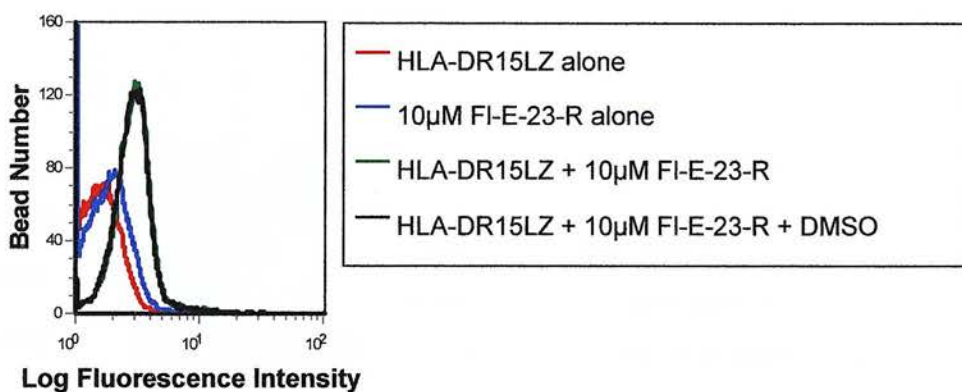


Figure 6.5c shows peptide binding to the HLA-DR15LZ TBB at the highest concentration of peptide used. The peak log fluorescence intensity within the marked region increased from 43 (with 0.04 $\mu$ M FL-E-23-R) to 229 (with 4 $\mu$ M FL-E-23-R). The increase was not due to non-specific interactions with the coated beads as there was no significant increase in fluorescence in the absence of HLA-DR15LZ TBB on the coated-beads (Figure 6.5b). The peak log fluorescence intensity increased from 10 (with 0.04 $\mu$ M FL-E-23-R) to 16 (with 4 $\mu$ M FL-E-23-R).

In order to distinguish specific binding within the peptide-binding groove from non-specific binding to another part of the HLA-DR15LZ TBB protein, I examined the capacity of an unlabelled high affinity HLA-DR15 ligand ('AS346' – **SPHGWISLWKGFSEFIMFFSAGR** – p134-145 of  $\alpha$ 3(IV)NC1 (*Albachim Ltd. UK*)), and a non-binding peptide ('1634S' – **REELFALHGFSCP** (*Albachim Ltd. UK*)) to inhibit the binding of Fl-E-23-R to HLA-DR15LZ TBB (Figure 6.6). Figure 6.6 shows the peptide-specific nature of the fluorescent peptide binding to HLA-DR15LZ TBB. The fluorescent-tagged peptide is displaced by the unlabelled competitor peptide ('AS346'), whilst the control peptide ('1634S') has no effect on fluorescent peptide binding. The peak log fluorescence intensity decreased from 165 with 0.8 $\mu$ M AS346 to the baseline value of 112 with 16 $\mu$ M AS346. The peak log fluorescence intensity did not change significantly with 1634S (220 at 0.8 $\mu$ M and 212 at 16 $\mu$ M 1634S). The peak log fluorescence intensity for the beads combined with 8 $\mu$ M Fl-E-23-R without HLA-DR15LZ TBB was 114. This experiment was successfully repeated with the same result. The DMSO introduced with the 'AS346' did not account for the displacement of Fl-E-23-R as DMSO at an equivalent concentration had no effect on Fl-E-23-R binding (Figure 6.7). Therefore, Fl-E-23-R binding to HLA-DR15LZ TBB is specifically inhibited by a peptide with a high HLA-DR15 binding affinity, and not by a non-binding peptide indicating that the observed Fl-E-23-R binding is occurring at the peptide-binding groove.

**Figure 6.6 – HLA-DR15LZ TBB peptide binding competition**

250 $\mu$ l of concentrated HLA-DR15LZ TBB in PBS was added to 1ml of citrate buffer pH5.0/Protease Inhibitor Cocktail<sup>®</sup>/0.5% NP40/5% ethanol. To this mixture prepared fluorescent-tagged peptide, FI-E-23-R, was added such that the final concentration of peptide was 8 $\mu$ M. To this mixture increasing amounts of either 'AS346' (b) or '1634S' (c) were added such that their final concentrations were 0.8 $\mu$ M, 8 $\mu$ M or 16 $\mu$ M. These mixtures were incubated at 37°C overnight with gentle shaking. The mixtures were then neutralized as above before adding 80 $\mu$ l of 9E10 coated-beads (about  $5 \times 10^5$  beads) and incubating at room temperature for 4 hours using the Dynal Sample Mixer<sup>®</sup>. The beads were washed twice in 1ml PBS using the Dynal MPC<sup>®</sup> prior to resuspending in PBS and analysing as previously. This is representative of three peptide binding competition experiments.

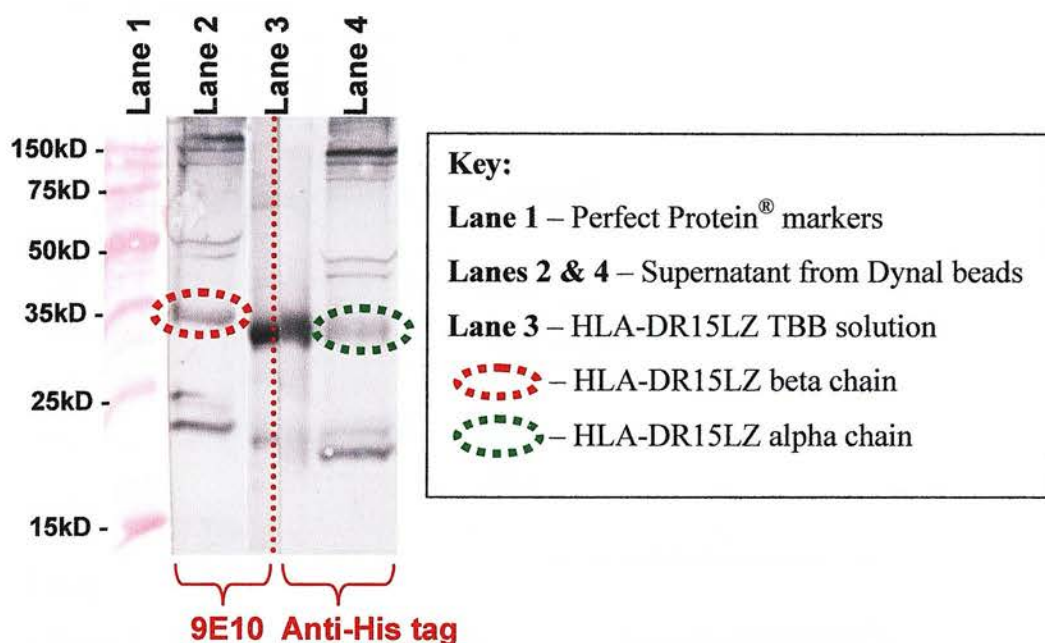
**Figure 6.7 – Lack of DMSO effect on HLA-DR15LZ TBB peptide binding**

250µl of concentrated HLA-DR15LZ TBB in PBS was added to 1ml of citrate buffer pH5.0/Protease Inhibitor Cocktail®/0.5% NP40/5% ethanol. To this mixture prepared fluorescent peptide, FI-E-23-R, was added such that the final concentration of peptide was 8µM. To one sample DMSO was added equivalent to the highest quantity used in the preceding experiment. These mixtures were incubated at 37°C overnight with gentle shaking. The mixtures were then neutralized as above before adding 80µl of 9E10 coated-beads and incubating at room temperature for 4 hours using the Dynal Sample Mixer®. The beads were washed twice in 1ml PBS using the Dynal MPC® prior to resuspending in PBS and analysing as previously.

It was disappointing that peptide binding could only be detected using high concentrations of FI-E-23-R. This in part reflects the unexpectedly low binding affinity of FI-E-23-R for HLA-DR15LZ TBB. Another factor was poor bead coating with 9E10 monoclonal antibody because significant quantities of HLA-DR15LZ TBB alpha and beta chains could be detected following capture by the 9E10 coated beads (Figure 6.8). Therefore, there is scope to improve the systems sensitivity further if required in future analyses.



Figure 6.8 – Assessment of HLA-DR15LZ TBB binding to beads



A sample of the supernatant fluid was removed once the coated-beads had been collected following HLA-DR15LZ capture and prior to washing the beads in PBS. The sample was separated by SDS-PAGE. The gel was electro-blotted onto nitrocellulose overnight prior to probing with either 9E10 or anti-His tag monoclonal antibody. The blot was developed using the three-layer approach and Sigma Fast<sup>™</sup> 3,3'-Diaminobenzidine hydrochloride.

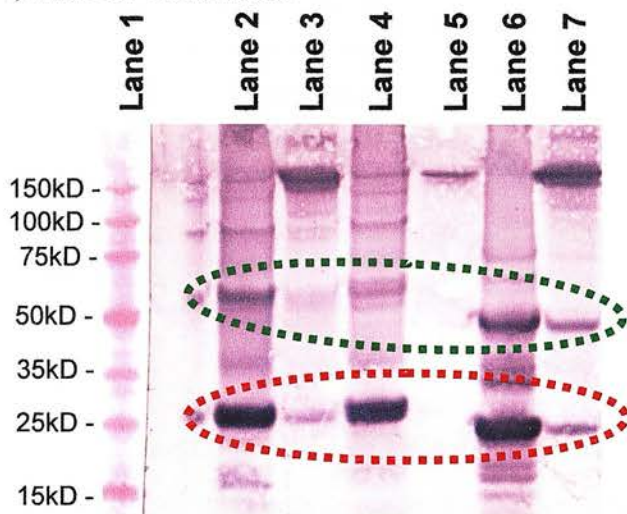
### 3 Single-chain Tetramer Building Blocks

#### 3.1 Integrity of $\alpha\beta$ association of the Purified Single-chain TBB

The integrity of the tertiary  $\alpha$  and  $\beta$  domain association of purified and refolded single-chain fusion proteins (HLA-DR15sc and HLA-DR7sc) was assessed using the heterodimer-specific L243 monoclonal antibody in an analogous experiment to that used in the assessment of HLA-DR15LZ TBB (Figure 6.9). No similar heterodimer-specific monoclonal antibody was available for the assessment of I-E<sup>d</sup>sc as 2G9 is capable of binding the urea-solubilised crude inclusion body preparation of I-E<sup>d</sup>sc (See Results III), and 14-4-4S binds free I-E<sup>d</sup> alpha chain as well as I-E<sup>d</sup> $\alpha\beta$  heterodimers (Spencer et al., 1993, Spencer and Kubo, 1989).

Figure 6.9 – L243 immunoprecipitation of HLA-DR15sc TBB and HLA-DR7sc TBB

a) Anti-HSV Immunoblot



**Key:**

**Lane 1** – Perfect Protein<sup>®</sup> markers

**Lane 2** – Unbound HLA-DR7sc


**Lane 3** – Eluted HLA-DR7sc


**Lane 4** – Unbound I-E<sup>d</sup>sc

**Lane 5** – Eluted I-E<sup>d</sup>sc

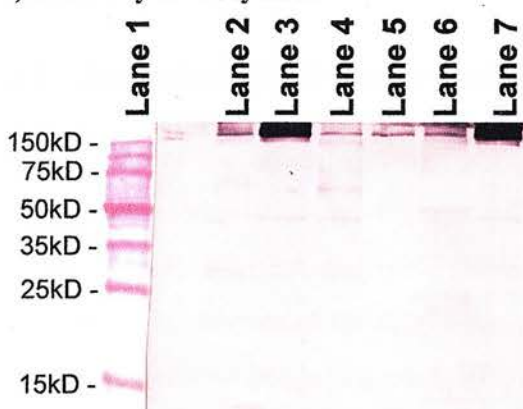
**Lane 6** – Unbound HLA-DR15sc

**Lane 7** – Eluted HLA-DR15sc

 – Monomeric single-chain fusion protein bands

 – Dimeric single-chain fusion protein bands

b) Secondary antibody alone





0.5ml of refolded HLA-DR15sc and HLA-DR7sc in PBS were separately immunoprecipitated using L243 and Protein A sepharose. Samples were collected from the antigen-L243 combinations following their passage through the Mobicol<sup>®</sup> microcolumn. These samples represented the L243-unbound postloads (Lanes 2, 4 & 6). Samples were also collected from the microcolumn eluates that represented the L243-bound fraction (Lanes 3, 5 & 7). The samples were separated by SDS-PAGE using a 4-12% NUPAGE<sup>®</sup> Bis-Tris gradient gel (*Invitrogen Ltd., UK*) before electro-blotting onto nitrocellulose overnight. The nitrocellulose membrane was probed with either the anti-HSV monoclonal antibody or the secondary antibody (anti-mouse IgGAP) alone before developing using the two-layer approach.

A small proportion of HLA-DR15sc TBB and HLA-DR7sc TBB were bound by L243 in solution indicating the correct tertiary  $\alpha\beta$  heterodimeric association. This can be seen by the presence of the expected 25kD band in Lanes 3 and 7. Interestingly, a proportion of the dimeric HLA-DR15sc TBB, and to a lesser extent HLA-DR7sc, also appears to have been immunoprecipitated as seen in Lanes 7 and 3 at around 50kD. The proportion immunoprecipitated is 5-10% although the correctly folded proportion could be much higher as the L243 concentration in this experiment was probably a limiting factor. These additional bands are not present in the I-E<sup>d</sup>sc eluate that was used as a negative control (Lane 5), nor are they present using the secondary antibody alone (Figure 6.9b), adding weight to the above findings.

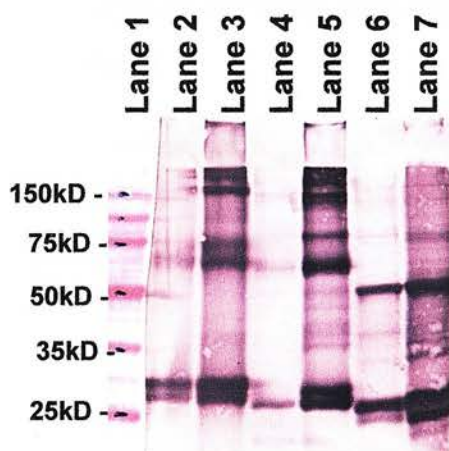
### 3.2 Assessment of Biotinylation of scTBB

One of the advantages of the *E.coli* expression system is the possibility of significant biotinylation of the recombinant single-chain fusion proteins by the endogenous *E.coli* BirA enzyme. The occurrence of this biotinylation was assessed by examining samples of the single-chain fusion proteins before and after adsorption onto avidin-coated beads (Figure 6.10). The blot developed using Extravidin<sup>®</sup> alone (Figure 6.10a) reveals only those proteins that are biotinylated, whereas the anti-HSV immunoblot (Figure 6.10b) detects all the recombinant scTBBs. Biotinylated proteins of the expected size are seen in comparing these blots, indicating that at least

a proportion of the recombinant proteins are indeed biotinylated during their formation. There is also a reduction in the quantity of these proteins following avidin adsorption, both confirming the above and highlighting the utility of using this interaction to adsorb the scTBBs on to a bead surface. Unfortunately, it would appear that the avidin beads used were a limiting factor given the presence of Extravidin<sup>®</sup> staining following adsorption (Figure 6.10a).

**Figure 6.10 – Assessment of Biotinylation of scTBB**

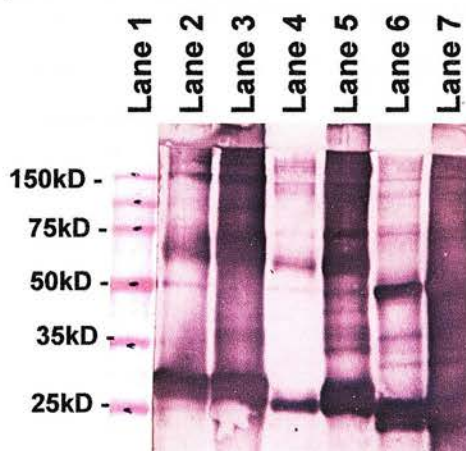
**a) Extravidin immunoblot**



**Key:**

- Lane 1** – Perfect Protein<sup>®</sup> markers
- Lane 2** – HLA-DR7sc Post-avidin beads
- Lane 3** – HLA-DR7sc Pre-avidin beads
- Lane 4** – I-E<sup>d</sup>sc Post-avidin beads
- Lane 5** – I-E<sup>d</sup>sc Pre-avidin beads
- Lane 6** – HLA-DR15sc Post-avidin beads
- Lane 7** – HLA-DR15sc Pre-avidin beads

**b) Anti-HSV immunoblot**

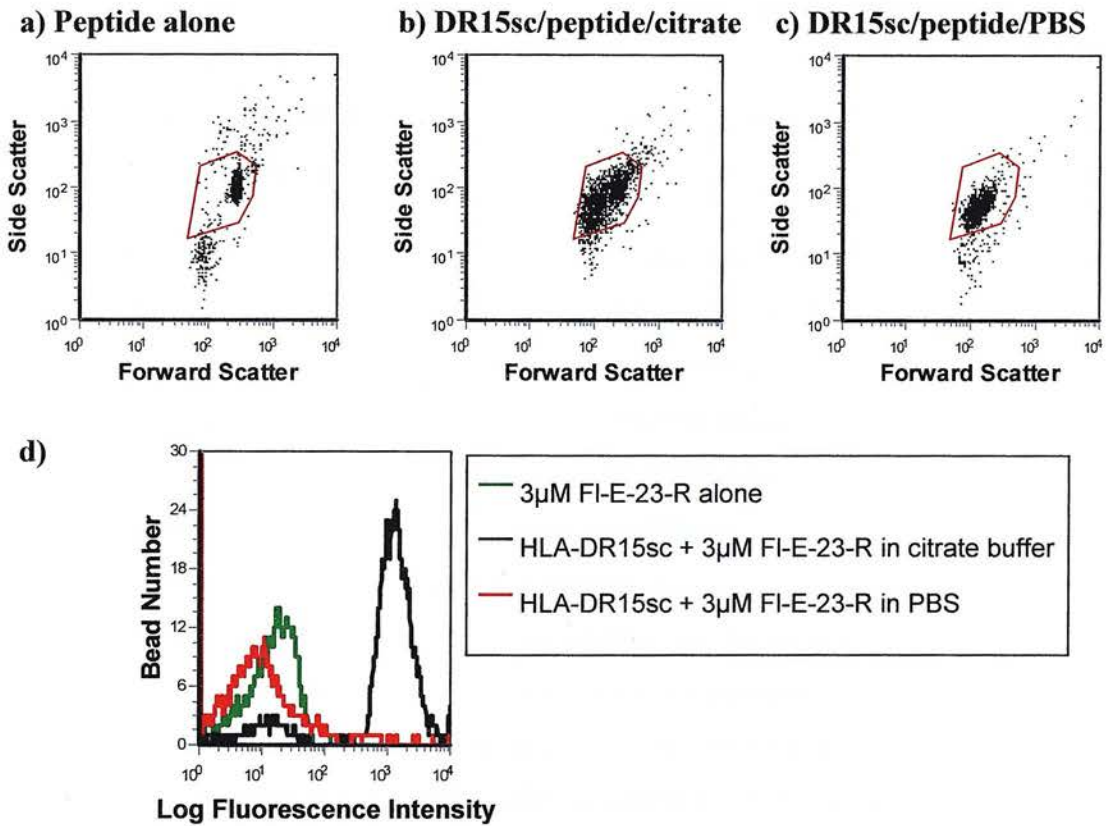


A sample of each of the three scTBB constructs was taken and mixed with 50µl of a 1:100 dilution of streptavidin-coated 1µm beads (*PolySciences Inc.*). The resulting mixture was incubated for 1 hour at room temperature with continuous mixing before pelleting the beads by centrifugation at 1800g for 30 seconds. Samples taken before and after combination with the streptavidin-coated beads were separated by SDS-PAGE and electro-blotted onto nitrocellulose overnight. The nitrocellulose gel was probed with either Extravidin® alone (*Sigma-Aldrich*®) or anti-HSV monoclonal antibody, and developed using the two-layer approach.

### 3.3 Peptide-Binding Assessment of Purified HLA-DR15sc TBB by FACS

I performed a pilot experiment to delineate the peptide-binding capacity of the purified refolded HLA-DR15sc TBB by loading the scTBB with fluorescent-tagged peptide under two pH conditions (Figure 6.11). This showed that in the absence of favourable peptide-binding conditions *i.e.* citrate buffer pH5.0, there was no increase in fluorescence above baseline and hence no specific peptide binding. This finding supported specific peptide binding to HLA-DR15sc. It was, therefore, important to determine the specificity of the binding and further optimise the peptide-binding conditions. In the first instance, all further peptide binding experiments were performed using citrate buffer pH5.0. Note that although 10000 events were captured for further analysis the total number of beads with any fluorescence is far less than this.

**Figure 6.11 – FACS analysis of HLA-DR15sc refolded with FI-E-23-R in the presence/absence of citrate buffer**



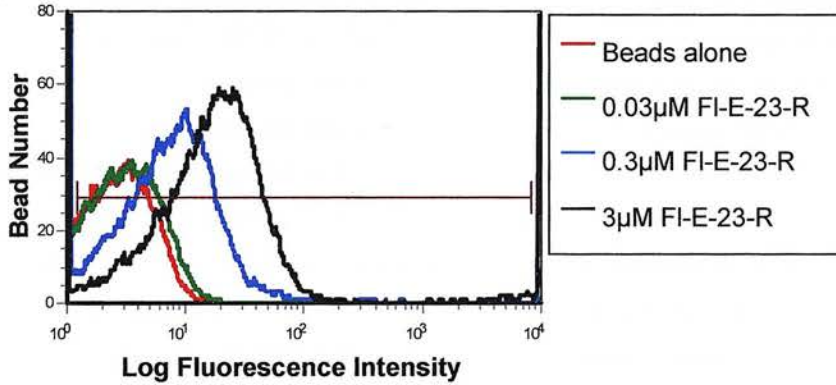
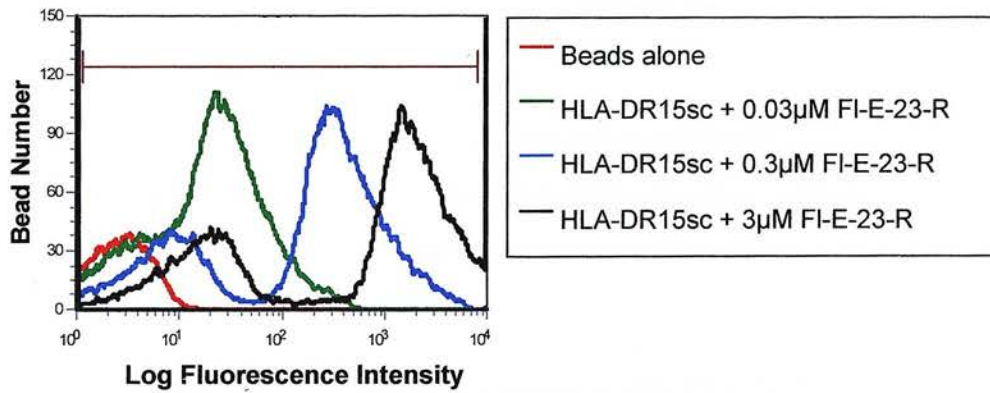
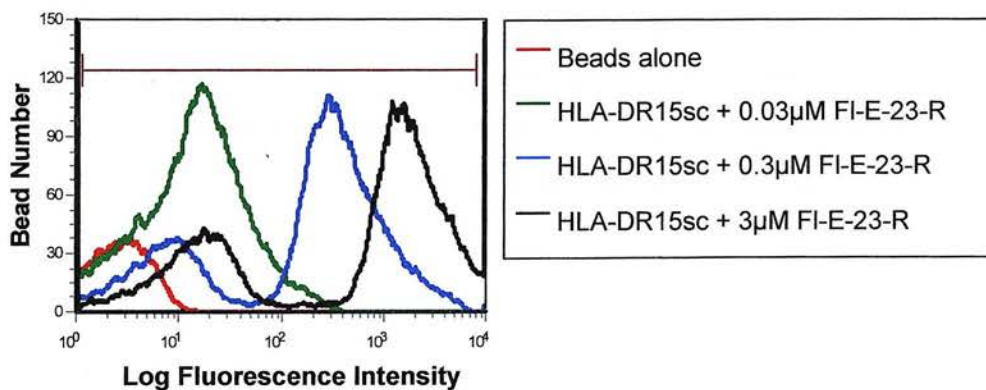
Two 500 $\mu$ l samples of HLA-DR15sc were taken and 5 $\mu$ l of 1mM FI-E-23-R peptide was added to each sample. The final concentration of FI-E-23-R was approximately 3 $\mu$ M. 1ml of citrate buffer pH5.0 was added to one sample, leaving the other in PBS overnight at 4°C. Both samples were separately mixed with 20 $\mu$ l of a 1:100 dilution of streptavidin-coated beads (approximately  $9 \times 10^6$  beads) at 4°C overnight. The beads were collected by centrifuging at 10000g for 2 minutes at room temperature, removing the supernatant and re-suspending in 1ml 0.45 $\mu$ m-filtered PBS. The beads were washed in this manner 3 times before analysing a 1:5 dilution using the Coulter Epics XL.MCL®. 10000 events were recorded for further analysis. The main population of beads was gated for analysis by comparing the three scatter diagrams (a-c) and gating of the maximal bead area in order to obtain the fluorescence histogram (d). This is representative of two refolding experiments.

Peptide-binding conditions were assessed using a series of experiments based upon the general principles of peptide-binding conditions outlined above. I decided to assess the effects of 0.5% NP40 (Buelow et al., 1994) and 5% ethanol (Falk et al., 2002) upon HLA-DR15sc peptide-binding in the context of a citrate buffer pH5.0. Non-specific binding of Fl-E-23-R to the streptavidin-coated beads without captured HLA-DR15sc was also assessed (Figure 6.12).

Non-specific binding of Fl-E-23-R to the streptavidin-coated beads was noted. There was a ten-fold increase in fluorescence over the range of Fl-E-23-R concentrations used (Figure 6.12a). In comparison, there was a striking increase in fluorescence of the beads with captured HLA-DR15sc incubated with the same range of Fl-E-23-R concentrations. There was a thousand-fold increase in fluorescence over the range of Fl-E-23-R concentrations used (Figure 6.12b). The addition of 5% ethanol, which is supposed to enhance peptide-binding (Falk et al., 2002) had no further effect (Figure 6.12c). The striking findings are the duality of the fluorescence peak and the disparity between the number of events captured and the actual number of fluorescent beads analysed. One possibility for both these findings is that the relative concentration of beads, HLA-DR15sc and Fl-E-23-R was not optimised.



Figure 6.12 – Optimising peptide-binding conditions of HLA-DR15sc with FI-E-23-R

**a) Beads with FI-E-23-R peptide alone in 0.5% NP40/5% Ethanol****b) Beads with DR15sc + FI-E-23-R peptide in 0.5% NP40****c) Beads with DR15sc + FI-E-23-R peptide in 0.5%NP40/5% Ethanol**

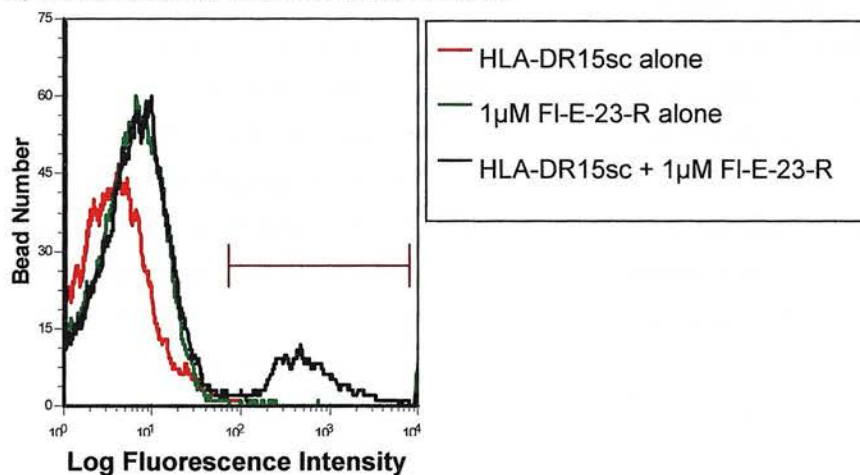
To 500µl samples of HLA-DR15sc TBB in PBS 1ml of either of two peptide-binding buffer solutions was added: citrate buffer pH5.0 with 0.5%NP40 (**NP**), or citrate buffer pH5.0 with 0.5%NP40+5% ethanol (**NP/Et**). To each of the resulting mixtures a series of reducing concentrations of the Fl-E-23-R peptide was added and the combinations mixed overnight at room temperature. Concurrently, the series of reducing concentrations of Fl-E-23-R peptide were also mixed with citrate buffer pH5.0/ 0.5%NP40/ 5%ethanol in the absence of HLA-DR15sc. The mixtures were neutralised using 80µl of 1M phosphate buffer pH8.0 before adding 10µl of a 1:100 dilution of streptavidin-coated beads (*PolySciences Inc.*) previously blocked using a solution of PBS/1% BSA overnight (approximately  $4.5 \times 10^6$  beads). The beads were mixed with the protein solutions for 4 hours at room temperature before centrifuging at 10000g for 10 minutes at room temperature, and resuspending in 1ml filtered PBS (0.45µm filter). The beads were washed in this manner 3 times before analysing a 1:5 dilution using the Coulter Epics XL.MCL<sup>®</sup>. 10000 events were recorded for further analysis. Peptide-binding was performed at room temperature in these experiments in order to minimize recombinant protein degradation from contaminants of these bacterially derived recombinant proteins.

The specificity of the peptide binding was examined by comparing Fl-E-23-R peptide binding in the presence of the unlabelled competitor peptide ‘AS346’ (high affinity for HLA-DR15), or the non-competitor peptide ‘1634S’ (negligible affinity for HLA-DR15) (Figure 6.13).

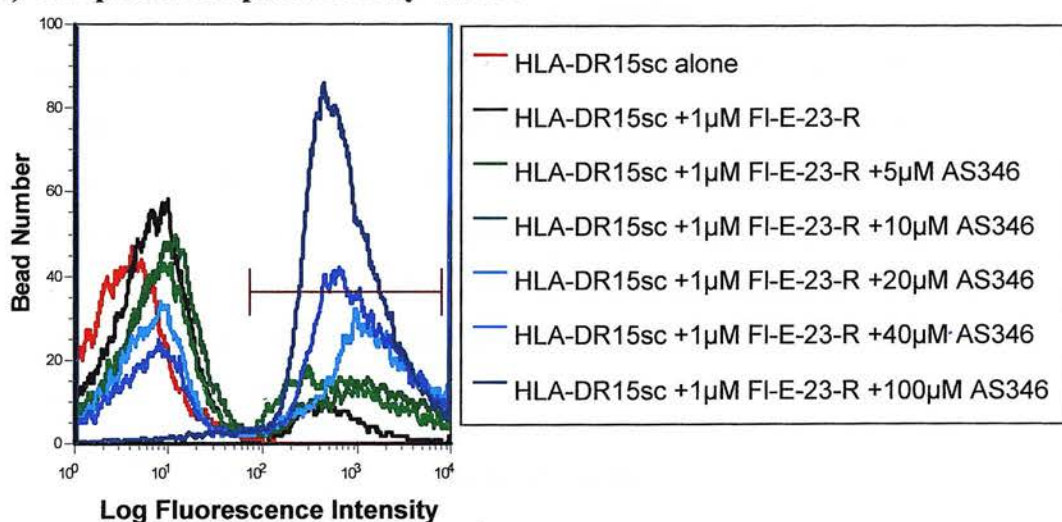
The distinct second peak of fluorescence with Fl-E-23-R peptide binding to HLA-DR15sc is clearly seen once more. Unexpectedly, the counts of fluorescence beads increased with increasing concentrations of the competitor peptide ‘AS346’. The expected competitive displacement and loss of fluorescence was not seen even at 100 fold greater concentration of the competitor peptide (Figure 6.13b). Furthermore, the lower fluorescence peak is lost at the highest concentration of ‘AS346’. In contrast, no effect was seen with the non-competitor peptide ‘1634S’ (Figure 6.13c).

Figure 6.13 – HLA-DR15sc peptide-binding inhibition (I)

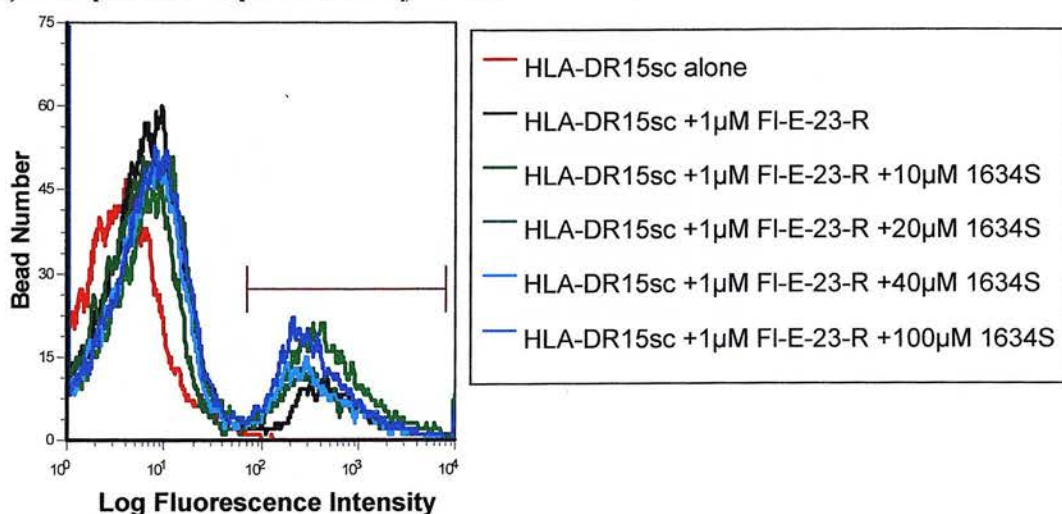
a) HLA-DR15sc binding to FI-E-23-R



b) Competitive displacement by 'AS346'



c) Competitive displacement by '1634S'

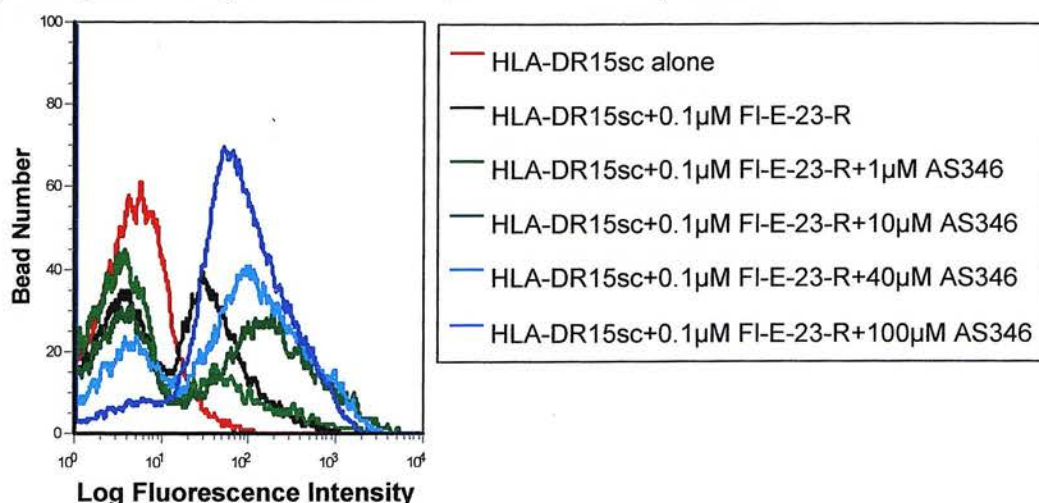


A series of reducing concentrations of both ‘AS346’ (b) and ‘1634S’ (c) were separately combined with 500µl of HLA-DR15sc in PBS and a final concentration of 1µM FI-E-23-R peptide in 1ml citrate buffer pH5.0/ 0.5%NP40/ 5%ethanol/ Bacterial Protease Inhibitor Cocktail® (*Sigma-Aldrich Inc.*). These solutions were gently mixed at room temperature overnight before neutralising with 80µl 1M phosphate buffer pH8.0 and adding 20µl of a 1:100 dilution of streptavidin-coated beads previously blocked in PBS/ 1% BSA. The beads were incubated for 4 hours at room temperature before collection by centrifuging at 10000g for 2 minutes. The beads were washed twice in 1ml PBS/ 1%BSA/ Bacterial Protease Inhibitor Cocktail® at 4°C by vortexing, prior to collecting by centrifugation, resuspending in PBS/ 1%BSA/ Bacterial Protease Inhibitor Cocktail®, and analysing using the Coulter Epics XL.MCL®. 10000 events were collected. This is representative of two peptide-binding inhibition experiments.

The experiment was repeated with ten-fold and one hundred-fold less fluorescent peptide in order to assess whether greater AS346:FI-E-23-R ratios would result in competitive displacement (Figure 6.14). The result mirrored that of the previous experiment, with the only effect seen being a reduction in the mean fluorescence of the fluorescent population of beads. Once again, there was a specific ‘AS346’-modulated enhancement of FI-E-23-R binding to HLA-DR15sc. Although unexpected, this does provide evidence of specific peptide to peptide-binding groove interaction.

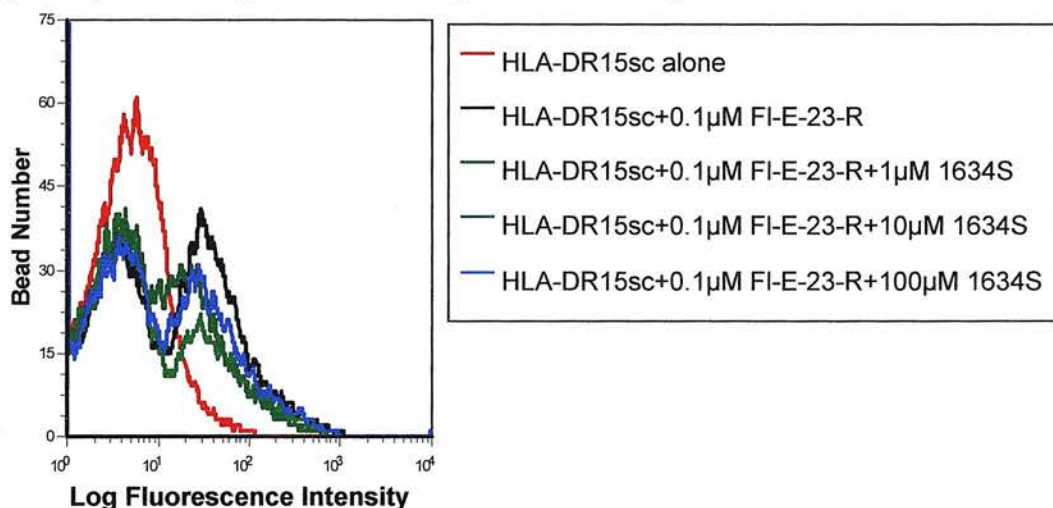
**Figure 6.14 - HLA-DR15sc peptide-binding inhibition (II)**

**a) Competitive displacement of 0.1µM FI-E-23-R by ‘AS346’**

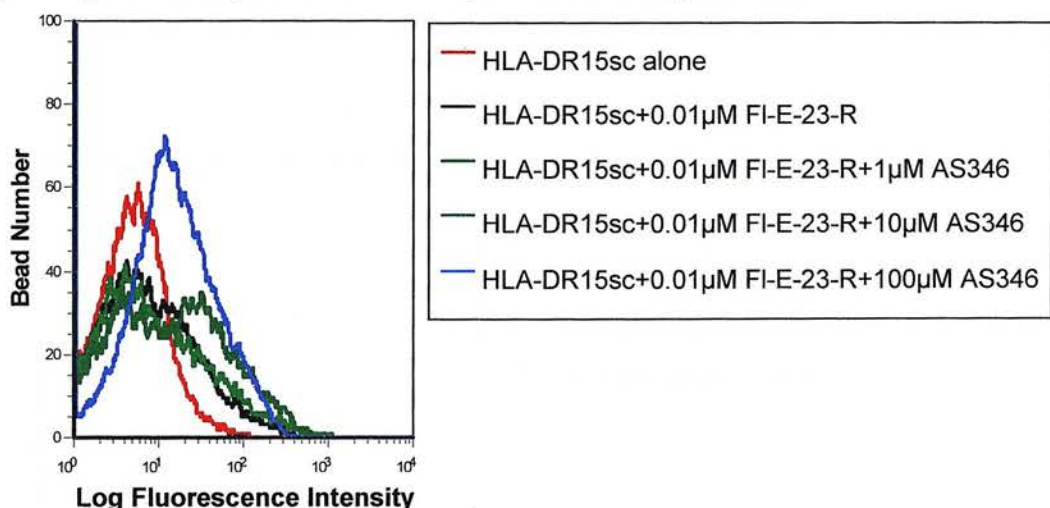




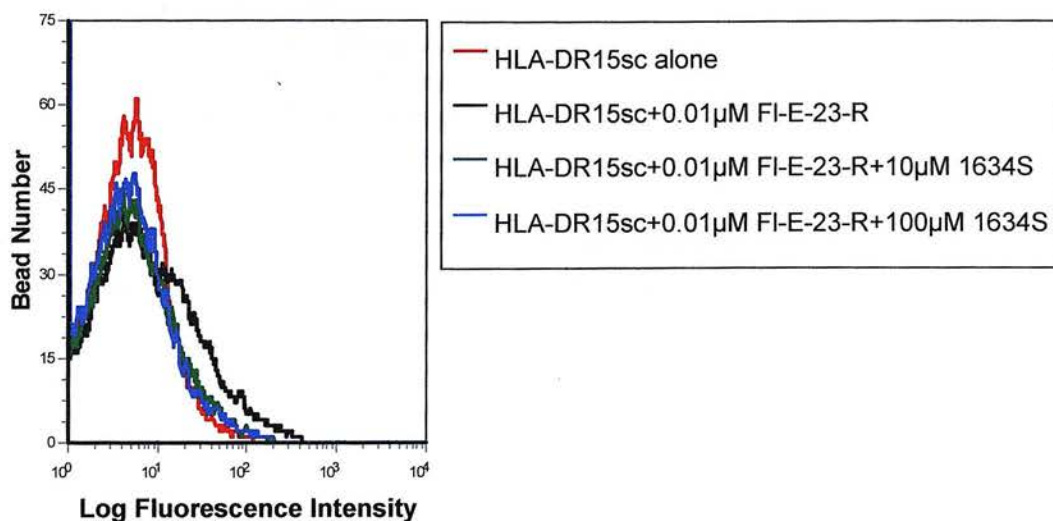
**b) Competitive displacement of 0.1μM FI-E-23-R by '1634S'**



**c) Competitive displacement of 0.01μM FI-E-23-R by 'AS346'**



**e) Competitive displacement of 0.01μM FI-E-23-R by '1634S'**

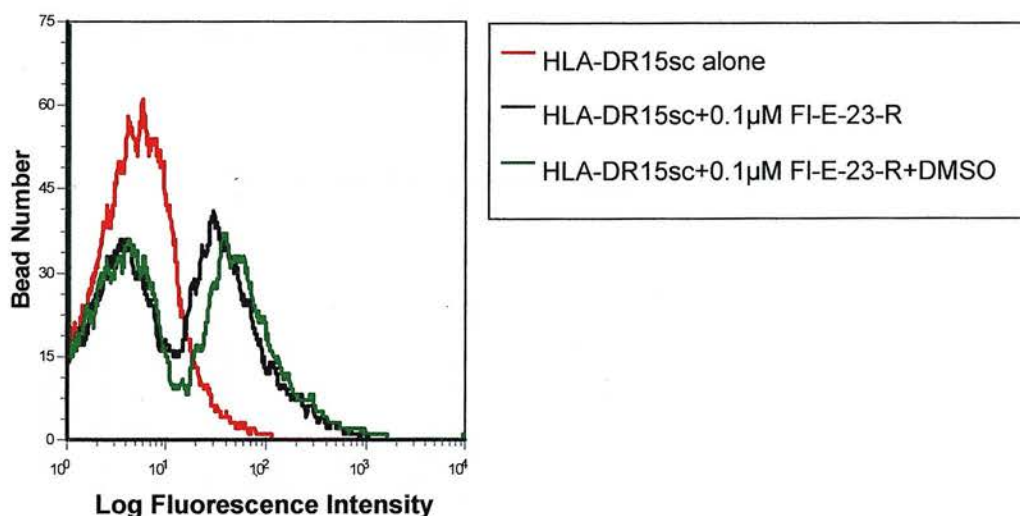




A series of reducing concentrations of both 'AS346' (a & c) and '1634S' (b & d) were separately combined with 500µl of HLA-DR15sc in PBS and a final concentration of either 0.1µM or 0.01µM FI-E-23-R peptide in 1ml citrate buffer pH5.0/ 0.5%NP40/ 5%ethanol/ Bacterial Protease Inhibitor Cocktail® (Sigma-Aldrich Inc.). These solutions were gently mixed and incubated with streptavidin-coated beads as previously before analysing using the Coulter Epics XL.MCL®. 10000 events were collected. This is representative of two peptide-binding inhibition experiments.

Given that 'AS346' was dissolved in a DMSO based solution, a further experiment was carried out in order to confirm the null effect of DMSO upon fluorescence. A sample of the fluorescein-tagged peptide was, therefore, refolded in the presence of an equivalent concentration of DMSO without 'AS346' (Figure 6.15). This experiment confirmed the null effect of DMSO upon fluorescence.

**Figure 6.15 – Effect of DMSO upon fluorescence intensity**

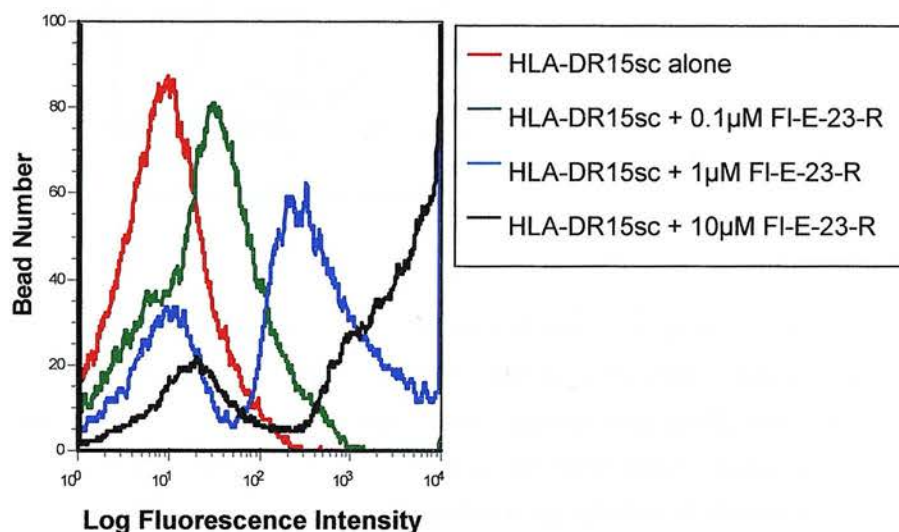


500µl of HLA-DR15sc in PBS was combined with a final concentration of 0.1µM FI-E-23-R peptide in 1ml citrate buffer pH5.0/ 0.5%NP40/ 5%ethanol/ Bacterial Protease Inhibitor Cocktail® (Sigma-Aldrich Inc.). DMSO was added to one sample in an amount equivalent to that found in 100µM 'AS346'. Further binding conditions and analysis remained unchanged.

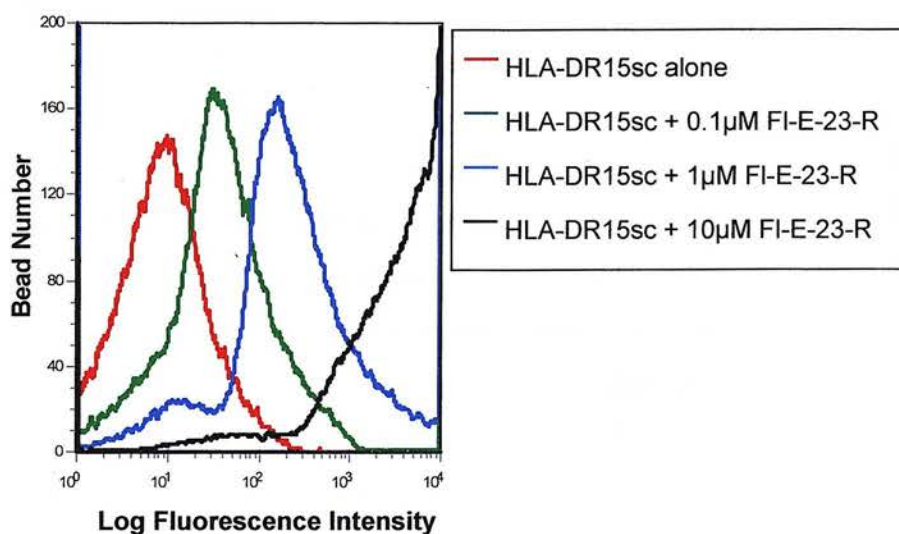
One possible explanation for the duality of the fluorescence peak was that the relative concentrations of beads and HLA-DR15sc were not optimal for the assay. This was assessed by reducing the amount of HLA-DR15sc by one fifth, in a series of peptide-binding experiments using three different bead quantities (Figure 6.16).

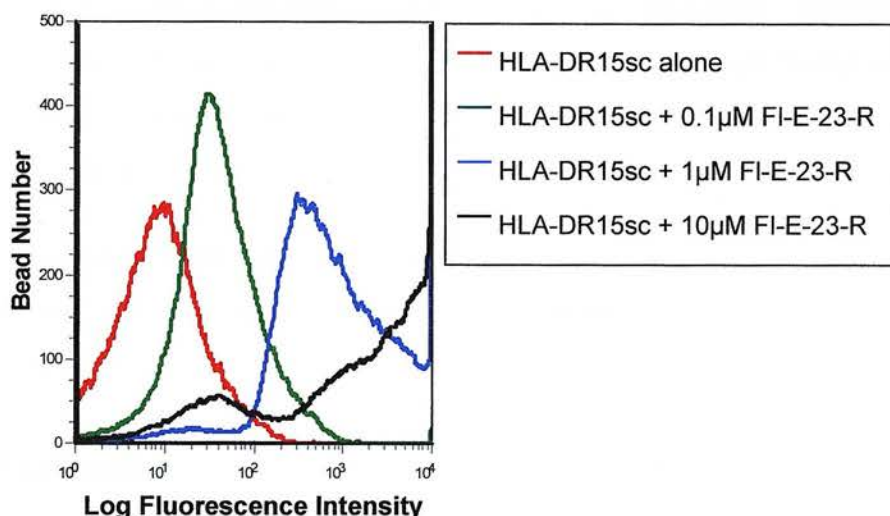
**Figure 6.16 – Optimisation of bead, HLA-DR15sc TBB and FI-E-23-R concentrations**

**a) Using 1µl of undiluted streptavidin-coated beads ( $4.5 \times 10^7$  beads)**



**b) Using 1µl of 1:10 dilution of streptavidin-coated beads ( $4.5 \times 10^6$  beads)**



**c) Using 1µl of 1:100 dilution of streptavidin-coated beads ( $4.5 \times 10^5$  beads)**

100µl of HLA-DR15sc in PBS was combined with FI-E-23-R peptide at a final concentration of 0.1µM, 1µM, or 10µM in 1ml citrate buffer pH5.0/ 0.5%NP40/ 5%ethanol/ Bacterial Protease Inhibitor Cocktail® (*Sigma-Aldrich Inc.*). These solutions were gently mixed at room temperature overnight before neutralising with 80µl 1M phosphate buffer pH8.0. Streptavidin-coated beads were added at one of three quantities (1µl neat suspension (a), 1µl of a 1:10 dilution in PBS (b) and 1µl of a 1:100 dilution in PBS (c)) having been previously blocked in PBS/ 1% BSA. Further binding conditions and analysis remained unchanged. The fluorescence intensity chromatograms were derived as previously and normalized at 0.1µM FI-E-23-R peptide. This is representative of two peptide-binding inhibition experiments.

Figure 6.16 suggests that the dual peak phenomenon was a result of less than optimal bead/scTBB/‘FI-E-23-R’ relative concentrations. At each bead concentration, the fluorescence level is seen to increase ten fold with each ten fold rise in peptide concentration. The peak log fluorescence intensity increased from a mean of 30 at 0.1µM FI-E-23-R, to 280 at 1µM FI-E-23-R, to 6500 at 10µM FI-E-23-R. At the optimal relative concentration (100µl of HLA-DR15sc, 0.1µM ‘FI-E-23-R’ peptide and 1µl of a 1:100 dilution of streptavidin-coated beads) a single fluorescence peak is demonstrated. This suggests that under these conditions, both the streptavidin-coated beads and the HLA-DR15sc TBB binding sites are saturated. Indeed, in reducing the bead quantity the actual fluorescent bead count increases (compare bead counts in

Figure 6.16a to c), indicating that with greater bead concentrations a greater proportion of the beads had little if any HLA-DR15sc TBB bound. This optimisation could be used to reassess the previous inhibition assays, although further adjustment of HLA-DR15sc amounts may be required if there is marked batch-to-batch variation in concentration.

In essence, the evaluation of HLA-DR15sc TBB has suggested that this recombinant protein is able to specifically bind peptide.

## 4 Discussion

The initial assessment of HLA-DR15LZ TBB by immunoprecipitation using the conformationally sensitive L243 monoclonal antibody would strongly suggest that the recombinant HLA-DR15LZ TBB formed is conformationally correct before, during and after nickel-chelation purification. Moreover, the results would imply that the addition of an L243-affinity column would be of value as a purification step in keeping with previous work (Arimilli et al., 1995, Kalandadze et al., 1996). However, it is certainly feasible for nickel-chelation chromatography to be the sole purification stage necessary, particularly if protein production is carried out in serum-free medium (Kuroda et al., 2000).

The ability of HLA-DR15LZ TBB to specifically bind peptide was initially assessed using standard ELISA techniques but this approach was unsuccessful because the fluorescein-tagged peptide bound too inefficiently to the HLA-DR15LZ TBB for satisfactory detection by ELISA. A novel FACS-based technique was developed using beads coated with human IgG<sub>4</sub> specific for the Fc segment of murine IgG to form the basis of a sensitive peptide-binding assay. This novel technique provided clear evidence of specific and inhibitable binding of peptide to HLA-DR15LZ TBB. The sensitivity of the technique requires further improvement through the optimisation of the solid phase scaffold constitution. Coating of the CELlection™ Dynabeads® (*Dynal Biotech UK*) with 9E10 can be optimised to achieve complete saturation of the beads, and in the same vein, the quantity of HLA-



DR15LZ TBB used to bind to the beads can also be optimised for the same reason. Optimisation can be checked using a fluorescent-tagged anti-murine IgG in the case of the former, and a rat anti-human HLA-DR (eg YD1/63.4.10 – *Abcam Limited (UK)* (Pawelec et al., 1982)) monoclonal antibody with a fluorescent-tagged anti-rat IgG secondary as the detecting antibody in the case of the latter. Importantly, the data clearly indicate that HLA-DR15LZ TBB in significant proportions is conformationally and functionally similar to native HLA-DR15.

Initial assessment of the scTBB fusion proteins began with an assessment of their conformational integrity. Due to a lack of a heterodimer-specific monoclonal antibody for I-E<sup>d</sup> peptide-binding domain, the nature of the peptide-binding domain of the human scTBB constructs alone was assessed using the monoclonal antibody L243. Immunoprecipitation of each of the refolded scTBB constructs revealed that a significant proportion of both HLA-DR7sc TBB and HLA-DR15sc TBB had the correct  $\beta_1$ - $\alpha_1$  association. Moreover, this finding extended to a proportion of apparently dimeric HLA-DRsc TBB proteins. This latter finding possibly indicates that although the L243 monoclonal antibody is heterodimer-specific, this does not equate to specificity for the correct tertiary structure of the peptide-binding domain given that the disulphide bond within the  $\beta_1$  domain is integral to its structure. This disulphide bond couples the carboxy-terminus of the  $\beta_1$  domain to the first strand of the anti-parallel  $\beta$ -sheet platform and is thought to serve as the “linchpin” to a stable tertiary structure (Chang et al., 2001). Further evaluation of these recombinant scTBB proteins involved an assessment of their biotinylation as work with recombinant MHC Class I produced in *E.coli* had suggested that further enzymatic biotinylation was required (Denkberg et al., 2000). Certainly, my preliminary findings would indicate that a significant proportion of the recombinant scTBB proteins produced have already been biotinylated within the *E.coli* inclusion bodies.

Using the bead-based FACS analysis of peptide binding, initial results indicated specific peptide binding to HLA-DR15sc TBB when refolded with the fluorescent-tagged peptide ‘Fl-E-23-R’. This result was reproduced by combining ‘Fl-E-23-R’ with HLA-DR15sc TBB in the presence of citrate buffer pH5.0. Peptide-binding experiments showed increasing peptide binding to HLA-DR15sc



TBB with increasing peptide concentrations. In order to clarify this further, a series of binding-inhibition experiments were performed using two unlabelled peptides, one of which ('AS346') was known to have a high affinity for native HLA-DR15 and so would act as a competitive inhibitor to the 'Fl-E-23-R' peptide. In the presence of the non-competitor peptide ('1634S') there was no alteration to the degree of 'Fl-E-23-R' binding to HLA-DR15sc TBB. Paradoxically there appeared to be increased fluorescence with increasing concentrations of the competitor peptide ('AS346'). A possible explanation for this is that the ratios of streptavidin-coated beads, HLA-DR15sc and 'Fl-E-23-R' require optimisation as suggested in Figure 6.16. A further explanation for this specific peptide to peptide-binding groove interaction is that the 'AS346' is affecting the conformation of the recombinant HLA-DR15sc in a manner that would improve its binding affinity, so allowing increased binding to the fluorescein-tagged peptide (Kasson et al., 2000, Natarajan et al., 1999, Rabinowitz et al., 1998, Sadegh-Nasseri and Germain, 1991). Certainly, work performed by Burrows' group would be in concordance with this hypothesis in that they also demonstrated the importance of peptide binding in keeping the  $\alpha_1$  and  $\beta_1$  domain helices in "relative register" (Chang et al., 2001). One dilemma with this as a possibility is that 'AS346' theoretically has a higher affinity for wild type HLA-DR15 than the fluorescein-tagged peptide (Phelps et al., 1998).

## **Chapter 7**

### **Conclusions**

# Chapter 7

## Conclusions

### 1 Introduction

Construction of MHC class II multimers is now well recognised to be very challenging. Even today, there are few reports of successful assembly of MHC class II multimers, and whilst very interesting data have been acquired with these reagents, it is striking that difficulties remain not only in their formation but also in their application (Hackett and Sharma, 2002). Rarely have these reagents been successfully transferred between laboratories, and unlike MHC class I multimers, commercially available reagents have only recently become available through *Beckman Coulter Immunomics*. Moreover, although the NIH Tetramer Facility is able to custom synthesise MHC class I tetramers, it has only recently been able to provide four MHC class II tetramers on a trial basis in collaboration with Dr W. Kwok (<http://www.niaid.nih.gov/reposit/tetramer/index.html>).

In this context I am not too disappointed that my three years as a training fellow did not yield functional multimers. I have described three strategies for the generation of recombinant MHC class II molecules suitable for formation into multimers in order to stain or stimulate populations of T cells bearing TCRs with particular MHC class II-peptide specificities. Two of these approaches generated recombinant MHC class II proteins that were shown to be functional. I believe that this work has resulted in a more complete understanding of the problems of functional MHC class II assembly, and of the importance of the many design decisions that must be made. Importantly, I am confident that the TBBs I have generated are likely to prove excellent substrates for MHC class II multimer formation.

In this chapter I discuss aspects of the design and production of MHC class II TBBs that my work has shown to be essential.

## 2 Formation of Tetramer Building Blocks

### 2.1 Maintaining MHC class II $\alpha$ and $\beta$ chain association

The importance of the association of MHC class II  $\alpha$  and  $\beta$  chains to the stability of the heterodimeric structure let alone its peptide-binding groove is well documented in the literature particularly in relation to the development of MHC class II tetramer technology (Scott et al., 1996). MHC class II  $\alpha\beta$  heterodimers are naturally associated through an interaction of their transmembrane domains as well as the presence of a bound peptide within the peptide-binding groove formed by the  $\alpha\beta$  heterodimer. In newly synthesised MHC class II molecules, this bound peptide is derived from the invariant chain protein (Ii) and is called CLIP (*class II-associated invariant-chain peptide*). CLIP must either dissociate or be displaced in order to allow an antigenic peptide to bind to the MHC class II molecule. As a result, “empty” recombinant MHC class II molecules are unstable structures.

Heterodimer association has been attempted using a combination of at least three techniques: covalently linked peptides (Kozono et al., 1994), carboxy terminal leucine zipper motifs (Smith et al., 1998), and carboxy terminal linkage to an immunoglobulin scaffold (Hamad et al., 1998).

My results using a covalently linked peptide to maintain the stability of the I-E<sup>d</sup>tBand3 construct indicated that this alone was not sufficient to maintain stability. Indeed similar findings have been reported with recombinant I-A<sup>s</sup> constructs (Reddy et al., 2003). However, other factors such as transcription/translation issues may have been the reasons for the lack of success of the I-E<sup>d</sup>tBirA and I-E<sup>d</sup>tBand3 constructs. Nonetheless, these early results underscore the importance of heterodimeric association.

Of the two alternative further methods of promoting heterodimeric association, leucine zipper constructs were rapidly emerging as the most versatile and most used. Their effectiveness at promoting MHC class II heterodimer formation had been well documented (Gauthier et al., 1998, Kalandadze et al., 1996,

Scott et al., 1996), and they had been successfully used to form recombinant HLA-DR in the *Drosophila* S2 expression system (Novak et al., 1999). Furthermore, the leucine-zipper of the heterodimeric associated constructs is likely to add a degree of flexibility that may improve TCR binding to a greater extent than the rather inflexible avidin-biotin backbone of the “standard” MHC tetramer construct (Casares et al., 1997, Hackett and Sharma, 2002). By comparison, the use of an immunoglobulin scaffold to solely promote chain pairing was not proving to be as versatile (N. Glaichenhaus, *personal communication*). Therefore, I decided to adapt a construct that had been successfully used in the formation of murine I-A<sup>u</sup> (Radu et al., 1998) with permission from Drs E.S. Ward and C.G. Radu. The adaptation of the construct involved the alignment of the extracellular portions of the I-A<sup>u</sup>  $\alpha$  and  $\beta$  chains with the respective chains from I-E<sup>d</sup>, HLA-DR15 and HLA-DR7 in order to align the acid-base leucine zipper motif correctly for the two chains to be precisely paired. The possibility of covalently linking a peptide to the amino-terminus of the  $\beta_1$  chain to further enhance both chain pairing and peptide loading remained. This adaptation process also opened the possibility of alternative purification strategies through the carboxy terminal c-myc and polyhistidine tags.

A novel technique for maintaining the peptide-binding domain of MHC class II proteins was developed by Burrows’ group (Burrows et al., 1998). This method exploited the functional role of the  $\alpha_1$ - $\beta_1$  domains of MHC class II molecules as the peptide-binding “superdomain” (Brown et al., 1993) as compared to the  $\alpha_2$ - $\beta_2$  domains that appear to act as the “superdomain” for CD4 co-receptor interactions (König, 2002, König et al., 1995). The method involved the linkage of the carboxy-terminus of the  $\beta_1$  domain to the amino-terminus of the  $\alpha_1$  domain in such a manner as to retain their quaternary peptide-binding association. Burrows’ group have demonstrated a very slow off-rate of the single-chain fusion protein construct once bound to the TCR, and have successfully used it to stain antigen-specific T cells in its monomeric form (Burrows et al., 1998). This finding is intriguing given that the heterodimeric constructs appear to require a degree of CD4<sup>+</sup> T cell activation for their tetramer staining (Kwok, 2003) and the CD4-MHC interaction aids in the stability of the immune synapse, with the latter occurring through the  $\alpha_2$  and  $\beta_2$



MHC class II domains (König, 2002). Acknowledging the early success of this system, however, I used it as the basis of my construct. Comparisons were first made between the RT1.B construct formed by Burrows' group and the sequence crystallographic structures of HLA-DR1, HLA-DR15, HLA-DR7 and I-E<sup>d</sup>. Once these comparisons had been made, recombinant proteins were successfully produced using the pET25b bacterial protein expression system. Again, the possibility of covalent peptide linkage to the amino terminus of the  $\beta_1$  domain was left open during construct design.

The latter two strategies were used in parallel in order to increase the chances of a successful outcome. Furthermore, these two contrasting methods of TBB formation can be assessed in parallel, which may well shed more light on the kinetics of this evolving technology.

## 2.2 Recombinant MHC class II expression

As has been alluded to in the preceding chapters, although the production of recombinant MHC class I proteins for multimer formation is via relatively standardised bacterial expression, this is not the case for MHC class II proteins. Indeed, bacterial expression has only been used to form a few heterodimeric MHC class II proteins (Ferlin et al., 2000), and of these only HLA-DR1 and I-E<sup>k</sup> have been used to form multimers (Cameron et al., 2001, Cochran et al., 2001, Gütgemann et al., 1998). The primary drawback with bacterial expression systems is the need for *in vitro* refolding. In order to overcome this inherent drawback, insect cell expression systems have been used yielding several recombinant MHC class II proteins. There is little in the literature to suggest that one eukaryotic expression system is superior to another in terms of the yield of functional recombinant MHC class II proteins, with both baculovirus and *Drosophila* expression systems being successfully utilised (Ferlin et al., 2000, Hugues et al., 2002). Indeed, one group has tried both systems for the same recombinant MHC class II protein and found that the *Drosophila* expression system provided equivalent and possibly greater protein yield

than the baculovirus system with less experimental effort (Cameron et al., 2002). This would indicate that there is little to be gained in switching insect expression systems.

The difficulties encountered with HLA-DR7LZ construct would appear to reside at the DNA preparation stage of the HLA-DRB7z construct, and should be relatively straightforward to correct. Although using the baculovirus expression system, Fourneau *et al* (Fourneau et al., 2004) have recently shown that co-expressed chaperones *e.g.* calreticulin improve the yield of recombinant HLA-DR4. It is conceivable that such a system could also be of value using the *Drosophila melanogaster* expression system, indeed this group indicated that they had successfully used chaperone co-expression in the *Drosophila* system. This group also found that an imbalance in HLA-DR $\alpha$  and HLA-DR $\beta$  chain expression lead to limited heterodimer secretion, which could be in keeping with my own findings regarding HLA-DR7LZ. Furthermore, Fourneau *et al* suggest that replacement of the leader sequence with an optimised insect cell leader sequence could improve the final protein yield (Fourneau et al., 2004). Moreover, it is conceivable that changing cell culture conditions could also improve protein yield. Gauthier et al (Gauthier et al., 1998) reported a near doubling of recombinant HLA-DR2 yield from a baculovirus expression system using roller bottles as compared to spinner flasks, although it was unclear whether this was related to cell density. Advances continue to be made in cell culture technology, improving viable cell density with the promise of improved protein yield *eg* miniPERM Bioreactor<sup>®</sup> (Vivascience Ltd) (Schillo *et al*, *personal communication*).

Changing cell culture conditions together with two-stage purification using a combination of nickel-chelation and antibody-affinity (either using L243 or 9E10) chromatography should improve both the yield and purity of the final product. Certainly, one suggestion in the literature is that improving the purity of the recombinant MHC class II constructs used in multimerisation may aid in the detection of low avidity CD4<sup>+</sup> T cells (Kwok, 2003).

Despite the apparent ease of expression and purification of RT1.B in a simple bacterial expression vector without the need for affinity purification (Burrows et al., 1999), I encountered numerous problems with transfer of the constructs into a bacterial expression vector, and later with downstream purification. In order to overcome these issues, a different bacterial expression vector was utilised with the added benefit of protein tags that could be exploited for protein purification. Although Burrows briefly alluded to the use of a polyhistidine tag in his seminal paper (Burrows et al., 1998) this did not appear to be used thereafter, indeed in discussing my construct with him he suggested that such tags may affect the tertiary structure of the resulting protein. Nevertheless, all three recombinant single-chain fusion proteins were successfully formed using pET25b and purified by nickel-chelation chromatography from bacterial inclusion bodies. It is recognised that different vector/bacterial host combinations may have to be tried to obtain the best protein yield (Mierendorf et al., 1994), and that protein yield may be reduced or negated by mRNA secondary structures such as loops and hair-pins (Dr B. Morris, Senior Scientist, Novagen® product applications – *personal communication*).

## 2.3 Refolding Recombinant MHC class II Proteins

Under physiological conditions most proteins fold spontaneously into their correct conformation as determined by their amino acid sequence (Anfinsen, 1973). MHC class II molecules are no exception, however, their refolding within the endoplasmic reticulum is in association with MHC class II-associated invariant chain (Ii). A portion of the Ii polypeptide chain lies within the MHC class II peptide-binding groove, preventing the binding of peptides at this stage and also helping to maintain the heterodimeric association of the MHC class II  $\alpha$  and  $\beta$  chains. During this assembly process, the components are associated with the chaperone protein calnexin. Once assembly is complete, the Ii-MHC class II complex is released from calnexin for transport out of the endoplasmic reticulum. The invariant chain is believed to target delivery of the MHC class II molecules to a low-pH endosomal compartment (the MHC class II compartment – MIIC) where the invariant chain is

sequentially cleaved leaving CLIP still bound to the MHC class II molecule. CLIP is later released through the association of an MHC-like molecule, called HLA-DM in humans, allowing other peptides to bind. Empty MHC class II molecules are retained within the endoplasmic reticulum and degraded.

Bacterial expression systems are capable of producing large quantities of recombinant proteins rapidly, but the recombinant products tend to accumulate as insoluble inactive inclusion bodies. These aggregates are highly enriched for the recombinant protein and are protected from proteolytic cleavage whilst aggregated (Clark, 1998, Williams et al., 1982). Recovery of active proteins from these aggregates generally involves three steps: isolation and washing; solubilisation that inevitably results in denaturation of the proteins; and finally refolding of the solubilised protein. Whilst the first two stages can be performed efficiently, the final stage still entails a trial-and-error approach despite the increasing knowledge base regarding the competing reactions of refolding, misfolding and aggregation (Clark, 1998, Rudolph et al., 1997, Tsumoto et al., 2003).

Initial isolation then washing of the inclusion body pellet using solutions containing detergent (*eg* Triton X100) and low concentrations of chaotropes (*eg* urea) is designed to remove proteinaceous contaminants that may have been adsorbed onto the inclusion bodies and that may affect refolding yield (Clark, 1998). The inclusion body pellet is then solubilised using either high concentrations of chaotropes or ionic detergents (*eg* N-lauroylsarcosine). The solubilised inclusion bodies can then be further purified (*eg* ion exchange or metal affinity chromatography) to remove both proteinaceous and non-proteinaceous contaminants that may shift the aggregation-refolding balance towards aggregation of the desired recombinant protein (Clark, 1998).

The next stage is refolding of the recombinant protein such that the protein conformation returns to its native folded compact state. This process involves the removal of the solubilising denaturant, and in so doing correct refolding should ideally occur as the protein's conformation changes to a more compact structure. Using chaotropes allows the use of intermediate concentrations of these denaturants

to be utilized to positively affect refolding, including disulphide bond formation through mixed disulphide formation (Rudolph and Lilie, 1996, Tsumoto et al., 2003). Chaotropes can be removed using a multitude of techniques *eg* dilution, dialysis, and gel filtration in order to effect variable rates of removal that need to be optimised for each protein. Slower processes of chaotrope removal can successfully prevent aggregation of protein if the recombinant protein is not prone to aggregation at intermediate denaturant concentrations. In this way, higher protein concentrations can be used without reducing refolding yield through aggregation (Clark, 1998, Tsumoto et al., 2003).

For disulphide bonded proteins refolding also needs to promote disulphide bond formation through oxidation of the reduced cysteines. This can be encouraged through oxido-shuffling systems, *eg* reduced and oxidised glutathione (Ahmed et al., 1975, Saxenat and Wetlaufert, 1970), which are optimal at slightly alkaline pH. Such oxido-shuffling systems increase the rate and yield of correct disulphide bond formation by enhancing both the formation of disulphide bonds and the reshuffling of incorrect disulphide bonds. Correct disulphide bonds being relatively protected within stable native protein structures (Fischer et al., 1992, Lilie et al., 1998, Rudolph, 1996, Rudolph and Lilie, 1996). Both pH and temperature can also affect refolding yield, with the former more likely to be protein dependent (Altman et al., 1993, Burrows et al., 1999).

Refolding yield can be enhanced by a variety of co-solutes that either enhance refolding or suppress aggregation (Clark, 1998, Rudolph and Lilie, 1996, Tsumoto et al., 2003). These folding aids include the ‘folding enhancer’ glycerol (Gekkot and Timasheff, 1981, Meng et al., 2001, Ou et al., 2002) and the ‘aggregation suppressor’ L-arginine (Arora and Khanna, 1996). The presence of certain salts can also benefit refolding (Arakawa and Timasheff, 1982). With the refolding process acting as a bottleneck to protein production, chromatographic techniques are being developed to improve the final refolding yield. By immobilising the recombinant protein on a solid support, aggregation of partially refolded proteins can be minimised as the concentration of denaturant is gradually reduced (Colangeli et al., 1998, Li et al., 2004).



The difficulties of efficient refolding are increased in multi-domain, oligomeric, disulphide bonded proteins such as MHC class II proteins. This is the main reason why, with two notable exceptions (I-E<sup>k</sup> (Gütgemann et al., 1998) and HLA-DR1 (Cochran et al., 2000)), most recombinant MHC class II molecules used to generate MHC multimers have been produced in one of two eukaryotic expression systems (Ferlin et al., 2000). Burrows *et al* (Burrows et al., 1998, Burrows et al., 1999) appeared to have circumvented this issue to some extent through covalent linkage of the two portions of the MHC class II peptide binding ‘superdomain’. Although protein refolding is still necessary, the multidomain and heterodimeric nature of MHC class II proteins is evaded. Further stability was added through the use of covalently linked peptides (Burrows et al., 2000a, Chang et al., 2001).

The current literature on the refolding of MHC class II proteins produced in *E.coli* is limited. The main groups using this expression system use a combination of a dilutional refolding strategy in association with glycerol as a viscous stabiliser and reduced and oxidised glutathione as an oxido-shuffling system in order to refold heterodimeric MHC class II proteins (Altman et al., 1993, Cameron et al., 2002). Despite the single-chain fusion protein construction, the major problem that I encountered with the *E.coli* expression of these single-chain MHC class II constructs was predictably that of protein refolding and disulphide bond formation. This was solved using a refolding strategy that has the potential to be performed “on-column” to reduce the final effects of dilution on protein yield.

Further modifications to the refolding methodology may be needed for optimisation of the final yield, *eg* the use of glycerol and/or L-arginine. The possibility of covalently linking peptides to the constructs remains a further way of optimising functional yield, and is currently being investigated in my former laboratory. McMichael’s group in Oxford have found that the inclusion of a linked peptide improves both yield and stability of recombinant HLA-DR1 produced using the *E.coli* expression system, although they indicated that linker design is critical and likely to vary between epitopes (Cunliffe et al., 2002, Wyer et al., 2001). Investigators have compared the staining ability of multimers containing covalently attached peptide to those loaded with exogenous peptide and have found similar

levels of staining under standard conditions (Kwok et al., 2002). These refolding steps may need to be preceded by a further purification step to improve final purity and refolding yield. Anion exchange chromatography may, therefore, need to be revisited prior to nickel-chelation chromatography as the polishing step. In terms of the latter, Burrows *et al* found that a six-histidine tag resulted in reduced thermal stability of their rat RT1.B construct above 60°C, although the construct appeared to be stable at physiological temperatures (Burrows et al., 1999). It is not clear whether or not the addition of the polyhistidine tag, HSV tag and/or the BirA site-specific biotinylation sequence will have detrimentally affected the functional stability of my single-chain MHC class II constructs in terms of antigen-specific T cell activation. The BirA sequence is a necessary part of the current multimerisation, whilst the other two tags provide a means of purification and identification of the recombinant proteins.

### 3 Functional Assessment of Tetramer Building Blocks

Functional assessment of recombinant MHC class II molecules used in multimer formation can be undertaken using biochemical and biological assays, usually in that order (see (Scott et al., 1996)).

A number of biochemical approaches have been reported in the literature. The most commonly employed has been the assessment of binding to monoclonal antibodies that are highly conformationally sensitive. L243 has been used in the purification of recombinant HLA-DR (Arimilli et al., 1995, Godkin et al., 2001, Kalandadze et al., 1996, Natarajan et al., 1999, Stern and Wiley, 1992), and has also been used to specifically assess the conformational integrity of the recombinant protein (Cunliffe et al., 2002). 14-4-4S has been used to confirm the conformational integrity of recombinant I-E<sup>d</sup> (Casares et al., 1997), with a panel of conformationally sensitive monoclonal antibodies being used to immunoprecipitate recombinant HLA-DR1 (Zhu et al., 1997). However, the absence of binding to a conformationally sensitive monoclonal antibody does not necessarily imply a lack of functional

integrity *e.g.* the recombinant HLA-DR15 T cell receptor ligand produced by Chang *et al* (Chang *et al.*, 2001) does not bind to L243 but does stimulate antigen-specific T cells (G. Burrows, *personal communication*).

A second biochemical approach has been the use of spectroscopic techniques. Circular dichroism has been used to assess the secondary structure of recombinant I-A<sup>u</sup> (Radu *et al.*, 1998) and the single-chain fusion protein of RT1.B (Burrows *et al.*, 1999). Surface plasmon resonance spectroscopy has been used to assess the binding kinetics of recombinant HLA-DR2 – MBP peptide to its cognate TCR (Appel *et al.*, 2000, Boniface *et al.*, 1998, Scott *et al.*, 1996).

Finally, biochemical assays of peptide binding have been used. Cochran *et al* (Cochran *et al.*, 2000) crudely assessed specific peptide binding to recombinant HLA-DR1 through the prevention of SDS-induced HLA-DR1 chain dissociation at room temperature. Kwok *et al* (Kwok *et al.*, 2000) used a competition peptide binding assay in order to assess specific peptide binding to recombinant HLA-DQ6.

Biological assessment has been broadly based around assays of the ability of the recombinant MHC class II – peptide multimers to stain and/or stimulate their cognate antigen-specific T cells. In their seminal paper, Altman *et al* (Altman *et al.*, 1996) showed staining by MHC class I – peptide tetramers correlated with peptide-dependent cytotoxicity, with these tetramers being able to stain antigen-specific CD8<sup>+</sup> T cells present in freshly isolated PBMCs, as well as antigen-specific CD8<sup>+</sup> T cell lines and clones. Subsequent groups working with MHC class II – peptide multimers have shown the ability of these multimers to stain antigen-specific CD4<sup>+</sup> T cell lines (Kuroda *et al.*, 2000) and hybridomas (Crawford *et al.*, 1998, Liu *et al.*, 2000, Malherbe *et al.*, 2000, Novak *et al.*, 1999), as well as antigen-specific CD4<sup>+</sup> T cells present in freshly isolated PBMCs (Crawford *et al.*, 1998, Novak *et al.*, 1999). In terms of antigen-specific CD4<sup>+</sup> T cell stimulation, this has been assessed using a variety of methods in both T cell clones and freshly isolated PBMCs:

- T cell proliferation assays using both soluble and immobilised MHC class II – peptide multimers (Appel et al., 2000, Casares et al., 1999, Hamad et al., 1998, Quarsten et al., 2001, Radu et al., 1998).
- Cytokine release assays *e.g.* IL-2 (Kotzin et al., 2000, Radu et al., 2000, Radu et al., 1998), IL-5 and interferon- $\gamma$  (Buckner et al., 2002).
- An assessment of CD4<sup>+</sup> T cell activation markers *e.g.* CD69 and CD25 (Cochran et al., 2000).
- Antigen-specific inhibition of T cell proliferation by single-chain recombinant T cell ligand (Burrows et al., 1998)

Functional assessment of the TBBs that I have developed used most of the biochemical techniques mentioned above. First, the majority of HLA-DR15LZ and a substantial fraction of both HLA-DR15sc and HLA-DR7sc bound to L243. Binding to this antibody demonstrated that these constructs had heterodimeric peptide-binding superdomains that were ‘conformationally correct’. Binding of L243 to HLA-DR15sc contrasts with the findings of G. Burrows whose group could not demonstrate L243 binding to their own HLA-DR15sc fusion protein. Our two constructs differ significantly in two areas: Burrow’s HLA-DR15sc construct does not contain a short linker sequence between the  $\beta_1$  and  $\alpha_1$  domains of the fusion protein, and neither does it have a carboxy BirA sequence with adjoining tags. These difference could account for this observed difference in L243 binding. Second, HLA-DR15LZ and HLA-DR15sc were shown to bind peptides specifically. This important finding was made using a novel fluid phase peptide-binding assay using micro-beads and FACS technology. Bead-FACS is used and continues to be developed for many analytes including cytokine assays and nucleoprotein interactions (Kellar and Iannone, 2002, Kellar et al., 2001, Vignali, 2000). One development has been the use of beads as solid supports on which to assess protein-protein interactions, more specifically peptide binding to HLA-A and HLA-B proteins (Chersi et al., 2000). As an extension of this technique, I developed a method to assess specific peptide binding to the recombinant TBBs.

The next logical stage in functional assessment of the TBBs made would be biological analysis. Suitable reagents for this only became available since I finished my period of research. My former laboratory has made HLA-DR15 restricted T cell hybridomas and is in the process of demonstrating their activation by peptide-loaded TBBs at the time of writing.

## 4 Sensitivity and Specificity of MHC Class II Multimers

Although one of the first hurdles in the application of MHC class II multimers has been their reliable production, the consistent problems now faced by researchers using MHC class II multimers are the apparent low number of antigen-specific T cells within the circulation as well as their low avidity. This has resulted in the currently published detection limits of this technology being reached (Kotzin et al., 2000, Meyer et al., 2000).

In terms of the problem of low abundance, groups involved in this area are trying to extend the detection capacity of this technique, with reports of an *ex vivo* detection of between 1:15000 (0.006%) (Kwok, 2003) and 1:33000 (0.003%) (Danke and Kwok, 2003), and even 1:80000 (0.0001%) using a magnetic bead enrichment technique (Day et al., 2003, Lucas et al., 2004). At the same time, researchers have tried using other techniques to tip the balance in their favour. Transgenic mouse models have been used with varying success (Gütgemann et al., 1998, Malherbe et al., 2000, Radu et al., 2000). Others have resorted to a period of *in vitro* peptide stimulation to increase antigen-specific T cell numbers (Kwok et al., 2002). However, this latter technique diminishes to some extent the promise of tetramer technology in being able to identify and characterise antigen-specific T cells *ex vivo* without any *in vitro* manipulation that could affect T cell characteristics (Cameron et al., 2002). Indeed, in order to minimise the antigen-specific T cell activation resulting from MHC-peptide multimer staining, new reversible staining protocols have been developed for MHC class I multimers to reduce the effect of prolonged staining on T cell characteristics. These protocols are based on the streptagII-



StrepTactin interaction that can be dissociated using d-biotin (Knabel et al., 2002). This is significant given that MHC multimers have been documented to activate T cells (Nepom et al., 2002, Novak et al., 2001b).

With regards to the problem of low avidity, higher order multimers may well be an answer as these would increase the overall avidity of the pMHC complex, improving the detection of lower avidity T cells (Malherbe et al., 2000). Taking this idea further may entail using microbeads as has been used with MHC Class I constructs (Bodinier et al., 2000, Luxembourg et al., 1998, Prakken et al., 2000). Mallet-Designé *et al* have successfully constructed such multimers using liposomes to form artificial antigen presenting cells (AAPC). These liposomal AAPCs incorporating MHC class II tetramers were used to stain low frequency low avidity CD4<sup>+</sup> T cells that could not be stained using the standard MHC class II tetramer construct (Mallet-Designé et al., 2003). Moreover, some have suggested that the rigidity of the “standard” avidin-biotin tetramer construct may be a hindrance to optimal TCR contact, advocating a switch to a more flexible scaffold *eg* the leucine zipper dimerisation domain with its flexible linker (Casares et al., 1997).

One contentious issue in this area of T cell detection is that of staining conditions. FACS staining protocols are being developed to reduce background staining and improve the detection of low frequency cells *e.g.* Single Epitope Multiple Staining (SEMS) technique (Townsend et al., 2001), neuraminidase treatment and detection of intracellular calcium flux (Reddy et al., 2003). However, such techniques aimed at improving the sensitivity of multimer staining may not necessarily improve the staining of low avidity CD4<sup>+</sup> T cells directed to self-antigens (Gebe et al., 2003). Despite the presence of background staining, MHC multimer labelling has been noted to be specific, with single amino acid substitutions of the bound peptide critically affecting T cell binding (Jang et al., 2003). Cameron *et al* demonstrated a reduction in oligomer staining at 4°C and T cells made anergic by an anti-CD3 monoclonal antibody (Cameron et al., 2001). The latter finding was replicated by another research group (Quarsten et al., 2001). However, other groups have produced opposing data in terms of T cell activation status. Reichstetter *et al* were able to demonstrate that paraformaldehyde fixation did not abrogate oligomer

staining (Reichstetter et al., 2000), whilst other groups have used anti-CD3 and/or anti-TCR monoclonal antibodies to enhance oligomer staining (Kotzin et al., 2000, Radu et al., 2000, Reddy et al., 2003). The role of staining temperature appears to have been clarified to some extent, with the suggestion that the variability of staining with temperature is related to T cell avidity (Reichstetter et al., 2000). Cunliffe *et al* (Cunliffe et al., 2002) have also investigated the conditions used for tetramer staining. Although this group found a variable element of background non-specific staining of 0.01–0.03% in fresh PBMCs, they noted a detection sensitivity of 5:10000 (0.05%) using the same cells. Furthermore, although they noted 90% staining of target T cells at room temperature, this rose to 99% at 37°C and fell to 30% on ice. No increase in staining intensity was seen beyond 1 hour. It would therefore appear that each variable needs adjusting to optimise the staining characteristics of each peptide/MHC class II multimer.

In order to improve the sensitivity of MHC class II multimers it is necessary to load them homogeneously with the relevant antigenic peptide. In attempting to improve this, many have covalently linked the peptide to the  $\beta$  chain of the MHC class II (Crawford et al., 1998). However, as well as causing the manufacture of MHC class II multimers to become more cumbersome, this method may have detrimental effects on T cell recognition by affecting the TCR binding of some T cells (Rees et al., 1999). The use of thrombin cleavage of the linker may well be a necessary part of using this particular strategy. However, one group of researchers has raised one proviso to the use of synthetic antigens. They have demonstrated that peptide conformation may be affected by manufacture as well as sequence, and this may well have a bearing on the peptide loading of MHC multimers (Peterson et al., 1999, Viner et al., 1996). One group has recently developed a novel peptide loading methodology using recombinant MHC class II proteins associated with covalently linked invariant chain peptide (CLIP) as precursors to *in vitro* peptide exchange. The covalently linked CLIP peptide can be cleaved by thrombin from the recombinant MHC protein *in vitro* to allow efficient peptide exchange with a peptide of interest, so improving functional yield whilst allowing a degree of ease in peptide loading (Day et al., 2003, Jang et al., 2003). The difficulties in defining the exact T cell

antigenic epitopes adds further difficulty, although here the multimers may prove themselves to be useful through epitope mapping (Kwok et al., 2001, Stone et al., 2005). The latter two techniques may prove effective in combination.

## 5 Application of MHC Class II Multimers

Over the period in which I have been generating TBBs several groups have published results of their own attempts to apply these reagents, and as a result the scope of potential applications has become clearer.

The multimers produced to date by a limited number of research groups have been found to stain antigen-specific T cells in a consistent manner (Cameron et al., 2002) resulting in their activation as evidenced by *e.g.* IL-2 production (Casares et al., 1997, Radu et al., 1998). Moreover, the level of multimer binding has been demonstrated to be proportional to the TCR affinity and expression level (Crawford et al., 1998). Further assessment revealed that these soluble MHC class II multimers had a variety of effects on their cognate T cell, from anergy, likely to be a result of a lack of co-stimulation (Appel et al., 2001), through to T<sub>H</sub>2 differentiation with IL-4 production in both resting and activated T cells (Casares et al., 2001a, Casares et al., 1999). These variations in response may well be due to both the extent of TCR engagement, as well as the physical form of the ligand and the context in which it is presented. The importance of TCR cross-linking and clustering for T cell activation has also been elegantly demonstrated using MHC multimers. These experiments revealed that at least one dimeric pMHC complex is needed to stimulate an antigen-specific T cell through dimerisation of its receptors, with the T cell responding to the number of MHC molecules engaged in the multimer (Boniface et al., 1998, Cochran et al., 2000). This would theoretically improve the sensitivity of the T cell to minor changes in the pMHC as the whole process becomes more kinetic, involving serial TCR engagement (Lanzavecchia, 1997, Valitutti et al., 1995) and clustering (Reich et al., 1997) leading to more finely tuned T cell activation (Lanzavecchia et al., 1999, Lanzavecchia and Sallusto, 2000). Taking this a stage further, CD4<sup>+</sup> T cell

activation can be studied using pMHC class II tetramers as they more closely recreate physiological T cell activation (Mallone and Nepom, 2004).

One rather novel use of this technology has been the identification of T cell epitopes by loading MHC class II tetramers with an overlapping panel of peptides and using these to stain T cells. The immunodominant CD4<sup>+</sup> T cell epitopes can be rapidly identified using this technique. Additional subdominant epitopes that may have partial agonist functions can also be identified in combination with cytokine screening. This has been successfully used by William Kwok's group to identify the immunodominant T cell epitopes of HSV-2 VP16 protein in HLA-DRB1\*0401 and \*0404 restricted CD4<sup>+</sup> T cells (Kwok et al., 2001, Novak et al., 2001a).

MHC class II multimers have been used to look more closely at the cellular arm of the immune response in TCR transgenic mouse models. Gütgemann *et al* used cytochrome c/I-E<sup>k</sup> tetramer staining in order to demonstrate that following the oral administration cytochrome c to TCR transgenic mice there was a rapid activation of cytochrome c - specific T cells followed by a decline in their numbers (Gütgemann et al., 1998). Using the same tetramer with two transgenic mouse strains Baldwin *et al* were able to demonstrate that thymic negative selection was independent of positive selection, with those thymocytes having the greatest degree of tetramer binding being more efficiently eliminated (Baldwin et al., 1999). The presence and importance of TCR plasticity has also been demonstrated using MHC class II tetramers. Using HLA-DRB1\*0401 and HLA-DRB1\*0404 tetramers loaded with influenza virus haemagglutinin peptide (HA<sub>307-319</sub>), Gebe *et al* established that a proportion of CD4<sup>+</sup> T cells were cross-reactive between these two HLA-DR alleles, but that the pattern of cytokine production depended upon the DR-allele (Gebe et al., 2001).

Having followed CD8<sup>+</sup> T cells over the course of an infection, the opportunity had now come to apply the same techniques to CD4<sup>+</sup> T cells in non-TCR transgenic models. Unfortunately, this has highlighted one of the main problems of using MHC class II multimers, namely the relatively low frequency of antigen-specific CD4<sup>+</sup> T cells in circulation. This is presumed to be due to the relatively

small “burst size” of the CD4<sup>+</sup> T cell response which is often below the lower limit of specific fluorescence detection (about 0.01%) (Nepom, 2003). William Kwok’s group have used HLA-DR4 tetramers loaded with HA<sub>307-319</sub> in conjunction with CFSE staining to identify antigen-specific T cells in the peripheral blood of a HLA-DR4 donor who had been immunised with influenza vaccine 8 months previously (Novak et al., 1999). This identification, however, required a period of *in vitro* stimulation with influenza vaccine/ HA<sub>307-319</sub> to allow detection of the specific T cells above background, with the CFSE stain enabling the calculation of the number of cell divisions undertaken by the cells identified. Further study revealed that almost all of the antigen-specific T cells identified after 4 days of *in vitro* culture could be found in the activated CD4<sup>high</sup> population of T cells as a result of *in vitro* stimulation (Novak et al., 2001b). A more recent study by the group has not only achieved direct *ex vivo* identification of HA peptide specific CD4<sup>+</sup> T cells, but has used multicolour FACS to explore the phenotype of these cells (Danke and Kwok, 2003). The same group has produced HLA-DQ6 tetramers loaded with a series of HSV-2 VP16 peptides to isolate and characterise HSV-2-specific HLA-DQ6 restricted T cells from the peripheral blood of a HSV-2 seropositive individual (Kwok et al., 2000). Using TCR transgenic mice and I-E<sup>k</sup> tetramers loaded with MCC peptide Savage *et al* demonstrated that the T cell repertoire narrows following a secondary immune response with a loss of lower affinity T cells. This finding was based on the half-life of tetramer binding (Savage et al., 1999). MHC class II tetramers have also been used to analyse human memory CD4<sup>+</sup> T cells specific for hepatitis C virus *ex vivo*. This was possible using magnetic bead enrichment and without a period of *in vitro* culture of the PBMCs (Day et al., 2003). Multimers have been used in the setting of non-viral human infections with a small degree of success given the complexity of possible peptide antigens. In the case of Lyme disease caused by infection with *Borrelia burgdorferi*, HLA-DR4 tetramers were produced loaded with a bacterial outer-surface protein A (OspA) peptide based on murine mapping studies in HLA-DR4 transgenic mice. These multimers were used in eight patients diagnosed with Lyme disease, only one of whom was homozygous for HLA-DRB1\*0401. Despite the large number of less than perfect characteristics about this study in terms of peptide specificity and HLA matching, the group were able to



identify and clone Osp A-specific T cells, characterising these clones using intracellular cytokine staining. This was performed directly from *ex vivo* PBMCs (Meyer et al., 2000).

One of the great promises of MHC class II multimers was the possibility of studying autoimmune disease processes. However, this area of research is likely to involve pMHC-TCR interactions at the lower end of the affinity/avidity spectrum, and certainly lower than foreign antigen specific T cells, stretching the sensitivity of this group of multimers beyond their current detection limits. This assumption was confirmed using MHC class I tetramers to look for influenza-nucleoprotein NP<sub>366-374</sub>-specific T cells in influenza nucleoprotein-transgenic mice (B10NP mice). This confirmed that it was the low avidity self-specific T cell that escaped from thymic deletion (Visser et al., 2000). More recently, Gebe *et al* (Gebe et al., 2003) confirmed the low structural and functional avidity of self-reactive CD4<sup>+</sup> T cells. This group defined structural avidity as the ability of T cells to bind MHC tetramers, and functional avidity as the concentration of peptide required to obtain half-maximal T cell proliferation. Various groups have made initial forays into this area with variable results. Radu *et al* induced experimental autoimmune encephalitis (a model for multiple sclerosis) in TCR transgenic mice. Using I-A<sup>u</sup> tetramers covalently linked to rat MBP<sub>1-11</sub> (the core MBP<sub>1-9</sub> sequence of this being identical to its murine counterpart) this group were able to detect the expansion of MBP<sub>1-9</sub>-specific T cells during the primary immune response to MBP in a manner akin to the response to an infectious agent. The result would indicate an escape from central tolerance. However, the low frequency of these cells in naïve mice precluded their detection despite the use of a TCR transgenic mouse (Radu et al., 2000). A similar result was obtained by Liu *et al* using I-A<sup>g7</sup> tetramers covalently linked to one of two glutamic acid decarboxylase peptides in NOD mice, a murine model of type I diabetes mellitus (Liu et al., 2000).

Results have been more disappointing in human subjects, particularly where HLA type and antigenic peptide specificity are not as clearly defined. Kotzin *et al* used HLA-DR4 tetramers covalently linked to one of two peptides found to be immunodominant in HLA-DRB1\*0401 and \*0101 transgenic mice susceptible to

collagen induced arthritis – human type II collagen peptide 259-272 or human cartilage glycoprotein peptide 263-275 (Kotzin et al., 2000). Unfortunately, no antigen-specific T cells were identified in either the peripheral blood or synovial fluid of patients with rheumatoid arthritis. This negative result has many possible explanations including patient HLA type, the nature of the immunodominant peptide in man as compared to mice, T cell affinity and avidity, the presence of immunosuppressive agents, as well as the lag time between disease onset and T cell assessment. Two groups have used MHC class II multimers to characterise antigen-specific T cells obtained from human subjects with coeliac disease or relapsing polychondritis. In one, Quarsten *et al* generated HLA-DQ2 multimers carrying covalently-linked gliadin epitopes that specifically stained the corresponding gliadin-specific human T cell lines without exhibiting any cross-reactive staining for DQ2-restricted T cells specific for different peptides (Quarsten et al., 2001). In another, Buckner *et al* formed HLA-DR4 multimers loaded with a human type II collagen peptide in order to identify human type II collagen peptide 261-273-specific T cell clones from a heterozygous patient with relapsing polychondritis (Buckner et al., 2002). In this last study the group found CD4<sup>high</sup> T cells that could be stimulated in a peptide-specific manner by the HLA-DR4 monomers, but at the same time were not stained by the same multimers, suggesting that they may represent recently activated peptide-specific T cells. In contrast to this, a recent study, looking at the presence of GAD65-specific T cells in newly diagnosed insulin-dependent diabetics and “at risk” subjects, found that tetramer staining using GAD65 peptide-loaded HLA-DR4 multimers occurred within the activated CD25<sup>+</sup>/CD4<sup>high</sup> T cell population. However, this staining could only be achieved following incubation of PBMCs with HLA-DR4 monomers, highlighting the need for activation and *ex vivo* amplification for tetramer staining (Reijonen et al., 2002).

*In situ* staining of tissue sections using MHC class II tetramers has been achieved using a similar technique to that used with MHC class I tetramers (Bischof et al., 2004). Using multimers in association with monoclonal antibodies in a multicolour FACS analysis to characterise CD4<sup>+</sup> T cell phenotype has also been achieved (Bischof et al., 2004, Danke and Kwok, 2003).

A role for MHC multimers at a therapeutic level has also been raised (Eisenbarth and Nepom, 2002). Certainly, the group led by Teodor-Doru Brumeanu have made advances in this field. They have demonstrated antigen-specific T cell downregulation through the use of doxorubicin chemically bound to dimeric I-E<sup>d</sup> chimeras in mice (Casares et al., 2001b). Moreover, using soluble dimeric I-E<sup>d</sup> they were able to halt the development of diabetes in a double transgenic mouse model of type I insulin dependent diabetes mellitus. This was found to be due to a combination of effects including the induction of anergy in antigen-specific splenic T cells and the stimulation of IL-10-secreting T<sub>R</sub>1 cells in the pancreas (Casares et al., 2002).

Much promise remains in developing and using MHC class II multimers. Their capacity to identify and characterise antigen-specific T cells in infectious and autoimmune disease processes will help in our understanding of these and may lead to new therapeutic strategies. This could also be used to characterise clinical heterogeneity within disease processes and even delineate responders from non-responders in therapeutic strategies. The possibility of using these multimers as therapy has even been raised, although safety and regulatory issues remain (Ferlin et al., 2000, Nepom et al., 2002). Despite all this promise many hurdles remain.

## 6 Future Work

As a result of my work the first hurdle to the use of MHC class II tetramer technology in anti-glomerular basement membrane disease has been overcome. I have shown the consistent production and functionality of recombinant HLA-DR15 TBB and HLA-DR7 TBB using two different methods. Furthermore, with the successful formation of the I-E<sup>d</sup>sc TBB, the possibility remains of using this construct in the murine model of AIHA. This would enable the parallel assessment of construct design and functionality in a separate disease model whose antigenic epitope has been relatively well delineated (Elson and Barker, 2000, Perry et al.,

1996). Colleagues within my former laboratory have both reproduced my findings and continued the development of the recombinant TBB constructs.

Further possible improvements in both heterodimer and fusion-protein TBB expression systems have been discussed. In summary, the following adaptations could be assessed in terms of their efficacy in improving recombinant protein yield:

- Covalent peptide linkage is currently being assessed within my former laboratory with regard to the single chain fusion protein constructs. However, this could also be considered for the leucine zipper associated heterodimeric constructs. Of interest would be the use of a covalently linked CLIP peptide that could then be exchanged for a peptide of interest once the recombinant MHC class II protein had been expressed (Day et al., 2003).
- Within the *Drosophila* expression system, the use of an insect cell leader sequence as well as the co-expression of chaperone protein *eg* calreticulin (Fourneau et al., 2004).
- Alteration of *Drosophila* culture conditions *eg* roller bottles (Gauthier et al., 1998).
- The use of anion exchange chromatography in association with metal affinity chromatography for the purification of the single-chain fusion protein constructs prior to refolding.
- The use of glycerol and L-arginine during the refolding of the single-chain fusion protein constructs.

Aside from the possibilities above, the biological evaluation of the recombinant MHC class II constructs formed to date requires completion. With the recent formation of Goodpasture antigen-specific HLA-DR15 restricted T cell hybridomas within my former laboratory, an assessment of these constructs *in vitro* has been initiated. Preliminary results indicate that these hybridomas are weakly responsive to both heterodimer and fusion-protein TBBs. It is hoped that the HLA-

DR15 transgenic mice lacking their murine MHC class II proteins developed within my former laboratory will form the basis of *ex vivo* assessments of my HLA-DR15 constructs.

With the successful biological evaluation of the TBB constructs, the next stage would be the formation and biological evaluation of multimeric assemblies. There are two feasible strategies: the “standard” tetramer design using the avidin-biotin interaction, or the use of higher order cross-linking using microbeads or liposomes as a scaffold.

The “standard” tetramer design would first require biotinylation of the heterodimeric TBB constructs using the recombinant BirA holoenzyme, the single-chain fusion proteins appearing to be already biotinylated to some extent during their synthesis. This is the more usual multimerisation strategy in terms of the heterodimeric TBBs, and the leucine zipper domains would improve the flexibility of MHC-TCR interactions so enhancing the avidity of the multimer. There would be no such flexibility in the case of the single-chain fusion proteins, and so the avidity of such multimers may require further optimisation through higher order multimerisation.

In terms of higher order cross-linking, both microbead and liposomal scaffolds have been successfully used in the case of MHC class I multimers (Bodinier et al., 2000, Luxembourg et al., 1998, Prakken et al., 2000), with promising early indications that both can be adapted for use with MHC class II multimers in order to improve their avidity. Kwok’s group have engineered artificial antigen presenting cells using microbeads coated with recombinant HLA-DR4 tetramers based on the “standard” avidin-biotin scaffold (Maus et al., 2003). The beads were used on CD4<sup>+</sup> T cell lines, so excluding possible non-specific phagocytosis by *e.g.* macrophages. This group found that indirect conjugation of the MHC class II tetramers via a monoclonal antibody resulted in both more efficient coating of the beads and a better functional outcome. This finding may be due to several factors including the directional binding of the tetramers to the beads, less harsh binding conditions, and the greater flexibility afforded to the tetramers that



would in turn improve the avidity of the construct. Teyton's group have successfully engineered liposomal artificial antigen presenting cells, linking the MHC class II tetramers to these via either a polyhistidine tag or an avidin-biotin interaction (Mallet-Designe et al., 2003). This technique was noted to improve the structural avidity of the MHC class II multimers, allowing the *ex vivo* identification of naïve antigen-specific CD4<sup>+</sup> T cells without the need for a period of activation, and without increasing background staining. However, these encouraging results identifying naïve CD4<sup>+</sup> T cells need to be tempered by the technical difficulties found by the authors in consistent liposome production. Certainly, my TBB constructs would be usable in this manner with either technique via their polyhistidine tags.

With the establishment functional multimeric TBB constructs, the intention would be to use these in order to gain a greater understanding of the role of auto-antigen specific CD4<sup>+</sup>T cells in a defined autoimmune process. The evidence to date would suggest that the use of “standard” MHC class II tetramers to stain *ex vivo* auto-antigen specific CD4<sup>+</sup> T cells is unlikely to succeed for a variety of reasons without the concomitant use of *eg* transgenic animal models or a period of *in vitro* expansion to improve CD4<sup>+</sup> T cell numbers. Therefore, although it may be worthwhile comparing the TBB constructs using the “standard” tetramer design before embarking on higher order multimerisation using microbeads, the use of higher order cross-linking in combination with developing FACS techniques (*eg* SEMS (Townsend et al., 2001)) places the *ex vivo* assessment of low affinity auto-antigen specific CD4<sup>+</sup> T cells within reach. Moreover, it would be of interest to compare the lower and higher order multimers in terms of the information that the techniques provide concerning auto-antigen specific CD4<sup>+</sup> T cells. This would be best achieved using transgenic animal models in order to improve “standard” tetramer staining, so allowing an assessment of whether a period of *in vitro* expansion significantly alters CD4<sup>+</sup> T cell phenotype. The pMHC class II tetramer constructs could be used as specific *in vitro* CD4<sup>+</sup> T cell activation reagents (Buckner et al., 2002, Reijonen et al., 2002).

Forays into autoimmune disease using MHC class II tetramers have not been exceedingly successful to date. Although these forays have investigated important

diseases in terms of their prevalence, they have been hampered to a greater or lesser extent by lack of HLA-restriction homogeneity and the presence of multiple possible auto-antigenic specificities. These factors are better defined in the case of Goodpasture's disease, improving the probability of the successful use of MHC class II multimer technology in a human autoimmune disease. I have formed complementary MHC class II TBB constructs with respect to Goodpasture's disease: HLA-DRB1\*1501 has strong positive associations and HLA-DRB1\*0701 has strong negative associations with the disease as a direct effect of the alleles themselves (Phelps and Rees, 1999). These constructs can be used in parallel to analyse antigen-specific CD4<sup>+</sup> T cell phenotypes in relation to disease and control populations, and so try to delineate any differences in CD4<sup>+</sup> T cell responses in relation to these two presentation strategies. As Goodpasture's disease tends not to follow a relapsing-remitting course, its kinetics with respect to changes in CD4<sup>+</sup> T cell phenotype and avidity can be more readily followed from near to the point of disease initiation through to its natural or therapeutically induced remission. Recent work in insulin-dependent diabetes mellitus would suggest that it is not the antigen responsiveness *per se*, but rather the balance of T cell phenotypes that leads to an autoimmune process (Arif et al., 2004). The constructs that I have formed would be ideally placed to further investigate this suggestion. Furthermore, although the Goodpasture antigen has been well characterised, and as a result the peptide antigens that would be utilised within the MHC class II multimeric constructs have been better defined, the possibility remains of confirming these epitopes using the MHC class II constructs and overlapping peptide panels to perform an epitope mapping exercise (Kwok et al., 2001). This may be of relevance given that different epitopes may predominate over the natural history of the disease process, with these epitopes being affected by both differences between individuals as well as APCs (Reijonen et al., 1999, Reijonen et al., 2003). Such epitope spreading may complicate the interpretation of negative results, and in this setting epitope mapping using the complementary MHC class II TBB constructs could be of value.

## **Chapter 8**

## **References**

## Chapter 8

### References

- Abastado, J.-P., Lone, Y.-C., Casrouge, A., Boulot, G. and Kourlisky, P. (1995) Dimerization of soluble major histocompatibility complex-peptide complexes is sufficient for activation of T cell hybridoma and induction of unresponsiveness. *Journal of Experimental Medicine*, **182**, 439 - 447.
- Abbas, A. K., Murphy, K. M. and Sher, A. (1996) Functional diversity of helper T lymphocytes. *Nature*, **383**, 787-793.
- Ahmed, A. K., Schaffer, S. W. and Wetlaufer, D. B. (1975) Nonenzymic reactivation of reduced bovine pancreatic ribonuclease by air oxidation and by glutathione oxidoreduction buffers. *Journal of Biological Chemistry*, **250**, 8477-8482.
- Alderwegen, I. E. v., Bruijn, J. A. and Heer, E. d. (1997) T cell subsets in immunologically-mediated glomerulonephritis. *Histology and Histopathology*, **12**, 241 - 250.
- Altman, J. D., Henner, D., Nilsson, B., Anderson, S. and Kuntz, I. D. (1991) Intracellular expression of BPTI fusion protein and single column cleavage/affinity purification by chymotrypsin. *Protein Engineering*, **4**, 593-600.
- Altman, J. D., Moss, P. A. H., Goulder, P. J. R., Barouch, D. H., McHeyzer-Williams, M. G., Bell, J. I., McMichael, A. J. and Davis, M. M. (1996) Phenotypic analysis of antigen-specific T lymphocytes. *Science*, **274**, 94-96.
- Altman, J. D., Reay, P. A. and Davis, M. M. (1993) Formation of functional peptide complexes of class II major histocompatibility complex proteins from subunits produced in *Escherichia coli*. *Proceedings of the National Academy of Science (USA)*, **90**, 10330-10334.
- AmershamBiosciences (1997) Uppsala, pp. 1 - 4.
- AmershamPharmaciaBiotech (2001) Uppsala, pp. 57 - 60.
- Amrani, A., Verdaguer, J., Serra, P., Tafuro, S., Tan, R. and Santamaria, P. (2000) Progression of autoimmune diabetes driven by avidity maturation of a T-cell population. *Nature*, **406**, 739 - 742.
- Anderton, S. M., Radu, C. G., Lowrey, P. A., Ward, E. S. and Wraith, D. C. (2001) Negative selection during the peripheral immune response to antigen. *Journal of Experimental Medicine*, **193**, 1-11.

- Anfinsen, C. B. (1973) Principles that Govern the Folding of Protein Chains. *Science*, **181**, 223 - 230.
- Appel, H., Gauthier, L., Pyrdol, J. and Wucherpfennig, K. W. (2000) Kinetics of T-cell receptor binding by bivalent HLA-DR peptide complexes that activate antigen-specific human T-cells. *Journal of Biological Chemistry*, **275**, 312 - 321.
- Appel, H., Seth, N. P., Gauthier, L. and Wucherpfennig, K. W. (2001) Anergy induction by dimeric TCR ligands. *Journal of Immunology*, **166**, 5279 - 5285.
- Arakawa, T. and Timasheff, S. N. (1982) Preferential Interactions of Proteins with Salts in Concentrated Solutions. *Biochemistry*, **21**, 6545 - 6552.
- Arif, S., Tree, T. I., Astill, T. P., Tremble, J. M., Bishop, A. J., Dayan, C. M., Roep, B. O. and Peakman, M. (2004) Autoreactive T cell responses show proinflammatory polarization in diabetes but a regulatory phenotype in health. *Journal of Clinical Investigation*, **113**, 451-463.
- Arimilli, S., Cardoso, C., Mukku, P., Baichwal, V. and Nag, B. (1995) Refolding and reconstitution of functionally active complexes of human leucocyte antigen DR2 and myelin basic protein peptide from recombinant  $\alpha$  and  $\beta$  polypeptide chains. *Journal of Biological Chemistry*, **270**, 971 - 977.
- Arora, D. and Khanna, N. (1996) Method for increasing the yield of properly folded recombinant human gamma interferon from inclusion bodies. *Journal of Biotechnology*, **52**, 127-133.
- Avrameas, S. (1969) Indirect immunoenzyme techniques for the intracellular detection of antigens. *Immunochemistry*, **6**, 825 - 831.
- Baldwin, K. K., Trenchak, B. P., Altman, J. D. and Davis, M. M. (1999) Negative selection of T cells occurs throughout thymic development. *Journal of Immunology*, **163**, 689-698.
- Becker, D., Mohamedzadeh, M., Reske, K. and Knop, J. (1992) Increased level of intracellular MHC class II molecules in murine langerhans cells following in vivo and in vitro administration of contact allergens. *The Journal of Investigative Dermatology*, **99**, 545-549.
- Beckett, D., Kovaleva, E. and Schatz, P. J. (1999) A minimal peptide substrate in biotin holoenzyme synthetase-catalysed biotinylation. *Protein Science*, **8**, 921-929.
- Bhan, A. K., Schneeberger, E. E., Collins, A. B. and McCluskey, R. T. (1978) Evidence for a pathogenic role of cell-mediated immune mechanism in experimental glomerulonephritis. *Journal of Experimental Medicine*, **148**, 246 - 260.
- Bischof, F., Hofmann, M., Schumacher, T. N. M., Vyth-Dreese, F. A., Weissert, R., Schild, H., Kruisbeek, A. M. and Melms, A. (2004) Analysis of Autoreactive CD4 T Cells in Experimental Autoimmune Encephalomyelitis after Primary and Secondary Challenge Using MHC Class II Tetramers. *The Journal of Immunology*, **172**, 2878-2884.



- Blattman, J. N., Sourdive, D. J. D., Murali-Krishna, K., Ahmed, R. and Altman, J. D. (2000) Evolution of the T cell repertoire during primary, memory and recall responses to viral infection.*Journal of Immunology*, **165**, 6081-6090.
- Bodinier, M., Peyrat, M., Tournay, C., Davodeau, F., Romagne, F., Bonneville, M. and Lang, F. (2000) Efficient detection and immunomagnetic sorting of specific T cells using multimers of MHC class I and peptide with reduced CD8 binding.*Nature Medicine*, **6**, 707 - 710.
- Bolton, W. K., Chandra, M., Tyson, T. M., Kirkpatrick, P. R., Sadovnic, M. J. and Sturgill, B. C. (1988) Transfer of experimental glomerulonephritis in chickens by mononuclear cells.*Kidney International*, **34**, 598 - 610.
- Bolton, W. K., Donald J. Innes, J., Sturgill, B. C. and Kaiser, D. L. (1987) T-cells and macrophages in rapidly progressive glomerulonephritis: Clinicopathological correlations.*Kidney International*, **32**, 869 - 876.
- Bolton, W. K., Tucker, F. L. and Sturgill, B. C. (1984) New avian model of experimental glomerulonephritis consistent with mediation by cellular immunity: Nonhumorally mediated glomerulonephritis in chickens.*Journal of Clinical Investigation*, **73**, 1263 - 1276.
- Boniface, J. J., Rabinowitz, J. D., Wülfing, C., Hampl, J., Reich, Z., Altman, J. D., Kantor, R. M., Beeson, C., McConnell, H. M. and Davis, M. M. (1998) Initiation of signal transduction through the T cell receptor requires the multivalent engagement of peptide/MHC ligands.*Immunity*, **9**, 459 - 466.
- Borza, D.-B., Bondar, O., Todd, P., Sundaramoorthy, M., Sado, Y., Ninomiya, Y. and Hudson, B. G. (2002) Quaternary Organization of the Goodpasture Autoantigen, the alpha 3(IV) Collagen Chain. SEQUESTRATION OF TWO CRYPTIC AUTOEPITOPES BY INTRAPROTOMER INTERACTIONS WITH THE alpha 4 AND alpha 5 NC1 DOMAINS.*Journal of Biological Chemistry*, **277**, 40075-40083.
- Borza, D.-B., Netzer, K.-O., Leinonen, A., Todd, P., Cervera, J., Saus, J. and Hudson, B. G. (2000) The Goodpasture autoantigen: Identification of multiple cryptic epitopes on the NC1 domain of the  $\alpha$ 3(IV) collagen chain.*Journal of Biological Chemistry*, **275**, 6030 - 6037.
- Bousso, P., Michel, F., Pardigon, N., Bercovici, N., Liblau, R., Kourilsky, P. and Abastado, J.-P. (1997) Enrichment of antigen-specific T lymphocytes by panning on immobilised MHC-peptide complexes.*Immunology Letters*, **59**, 85-91.
- Braunstein, N., Germain, R., Loney, K. and Berkowitz, N. (1990) Structurally interdependent and independent regions of allelic polymorphism in class II MHC molecules. Implications for Ia function and evolution.*Journal of Immunology*, **145**, 1635 - 1645.

- Brown, J. H., Jardetzky, T. S., Gorga, J. C., Stern, L. J., Urban, R. G., Strominger, J. L. and Wiley, D. C. (1993) Three-dimensional structure of the human class II histocompatibility antigen HLA-DR1. *Nature*, **364**, 33 - 39.
- Buckner, J. H., Landeghen, M. V., Kwok, W. W. and Tsarknaridis, L. (2002) Identification of type II collagen peptide 261-273-specific T cell clones in a patient with relapsing polychondritis. *Arthritis and Rheumatism*, **46**, 238 - 244.
- Buelow, R., Kuo, S., Paborsky, L., Wilson, K. J. and Rothbard, J. B. (1994) Detergent-enhanced dissociation of endogenous peptides from PI-DRB1\*0401. *European Journal of Immunology*, **24**, 2181 - 2185.
- Bunch, T. A., Grinblat, Y. and Goldstein, L. S. B. (1988) Characterisation and use of the *Drosophila* metallothionein promoter in cultured *Drosophila melongaster* cells. *Nucleic Acids Research*, **16**, 1043-1061.
- Burrows, G. G., Adlard, K. L., Bruce F. Bebo, J., Chang, J. W., Tenditnyy, K., Vandenbark, A. A. and Offner, H. (2000a) Regulation of encephalitogenic T cells with recombinant TCR ligands. *Journal of Immunology*, **164**, 6366-6371.
- Burrows, G. G., Bruce F. Bebo, J., Adlard, K. L., Vandenbark, A. A. and Offner, H. (1998) Two-domain MHC class II molecules form stable complexes with myelin basic protein 69-89 peptide that detect and inhibit rat encephalitogenic T cells and treat experimental autoimmune encephalomyelitis. *Journal of Immunology*, **161**, 5987-5996.
- Burrows, G. G., Chang, J. W., Bächinger, H.-P., Bourdette, D. N., Offner, H. and Vandenbark, A. A. (1999) Design, engineering and production of functional single-chain T cell receptor ligands. *Protein Engineering*, **12**, 771-778.
- Burrows, S. R., Kienzle, N., Winterhalter, A., Bharadwaj, M., Altman, J. D. and Brooks, A. (2000b) Peptide-MHC class I tetrameric complexes display exquisite ligand specificity. *Journal of Immunology*, **165**, 6229-6234.
- Busch, D. H., Kersiek, K. M. and Pamer, E. G. (2000) Differing roles of inflammation and antigen in T cell proliferation and memory generation. *Journal of Immunology*, **164**, 4063-4070.
- Busch, D. H. and Pamer, E. G. (1999) T cell affinity maturation by selective expansion during infection. *Journal of Experimental Medicine*, **189**, 701 - 709.
- Busch, D. H., Pilip, I. M., Vijn, S. and Pamer, E. G. (1998) Coordinate regulation of complex T cell populations responding to bacterial infection. *Immunity*, **8**, 353-362.
- Buslepp, J., Zhao, R., Donnini, D., Loftus, D., Saad, M., Appella, E. and Collins, E. J. (2001) T cell activity correlates with oligomeric peptide-Major Histocompatibility Complex binding on T cell surface. *Journal of Biological Chemistry*, **276**, 47320 - 47328.

- Butkowski, R. R., Langeveld, J. P. M., Wieslander, J., Hamilton, J. and Hudson, B. G. (1987) Localisation of the Goodpasture epitope to a novel chain of basement membrane collagen. *The Journal of Biological Chemistry*, **262**, 7874-7877.
- Buus, S. (1999) Description and prediction of peptide-MHC binding: the 'human MHC project'. *Current Opinion in Immunology*, **11**, 209-213.
- Buus, S., Sette, A., Colon, S. M., Miles, C. and Grey, H. M. (1987) The relation between Major Histocompatibility Complex (MHC) restriction and the capacity of Ia to bind to immunogenic peptides. *Science*, **235**, 1353-1358.
- Cairns, L. S., Phelps, R. G., Bowie, L., Hall, A. M., Saweirs, W. W. M., Rees, A. J. and Barker, R. N. (2003) The Fine Specificity and Cytokine Profile of T-Helper Cells Responsive to the {alpha}3 Chain of Type IV Collagen in Goodpasture's Disease. *Journal of the American Society of Nephrology*, **14**, 2801-2812.
- Cairns, L. S., Phelps, R. G., Rees, A. J. and Barker, R. N. (1999) Mapping autoreactive T-cell epitopes on the Goodpasture Antigen. *Immunology*, **98**, 33.
- Callan, M. F. C., L.Tan, Annels, N., G.S.Ogg, Wilson, J. D. K., O'Callaghan, C. A., Steven, N., McMichael, A. J. and Rickinson, A. B. (1998) Direct visualisation of antigen-specific CD8+ T cells during the primary immune response to Epstein-Barr virus in vivo. *Journal of Experimental Medicine*, **187**, 1395-1402.
- Cameron, T. O., Cochran, J. R., Yassine-Diab, B., Sékaly, R.-P. and Stern, L. J. (2001) Cutting Edge: Detection of antigen-specific CD4+ T cells by HLA-DR1 oligomers is dependent on the T cell activation state. *Journal of Immunology*, **166**, 741 - 745.
- Cameron, T. O., Norris, P. J., Patel, A., Moulon, C., Rosenberg, E. S., Mellins, E. D., Wedderburn, L. R. and Stern, L. J. (2002) Labeling antigen-specific CD4<sup>+</sup> T cells with class II MHC oligomers. *Journal of Immunological Methods*, **268**, 51 - 69.
- Cammarota, G., Scheirle, A., Takacs, B., Doran, D. M., Knorr, R., Bannwarth, W., Guardiola, J. and Sinigaglia, F. (1992) Identification of a CD4 binding site on the  $\beta_2$  domain of HLA-DR molecules. *Nature*, **356**, 799 - 801.
- Campbell, A. M., Kessler, P. D. and Fambrough, D. M. (1992) The alternative carboxyl termini of avian cardiac and brain sarcoplasmic reticulum/endoplasmic reticulum Ca<sup>2+</sup>-ATPases are on opposite sides of the membrane. *Journal of Biological Chemistry*, **267**, 9321 - 9325.
- Casares, S., Bona, C. A. and Brumeanu, T. D. (1997) Engineering and characterisation of a murine MHC class II-immunoglobulin chimera expressing an immunodominant CD4 T viral epitope. *Protein Engineering*, **10**, 1295 - 1301.

- Casares, S., Bona, C. A. and Brumeanu, T.-D. (2001a) Enzymatically mediated engineering of multivalent MHC class II-peptide chimeras.*Protein Engineering*, **14**, 195 - 200.
- Casares, S., Hurtado, A., McEvoy, R. C., Sarukhan, A., Boehmer, H. v. and Brumeanu, T.-D. (2002) Down-regulation of diabetogenic CD4<sup>+</sup> T cells by a soluble dimeric peptide-MHC class II chimera.*Nature Immunology*, **3**, 383 - 391.
- Casares, S., Stan, A. C., Bona, C. A. and Brumeanu, T.-D. (2001b) Antigen-specific downregulation of T cells by doxorubicin delivered through a recombinant MHC II - peptide chimera.*Nature Biotechnology*, **19**, 142 - 147.
- Casares, S., Zong, C. S., Radu, D. L., Miller, A., Bona, C. A. and Brumeanu, T.-D. (1999) Antigen-specific signalling by a soluble, dimeric peptide/major histocompatibility complex class II/Fc chimera leading to T helper cell type 2 differentiation.*Journal of Experimental Medicine*, **190**, 543 - 553.
- Chan, O. and J. Shlomchik, M. (1998) A New Role for B Cells in Systemic Autoimmunity: B Cells Promote Spontaneous T Cell Activation in MRL-lpr/lpr Mice.*Journal of Immunology*, **160**, 51-59.
- Chan, O. T. M., Hannum, L. G., Haberman, A. M., Madaio, M. P. and Shlomchik, M. J. (1999) A novel mouse with B cells but lacking serum antibody reveals an antibody-independent role for B cells in murine lupus.*Journal of Experimental Medicine*, **189**, 1639 - 1647.
- Chang, H.-C., Bao, Z.-Z., Yao, Y., Tse, A. G. D., Goyarts, E. C., Madsen, M., Kawasaki, E., Brauer, P. P., Sacchettini, J. C., Nathenson, S. G. and Reinherz, E. L. (1994) A general method for facilitating heterodimeric pairing between two proteins: Application to expression of  $\alpha$  and  $\beta$  T-cell receptor extracellular segments.*Proceedings of the National Academy of Science (USA)*, **91**, 11408 - 11412.
- Chang, J. W., Mechling, D. E., Bächingers, H.-P. and Burrows, G. G. (2001) Design, engineering, and production of human recombinant T cell receptor ligands derived from human leucocyte antigen DR2.*Journal of Biological Chemistry*, **276**, 24170 - 24176.
- Chersi, A., Rosano, L. and Tanigaki, N. (2000) Polystyrene beads coated with antibodies directed to HLA class I intracytoplasmic domain: the use in quantitative measurement of peptide-HLA class I binding by flow cytometry.*Human Immunology*, **61**, 1298-1306.
- Chicz, R. M., Urban, R. G., Gorga, J. C., Vignali, D. A. A., Lane, W. S. and Strominger, J. L. (1993) Specificity and promiscuity among naturally processed peptides bound to HLA-DR alleles.*Journal of Experimental Medicine*, **178**, 27 - 47.

- Chicz, R. M., Urban, R. G., Lane, W. S., Gorga, J. C., Stern, L. J., Vignali, D. A. A. and Strominger, J. L. (1992) Predominant naturally processed peptides bound to HLA-DR1 are derived from MHC-related molecules and are heterogenous in size. *Nature*, **358**, 764 - 768.
- Chopra, S. (1999) University of Aberdeen, Aberdeen, pp. 135.
- Clark, E. D. B. (1998) Refolding of recombinant proteins. *Current Opinion in Biotechnology*, **9**, 157 – 163.
- Cochran, J. R., Cameron, T. O. and Stern, L. J. (2000) The relationship of MHC-peptide binding and T cell activation probed using chemically defined MHC class II oligomers. *Immunity*, **12**, 241-250.
- Cochran, J. R., Cameron, T. O., Stone, J. D., Lubetsky, J. B. and Stern, L. J. (2001) Receptor Proximity, Not Intermolecular Orientation, Is Critical for Triggering T-cell Activation. *Journal of Biological Chemistry*, **276**, 28068-28074.
- Colangeli, R., Heijbel, A., Williams, A. M., Manca, C., Chan, J., Lyashchenko, K. and Laura Gennaro, M. (1998) Three-step purification of lipopolysaccharide-free, polyhistidine-tagged recombinant antigens of Mycobacterium tuberculosis. *Journal of Chromatography B: Biomedical Sciences and Applications*, **714**, 223-235.
- Coligan, J. E., Kruisbeek, A. M., Margulies, D. H., Shevach, E. M. and Strober, W. (Eds.) (2001) *Ligand-Receptor Interactions in the Immune System*, John Wiley & Sons Inc., New York.
- Cosson, P. and Bonifacio, J. S. (1992) Role of transmembrane domain interactions in the assembly of class II MHC molecules. *Science*, **258**, 659 - 662.
- Crawford, F., Kozono, H., White, J., Marrack, P. and Kappler, J. (1998) Detection of antigen-specific T cells with multivalent soluble class II MHC covalent peptide complexes. *Immunity*, **8**, 675-682.
- Cunliffe, S. L., Wyer, J. R., Sutton, J. K., Lucas, M., Harcourt, G., Klenerman, P., McMichael, A. J. and Kelleher, A. D. (2002) Optimization of peptide linker length in production of MHC class II/peptide tetrameric complexes increases yield and stability, and allows identification of antigen-specific CD4+T cells in peripheral blood mononuclear cells. *European Journal of Immunology*, **32**, 3366 - 3375.
- Cunningham, M. A., Huang, X. R., Dowling, J. P., Tipping, P. G. and Holdsworth, S. R. (1999) Prominence of cell-mediated immunity effectors in "pauci-immune" glomerulonephritis. *Journal of the American Society of Nephrology*, **10**, 499 - 506.
- Danke, N. A. and Kwok, W. W. (2003) HLA Class II-Restricted CD4+ T Cell Responses Directed Against Influenza Viral Antigens Postinfluenza Vaccination. *Journal of Immunology*, **171**, 3163-3169.



- David, M., Borza, D.-B., Leinonen, A., Belmont, J. M. and Hudson, B. G. (2001) Hydrophobic Amino Acid Residues Are Critical for the Immunodominant Epitope of the Goodpasture Autoantigen. A MOLECULAR BASIS FOR THE CRYPTIC NATURE OF THE EPITOPE. *Journal of Biological Chemistry*, **276**, 6370-6377.
- Davis, M. M., Boniface, J. J., Reich, Z., Lyons, D., Hamp, J., Arden, B. and Chien, Y.-h. (1998) Ligand recognition by  $\alpha\beta$  T cell receptors. *Annual Review of Immunology*, **16**, 523 - 544.
- Day, C. L., Seth, N. P., Lucas, M., Appel, H., Gauthier, L., Lauer, G. M., Robbins, G. K., Szczepiorkowski, Z. M., Casson, D. R., Chung, R. T., Bell, S., Harcourt, G., Walker, B. D., Klenerman, P. and Wucherpfennig, K. W. (2003) Ex vivo analysis of human memory CD4 T cells specific for hepatitis C virus using MHC class II tetramers. *Journal of Clinical Investigation*, **112**, 831 - 842.
- Dehan, P., Weber, M., Zhang, X., Reeders, S. T., Foidart, J.-M. and Tryggvason, K. (1996) Sera from patients with anti-GBM nephritis including Goodpasture syndrome show heterogenous reactivity to recombinant NC1 domain of type IV collagen  $\alpha$  chains. *Nephrology Dialysis and Transplantation*, **11**, 2215 - 2222.
- Denkberg, G., Cohen, C. J. and Reiter, Y. (2001) Critical role for CD8 in binding of MHC tetramers to TCR: CD8 antibodies block specific binding of human tumor-specific MHC-peptide tetramers to TCR. *Journal of Immunology*, **167**, 270 - 276.
- Denkberg, G., Cohen, C. J., Segal, D., Kirkin, A. F. and Reiter, Y. (2000) Recombinant human single-chain MHC-peptide complexes made from *E.coli* by *in vitro* refolding: functional single-chain MHC-peptide complexes and tetramers with tumour associated antigens. *European Journal of Immunology*, **30**, 3522 - 3532.
- Derby, M. A., Wang, J., Margulies, D. H. and Berzofsky, J. A. (2001) Two intermediate-avidity cytotoxic T lymphocyte clones with a disparity between functional avidity and MHC tetramer staining. *International Immunology*, **13**, 817 - 824.
- Derry, C. J., Dunn, M. J., Rees, A. J. and Pusey, C. D. (1991) Restricted specificity of the autoantibody response in Goodpasture's syndrome demonstrated by two-dimensional Western blotting. *Clinical Experimental Immunology*, **86**, 457 - 463.
- Derry, C. J., Ross, C. N., Lombard, G., Mason, P. D., Rees, A. J., Lechler, R. I. and Pusey, C. D. (1995) Analysis of T cell responses to the autoantigen in Goodpasture's disease. *Clinical and Experimental Immunology*, **100**, 262-268.
- Doherty, P. C. (1998) The numbers game for virus-specific CD8<sup>+</sup> T cells. *Science*, **280**, 227.

- Dornmair, K. and McConnell, H. M. (1990) Refolding and reassembly of separate  $\alpha$  and  $\beta$  chains of class II molecules of the major histocompatibility complex leads to increased peptide-binding capacity. *Proceedings of the National Academy of Science (USA)*, **87**, 4134-4138.
- Drake III, D. R. and Braciale, T. J. (2001) Cutting Edge: Lipid raft integrity affects the efficiency of MHC Class I tetramer binding and cell surface TCR arrangement on CD8<sup>+</sup> T cells. *Journal of Immunology*, **166**, 7009 - 7013.
- Dunbar, P. R. and Ogg, G. S. (2002) Oligomeric MHC molecules and their homologues: State of the art. *Journal of Immunological Methods*, **268**, 3 - 7.
- Dunbar, P. R., Ogg, G. S., Chen, J., Rust, N., Bruggen, P. v. d. and Cerundolo, V. (1998) Direct isolation, phenotyping and cloning of low-frequency antigen-specific cytotoxic T lymphocytes from peripheral blood. *Current Biology*, **8**, 413-416.
- Dutoit, V., Rubio-Godoy, V., Doucey, M.-A., Batard, P., Lienard, D., Rimoldi, D., Speiser, D., Guillaume, P., Cerottini, J.-C., Romero, P. and Valmori, D. (2002) Functional Avidity of Tumor Antigen-Specific CTL Recognition Directly Correlates with the Stability of MHC/Peptide Multimer Binding to TCR. *Journal of Immunology*, **168**, 1167-1171.
- Echchakir, H., Dorothee, G., Vergnon, I., Menez, J., Chouaib, S. and Mami-Chouaib, F. (2002) Cytotoxic T lymphocytes directed against a tumor-specific mutated antigen display similar HLA tetramer binding but distinct functional avidity and tissue distribution. *Proceedings of the National Academy of Science (USA)*, **99**, 9358-9363.
- Eisenbarth, G. S. and Nepom, G. T. (2002) Class II peptide multimers: promise for type 1A diabetes? *Nature Immunology*, **3**, 344 - 345.
- Elson, C. J. and Barker, R. N. (2000) Helper T cell in antibody-mediated, organ-specific autoimmunity. *Current Opinion in Immunology*, **12**, 664-669.
- Evan, G. I., Lewis, G. K., Ramsay, G. and Bishop, J. M. (1985) Isolation of monoclonal antibodies specific for human c-myc proto-oncogene product. *Molecular and Cellular Biology*, **5**, 3610 - 3616.
- Fahmy, T. M., Bieler, J. G., Edidin, M. and Schneck, J. P. (2001) Increased TCR avidity after T cell activation: A mechanism for sensing low-density antigen. *Immunity*, **14**, 135 -143.
- Falk, K., Lau, J. M., Santambrogio, L., Esteban, V. M., Puentes, F., Rötzschke, O. and Strominger, J. L. (2002) Ligand exchange of Major Histocompatibility Complex Class II proteins is triggered by H-bond donor groups of small molecules. *Journal of Biological Chemistry*, **277**, 2709 - 2715.
- Falk, K., Rötzschke, O., Stevanović, S., Jung, G. and Rammensee, H.-G. (1991) Allele-specific motifs revealed by sequencing of self-peptides eluted from MHC molecules. *Nature*, **351**, 290 - 296.

- Ferlin, W., Glaichenhaus, N. and Mougneau, E. (2000) Present difficulties and future promise of MHC multimers in autoimmune exploration. *Current Opinion in Immunology*, **12**, 670-675.
- Ferrario, F., Castiglione, A., Colasanti, G., Belgioioso, G. B. D., Bertoli, S. and D'Amico, G. (1985) The detection of monocytes in human glomerulonephritis. *Kidney International*, **28**, 513 - 519.
- Fischer, B., Sumner, I. and Goodenough, P. (1992) Isolation and renaturation of bio-active proteins expressed in *Escherichia coli* as inclusion bodies. *Arzneimittel-Forschung*, **42**, 1512 - 1515.
- Fisher, M., Pusey, C. D., Vaughan, R. W. and Rees, A. J. (1997) Susceptibility to anti-glomerular basement membrane disease strongly associated with HLA-DRB1 genes. *Kidney International*, **51**, 222-229.
- Ford, D. and Burger, D. (1983) Precursor frequency of antigen-specific T cells: Effects of sensitisation *in Vivo* and *in Vitro*. *Cellular Immunology*, **79**, 334 - 344.
- Fourneau, J.-M., Cohen, H. and van Endert, P. M. (2004) A chaperone-assisted high yield system for the production of HLA-DR4 tetramers in insect cells. *Journal of Immunological Methods*, **285**, 253-264.
- Frayser, M., Sato, A. K., Xu, L. and Stern, L. J. (1999) Empty and peptide-loaded Class II Major Histocompatibility Complex proteins produced by expression in *Escherichia coli* and folding *in vitro*. *Protein Expression and Purification*, **15**, 105 - 114.
- Fremont, D. H., Hendrickson, W. A., Marrack, P. and Kappler, J. (1996) Structures of an MHC class II molecule with covalently bound single peptides. *Science*, **272**, 1001-1004.
- Fu, X. T. and Karr, R. W. (1994) HLA-DR alpha chain residues located on the outer loops are involved in nonpolymorphic and polymorphic antibody-binding epitopes. *Human Immunology*, **39**, 253 - 260.
- Garboczi, D. N., Hung, D. T. and Wiley, D. C. (1992) HLA-A2-peptide complexes: Refolding and crystallization of molecules expressed in *Escherichia coli* and complexed with single antigenic peptides. *Proceedings of the National Academy of Science (USA)*, **89**, 3429 - 3433.
- Gauthier, L., Smith, K. J., Pyrdol, J., Kalandadze, A., Strominger, J. L., Wiley, D. C. and Wucherpfennig, K. W. (1998) Expression and crystallization of the complex of HLA-DR2 (DRA, DRB1\*1501) and an immunodominant peptide of human myelin basic protein. *Proceedings of the National Academy of Science (USA)*, **95**, 11828 - 11833.
- Gebe, J. A., Falk, B. A., Rock, K. A., Kochik, S. A., Heninger, A. K., Reijonen, H., Kwok, W. W. and Nepom, G. T. (2003) Low-avidity recognition by CD4+ T cells directed to self-antigens. *European Journal of Immunology*, **33**, 1409 - 1417.

- Gebe, J. A., Novak, E. J., Kwok, W. W., Farr, A. G., Nepom, G. T. and Buckner, J. H. (2001) T cell selection and differential activation on structurally related HLA-DR4 ligands.*Journal of Immunology*, **167**, 3250 - 3256.
- Gekkot, K. and Timasheff, S. N. (1981) Mechanism of Protein Stabilization by Glycerol: Preferential Hydration in Glycerol-Water Mixtures?*Biochemistry*, **20**, 4667 - 4676.
- Germain, R. N. and Hendrix, L. R. (1991) MHC class II structure, occupancy and surface expression determined by post-endoplasmic reticulum antigen binding.*Nature*, **353**, 134 - 139.
- Glimcher, L. H., Kim, K. J., Green, I. and Paul, W. E. (1982) Ia antigen-bearing B cell tumor lines can present protein antigen and alloantigen in a major histocompatibility complex-restricted fashion to antigen-reactive T cells.*Journal of Experimental Medicine*, **155**, 445 - 459.
- Godkin, A. J., Smith, K. J., Willis, A., Tejada-Simon, M. V., Zhang, J., Elliott, T. and Hill, A. V. S. (2001) Naturally processed HLA class II peptides reveal highly conserved immunogenic flanking region sequence preferences that reflect antigen processing rather peptide-MHC interactions.*Journal of Immunology*, **166**, 6720 - 6727.
- Gorga, J. C., Horejsí, V., Johnson, D. R., Raghupathy, R. and Strominger, J. L. (1987) Purification and characterisation of Class II histocompatibility antigens from a homozygous human B cell line.*Journal of Biological Chemistry*, **262**, 16087 - 16094.
- Gunnarsson, A., Hellmark, T. and Wieslander, J. (2000) Molecular properties of the Goodpasture Epitope.*Journal of Biological Chemistry*, **275**, 30844 - 30848.
- Gütgemann, I., Fahrner, A. M., Altman, J. D., Davis, M. M. and Chien, Y.-h. (1998) Induction of rapid T cell activation and tolerance by systemic presentation of an orally administered antigen.*Immunity*, **8**, 667-673.
- Guy, K., Heyning, V. V., Cohen, B. B., Deane, D. L. and Steel, C. M. (1982) Differential expression and serologically distinct subpopulations of human Ia antigens detected with monoclonal antibodies to Ia alpha and beta chains.*European Journal of Immunology*, **12**, 942 - 948.
- Hackett, C. J. and Sharma, O. K. (2002) Frontiers in peptide-MHC class II multimer technology.*Nature Immunology*, **3**, 887 - 889.
- Hamad, A. R. A., O'Herrin, S. M., Lebowitz, M. S., Srikrishnan, A., Bieler, J., Schneck, J. and Pardoll, D. (1998) Potent T cell activation with dimeric peptide-major histocompatibility complex class II ligand: The role of CD4 coreceptor.*The Journal of Experimental Medicine*, **188**, 1633-1640.
- Hanahan, D. (1983) Studies on transformation of *Escherichia coli* with plasmids.*Journal of Molecular Biology*, **166**, 557 - 580.

- Hayakawa, K., Ishii, R., Yamasaki, K., Kishimoto, T. and Hardy, R. R. (1987) Isolation of high-affinity memory B cells: Phycoerythrin as a probe for antigen-binding cells. *Proceedings of the National Academy of Sciences (USA)*, **84**, 1379 - 1383.
- Hellmark, T., Burkhardt, H. and Wieslander, J. (1999a) Goodpasture Disease - Characterisation of a single conformational epitope as the target of pathogenic autoantibodies. *Journal of Biological Chemistry*, **274**, 25862-25868.
- Hellmark, T., Johansson, C. and Wieslander, J. (1994) Characterisation of anti-GBM antibodies involved in Goodpasture's syndrome. *Kidney International*, **46**, 823 - 829.
- Hellmark, T., Segelmark, M., Unger, C., Burkhardt, H., Saus, J. and Wieslander, J. (1999b) Identification of a clinically relevant immunodominant region of collagen IV in Goodpasture disease. *Kidney International*, **55**, 936-944.
- Hellmark, T., Segelmark, M. and Wieslander, J. (1997) Anti-GBM antibodies in Goodpasture syndrome; anatomy of an epitope. *Nephrology Dialysis and Transplantation*, **12**, 646 - 648.
- Hickling, J. K. (1999), Measuring human T-lymphocyte function. *Expert Reviews in Molecular Medicine*.
- Hochuli, E., Döbeli, H. and Schacher, A. (1987) New metal chelate adsorbent selective for proteins and peptides containing neighbouring histidine residues. *Journal of Chromatography*, **411**, 177 - 184.
- Holdsworth, S. R., Kitching, A. R. and Tipping, P. G. (1999) Th1 and Th2 T helper cell subsets affect patterns of injury and outcomes in glomerulonephritis. *Kidney International*, **55**, 1198 - 1216.
- Hooke, D. H., Gee, D. C. and Atkins, R. C. (1987) Leukocyte analysis using monoclonal antibodies in human glomerulonephritis. *Kidney International*, **31**, 964 - 972.
- Horton, R. M., Cai, Z., Ho, S. N. and Pease, L. R. (1990) Gene splicing by overlap extension: Tailor made genes using the polymerase chain reaction. *Biotechniques*, **8**, 528 - 535.
- Huang, B., Yachou, A., Fleury, S., Hendrickson, W. A. and Sekaly, R.-P. (1997a) Analysis of the contact sites on the CD4 molecule with Class II MHC molecule: Co-ligand versus co-receptor function. *Journal of Immunology*, **158**, 216 - 225.
- Huang, X. R., Holdsworth, S. R. and Tipping, P. G. (1994) Evidence for delayed-type hypersensitivity mechanisms in glomerular crescent formation. *Kidney International*, **46**, 69 - 78.
- Huang, X. R., Tipping, P. G., Apostolopoulos, J., Oettinger, C., D'Souza, M., Milton, G. and Holdsworth, S. R. (1997b) Mechanisms of T cell-induced glomerular injury in anti-glomerular basement membrane (GBM) glomerulonephritis in rats. *Clinical and Experimental Immunology*, **109**, 134 - 142.



- Hudson, B. G., Kalluri, R., Gunwar, S., Noelken, M. E., Mariyama, M. and Reeders, S. T. (1993a) Molecular characteristics of the Goodpasture autoantigen. *Kidney International*, **43**, 135-139.
- Hudson, B. G., Reeders, S. T. and Tryggvason, K. (1993b) Type IV collagen: structure, gene organisation, and role in human diseases. Molecular basis of Goodpasture and Alport syndromes and diffuse leiomyomatosis. *Journal of Biological Chemistry*, **268**, 26033 - 26036.
- Hudson, B. G., Tryggvason, K., Sundaramoorthy, M. and Neilson, E. G. (2003) Alport's Syndrome, Goodpasture's Syndrome, and Type IV Collagen. *The New England Journal of Medicine*, **348**, 2543-2556.
- Huey, B., McCormick, K., Capper, J., Ratliff, C., Colombe, B. W., Garovoy, M. R. and Wilson, C. B. (1993) Association of HLA-DR and HLA-DQ types with anti-GBM nephritis by sequence-specific oligonucleotide probe hybridisation. *Kidney International*, **44**, 307 - 312.
- Hugues, S., Malherbe, L., Filippi, C. and Glaichenhaus, N. (2002) Generation and use of alternative multimers of peptide/MHC complexes. *Journal of Immunological Methods*, **268**, 83 - 92.
- Hunt, D. F., Henderson, R. A., Shabanowitz, J., Sakaguchi, K., Michel, H., Sevilir, N., Cox, A. L., Appella, E. and Engelhard, V. H. (1992) Characterization of Peptides Bound to the Class I MHC Molecule HLA-A2.1 by Mass Spectrometry. *Science*, **255**, 1261 - 1263.
- Ivey-Hoyle, M. (1991) Recombinant gene expression in cultured *Drosophila melanogaster* cells. *Current Opinion in Biotechnology*, **2**, 704 - 707.
- Janeway, C. A., Travers, P., Walport, M. and Shlomchik, M. (2001) *Immunobiology - The immune system in health and disease*, 5<sup>th</sup> ed. New York, Garland Publishing.
- Jang, M.-H., Seth, N. P. and Wucherpfennig, K. W. (2003) Ex Vivo Analysis of Thymic CD4 T Cells in Nonobese Diabetic Mice with Tetramers Generated from I-Ag7/Class II-Associated Invariant Chain Peptide Precursors. *The Journal of Immunology*, **171**, 4175-4186.
- Kalandadze, A., Galleno, M., Foncerrada, L., Strominger, J. L. and Wucherpfennig, K. W. (1996) Expression of recombinant HLA-DR2 molecules: Replacement of the hydrophobic transmembrane region by a leucine zipper dimerization motif allows the assembly and secretion of soluble DR $\alpha\beta$  heterodimers. *Journal of Biological Chemistry*, **271**, 20156 - 20162.
- Kalluri, R., Danoff, T. M., Okada, H. and Neilson, E. G. (1997) Susceptibility to anti-glomerular basement membrane disease and Goodpasture syndrome is linked to MHC class II genes and the emergence of T cell-mediated immunity in mice. *Journal of Clinical Investigation*, **100**, 2263-2275.
- Kalluri, R., Gunwar, S., Reeders, S. T., Morrison, K. C., Mariyama, M., Ebner, K. E., Noelken, M. E. and Hudson, B. G. (1991) Goodpasture Syndrome - Localisation of the epitope for the

autoantibodies to the carboxyl-terminal region of the  $\alpha 3(\text{IV})$  chain of basement membrane collagen. *Journal of Biological Chemistry*, **266**, 24018 - 24024.

Kalluri, R., Sun, M. J., Hudson, B. G. and Neilson, E. G. (1996) The Goodpasture autoantigen: Structural delineation of two immunologically privileged epitopes on  $\alpha 3(\text{IV})$  chain of type IV collagen. *Journal of Biological Chemistry*, **271**, 9062 - 9068.

Kasson, P. M., Rabinowitz, J. D., Schmitt, L., Davis, M. M. and McConnell, H. M. (2000) Kinetics of peptide binding to the Class II MHC protein I-E<sup>k</sup>. *Biochemistry*, **39**, 1048 - 1058.

Kellar, K. L. and Iannone, M. A. (2002) Multiplexed microsphere-based flow cytometric assays. *Experimental Hematology*, **30**, 1227 - 1237.

Kellar, K. L., Kalwar, R. R., Dubois, K. A., Crouse, D., Chafin, W. D. and Kane, B. E. (2001) Multiplexed fluorescent bead-based immunoassays for quantitation of human cytokines in serum and culture supernatants. *Cytometry*, **45**, 27 - 36.

Kelso, A. (1995) Th1 and Th2 subsets: paradigms lost? *Immunology Today*, **16**, 374 - 379.

Knabel, M., Franz, T. J., Schiemann, M., Wulf, A., Villmow, B., Schmidt, B., Bernhard, H., Wagner, H. and Busch, D. H. (2002) Reversible MHC multimer staining for functional isolation of T-cell populations and effective adoptive transfer. *Nature Medicine*, **8**, 631 - 637.

König, R. (2002) Interactions between MHC molecules and co-receptors of the TCR. *Current Opinion in Immunology*, **14**, 75 - 83.

König, R., Shen, X. and Germain, R. N. (1995) Involvement of both Major Histocompatibility Complex Class II  $\alpha$  and  $\beta$  chains in CD4 function indicates a role for ordered oligomerization in T cell activation. *Journal of Experimental Medicine*, **182**, 779 - 787.

Kotzin, B. L., Falta, M. T., Crawford, F., Rosloniec, E. F., Bill, J., Marrack, P. and Kappler, J. (2000) Use of soluble peptide-DR4 tetramers to detect synovial T cells specific for cartilage antigens in patients with rheumatoid arthritis. *Proceedings of the National Academy of Science (USA)*, **97**, 291-296.

Kozono, H., Parker, D., White, J., Marrack, P. and Kappler, J. (1995) Multiple binding sites for bacterial superantigens on soluble class II MHC molecules. *Immunity*, **3**, 187 - 196.

Kozono, H., White, J., Clements, J., Marrack, P. and Kappler, J. (1994) Production of soluble MHC class II proteins with covalently bound single peptides. *Nature*, **369**, 151-154.

Kuhelj, R., Dolinar, M., Pungercar, J. and Turk, V. (1995) The preparation of catalytically active human cathepsin B from its precursor expressed in *Escherichia coli* in the form of inclusion bodies. *European Journal of Biochemistry*, **229**, 533 - 539.

- Kuroda, M. J., Schmitz, J. E., Barouch, D. H., Craiu, A., Allen, T. M., Sette, A., Watkins, D. I., Forman, M. A. and Letvin, N. L. (1998) Analysis of Gag-specific Cytotoxic T Lymphocytes in Simian Immunodeficiency Virus-infected Rhesus Monkeys by Cell Staining with a Tetrameric Major Histocompatibility Complex Class I-Peptide Complex. *Journal of Experimental Medicine*, **187**, 1373-1381.
- Kuroda, M. J., Schmitz, J. E., Lekutis, C., Nickerson, C. E., Lifton, M. A., Franchini, G., Harouse, J. M., Cheng-Mayer, C. and Letvin, N. L. (2000) Human Immunodeficiency Virus Type I envelope epitope-specific CD4+ T lymphocytes in Simian/Human Immunodeficiency Virus-infected and vaccinated Rhesus monkeys detected using a peptide-Major Histocompatibility Complex Class II tetramer. *Journal of Virology*, **74**, 8751 - 8756.
- Kwok, W. W. (2003) Challenges in staining T cells using HLA class II tetramers. *Clinical Immunology*, **106**, 23 - 28.
- Kwok, W. W., Gebe, J. A., Liu, A., Agar, S., Ptacek, N., Hammer, J., Koelle, D. M. and Nepom, G. T. (2001) Rapid epitope identification from complex class-II- restricted T-cell antigens. *Trends in Immunology*, **22**, 583 - 588.
- Kwok, W. W., Liu, A. W., Novak, E. J., Gebe, J. A., Ettinger, R. A., Nepom, G. T., Reymond, S. N. and Koelle, D. M. (2000) HLA-DQ tetramers identify epitope-specific T cells in peripheral blood of herpes simplex virus type 2-infected individuals: Direct detection of immunodominant antigen-responsive cells. *Journal of Immunology*, **164**, 4244-4249.
- Kwok, W. W., Ptacek, N. A., Liu, A. W. and Buckner, J. H. (2002) Use of class II tetramers for the identification of CD4+ T cells. *Journal of Immunological Methods*, **268**, 71 - 81.
- Labeta, M. O., Fernandez, N. and Festenstein, H. (1988) Solubilisation effect of Nonidet P-40, triton X-100 and CHAPS in the detection of MHC-like glycoproteins. *Journal of Immunological Methods*, **112**, 133 - 138.
- Lampson, L. A. and Levy, R. (1980) Two populations of Ia-like molecules on a human B cell line. *Journa of Immunology*, **125**, 293 - 299.
- Landschulz, W. H., Johnson, P. F. and McKnight, S. L. (1988) The Leucine Zipper: A Hypothetical Structure Common to a New Class of DNA Binding Proteins. *Science*, **240**, 1759 -1764.
- Lanzavecchia, A. (1997) Understanding the mechanisms of sustained signaling and T cell activation. *Journal of Experimental Medicine*, **185**, 1717 - 1719.
- Lanzavecchia, A., Iezzi, G. and Viola, A. (1999) From TCR engagement to T cell activation: A kinetic view of T cell behavior. *Cell*, **96**, 1-4.
- Lanzavecchia, A. and Sallusto, F. (2000) From synapse to immunological memory: the role of sustained T cell stimulation. *Current Opinion in Immunology*, **12**, 92-98.

- Latek, R. R., Suri, A., Petzold, S. J., Nelson, C. A., Kanagawa, O., Unanue, E. R. and Fremont, D. H. (2000) Structural basis of peptide binding and presentation by the diabetes-associated MHC Class II molecule of NOD mice. *Immunity*, **12**, 699-710.
- Leinonen, A., Netzer, K.-O., Boutaud, A., Gunwar, S. and Hudson, B. G. (1999) Goodpasture antigen: Expression of the full length alpha3(IV) chain of collagen IV and localisation of epitopes exclusively to the noncollagenous domain. *Kidney International*, **55**, 926-935.
- Lerner, R. A., Glassock, R. J. and Dixon, F. J. (1967) The role of anti-glomerular basement membrane antibody in the pathogenesis of human glomerulonephritis. *Journal of Experimental Medicine*, **126**, 989 - 1004.
- Levy, J. B., Coulthart, A. and Pusey, C. D. (1997) Mapping B cell epitopes in Goodpasture's Disease. *Journal of the American Society of Nephrology*, **8**, 1698 - 1705.
- Levy, J. B., Turner, A. N., George, A. J. T. and Pusey, C. D. (1996) Epitope analysis of the Goodpasture antigen using a resonant mirror biosensor. *Clinical and Experimental Immunology*, **106**, 79-85.
- Li, M., Su, Z.-G. and Janson, J.-C. (2004) In vitro protein refolding by chromatographic procedures. *Protein Expression and Purification*, **33**, 1-10.
- Li, S., Holdsworth, S. R. and Tipping, P. G. (1997) Antibody independent crescentic glomerulonephritis in  $\mu$  chain deficient mice. *Kidney International*, **51**, 672 - 678.
- Lightstone, L., Salama, A., Mosley, K., Chaudhry, A., Pusey, C. and Lechler, R. (2001) Regulatory T-cell populations in anti-GBM disease and Alport's syndrome. *Immunology*, **104**, 8.
- Lilie, H., Schwarz, E. and Rudolph, R. (1998) Advances in refolding of proteins produced in *E. coli*. *Current Opinion in Biotechnology*, **9**, 497-501.
- Lim, D.-G., Bourcier, K. B., Freeman, G. J. and Hafler, D. A. (2000) Examination of CD8<sup>+</sup> T cell function in humans using MHC Class I tetramers: Similar cytotoxicity but variable proliferation and cytokine production among different clonal CD8<sup>+</sup> T cells specific to a single viral epitope. *Journal of Immunology*, **165**, 6214 - 6220.
- Liu, C.-P., Jiang, K., Wu, C.-H., Lee, W.-H. and Lin, W.-J. (2000) Detection of glutamic acid decarboxylase-activated T cells with I-A<sup>g</sup> tetramers. *Proceedings of the National Academy of Science (USA)*, **97**, 14596-14601.
- Liu, C.-P., Parker, D., Kappler, J. and Marrack, P. (1997) Selection of Antigen-specific T Cells by a Single IEk Peptide Combination. *Journal of Experimental Medicine*, **186**, 1441-1450.
- Lucas, M., Day, C. L., Wyer, J. R., Cunliffe, S. L., Loughry, A., McMichael, A. J. and Klenerman, P. (2004) Ex Vivo Phenotype and Frequency of Influenza Virus-Specific CD4 Memory T Cells. *The Journal of Virology*, **78**, 7284-7287.

- Luo, A. M., Fox, J. and Bolton, W. K. (1996) Experimental Autoimmune Glomerulonephritis (EAG): Searching for epitope(s).*Journal of the American Society of Nephrology*, **7**, 1709.
- Luxembourg, A. T., Borrow, P., Teyton, L., Brunmark, A. B., Peterson, P. A. and Jackson, M. R. (1998) Biomagnetic isolation of antigen-specific CD8<sup>+</sup> T cells usable in immunotherapy.*Nature Biotechnology*, **16**, 281-285.
- Maas, K., Chan, S., Parker, J., Slater, A., Moore, J., Olsen, N. and Aune, T. M. (2002) Cutting Edge: Molecular portrait of human autoimmune disease.*Journal of Immunology*, **169**, 5 - 9.
- Magil, A. B. and Wadsworth, L. D. (1981) Monocytes in human glomerulonephritis: An electron microscopic study.*Laboratory Investigation*, **45**, 77 - 81.
- Magil, A. B. and Wadsworth, L. D. (1982) Monocyte involvement in glomerular crescents: A histochemical and ultrastructural study.*Laboratory Investigation*, **47**, 160 - 166.
- Maile, R., Wang, B., Schooler, W., Meyer, A., Collins, E. J. and Frelinger, J. A. (2001) Antigen-specific modulation of an immune response by in vivo administration of soluble MHC Class I tetramers.*Journal of Immunology*, **167**, 3708 - 3714.
- Malherbe, L., Filippi, C., Julia, V., Foucras, G., Moro, M., Appel, H., Wucherpfennig, K., Guéry, J.-C. and Glaichenhaus, N. (2000) Selective activation and expansion of high-affinity CD4<sup>+</sup> T cells in resistant mice upon infection with *Leishmania major*.*Immunity*, **13**, 771 - 782.
- Mallet-Designé, V. I., Stratmann, T., Homann, D., Carbone, F., Oldstone, M. B. A. and Teyton, L. (2003) Detection of Low-Avidity CD4<sup>+</sup> T Cells Using Recombinant Artificial APC: Following the Antiovalbumin Immune Response.*The Journal of Immunology*, **170**, 123-131.
- Mallone, R. and Nepom, G. T. (2004) MHC Class II tetramers and the pursuit of antigen-specific T cells: define, deviate, delete.*Clinical Immunology*, **110**, 232 - 242.
- Manz, R., Assenmacher, M., Pflüger, E., Miltenyi, S. and Radbruch, A. (1995) Analysis and sorting of live cells according to secreted molecules, relocated to a cell-surface affinity matrix.*Proceedings of the National Academy of Science (USA)*, **92**, 1921 - 1925.
- Marelli-Berg, F., Levy, J. B., Waller, H., Phelps, R. G., Turner, A. N., Lombardi, G., Pusey, C. D. and Lechler, R. I. (1996) Characterisation of autoantigen specific T cell responses in Goodpasture's Disease.*Journal of the American Society of Nephrology*, **7**, 1709.
- Markovic-Lipkovski, J., Muller, C., Risler, T., Bohle, A. and Muller, G. (1990) Association of glomerular and interstitial mononuclear leukocytes with different forms of glomerulonephritis.*Nephrology Dialysis Transplantation*, **5**, 10-17.
- Marrack, P., Ignatowicz, L., Kappler, J. W., Boymel, J. and Freed, J. H. (1993) Comparison of peptides bound to spleen and thymus class II.*Journal of Experimental Medicine*, **178**, 2173-2183.



- Marsh, S. G. E., Parham, P. and Barber, L. D. (2000) *The HLA FactsBook, First. London*, Academic Press.
- Matsui, K., Boniface, J. J., Reay, P. A., Schild, H., Groth, B. F. D. S. and Davis, M. M. (1991) Low affinity interaction of peptide-MHC complexes with T cell receptors. *Science*, **254**, 1788 - 1791.
- Matsui, K., Boniface, J. J., Steffner, P., Reay, P. A. and Davis, M. M. (1994) Kinetics of T-cell receptor binding to peptide/I-E<sup>k</sup> complexes: Correlation of the dissociation rate with T-cell responsiveness. *Proceedings of the National Academy of Science (USA)*, **91**, 12862 - 12866.
- Maus, M. V., Riley, J. L., Kwok, W. W., Nepom, G. T. and June, C. H. (2003) HLA tetramer-based artificial antigen-presenting cells for stimulation of CD4<sup>+</sup> T cells. *Clinical Immunology*, **106**, 16 - 22.
- McHeyzer-Williams, M. G., Altman, J. D. and Davis, M. M. (1996) Enumeration and characterization of memory cells in the Th compartment. *Immunological Reviews*, **150**, 5 - 21.
- McHeyzer-Williams, M. G. and Davis, M. M. (1995) Antigen-specific development of primary and memory T cells in vivo. *Science*, **268**, 106 - 111.
- McHeyzer-Williams, M. G., Nossal, G. J. V. and Lalor, P. A. (1991) Molecular characterization of single memory B cells. *Nature*, **350**, 502 - 505.
- McMichael, A. J. and Kelleher, A. (1999) The arrival of HLA class II tetramers. *Journal of Clinical Investigation*, **104**, 1669-1670.
- McMichael, A. J. and O'Callaghan, C. A. (1998) A new look at T cells. *Journal of Experimental Medicine*, **187**, 1367-1371.
- Meng, F.-G., Park, Y.-D. and Zhou, H.-M. (2001) Role of proline, glycerol, and heparin as protein folding aids during refolding of rabbit muscle creatine kinase. *The International Journal of Biochemistry & Cell Biology*, **33**, 701-709.
- Mengle-Gaw, L., Conner, S., McDevitt, H. O. and Fathman, C. G. (1984) Gene conversion between murine class II major histocompatibility complex loci. Functional and molecular evidence from the bm 12 mutant. *Journal of Experimental Medicine*, **160**, 1184 - 1194.
- Merkel, F., Kalluri, R., Marx, M., Enders, U., Stevanovic, S., Giegerich, G., Neilson, E. G., Rammensee, H.-G., Hudson, B. G. and Weber, M. (1996) Autoreactive T-cells in Goodpasture's syndrome recognize the N-terminal NC1 domain on  $\alpha 3$  type IV collagen. *Kidney International*, **49**, 1127-1133.
- Meyer, A. L., Trollmo, C., Crawford, F., Marrack, P., Steere, A. C., Huber, B. T., Kappler, J. and Hafler, D. A. (2000) Direct enumeration of Borrelia-reactive CD4 T cells *ex vivo* by using

- MHC class II tetramers.*Proceedings of the National Academy of Science USA*, **97**, 11433-11438.
- Meyers, K. E. C., Kinniry, P. A., Kalluri, R., Neilson, E. G. and P.Madaio, M. (1998) Human Goodpasture anti- $\alpha$ 3(IV)NC1 autoantibodies share structural determinants.*Kidney International*, **53**, 402 - 407.
- Mierendorf, R., Yeager, K. and Novy, R. (1994) The pET system: Your choice for expression.*in**Novations*, **1**, 1 - 3.
- Moris, A., Teichgräber, V., Gauthier, L., Bühring, H.-J. and Rammensee, H.-G. (2001) Cutting Edge: Characterization of allorestricted and peptide-selective alloreactive T cells using HLA-tetramer selection.*Journal of Immunology*, **166**, 4818 - 4821.
- Mosmann, T. R. and Sada, S. (1996) The expanding universe of T-cell subsets: Th1, Th2 and more.*Immunology Today*, **17**, 138 - 146.
- Mottez, E., Jaulin, C., Godeau, F., Choppin, J., Levy, J.-P. and Kourilsky, P. (1991) A single-chain murine class I major transplantation antigen.*European Journal of Immunology*, **21**, 467 - 471.
- Murali-Krishna, K., Altman, J. D., Suresh, M., Sourdive, D. J. D., Zajac, A. J., Miller, J. D., Slansky, J. and Ahmed, R. (1998) Counting antigen-specific CD8 T cells: A reevaluation of bystander activation during viral infection.*Immunity*, **8**, 177-187.
- Nag, B., Arimilli, S., Koukis, B., Rhodes, E., Baichwal, V. and Sharma, S. D. (1994) Intramolecular charge heterogeneity in purified major histocompatibility class II  $\alpha$  and  $\beta$  polypeptide chains.*Journal of Biological Chemistry*, **269**, 10061 - 10070.
- Nag, B., Arimilli, S., Mukku, P. V. and Astafieva, I. (1996) Functionally active recombinant  $\alpha$  and  $\beta$  chain-peptide complexes of human major histocompatibility class II molecules.*Journal of Biological Chemistry*, **271**, 10413 - 10418.
- Natarajan, S. K., Assadi, M. and Sadegh-Nasseri, S. (1999) Stable peptide binding to MHC Class II molecule is rapid and is determined by a receptive conformation shaped by prior association with low affinity peptides.*Journal of Immunology*, **162**, 4030 - 4036.
- Neale, T. J., Tipping, P. G., Carson, S. D. and Holdsworth, S. R. (1988) Participation of cell-mediated immunity in deposition of fibrin in glomerulonephritis.*Lancet*, 421 - 424.
- Neilson, E. G., Kalluri, R., Sun, M. J., Gunwar, S., Danoff, T., Mariyama, M., Myers, J. C., Reeders, S. T. and Hudson, B. G. (1993) Specificity of Goodpasture Autoantibodies for the recombinant noncollagenous domains of human type (IV) collagen.*Journal of Biological Chemistry*, **268**, 8402 - 8405.

- Nepom, B. S., Nepom, G. T., Coleman, M. and Kwok, W. W. (1996) Critical contribution of beta chain residue 57 in peptide binding ability of both HLA-DR and -DQ molecules. *Proceedings of the National Academy of Sciences (USA)*, **93**, 7202-7206.
- Nepom, G. T. (2003) MHC multimers: expanding the clinical toolkit. *Clinical Immunology*, **106**, 1-4.
- Nepom, G. T., Buckner, J. H., Novak, E. J., Reichstetter, S., Reijonen, H., Gebe, J., Wang, R., Swanson, E. and Kwok, W. W. (2002) HLA Class II tetramers: Tools for direct analysis of antigen-specific CD4<sup>+</sup> T cells. *Arthritis and Rheumatism*, **46**, 5 - 12.
- Netzer, K.-O., Leinonen, A., Boutaud, A., Borza, D.-B., Todd, P., Gunwar, S., Langeveld, J. P. M. and Hudson, B. G. (1999) The Goodpasture autoantigen: Mapping the major conformational epitope(s) of  $\alpha 3(\text{IV})$  collagen to residues 17-31 and 127-141 of the NC1 domain. *Journal of Biological Chemistry*, **274**, 11267 - 11274.
- Nikolic-Paterson, D. J. (2001) T-cell-specific therapy in autoimmune glomerulonephritis. *American Journal of Kidney Disease*, **38**, 1321 - 1328.
- Nolasco, F. E. B., Cameron, J. S., Hartley, B., Coelho, A., Hildreth, G. and Reuben, R. (1987) Intraglomerular T cells and monocytes in nephritis: Study with monoclonal antibodies. *Kidney International*, **31**, 1160 - 1166.
- Novak, E. J., Liu, A. W., Gebe, J. A., Falk, B. A., Nepom, G. T., Koelle, D. M. and Kwok, W. W. (2001a) Tetramer-guided epitope mapping: Rapid identification and characterization of immunodominant CD4<sup>+</sup> T cell epitopes from complex antigens. *Journal of Immunology*, **166**, 6665 - 6670.
- Novak, E. J., Liu, A. W., Nepom, G. T. and Kwok, W. W. (1999) MHC class II tetramers identify peptide-specific human CD4<sup>+</sup> T cells proliferating in response to influenza A antigen. *Journal of Clinical Investigation*, **104**, R63-R67.
- Novak, E. J., Masewicz, S. A., Liu, A. W., Lernmark, Å., Kwok, W. W. and Nepom, G. T. (2001b) Activated human epitope-specific T cells identified by class II tetramers reside within a CD4<sup>high</sup> proliferating subset. *International Immunology*, **13**, 799 - 806.
- Oelke, M., Kurokawa, T., Hentrich, I., Behringer, D., Cerundolo, V., Lindemann, A. and Mackensen, A. (2000) Functional characterisation of CD8<sup>+</sup> antigen-specific cytotoxic T lymphocytes after enrichment based on cytokine secretion: Comparison with the MHC-tetramer technology. *Scandinavian Journal of Immunology*, **52**, 544-549.
- Ogg, G. S., Jin, X., Bonhoeffer, S., Dunbar, P. R., Nowak, M. A., Monard, S., Segal, J. P., Cao, Y., Rowland-Jones, S. L., Cerundolo, V., Hurley, A., Markowitz, M., Ho, D. D., Nixon, D. F. and McMichael, A. J. (1998) Quantitation of HIV-1-specific cytotoxic T lymphocytes and plasma load of viral RNA. *Science*, **279**, 2103 - 2106.

- Ogg, G. S. and McMichael, A. J. (1998) HLA-peptide tetrameric complexes.*Immunology News*, 124-126.
- O'Shea, E. K., Lumb, K. J. and Kim, P. S. (1993) Peptide 'Velcro': Design of a heterodimeric coiled coil.*Current Biology*, **3**, 658 - 667.
- Ou, W.-B., Park, Y.-D. and Zhou, H.-M. (2002) Effect of osmolytes as folding aids on creatine kinase refolding pathway.*The International Journal of Biochemistry & Cell Biology*, **34**, 136-147.
- Ozato, K., Mayer, N. and Sachs, D. H. (1980) Hybridoma cell lines secreting monoclonal antibodies to mouse H-2 and Ia antigens.*The Journal of Immunology*, **124**, 533-540.
- Ozato, K. and Sachs, D. H. (1982) Detection of at least two distinct mouse I-E antigen molecules by the use of a monoclonal antibody.*The Journal of Immunology*, **128**, 807-810.
- Pawelec, G. P., Shaw, S., Ziegler, A., Muller, C. and Wernet, P. (1982) Differential inhibition of HLA-D- or SB-directed secondary lymphoproliferative responses with monoclonal antibodies detecting human Ia-like determinants.*Journal of Immunology*, **129**, 1070 - 1075.
- Penadés, J. R., Bernal, D., Revert, F., Johansson, C., Fresquet, V. J., Cervera, J., Wieslander, J., Quinones, S. and Saus, J. (1995) Characterisation and expression of multiple alternatively spliced transcripts of the Goodpasture antigen gene region: Goodpasture antibodies recognize recombinant proteins representing the autoantigen and one of its alternative forms.*European Journal of Biochemistry*, **229**, 754 - 760.
- Perry, F. E., Barker, R. N., Mazza, G., Day, M. J., Wells, A. D., Shen, C. R., Schofield, A. E. and Elson, C. J. (1996) Autoreactive T cell specificity in autoimmune hemolytic anemia of the NZB mouse.*European Journal of Immunology*, **26**, 136 - 141.
- Peterson, D. A., DiPaolo, R. J., Kanagawa, O. and Unanue, E. R. (1999) Quantitative analysis of the T cell repertoire that escapes negative selection.*Immunity*, **11**, 453-462.
- Phelps, R. G. (2000) Immune recognition of glomerular antigens.*Experimental Nephrology*, **8**, 226 - 234.
- Phelps, R. G., Jones, V., Turner, A. N. and Rees, A. J. (2000) Properties of HLA class II molecules divergently associated with Goodpasture's disease.*International Immunology*, **12**, 1135-1143.
- Phelps, R. G., L.Jones, V., Coughlan, M., Turner, A. N. and Rees, A. J. (1998) Presentation of the Goodpasture autoantigen to CD4 T cells is influenced more by processing constraints than by HLA class II peptide binding preferences.*Journal of Biological Chemistry*, **273**, 11440-11447.
- Phelps, R. G. and Rees, A. J. (1999) The HLA complex in Goodpasture's disease: A model for analyzing susceptibility to autoimmunity.*Kidney International*, **56**, 1638-1653.

- Phelps, R. G. and Turner, A. N. (2000) In *Comprehensive Clinical Nephrology*(Eds, Johnson, R. J. and Feehally, J.) Mosby, London, pp. 5.27.1 - 5.27.10.
- Phelps, R. G., Turner, A. N. and Rees, A. J. (1996) Direct identification of naturally processed autoantigen-derived peptides bound to HLA-DR15.*Journal of Biological Chemistry*, **271**, 18549-18553.
- Porto, J., Johansen, T., Catipovic, B., Parfit, D., Tuveson, D., Gether, U., Kozlowski, S., Fearon, D. and Schneck, J. (1993) A Soluble Divalent Class I Major Histocompatibility Complex Molecule Inhibits Alloreactive T Cells at Nanomolar Concentrations.*Proceedings of the National Academy of Sciences (USA)*, **90**, 6671-6675.
- Prakken, B., Wauben, M., Genini, D., Samodal, R., Barnett, J., Mendivil, A., Leoni, L. and Albani, S. (2000) Artificial antigen-presenting cells as a tool to exploit the immune 'synapse'.*Nature Medicine*, **6**, 1406 - 1410.
- Pusey, C., Holland, M., Cashman, S., Sinico, R., Lloveras, J., Evans, D. and Lockwood, C. (1991) Experimental autoimmune glomerulonephritis induced by homologous and isologous glomerular basement membrane in Brown-Norway rats.*Nephrology Dialysis Transplantation*, **6**, 457-465.
- Quarsten, H., McAdam, S. N., Jensen, T., Arentz-Hansen, H., Molberg, Ø., Lundin, K. E. A. and Sollid, L. M. (2001) Staining of celiac disease-relevant T cells by peptide-DQ2 multimers.*Journal of Immunology*, **167**, 4861 - 4868.
- Rabinowitz, J. D., Vrljic, M., Kasson, P. M., Liang, M. N., Busch, R., Boniface, J. J., Davis, M. M. and McConnell, H. M. (1998) Formation of highly peptide-receptive state of class II MHC.*Immunity*, **9**, 699 - 709.
- Radu, C. (1999) In *British Society of Immunology*Harrogate International Centre.
- Radu, C. G., Anderton, S. M., Firan, M., Wraith, D. C. and Ward, E. S. (2000) Detection of autoreactive T cells in H-2<sup>u</sup> mice using peptide-MHC multimers.*International Immunology*, **12**, 1553-1560.
- Radu, C. G., Ober, B. T., Colantonio, L., Qadri, A. and Ward, E. S. (1998) Expression and characterization of recombinant soluble peptide: I-A complexes associated with murine experimental autoimmune diseases.*Journal of Immunology*, **160**, 5915-5921.
- Reddy, J., Bettelli, E., Nicholson, L., Waldner, H., Jang, M.-H., Wucherpfennig, K. W. and Kuchroo, V. K. (2003) Detection of Autoreactive Myelin Proteolipid Protein 139–151-Specific T Cells by Using MHC II (IAs) Tetramers.*The Journal of Immunology*, **170**, 870 – 877.



- Rees, A. J., Peters, D. K., Amos, N., Welsh, K. I. and Batchelor, J. R. (1984) The influence of HLA-linked genes on the severity of anti-GBM antibody-mediated nephritis. *Kidney International*, **26**, 444 - 450.
- Rees, W., Bender, J., Teague, T. K., Kedl, R. M., Crawford, F., Marrack, P. and Kappler, J. (1999) An inverse relationship between T cell receptor affinity and antigen dose during CD4<sup>+</sup> T cell responses *in vivo* and *in vitro*. *Proceedings of the National Academy of Science (USA)*, **96**, 9781 - 9786.
- Reich, Z., Boniface, J. J., Lyons, D. S., Borochoy, N., Watchel, E. J. and Davis, M. M. (1997) Ligand-specific oligomerisation of T-cell receptor molecules. *Nature*, **387**, 617 - 620.
- Reichstetter, S., Ettinger, R. A., Liu, A. W., Gebe, J. A., Nepom, G. T. and Kwok, W. W. (2000) Distinct T cell interactions with HLA Class II tetramers characterize a spectrum of TCR affinities in the human antigen-specific T cell response. *Journal of Immunology*, **165**, 6994-6998.
- Reijonen, H., Elliott, J. F., van Endert, P. and Nepom, G. (1999) Differential Presentation of Glutamic Acid Decarboxylase 65 (GAD65) T Cell Epitopes Among HLA-DRB1\*0401-Positive Individuals. *The Journal of Immunology*, **163**, 1674-1681.
- Reijonen, H., Kwok, W. W. and Nepom, G. T. (2003) Detection of CD4<sup>+</sup> Autoreactive T Cells in T1D Using HLA Class II Tetramers. *Annals of the New York Academy of Sciences*, **1005**, 82-87.
- Reijonen, H., Novak, E. J., Kochik, S., Heninger, A., Liu, A. W., Kwok, W. W. and Nepom, G. T. (2002) Detection of GAD65-Specific T-Cells by Major Histocompatibility Complex Class II Tetramers in Type 1 Diabetic Patients and At-Risk Subjects. *Diabetes*, **51**, 1375-1382.
- Reinherz, E. L., Tan, K., Tang, L., Kern, P., Liu, J.-h., Xiong, Y., Hussey, R. E., Smolyar, A., Hare, B., Zhang, R., Joachimiak, A., Chang, H.-C., Wagner, G. and Wang, J.-h. (1999) The crystal structure of a T cell receptor in complex with peptide and MHC class II. *Science*, **286**, 1913 - 1921.
- Reynolds, J., Cashman, S. J., Evans, D. J. and Pusey, C. D. (1991) Cyclosporin A in the prevention and treatment of experimental autoimmune glomerulonephritis in the brown Norway rat. *Clinical Experimental Immunology*, **85**, 28 - 32.
- Reynolds, J., Norgan, V. A., Bhambra, U., Smith, J., Cook, H. T. and Pusey, C. D. (2002) Anti-CD8 monoclonal antibody therapy is effective in the prevention and treatment of experimental autoimmune glomerulonephritis. *Journal of the American Society of Nephrology*, **13**, 359 - 369.

- Reynolds, J. and Pusey, C. D. (1994) *In vivo* treatment with a monoclonal antibody to T helper cells in experimental autoimmune glomerulonephritis in the BN rat. *Clinical Experimental Immunology*, **95**, 122 - 127.
- Reynolds, J., Sallie, B. A., Syrganis, C. and Pusey, C. D. (1993) The role of T-helper lymphocytes in priming for experimental autoimmune glomerulonephritis in the BN rat. *Journal of Autoimmunity*, **6**, 571 - 585.
- Reynolds, J., Tam, F. W. K., Chandraker, A., Smith, J., Karkar, A. M., Cross, J., Peach, R., Sayegh, M. H. and Pusey, C. D. (2000) CD28-B7 blockade prevents the development of experimental autoimmune glomerulonephritis. *Journal of Clinical Investigation*, **105**, 643 - 651.
- Rhode, P. R., Burkhardt, M., Jiao, J.-a., Siddiqui, A. H., Huang, G. P. and Wong, H. C. (1996) Single-chain MHC class II molecules induce T cell activation and apoptosis. *Journal of Immunology*, **157**, 4885 - 4891.
- Robert, B., Guillaume, P., Luescher, I., Romero, P. and Mach, J.-P. (2000) Antibody-conjugated MHC class I tetramers can target tumor cells for specific lysis by T lymphocytes. *European Journal of Immunology*, **30**, 3165-3170.
- Robson, M. G. (2000) In *Rheumatology Section, Division of Medicine* Imperial College School of Medicine, London, pp. 197.
- Roncarolo, M.-G. and Levings, M. K. (2000) The role of different subsets of T regulatory cells in controlling autoimmunity. *Current Opinion in Immunology*, **12**, 676-683.
- Rosenkranz, A. R., Knight, S., Sethi, S., Alexander, S. I., Cotran, R. S. and Mayadas, T. N. (2000) Regulatory interactions of  $\alpha\beta$  and  $\gamma\delta$  T cells in glomerulonephritis. *Kidney International*, **58**, 1055 - 1066.
- Rothenhausler, B., Dornmair, K. and McConnell, H. (1990) Specific Binding of Antigenic Peptides to Separate  $\alpha$  and  $\beta$  Chains of Class II Molecules of the Major Histocompatibility Complex. *Proceedings of the National Academy of Sciences (USA)*, **87**, 352 - 354.
- Rovin, B. H. and Schreiner, G. F. (1991) Cell-mediated immunity in glomerular disease. *Annual Reviews in Medicine*, **42**, 25 - 33.
- Ruberti, G., Sellins, K., Hill, C., Germain, R., Fathman, C. and Livingstone, A. (1992) Presentation of antigen by mixed isotype class II molecules in normal H-2d mice. *The Journal of Experimental Medicine*, **175**, 157-162.
- Rudensky, A. Y., Preston-Hurlburt, P., Al-Ramadi, B. K., Rothbard, J. and Jr, C. A. J. (1992) Truncation variants of peptides isolated from MHC class II molecules suggest sequence motifs. *Nature*, **359**, 429 - 431.

- Rudensky, A. Y., Preston-Hurlburt, P., Hong, S.-C., Barlow, A. and Janeway, C. A. (1991) Sequence analysis of peptides bound to MHC class II molecules. *Nature*, **353**, 622 - 627.
- Rudolph, R. (1996) In *Protein Engineering: Principles and Practice*(Eds, Cleland, J. L. and Craik, C. S.) Wiley-Liss, New York, pp. 283 - 298.
- Rudolph, R., Böhm, G., Lilie, H. and Jaeniche, R. (1997) In *Protein function - A practical approach*(Ed, Creighton, T. E.) Oxford University Press, Oxford.
- Rudolph, R. and Lilie, H. (1996) In vitro folding of inclusion body proteins. *FASEB Journal*, **10**, 49 - 56.
- Ryan, J. J., P.J.Mason, C.D.Pusey and N.Turner (1998) Recombinant alpha-chains of type IV collagen demonstrate that the amino terminal of the Goodpasture autoantigen is crucial for antibody recognition. *Clinical Experimental Immunology*, **113**, 17-27.
- Sadegh-Nasseri, S. and Germain, R. N. (1991) A role for peptide in determining MHC class II structure. *Nature*, **353**, 167 - 170.
- Salama, A. D., Chaudhry, A., Ryan, J., Lightstone, L., Pusey, C. D. and Lechler, R. I. (1999) T cell responses in Goodpasture's disease. *Immunology*, **98**, 35.
- Salama, A. D., Chaudry, A. N., Ryan, J. J., Eren, E., Levy, J. B., Pusey, C. D., Lightstone, L. and Lechler, R. I. (2001) In Goodpasture's Disease, CD4<sup>+</sup> T cells escape thymic deletion and are reactive with the autoantigen  $\alpha 3(\text{IV})\text{NC1}$ . *Journal of the American Society of Nephrology*, **12**, 1908 - 1915.
- Sambrook, J., Fritsch, E. F. and Maniatis, T. (1989) *Molecular cloning - A laboratory manual*, Second. New York, Cold Spring Harbor Laboratory Press.
- Saus, J., Wieslander, J., Langeveld, J. P. M., Quinones, S. and Hudson, B. G. (1988) Identification of the Goodpasture Antigen as the  $\alpha 3(\text{IV})$  chain of collagen IV. *Journal of Biological Chemistry*, **263**, 13374 - 13380.
- Savage, C. O., Pusey, C. D., Bowman, C., Rees, A. J. and Lockwood, C. M. (1986) Antiglomerular basement membrane antibody mediated disease in the British Isles 1980-4. *British Medical Journal Clinical Research Ed*, **292**, 301-4.
- Savage, P. A., Boniface, J. J. and Davis, M. M. (1999) A kinetic basis for T cell receptor repertoire selection during an immune response. *Immunity*, **10**, 485-492.
- Saxenat, V. P. and Wetlaufert, D. B. (1970) Formation of Three-Dimensional Structure in Proteins. I. Rapid Nonenzymic Reactivation of Reduced Lysozyme. *Biochemistry*, **9**, 5015 - 5023.

- Schatz, P. J. (1993) Use of peptide libraries to map the substrate specificity of a peptide-modifying enzyme: A 13 residue consensus peptide specifies biotinylation in *Escherichia coli*. *Biotechnology*, **11**, 1138 - 1143.
- Scheirle, A., Takacs, B., Kremer, L., Marin, F. and Sinigaglia, F. (1992) Peptide binding to soluble HLA-DR4 molecules produced by insect cells. *Journal of Immunology*, **149**, 1994 - 1999.
- Scott, C. A., Garcia, K. C., Carbone, F. R., Wilson, I. A. and Teyton, L. (1996) Role of chain pairing for the production of functional soluble IA major histocompatibility complex class II molecules. *Journal of Experimental Medicine*, **183**, 2087-2095.
- Scott, C. A., Garcia, K. C., Stura, E. A., Peterson, P. A., Wilson, I. A. and Teyton, L. (1998) Engineering protein for X-ray crystallography: The murine Major Histocompatibility Complex class II molecule I-A(d). *Protein Science*, **7**, 413 - 418.
- Segelmark, M., Butkowski, R. and Wieslander, J. (1990) Antigen restriction and IgG subclasses among anti-GBM autoantibodies. *Nephrology Dialysis and Transplantation*, **5**, 991 - 996.
- Sette, A., Southwood, S., O'Sullivan, D., Gaeta, F. C. A., Sidney, J. and Gray, H. M. (1992) Effect of pH on MHC class II-peptide interactions. *Journal of Immunology*, **148**, 844 - 851.
- Skinner, P. J., Daniels, M. A., Schmidt, C. S., Jameson, S. C. and Haase, A. T. (2000) Cutting Edge: In situ tetramer staining of antigen-specific T cells in tissues. *Journal of Immunology*, **165**, 613-617.
- Smith, K. J., Pyrdol, J., Gauthier, L., Wiley, D. C. and Wucherpfennig, K. W. (1998) Crystal structure of HLA-DR2 (DRA\*0101, DRB1\*1501) complexed with a peptide from human myelin basic protein. *Journal of Experimental Medicine*, **188**, 1511 - 1520.
- Spencer, J. S., Freed, J. H. and Kubo, R. T. (1993) Expression and function of mixed isotype MHC class II molecules in normal mice. *Journal of Immunology*, **151**, 6822-32.
- Spencer, J. S. and Kubo, R. T. (1989) Mixed isotype class II antigen expression. A novel class II molecule is expressed on a murine B cell lymphoma. *Journal of Experimental Medicine*, **169**, 625-40.
- Stebay, R. W. (1962) Glomerulonephritis induced in sheep by injections of heterologous glomerular basement membrane and Freund's complete adjuvant. *Journal of Experimental Medicine*, **116**, 253 - 272.
- Stern, L. J., Brown, J. H., Jardetzky, T. S., Gorga, J. C., Urban, R. G., Strominger, J. L. and Wiley, D. C. (1994) Crystal structure of the human Class II MHC protein HLA-DR1 complexed with an influenza virus peptide. *Nature*, **368**, 215 - 221.
- Stern, L. J. and Wiley, D. C. (1992) The human class II MHC protein HLA-DR1 assembles as empty  $\alpha\beta$  heterodimers in the absence of antigenic peptide. *Cell*, **68**, 465 - 477.

- Stöckel, J., Döring, K., Malotka, J., Jähnig, F. and Dornmair, K. (1997) Pathway of detergent-mediated and peptide ligand-mediated refolding of heterodimeric class II major histocompatibility complex (MHC) molecules. *European Journal of Biochemistry*, **248**, 684 - 691.
- Stöckel, J., Meinel, E., Hahnel, C., Malotka, J., Seitz, R., Drexler, K., Wekerle, H. and Dornmair, K. (1994) Refolding of human class II major histocompatibility complex molecules isolated from *Escherichia coli*. *Journal of Biological Chemistry*, **269**, 29571-29578.
- Stone, J. D., Demkowicz, W. E., Jr. and Stern, L. J. (2005) HLA-restricted epitope identification and detection of functional T cell responses by using MHC-peptide and costimulatory microarrays. *Proceedings of the National Academy of Sciences*, **102**, 3744 - 3749.
- Studier, F. W. and Moffatt, B. A. (1986) Use of bacteriophage T7 RNA polymerase to direct selective high-level expression of cloned genes. *Journal of Molecular Biology*, **189**, 113-130.
- Sundaramoorthy, M., Meiyappan, M., Todd, P. and Hudson, B. G. (2002) Crystal Structure of NC1 Domains. STRUCTURAL BASIS FOR TYPE IV COLLAGEN ASSEMBLY IN BASEMENT MEMBRANES. *Journal of Biological Chemistry*, **277**, 31142-31153.
- Theofilopoulos, A. N. (1995) The basis of autoimmunity: Part I - Mechanisms of aberrant self-recognition. *Immunology Today*, **16**, 90 - 98.
- Thompson, J. D., Gibson, T. J., Plewniak, F., Jeanmougin, F. and Higgins, D. G. (1997) The ClustalX windows interface: flexible strategies for multiple sequence alignment aided by quality analysis tools. *Nucleic Acid Research*, **24**, 4876 - 4882.
- Tipping, P. G., Huang, X. R., Qi, M., Van, G. Y. and Tang, W. W. (1998) Crescentic glomerulonephritis in CD4- and CD8- deficient mice. *American Journal of Pathology*, **152**, 1541 - 1548.
- Tipping, P. G., Neale, T. J. and Holdsworth, S. R. (1985) T lymphocyte participation in antibody-induced experimental glomerulonephritis. *Kidney International*, **27**, 530 - 537.
- Tough, D. F. and Sprent, J. (1998) Anti-viral immunity: Spotting virus-specific T cells. *Current Biology*, **8**, R498-R501.
- Townsend, S. E., Goodnow, C. C. and Cornall, R. J. (2001) Single epitope multiple staining to detect ultralow frequency B cells. *Journal of Immunological Methods*, **249**, 137-146.
- Tsumoto, K., Ejima, D., Kumagai, I. and Arakawa, T. (2003) Practical considerations in refolding proteins from inclusion bodies. *Protein Expression and Purification*, **28**, 1-8.
- Turner, A. N. and Rees, A. J. (1996) Goodpasture's disease and Alport's syndromes. *Annual Review of Medicine*, **47**, 377-386.



- Turner, N., Forstova, J., Rees, A., D.Pusey, C. and Mason, P. J. (1994) Production and characterisation of recombinant Goodpasture antigen in insect cells.*Journal of Biological Chemistry*, **269**, 17141-17145.
- Turner, N., Mason, P. J., Brown, R., Fox, M., Povey, S., Rees, A. and Pusey, C. D. (1992) Molecular cloning of the human Goodpasture antigen demonstrates it to be the alpha 3 chain of type IV collagen.*Journal of Clinical Investigation*, **89**, 592-601.
- Valitutti, S., Müller, S., Cella, M., Padovan, E. and Lanzavecchia, A. (1995) Serial triggering of many T-cell receptors by a few peptide-MHC complexes.*Nature*, **375**, 148 - 151.
- VanBleek, G. M. and Nathenson, S. G. (1990) Isolation of an endogenously processed immunodominant viral peptide from the class I H-2Kb molecule.*Nature*, **348**, 213 - 216.
- Vignali, D. A. A. (2000) Multiplexed particle-based flow cytometric assays.*Journal of Immunological Methods*, **243**, 243-255.
- Viner, N. J., Nelson, C. A., Deck, B. and Unanue, E. R. (1996) Complexes generated by the binding of free peptides to class II MHC molecules are antigenically diverse compared with those generated by intracellular processing.*Journal of Immunology*, **156**, 2365-2368.
- Visser, K. E. d., Cordaro, T. A., Kioussis, D., Haanen, J. B. A. G., Schumacher, T. N. M. and Kruisbeek, A. M. (2000) Tracing and characterisation of the low-avidity self-specific T cell repertoire.*European Journal of Immunology*, **30**, 1458-1468.
- Vogt, A. B., Kropshofer, H., Kalbacher, H., Kalbus, M., Rammensee, H.-G., Coligan, J. E. and Martin, R. (1994) Ligand motifs of HLA-DRB5\*0101 and DRB1\*1501 molecules delineated from self-peptides.*Journal of Immunology*, **153**, 1665 - 1673.
- Waldrop, S. L., Pitcher, C. J., Peterson, D. M., Maino, V. C. and Picker, L. J. (1997) Determination of antigen-specific memory/effector CD4+ T cell frequencies by flow cytometry: Evidence for a novel, antigen-specific homeostatic mechanism in HIV-associated immunodeficiency.*Journal of Clinical Investigation*, **99**, 1739 - 1750.
- Wallny, H.-J., Sollami, G. and Karjalainen, K. (1995) Soluble mouse major histocompatibility complex class II molecules produced in *Drosophila* cells.*European Journal of Immunology*, **25**, 1262-1266.
- Wieslander, J., Barr, J. F., Butkowski, R. J., Edwards, S. J., Bygren, P., Heinegard, D. and Hudson, B. G. (1984) Goodpasture antigen of the glomerular basement membrane: localization to noncollagenous regions of type IV collagen.*Proceedings of the National Academy of Sciences (U S A)*, **81**, 3838 - 3842.
- Wieslander, J., Kataja, M. and Hudson, B. G. (1987) Characterization of the human Goodpasture antigen.*Clinical Experimental Immunology*, **69**, 332 - 340.

- Wieslander, J., Langeveld, J., Butkowski, R., Jodlowski, M., Noelken, M. and Hudson, B. G. (1985) Physical and immunochemical studies of the globular domain of type IV collagen - Cryptic properties of the Goodpasture antigen. *Journal of Biological Chemistry*, **260**, 8564 - 8570.
- Williams, D. C., Frank, R. M. V., Muth, W. L. and Burnett, J. P. (1982) Cytoplasmic Inclusion Bodies in *Escherichia coli* Producing Biosynthetic Human Insulin Proteins. *Science*, **Vol. 215**, 687 - 689.
- Wilson, C. B. and Dixon, F. J. (1973) Anti-glomerular basement membrane antibody-induced glomerulonephritis. *Kidney International*, **3**, 74 - 89.
- Wu, J., Hicks, J., Borillo, J., II, W. F. G. and Lou, Y.-H. (2002) CD4<sup>+</sup> T cells specific to a glomerular basement membrane antigen mediated glomerulonephritis. *Journal of Clinical Investigation*, **109**, 517 - 524.
- Wucherpfennig, K. W., Sette, A., Southwood, S., Oseroff, C., Matsui, M., Strominger, J. L. and Hafler, D. A. (1994) Structural requirements for binding of an immunodominant myelin basic protein peptide to DR2 isotypes and for its recognition by human T cell clones. *Journal of Experimental Medicine*, **179**, 279 - 290.
- Wyer, J. R., Cunliffe, S. L., Kelleher, A. D., Sutton, J. K. and McMichael, A. J. (2001) Production of MHC Class II tetrameric complexes and optimisation of peptide linker length. *Immunology*, **104**, 71.
- Xu, X.-N. and Screaton, G. R. (2002) MHC/peptide tetramer-based studies of T cell function. *Journal of Immunological Methods*, **268**, 21 - 28.
- Yang, J., Shi, R., Goodman, J. and Mohankumar, T. (2002) A new method for the production of MHC Class II/peptide complexes associated by Fos and Jun dimerization domains. *Human Immunology*, **63**, S4.
- Yee, C., Savage, P. A., Lee, P. P., Davis, M. M. and Greenberg, P. D. (1999) Isolation of high avidity melanoma-reactive CTL from heterogeneous populations using peptide-MHC tetramers. *Journal of Immunology*, **162**, 2227-2234.
- Young, N. T. and Darke, C. (1994) Molecular characterization of the HLA-DR2LUM haplotype. *Tissue Antigens*, **43**, 28 - 33.
- Zhang, J., Markovic-Plese, S., Lacet, B., Raus, J., Weiner, H. L. and Hafler, D. A. (1994) Increased frequency of interleukin 2-responsive T cells specific for myelin basic protein and proteolipidprotein in peripheral blood and cerebrospinal fluid of patients with multiple sclerosis. *Journal of Experimental Medicine*, **179**, 973 - 974.
- Zhu, X., Bavari, S., Ulrich, R., Sadegh-Nasseri, S., Ferrone, S., McHugh, L. and Mage, M. (1997) A recombinant single-chain human class II MHC molecule (HLA-DR1) as a covalently linked

heterotrimer of  $\alpha$  chain,  $\beta$  chain, and antigenic peptide, with immunogenicity *in vitro* and reduced affinity for bacterial superantigens. *European Journal of Immunology*, **27**, 1933-1941.

## **Appendices**

## Appendix 1

### Heterodimeric MHC Class II Oligonucleotide Primers

#### 1 I-E<sup>d</sup> Heterodimer Constructs

##### 1.1 BirA1 Sequence

CGCTAGCGGC GGTGGACTGC ATCATATTCT GGATGCACAG AAAATGGTGT  
GGAATCATCG TTAAG

##### 1.2 BirA2 Sequence

GATCCTTAAC GATGATTCCA CACCATTTTC TGTGCATCCA GAATATGATG  
CAGTCCACCG CCGCTAGCGG TAC

##### 1.3 IE1 Sequence

AAGGGAATTC GAGCTC

##### 1.4 IE2 Sequence

CTCGAGTGTC TCTGAC

##### 1.5 IE3 Sequence

CTCGAGGCCC ACGGTTTTTG G

##### 1.6 IE4 Sequence

GGTACCCCTA GATGTGGAC



## 2 HLA-DR Zipper Constructs

### 2.1 ZipDRAL2 Sequence

CGAATTGTCG ACATGTGATC ATCCAGGCCG

### 2.2 ZipDRAR Sequence

ATCGGATCCA GATCTCTCGA GTGACGAGTT CTCTGTAGTC TC

### 2.3 ZipDRBL Sequence

CGAATTCTCG AGGCCACGT TTCYTG Y = C or T

### 2.4 ZipDRBR Sequence

CGAATTCAAG CTTGGATCCG TCGACTGACG ACTTGCTCTG TGC

## 3 Peptide Binding cassette Construct

### 3.1 PCTop

GCTCGAGGGG AGATCTGGAG GTTCACTAGT GCCACGGGGC TCTGGAGGCG  
GTCGACGGTA C

### 3.2 PCBottom

CGTCGACCGC CTCCAGAGCC CCGTGGCACT AGTGAACCTC CAGATCTCCC  
CTCGAGCTGC A

## Appendix 2

### Single-chain MHC Class II Oligonucleotide Primers

#### SC1 Sequence

GAATTCCATG GGCTCTCGAG GCCCACGKTT YYT      K = G or T; Y = C or T

#### SCmH2 Sequence

ATAAGCGTCT TGAGCTCCGA CTCKCCGCGY

#### SCH2 Sequence

ATAAGCGTCT TGAGCTCCGA CTCGCCGCTG

#### SC3 Sequence

GTCGGAGCTC AAGACGCTAT CAAAGARGAA CA      R = A or G

#### SC4 Sequence

GATCGGTACC ATTGGTGATC G

#### SCm4 Sequence

GATCGGTACC GTTGGCATCT G

#### SC25L2

GGGAATTCAT ATGTCTCGAG GGGTACCAGC GGCGGTGGAC

#### SC25R2

GATCCTCTAG AGGAACGATG ATTCC

## Appendix 3

### Solutions

#### 1 Transformation and amplification of DNA in competent cells

All solutions were produced following the methods laid out in Sambrook *et al* (Sambrook et al., 1989).

#### 2 Agarose mini gels

All solutions were produced following the methods laid out in Sambrook *et al* (Sambrook et al., 1989).

#### 3 SDS-PAGE gels

All solutions and gels were produced following the methods laid out in Sambrook *et al* (Sambrook et al., 1989).

#### 4 Antibody purification

##### 4.1 Loading and wash buffer

0.1M sodium phosphate buffer (pH8.0) was formed by mixing 93.2ml of 1M  $\text{Na}_2\text{HPO}_4$  with 6.8ml 1M  $\text{NaH}_2\text{PO}_4$  in 900ml of  $\text{dH}_2\text{O}$ , adjusting pH if necessary. To this sodium chloride was added to a final concentration of 0.5M prior to filtering through a  $0.45\mu\text{m}$  filter (*PAL Gelman corporation*) and storing at room temperature

## **5 Bacterial inclusion body preparation**

### **5.1 Triton wash solution**

0.5% Triton X-100

1mM EDTA

The above was made in 1l of dH<sub>2</sub>O prior to storing at room temperature.

### **5.2 Inclusion body re-suspension solution**

6M Urea

50mM HEPES pH8

1M NaCl

The above was freshly prepared in dH<sub>2</sub>O prior to use.

## **6 Nickel chelation chromatography**

All solutions were passed through a 0.45µm filter (*PAL Gelman Corporation*) prior to use.

### **6.1 Column stripping solution**

100mM EDTA

1M NaCl

The above was formed in dH<sub>2</sub>O, adjusting to pH 8.0 using 1M NaOH to allow dissolution of EDTA.

## 6.2 Column metal loading solution

100mM NiCl<sub>2</sub>

10mM sodium acetate

The above was formed in dH<sub>2</sub>O, adjusting pH to 4.5 using 1M HCl prior to storing at room temperature.

## 6.3 Column wash solution for heterodimer

0.1M sodium phosphate buffer (pH8)

1M NaCl

10mM imidazole

The above was mixed in dH<sub>2</sub>O prior to filtering and storing at room temperature.

## 6.4 Column elution solution for heterodimer

To the above wash solution, EDTA was added to a final concentration of 0.1M, adjusting the pH with sodium hydroxide to 8.0.

## 6.5 Column wash solution for single chain

The following were mixed prior to adjusting the pH to 8.0, filtering and storing at room temperature:

6M urea

50mM HEPES

1M NaCl

10mM imidazole



## 6.6 Column elution solution for single chain

To the above solution, EDTA was added to a final concentration of 0.1M, adjusting the pH with sodium hydroxide to 8.0.

## 7 Miscellaneous solutions

### 7.1 Cell lysis solution

This solution was composed of the following:

50mM Tris.Cl (pH7.5)

150mM Sodium Chloride

1% NP40

5mM EDTA, 1mM phenylmethanesulphonyl fluoride (PMSF), 1mM Iodoacetamide, 1µg/ml Leupeptin and 1µg/ml Pepstatin A

Once formed the solution was stored at -20°C until required.

### 7.2 Immunoprecipitation solutions

All solutions were produced following the methods laid out in Sambrook *et al* (Sambrook et al., 1989).

### 7.3 Citrate buffer for peptide binding experiments

Stock solutions of 0.1M citric acid (19.21g/l) and 0.2M dibasic sodium phosphate were first formed. A pH5.0 buffer was then made by combining 24.3ml of 0.1M citric acid and 25.7ml 0.2M dibasic sodium phosphate and diluting to 100ml with dH<sub>2</sub>O.